

Transport and Behavior of Microplastic in Lake Systems

DISSERTATION

zur Erlangung des akademischen Grades eines Doktors

der Naturwissenschaften (Dr. rer. nat.)

in der Bayreuther Graduiertenschule für Mathematik und Naturwissenschaften

(BayNAT)

der Universität Bayreuth

Vorgelegt von

Hassan Elagami

aus Dakahliya, Ägypten

Bayreuth, 2022

Transport and Behavior of Microplastic in Lake Systems

DISSERTATION

zur Erlangung des akademischen Grades eines Doktors

der Naturwissenschaften (Dr. rer. nat.)

in der Bayreuther Graduiertenschule für Mathematik und Naturwissenschaften

(BayNAT)

der Universität Bayreuth

Vorgelegt von

Hassan Elagami

aus Dakahliya, Ägypten

Bayreuth, 2022

Die vorliegende Arbeit wurde in der Zeit von Oktober 2019 bis Oktober 2022 an der Universität Bayreuth am Lehrstuhl für Hydrologie und an der limnologischen Station unter Betreuung von Herrn Dr. Benjamin-Silas Gilfedder angefertigt.

Vollständiger Abdruck der von der Bayreuther Graduiertenschule für Mathematik und Naturwissenschaften (BayNAT) der Universität Bayreuth genehmigten Dissertation zur Erlangung des akademischen Grades eines Doktors der Naturwissenschaften (Dr. rer. nat).

Dissertation eingereicht am: 21.10.2022

Zulassung durch das Leitungsgremium: 02.11.2022

Wissenschaftliches Kolloquium: 15.03.2023

Amtierender Direktor: Prof. Dr. Hans Keppler

Prüfungsausschuss:

Dr. Benjamin-Silas Gilfedder (Gutachter)

Prof. Dr. Efstathios Diamantopoulos (Gutachter)

Prof. Dr. Jan Fleckenstein (Vorsitz)

Prof. Dr. Christian Laforsch

Acknowledgement

It is really difficult to know where to start with the acknowledgment as many people have contributed to this project. First and foremost, I would like to thank my main supervisor Dr. Benjamin-Silas Gilfedder, and the co-supervisors, PD Dr. Sven Frei, and Prof. Dr. Jan H. Fleckenstein for their support and constructive guidance. Dr. Benjamin-Silas Gilfedder and PD Dr. Sven Frei deserve special thanks for the long hours of work and support in all kinds of bad weather at Brombachsee.

Secondly, I would like to acknowledge Prof. Dr. Martin Obst and his team for their valuable help during the microscopy part. I would also like to thank Prof. Dr. Seema Agarwal and project C02 for providing us with all microplastic needed in the first part of this work.

Thirdly, I am particularly grateful to all of my colleagues, Jan-Pascal Boos, Johanna Schmidtmann, Pouyan Ahmadi, Franz Dichgans, Laura Wegner, Barbara Jakob, Stefan Peiffer, Luisa Hopp, Bouchra Marouane, Karel As, Katharina Blaurock, Xingyu Liu, Usman Munir, Isolde Baumann, Jutta Eckert, Silke Hammer, and Martina Rohr.

Fourthly, I would like to thank Dr. Gabriele Trommer and the team of the Water Management Office in Ansbach for providing us with all means of support including logistics and monitoring data during our field experiments at Brombachsee.

Last but not least, I would like to acknowledge the Collaborative Research Centre (CRC) 1357 Microplastic for funding my research. I also would like to express my sincere gratitude to Prof. Dr. Christian Laforsch, Prof. Dr. Andreas Greiner, Dr. Melanie Pöhlmann, Dr. Hannes Imhof, and Ramona Lechner for the excellent organization of the CRC 1357 project.

Table of content

0 Abstract	1
0 Zusammenfassung	3
Chapter 1: Introduction	6
1. Current state of knowledge	6
1.1 Sources of microplastic	6
1.2 Microplastic in lake systems	7
1.3 Factors controlling microplastic behavior in lakes.....	7
1.3.1. Physical properties of pristine microplastic particles.....	8
1.3.2 Lake hydrodynamics	8
1.3.3 Biofilms	9
1.3.4 Interaction between microplastic and lake organisms and natural particles	9
2. Aims of this work	10
3. Materials and methods	11
3.1 Microplastic particles	11
3.2 Laboratory measurements and lake model (study 1).....	12
3.3 CFD simulations (study 2)	13
3.4 Mesocosm experiments and random walk modeling (study 3).....	14
3.5 Modelling of microplastic interaction with lake organisms (study 4)	15
4. Summary of findings and discussion	16
4.1 Measurement of microplastic settling velocities and implications for residence time in thermally stratified lakes (study 1).....	16
4.2 Systematic evaluation of physical parameters affecting the terminal settling velocity of microplastic particles in lakes using CFD (study 2).	18
4.3 Quantifying microplastic residence times in lakes using mesocosm experiments and transport modelling (study 3)	19
4.4 Filter feeders are key to residence times of small microplastic particles in stratified lakes: a virtual experiment (study 4)	21

5. Conclusion and outlook.....	23
5.1 Conclusion.....	23
5.2 Research outlook	24
6. References	26
7. Contribution statement	31
Chapter 2: Publications	33
Study 1: Measurement of microplastic settling velocities and implications for residence times in thermally stratified lakes	33
Study 2: Systematic evaluation of physical parameters affecting the terminal settling velocity of microplastic particles in lakes using CFD	53
Study 3: Quantifying microplastic residence times in lakes using mesocosm experiments and transport modelling	79
Study 4: Filter feeders are key to small microplastic cycling in stratified lakes: a virtual experiment.....	119

0 Abstract

Lakes are important ecosystems, with an array of organisms that may be sensitive to microplastic. One of the primary controls on microplastic uptake is the residence time in the water column, which is governed by several physical, biological, and hydrodynamical factors existing in the lake. In this dissertation, we combined 4 interrelated studies to investigate the behavior of microplastic in lake systems and understand how this can affect their residence times in the lake water column, as well as the exposure time to lake organisms.

Study 1 combines systematic laboratory experiments and lake incubations to understand the effect of microplastic properties on the residence times and investigate how this affects their exposure time to lake organisms. This was followed by model calculations to estimate microplastic residence time, accumulation, and transfer between lake compartments in a stratified water column broadly based on Upper Lake Constance, Germany. A wide range of biodegradable and non-biodegradable microplastic particles with various sizes and densities were used. The laboratory experiments identified particle size and density as the primary controls on residence times. The microplastic particles that had been incubated for up to 30 weeks were colonized by a range of biofilms and associated extracellular polymeric substances. Although the settling velocity did not vary between pristine and colonized microplastic particles, the biofilms acted as an adhesive and increased the tendency for the formation of aggregates. Finally, the modelled residence times varied over a very wide range of time scales (10^{-1} to 10^5 d), depending on the particle size (1, 100, 500, 1000 μm). The long residence time for the smallest microplastic suggests that there is a high likelihood that these particles will be taken up at some stage by lake organisms.

Study 2 aims at evaluating the different factors that control the residence time of microplastic particles such as particle density, size, and shape as well as water temperature using computational fluid dynamics (CFD) simulations. The model was validated using the experimental results of study 1. The CFD model presented that particle size and density are the most important factors controlling the settling velocities of the particles under laminar conditions. By doubling the density of a given particle size, the settling velocity increased by ~380 and 480 % for irregular and regular particles respectively. Increases up to ~95 and 225% could be obtained by doubling the volume of irregular and regular particles respectively. Other factors such as particle shape and water temperature had less effect on the settling velocity of

microplastic than that of density and size. Finally, the CFD results still overestimated the settling velocities from the laboratory experiments although the initial and boundary conditions of the CFD model were defined according to the real experimental setup.

Study 3 combines a series of in-lake mesocosm experiments and random walk modelling to quantitatively analyze the processes governing microplastic transport in the lake water column. The experiments were conducted over one year using three size ranges of fluorescent microspheres (1-5, 28-48, and 53-63 μm), capturing stratified and unstable conditions within the mesocosm. The measured residence times of the smallest particles during lake turnover were ~ 12 times shorter than that in summer. The residence times from the random walk model for the smallest particles during thermal stratification using Stokes velocities were ~ 10 times longer than the measured residence times in the mesocosm. However, the modeled residence times using settling velocities measured in the laboratory and mesocosm were comparable to the real residence times in the mesocosm. Finally, the modeled residence times during lake turnover were 113 times longer than that in the mesocosm. We believe that these discrepancies are due to the interactions between small microplastic particles and existing particles, as well as the complex hydrodynamic and biological conditions in the lake water column.

Study 4 uses laboratory and virtual experiments to quantify microplastic residence times in a purely physical system controlled by sinking and mixing and compare this to a system where daphnia package microplastic into faecal pellets. The simulations were parametrized using data from Lake Constance, Germany, and Esthwaite Water, UK as well as from existing literature and our own laboratory experiments. The simulations showed that when neglecting the biological pathway, the residence times for the 0.5 and 5 μm particles (>15 years) have exceeded the retention time of both lakes. After adding daphnia to the system, the residence times were reduced to ~ 1 year. The large 15 μm particles had a residence time between 1 and 2.5 years in the abiotic system and <1.6 years after daphnia was included. These results emphasize the significance of considering lake ecology when assessing residence times.

The results from the four studies show the complexity of microplastic transport in lake systems as many interrelated physical, biological, and hydrodynamic processes are involved in their transport process in the lake water column.

0 Zusammenfassung

Seen sind wichtige Ökosysteme mit einer Vielzahl von Organismen, die empfindlich auf Mikroplastik reagieren können. Einer der wichtigsten Faktoren für die Aufnahme von Mikroplastik ist die Verweilzeit in der Wassersäule, die von mehreren physikalischen, biologischen und hydrodynamischen Faktoren abhängig ist. In dieser Dissertation haben wir vier zusammenhängende Studien kombiniert, um das Verhalten von Mikroplastik in Seen zu untersuchen und herauszufinden, wie dies die Verweilzeit in der Wassersäule des Sees und die Expositionszeit für Seeorganismen beeinflussen kann.

Studie 1 kombiniert Laborexperimente mit Mikroplastikinkubationen, um die Auswirkungen der physikalischen Eigenschaften von Mikroplastik auf die Verweilzeit und die Expositionszeit für Seeorganismen zu verstehen. Darauf folgten Modellsimulationen zur Ermittlung der Verweilzeit von Mikroplastik, der Akkumulation und des Transfers zwischen den Seekompartimenten in einer geschichteten Seewassersäule, die grundsätzlich auf dem Obersee (Bodensee) in Deutschland basiert. Verschiedene biologisch und nicht biologisch abbaubare Mikroplastikpartikel mit unterschiedlichen Größen und Dichten wurden verwendet. Von Laborexperimenten wurden die Partikelgröße und -dichte als die wichtigsten Einflussfaktoren auf die Verweilzeit ermittelt. Die Mikroplastikpartikel, die bis zu 30 Wochen lang inkubiert wurden, wurden von einer von Biofilmen und extrazellulären polymeren Substanzen besiedelt. Obwohl die Sinkgeschwindigkeit zwischen fabrikneuen und inkubierten Mikroplastikpartikeln nicht signifikant variierte, wirkte der Biofilm als Klebstoff und führte zur Bildung von Aggregaten. Schließlich variierten die modellierten Verweilzeiten je nach Partikelgröße (1, 100, 500, 1000 μm) über einen sehr weiten Bereich von Zeitskalen (10^{-1} bis 10^5 d). Die extrem langen Verweilzeiten von kleinen Mikroplastikpartikeln zeigen, dass sie mit hoher Wahrscheinlichkeit von den Seeorganismen aufgenommen würden.

Studie 2 bewertet die verschiedenen Faktoren, die die Verweilzeit von Mikroplastikpartikeln steuern, wie z. B. Partikeldichte, -größe und -form sowie die Wassertemperatur mit Hilfe von numerischen Strömungsmechanik (CFD) Modellierung. Das Modell wurde anhand von experimentellen Ergebnisse von Studie 1 validiert. Das CFD-Modell zeigte, dass Partikelgröße und -dichte die wichtigsten Faktoren sind, die die Sinkgeschwindigkeiten der Partikel unter laminaren Bedingungen steuern. Eine Verdoppelung der Dichte eines Partikels führte zu einer Erhöhung der Absetzgeschwindigkeit um 480 bis 380 % für regelmäßige bzw. unregelmäßige Partikel. Eine Verdoppelung des Partikelvolumens führte zu einer Steigerung von 225 bzw. 95

% für regelmäßige und unregelmäßige Partikel. Andere Faktoren wie die Form der Partikel und die Wassertemperatur hatten einen geringeren Einfluss auf die Sinkgeschwindigkeit von Mikroplastik als die Dichte und Größe. Auch die Ergebnisse der Sinkgeschwindigkeit aus dem CFD-Modell lagen nahe an den im Labor gemessenen Geschwindigkeiten aus Studie 1. Das liegt daran, dass die Anfangs- und Randbedingungen des CFD-Modells entsprechend dem realen Laboraufbau definiert wurden.

In Studie 3 wurde eine Reihe von Mesokosmen-Experimenten im See mit einer Random-Walk-Modellierung kombiniert, um die Prozesse, die den Mikroplastiktransport in der Wassersäule des Sees bestimmen, quantitativ zu analysieren. Die Experimente wurden über ein Jahr mit drei Größenbereichen von fluoreszierenden Mikrosphären (1-5, 28-48 und 53-63 μm) durchgeführt, wobei Temperaturschichtung im Sommer und Wasserzirkulation (Durchmischung) im Herbst innerhalb des Mesokosmos erfasst wurden. Die gemessene Verweilzeit der kleinsten Partikel während der Vollzirkulation der Wassersäule im Herbst war ~ 12 Mal kürzer als die im Sommer. Die Modellierungsergebnisse für die kleinsten Partikel während der Temperaturschichtung unter Verwendung des Stokes Modells waren ~ 10 Mal länger als die realen Verweilzeiten im Mesokosmos. Die modellierten Verweilzeiten unter Verwendung der im Labor und im Mesokosmos gemessenen Sinkgeschwindigkeiten waren jedoch mit den realen Verweilzeiten im Mesokosmos vergleichbar. Schließlich waren die modellierten Verweilzeiten für die kleinsten Partikel während der Vollzirkulation des Sees 113 Mal länger als die im Mesokosmos. Wir vermuten, dass diese Unstimmigkeiten von den Wechselwirkungen zwischen kleinen Mikroplastikpartikeln und vorhandenen Partikeln sowie von den komplexen hydrodynamischen und biologischen Bedingungen in der Wassersäule abhängig sind.

Studie 4 verwendet Labor- und virtuelle Experimente, um die Verweilzeiten von Mikroplastik in einem rein physikalischen System zu quantifizieren, das durch Sinken und Durchmischen gesteuert wird, und vergleicht dies mit einem System, in dem Daphnien kleinen Mikroplastikpartikel in Fäzes verpacken. Die Simulationen basieren auf den Literaturdaten aus dem Bodensee (Deutschland) und dem Esthwaite Water (Vereinigtes Königreich) sowie aus unseren eigenen Laborexperimenten parametrisiert. Die Simulationen zeigten, dass bei Vernachlässigung des biologischen Weges die Verweilzeiten für die 0,5 und 5 μm großen Partikel (>15 Jahre) die Wasseraustauschzeit von beiden Seen überschritten haben. Nach der Zugabe von Daphnien ins System wurden die Verweilzeiten auf ~ 1 Jahr reduziert. Die großen 15 μm Partikel hatten im abiotischen System eine Verweilzeit zwischen 1 und 2,5 Jahren und $<1,6$ Jahre, nachdem die Daphnien hinzugefügt wurden. Diese Ergebnisse heben die

Wichtigkeit der Berücksichtigung der Seeökologie bei der Ermittlung der Verweilzeiten von Mikroplastik hervor.

Die Ergebnisse der vier Studien zeigen, wie komplex der Transport von Mikroplastik in Seesystemen ist, da viele zusammenhängende physikalische, biologische und hydrodynamische Prozesse am Transportprozess in der Wassersäule des Sees beteiligt sind.

Chapter 1: Introduction

1. Current state of knowledge

1.1 Sources of microplastic

Innovations in the plastic industry have led to novel and low-cost synthetic polymers that are incorporated into all industrial and commercial applications. As of 2015, global plastic production has grown to ~322 million metric tons per year (Worm et al., 2017) and is likely to increase in the future. The majority of this plastic production is typically designed for single use, particularly as packaging (Geyer et al., 2017). After use, the plastic should be recycled, and reenter the production stream. However, life cycle studies estimated that a small portion of the plastic produced was recycled, while the majority of the produced plastic that was turned into waste was either incinerated or accumulated in landfills and the environment (Figure 1) (Geyer et al., 2017; Worm et al., 2017). This plastic waste is able to migrate through different environmental compartments carried by wind, erosion, and surface runoff (D’Avignon et al., 2022). During the transport of plastic debris in the environment, it is exposed to various physical, chemical, and biological degradation processes (Meides et al., 2021). The fragmentation and degradation processes in natural environments transform the large plastic debris (> 5 mm) into ‘secondary’ microplastic (100 nm to 5 mm) and /or nanoplastics (< 100 nm). While secondary microplastic results from the breakdown of macroplastic, primary microplastics are pellets designed for commercial purposes such as cosmetics. Surprisingly, a significant share of plastic debris found in the environment belongs to the microplastic fraction (Barnes et al., 2009; D’Avignon et al., 2022).

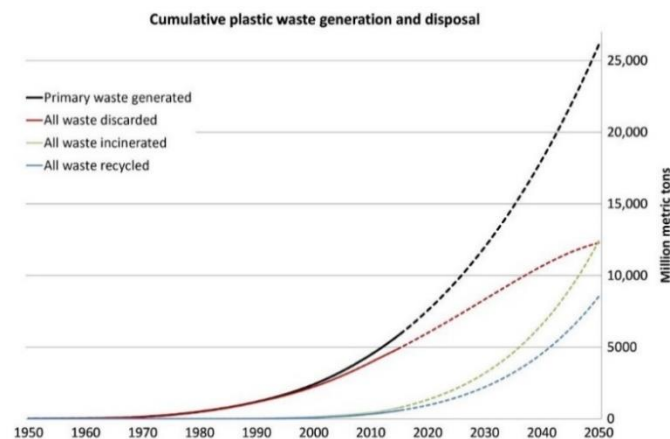


Figure 1: Cumulative plastic waste generation and disposal (in million metric tons). Solid lines show historical data from 1950 to 2015; dashed lines show projections of historical trends to 2050 (Geyer et al., 2017).

1.2 Microplastic in lake systems

Lakes are often used for drinking water, food supplies, recreational purposes, traffic, and active flood protection. They also play a vital role as a habitat for a wide range of organisms and are characterized by complex food webs which are related to biological, chemical, and hydrodynamic conditions in lake systems (Scherer et al., 2017). Microplastic pollution in lake systems originates predominantly from terrestrial sources such as effluents from sewage treatment plants (Sun et al., 2019), surface runoff (Wang et al., 2022), agriculture (Bigalke et al., 2022), and improper disposal of plastic waste. Due to the low-energy hydrodynamic regimes of lakes compared to that in river systems, lakes are considered permanent sinks for microplastic when microplastic is buried into lake sediment, or temporary sinks when the settled particles resuspend into the lake water column (D'Avignon et al., 2022). Once microplastic enters lake systems, it can reside for significant periods in the lake water column before it either reaches lake sediment or before being flushed out through outlets. This is attributed to the fact that microplastic particles are small in size ($< 5\text{mm}$), irregular in shape, and usually have polymer density close to that of lake water, allowing them to have a considerably low settling velocity and reside for substantial periods in the lake water column (months or even years) (Elagami et al., 2022). During microplastic residence time in the lake water column, it is exposed to a very wide range of lake organisms at various trophic levels (D'Avignon et al., 2022). Long residence times of pristine microplastic, especially in the complex food web in the epilimnion during thermal stratification increase the probability of uptake through filter feeders such as daphnia (Aljaibachi and Callaghan, 2018). This uptake probability by filter feeders is expected to be significant during the clear water phase when these organisms filter substantial portions of particulate organic carbon out of the lake epilimnion (Effler et al., 2015). Also, recent studies have shown that filter feeders are not able to distinguish between their food and microplastic (Aljaibachi and Callaghan, 2018). Once microplastic has entered the food chain, it can migrate to higher trophic levels either through direct or indirect ingestion by predators (D'Avignon et al., 2022; Nelms et al., 2018).

1.3 Factors controlling microplastic behavior in lakes

The current understanding is that the settling velocity and the residence times of microplastic in lake systems are controlled by several key factors such as particle properties (Waldschläger and Schüttrumpf, 2019), interaction with biofilm-building organisms as well as the formation of aggregates (Leiser et al., 2020; Rummel et al., 2017), interaction between microplastic and lake organisms such as daphnia and fish (D'Avignon et al., 2022; Cole et al., 2016;), and lake

hydrodynamics (Elagami et al., 2022). The following section discusses in detail the key factors affecting the transport and behavior of microplastic in lake systems that are investigated in this work, and how this affects the residence times of microplastic in lake systems.

1.3.1. Physical properties of pristine microplastic particles

Various studies have shown that the physical properties of pristine microplastic control the settling velocities of the particles and thus their residence times in the lake water column (Elagami et al., 2022; Leiser et al., 2020; Waldschläger and Schüttrumpf, 2019). Polymer density and particle size were identified as the most significant factors controlling the settling velocities of microplastic (Ahmadi et al., 2022; Waldschläger and Schüttrumpf, 2019). Also, microplastic particles are usually irregularly shaped and have large surface areas compared to that of perfect spheres. This leads to an increase in the hydrodynamical friction exerted on the sinking particle and thus an increase in the residence times of microplastic compared to that of spherical particles (Ahmadi et al., 2022). In addition, recent studies have shown that the hydrophobic nature of pristine microplastic increases the potential attachment of fine air bubbles existing in the water column to the surface of microplastic, increasing the buoyancy and residence time of the settling particles (Renner et al., 2020).

1.3.2 Lake hydrodynamics

During thermal stratification in summer, the residence times of the particles in the epilimnion and hypolimnion (e.g. microplastic, sediment particles, or dead zooplankton) are expected to be significantly longer than that in the laminar metalimnion (Elagami et al., 2022; Reynolds and Wiseman, 1982). This is attributed to the presence of turbulent mixing which is mainly caused by wind (Singh et al., 2019) in the epilimnion and by seiches in the hypolimnion caused (Kirillin et al., 2012). Turbulent mixing in the epilimnion and hypolimnion likely causes entrainment of the settling particles and increases their residence time in these zones (Reynolds and Wiseman, 1982). In the metalimnion, however, the residence times of the settling particles depend on the laminar settling velocity of the particles and the thickness of the layer. During lake turnover in autumn, the residence time of microplastic is likely to be significantly shorter than that during thermal stratification. This is due to the instability in the lake water column which leads to the onset of lake convection (Cannon et al., 2021). Also, the variations in water temperature within the lake water column are associated with changes in the density and the viscosity of water. This changes the drag forces exerted on the settling microplastic particles and influences their settling velocities and residence time (Ahmadi et al., 2022).

1.3.3 Biofilms

The hydrophobic nature of pristine microplastic favors biofilm formation (Lacerda et al., 2019; Rummel et al., 2017; Zettler et al., 2013). Various studies showed that the accumulation of biofilms on the surface of pristine microplastic can potentially alter the density of the particles and their settling velocities (Michels et al., 2018; Rummel et al., 2017). Other studies found non-significant differences between pristine and incubated particles (Elagami et al., 2022; Leiser et al., 2020). Recent studies have also shown that incubated microplastic particles tend to form aggregates as the extra polymeric substances (EPS matrix) act likely as an adhesive and favor the formation of aggregates (Elagami et al., 2022; Rummel et al., 2017). The settling velocities of the aggregates are expected to be higher than that of individual incubated particles (Michels et al., 2018). However, more research has to be done to investigate the biofouling process of microplastic, since this process varies between lakes depending on several factors such as water temperature that affects the metabolism of the biofilm-building organisms (Farhat et al., 2016).

1.3.4 Interaction between microplastic and lake organisms and natural particles

Filter feeders are very important for the nutrient cycle in lake systems (Sánchez et al., 2016) as they play a vital role in food webs, controlling primary production, and nutrient cycling (Bastviken et al., 1998; Stein et al., 1995). Using daphnia as an example of lake organisms, they do not selectively filter nutrients from the water column (Aljaibachi and Callaghan, 2018). During the clear water phase, when population densities of daphnia in the lake water column reach their maximum, most of the water in the epilimnion pass through these organisms (Effler et al., 2015). Once microplastic has been ingested, it can migrate to higher trophic levels through direct or indirect ingestion by predators (D'Avignon et al., 2022; Nelms et al., 2018). Ingested microplastic particles are also egested within the faecal pellets (Cole et al., 2016). Since fecal pellets are a source of food for organisms, the ingestion of microplastic-containing pellets of daphnia facilitates the transport of microplastic to higher trophic levels (Nelms et al., 2018), and subsequently, microplastic end up in large faecal material and sink faster than daphnia pellets (Pérez-Guevara et al., 2021). Also, some additional processes such as aggregation of microplastic with natural lake particles can significantly increase their settling velocity and lead to the rapid removal of microplastic from the lake water column, transporting microplastic to lake sediment. Recent studies have demonstrated that microplastic has been found in lake sediment in significant numbers, reaching the same magnitudes as those in the most contaminated marine sediments (D'Avignon et al., 2022).

2. Aims of this work

Despite decades of plastic pollution research in the marine environment (Bagaev and Chubarenko, 2017; Murawski et al., 2022), it is still in its infancy in limnic environments (Figure 2). The majority of the existing research dealing with microplastic transport in lakes was based on investigating the behavior of pristine and biofouled microplastic under controlled laboratory settings (Leiser et al., 2020; Waldschläger and Schüttrumpf, 2019). This resulted in a lack of understanding of the behavior of microplastic in a real lake water column. The primary aims of this work are to (i) develop a quantitative understanding of the primary factors influencing microplastic transport in the lake water column such as lake hydrodynamics, particle physical properties, and biofouling (ii) understand how this may influence the exposure of organisms to this emerging pollutant, and (iii) evaluate the biological pathway of microplastic through their uptake by filter feeders and how this affects their residence time in the lake water column.

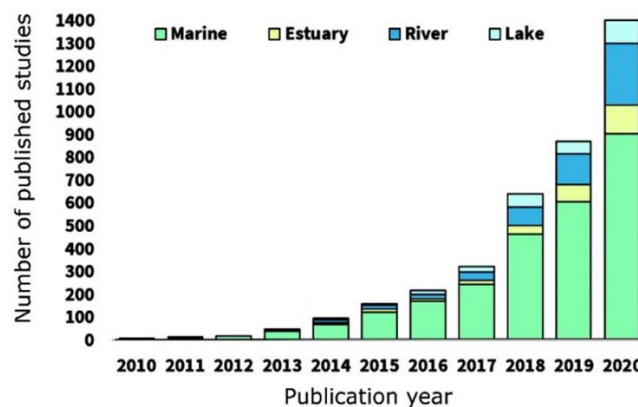


Figure 2: Number of studies on microplastic pollution for various waterbody types (D'Avignon et al., 2022).

Here we combined laboratory experiments, lake incubations, and lake models with computational fluid dynamics. Then, we performed microplastic addition experiments in an in-lake mesocosm during thermal stratification in summer and lake turnover in autumn and compared the results with results from a random walk model to quantitatively analyze the processes governing microplastic transport in lakes. Finally, we performed virtual experiments to quantify the residence times of small microplastic in a purely physical system controlled by sinking and mixing and compared this to a system where daphnia packages microplastic into faecal pellets. We expect that the residence times of microplastic in the lake water column are largely controlled by (i) density, size, shape, water temperature, and the hydrophobic adhesion of microplastic with fine air bubbles existing in the lake water column, (ii) biofilm accumulation on the surfaces of the particles, (iii) the hydrodynamic conditions existing in the lake water column, and (iv) packaging of the small particles in the faecal pellets of zooplankton.

3. Materials and methods

This research is divided into two main packages. The first package includes two studies (study 1 and study 2). Study 1 focuses on laboratory experiments and model calculations, while study 2 focuses on CFD modeling of the settling velocity based on the results from study 1. The second package also includes two studies (study 3 and study 4). Study 3 focuses on field experiments in an in-lake mesocosm and random walk calculations, while study 4 focuses on modelling the interaction of microplastic particles with daphnia. Here, a brief description of the material and methods, as well as the main objectives and structure of each study are presented.

3.1 Microplastic particles

In studies 1 and 2, a wide range of microplastic particles of various types, sizes, and shapes were used. The selected polymers captured the most dominant plastics used in the industry. The irregular microplastic particles used in studies 1 and 2 were produced by the Department of Macromolecular Chemistry at the University of Bayreuth, Germany from bio- and non-biodegradable polymers with an equivalent diameter ranging between 150 and 2200 μm (Table 1). The spherical polystyrene microplastic particles were supplied by Cospheric LLC with sizes of 1, 10, 500, and 1000 μm . Study 2 has also used virtual particles with different shapes and geometries in the CFD simulations.

Table 1: A list of all polymers used in studies 1 and 2, and their measured densities.

Polymer	Abbreviation	Density [g/cm ³]	Type
Polystyrene	PS	1.03	Non-biodegradable
Polyamide 66	PA66	1.12	Non-biodegradable
Polyvinylchloride	PVC	1.38	Non-biodegradable
Polycaprolactone	PCL	1.14	Biodegradable
Poly lactide	PLLA	1.20	Biodegradable
Polybutylenadipate terephthalate	PBAT	1.22	Biodegradable

For study 3, all microspheres were supplied by Cospheric LLC in green fluorescent dry powder (Table 2). The fluorescent dye had maximum excitation and emission wave lengths of 514 and 414 nm respectively. The particles used in this study were either polyethylene (size range between 28-48 and 53-63 μm) or particles from a propriety polymer with an unknown chemical structure (1-5 μm). Aqueous microplastic solutions with concentrations of 1.0 g l⁻¹ were

prepared in the laboratory prior to each experiment. Due to the hydrophobic nature of Cospheric particles, the stock solutions were prepared using distilled water and mixed with 0.1 g of surfactant (Tween 20) per 100 ml of water.

Table2: A list of polymer names, particle sizes, densities, and amount of the microplastic microspheres used in the mesocosm experiments.

Polymer	Density (g cm⁻³)	Amount (g)	Diameter (µm)	Time of experiment
Polyethylene	1.10	20	53-63	Summer 2021
Polyethylene	1.10	20	28-48	Summer 2021
Unknown (Proprietary Polymer)	1.30	5	1-5	Summer 2022
Unknown (Proprietary Polymer)	1.30	5	1-5	Autumn 2021

In study 4, wet ground 17.7 µm PS fragments (PS158N/L; INEOS Styrolution Group GmbH, Germany) and red 3 µm PS spheres (Polybead, Polysciences, Inc.; USA) were used in the feeding experiments of *Daphnia magna*. Additionally, spray dried fluorescent labelled (rhodamine B) 10.4 µm PS particles were used to analyze the degree of microplastic incorporation into the faeces. In the modelling, virtual PS particles with a density of 1.05 g/cm³ with particle diameters of 0.5, 5, and 15 µm were used.

3.2 Laboratory measurements and lake model (study 1)

Study 1 focuses on investigating the effect of particle properties, biofilm, and turbulent mixing on the transport behavior and residence time of microplastic particles. The physical properties of pristine microplastic particles such as particle size, density, and shape were measured prior to each experiment in the laboratory. The shape and size of the particles were estimated from their two-dimensional images captured by a light microscope and high-definition digital single-lens reflex camera. The laminar settling velocities of the particles were measured in an 18 cm x 18 cm x 1.1 m glass column filled with filtered lake water using a two-dimensional particle imaging velocimetry system (PIV) ILA 5150 (Figure 3). The measured settling velocities were then compared to the values calculated using the semi-empirical equation of Dietrich (1982). To quantify the effect of particle size and lake hydrodynamics on the residence time of microplastic particles in a stratified lake water column, the measured settling velocities of the 1, 10, 500, and 1000 µm spherical PS particles were added to a 3-box model to simulate the residence times in the epilimnion, metalimnion, and hypolimnion of a hypothetical stratified lake broadly based on Upper Lake Constance, Germany. Finally, the pristine (irregular)

particles were incubated in a pond at the University of Bayreuth in Germany for up to 30 weeks. The potential changes in microplastic properties and settling velocity of the incubated particles were measured in the laboratory. The structure of the biofilm and the potential formation of aggregates were characterized using confocal laser scanning microscopy (CLSM).

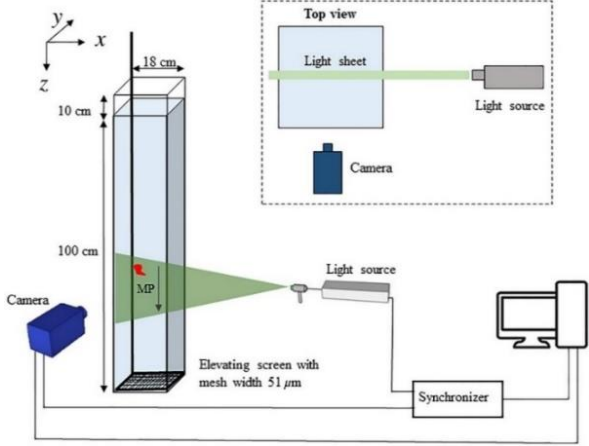


Figure 3: The water column and the setup of the two-dimensional particle image velocimetry system.

3.3 CFD simulations (study 2)

Study 2 aims at quantifying and evaluating the effects of key parameters such as particle size, polymer density, particle shape, and water temperature on the terminal settling velocity of the particles and comparing this to the settling velocity measurements from study 1 as well as to calculations using Dietrich (1982) and Waldschläger and Schüttrumpf (2019). The CFD model was validated using the results from the laboratory experiments in study 1. The terminal settling velocity was simulated using the solver overInterDyMFoam out of the open source C++ toolbox OpenFOAM v1812 (Weller et al., 1998). The shape of the selected particles was meshed using the SALOME 9.4 (IEEE Computer Society, 2007). The CFD simulations were run at ambient conditions for a laminar flow regime. The simulations were carried out until the particle reached terminal velocity. A schematic of the used setup in all the simulations is shown in Figure 4.

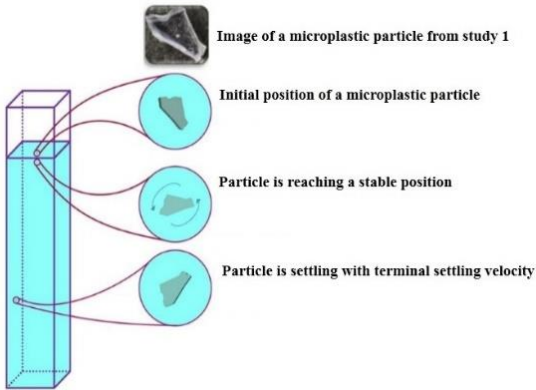


Figure 4: Schematic of the used setup in all the simulations

3.4 Mesocosm experiments and random walk modeling (study 3)

Study 3 aims at understanding and quantifying the effect of lake hydrodynamics and microplastic size on the distribution, concentration, and residence times of microplastic in the lake water column by performing settling velocity experiments in an in-lake mesocosm located at Brombachsee in the German state of Bavaria (Figure 5). The Großer Brombachsee is a 5.1 km long and ~ 2.0 km wide water reservoir with a maximum depth of ~ 32.5 m covering an area of ~8.50 km². The thermal stratification period extends from May until the end of October. Lake turnover typically begins in November. The mesocosm experiments were conducted over an extent of one year, capturing the changes in lake hydrodynamics associated with lake turnover in autumn and thermal stratifications in summer. The microplastic solutions were added to the mesocosm simultaneously by two people using metal watering cans fitted with wide sprinklers. The microplastic concentrations were measured in a 12 m deep and 3m diameter mesocosm (Aquatic Research Instruments, USA) using submersible field fluorometers from Albillia GGUN-FL24. The residence times of the particles were calculated from the measured microplastic concentrations in the mesocosm. The residence time in each compartment was defined as the time elapsed until 95% of the particles are lost from that compartment. The turbulence kinetic energy and eddy diffusivity were calculated from the water velocities inside the mesocosm captured by a three-dimensional acoustic doppler velocimeter (ADV, Nortek vector 300). Water temperatures inside and outside the mesocosm were measured using Hobo TidbiT temperature loggers at 1 m intervals to infer the stability and stratification of the water column. The mesocosm experiments were then followed by modelling of microplastic distributions and residence times in the mesocosm using a 1D random walk model. The model was run using three characteristic settling velocities. Firstly, Stokes equation was used to calculate the settling velocities of the small 1-5 μm particles. Secondly, the settling velocities of particles outside Stokes range (28-48 and 53-63 μm) were measured experimentally under laminar conditions using the PIV system in study 1. The measured velocities were then corrected to the water temperature of each lake compartment in the mesocosm. Finally, effective settling velocities for all microplastic sizes were calculated using the experimental data from the mesocosm.

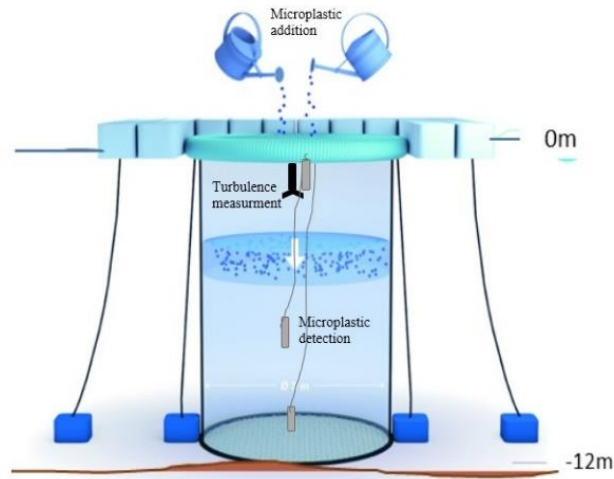


Figure 5: A sketch of the mesocosm setup at Großer Brombachsee

3.5 Modelling of microplastic interaction with lake organisms (study 4)

Study 4 aims at elucidating how lake size, daphnia population dynamics, ingestion of microplastic by daphnia, and egestion as part of their faeces influence the settling velocities and residence times of microplastic in the water column. Here we combined laboratory and virtual experiments to quantify microplastic residence times in a purely physical system controlled by sinking and mixing and compare this to a system where daphnia package microplastic into their faecal pellets which increases the settling velocity (Figure 6). The settling velocity measurement of the microplastic embedded faeces was measured in the laboratory in a 3 cm x 3 cm x 12 cm glass chamber using the same PIV system in study 1. The virtual experiments were conducted using Simulink toolbox MATLAB. This model is an extension of the lake model used in study 1. The simulations were parameterized using data from Lake Constance, Germany, and Esthwaite Water, UK as well as from existing literature and our own laboratory experiments.

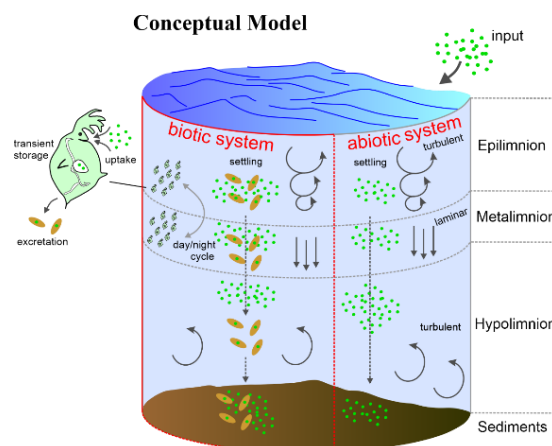


Figure 6: Conceptual model of the primary processes affecting microplastic transport and residence times in a stratified lake as implemented in the model.

4. Summary of findings and discussion

4.1 Measurement of microplastic settling velocities and implications for residence time in thermally stratified lakes (study 1).

<https://doi.org/10.1002/lno.12046>

In this work, we combine laboratory measurements of settling velocities under laminar conditions, theoretical calculations of settling velocities, and lake incubations with modeling of microplastic residence time in a stratified lake water column. We investigated the effects of particle size, polymer density, hydrophobicity of the particle surface, biofouling, and turbulent mixing on the residence times of microplastic in the lake water column. This aimed at understanding the transport, behavior, and accumulation of microplastic in the lake water column.

The experimental investigation of microplastic behavior showed that the settling velocity and residence time of the microplastics are mainly controlled by particle size and particle density. The settling velocities for the irregular particles ranged between ~ 0.30 and $\sim 50 \text{ mm s}^{-1}$. It was however difficult to quantify the effect of particle shape on the settling velocity as it was experimentally hard to isolate the effect of particle shape from that of size and density. This problem was exacerbated by the fact that all microplastic particles were similar in shape (irregular) and no fibers or special geometries such as cubes, discs, or cylinders were used in this work.

The settling velocities of the pristine microplastic particles seemed to be affected by the hydrophobic adhesion of the particles with the fine air bubbles inside the water column. This is expected to significantly increase the residence time of the settling pristine particles in the lake water column due to the increase in their buoyancy. Therefore, the calculated settling velocities using Dietrich (1982) were systematically higher than that from the experiments, especially for the biodegradable particles (Figure 7), as such processes are not considered in the conventional sediment transport model of Dietrich (1982).

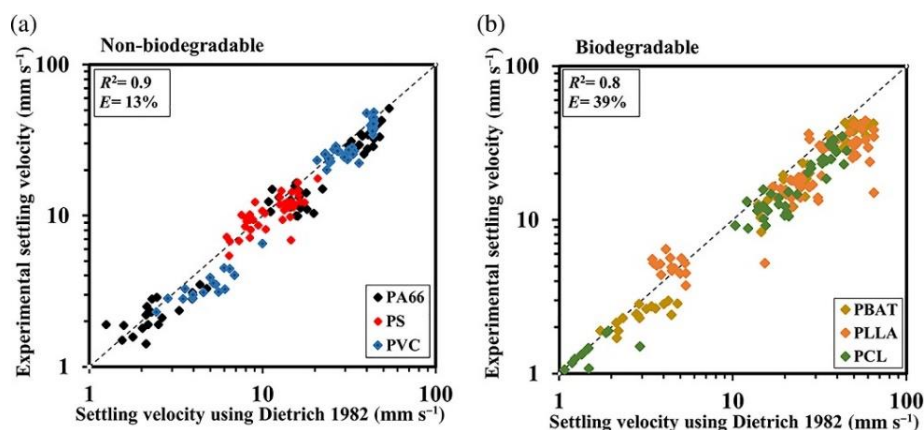


Figure 7: A comparison between the experimental settling velocities and Dietrich model, where E is the relative error (%), and R^2 (–) is the coefficient of determination. The dashed line presents the 1:1 line.

The lake incubations showed no substantial changes in the shapes, sizes, and densities of the incubated particles even after 30 weeks of incubation. The biofilm was formed in patches rather than coating the whole particle surface with biofilm. These patches did not cause any significant changes in the physical properties and settling velocities of the particles compared to pristine particles even after 30 weeks of incubation. This could be attributed to the “short” incubation periods of 6, 8, 10, and 30 weeks. The pond was also frozen for the first 3 weeks of incubation during the winter season which may explain the small volumes of biofilm. However, the presence of the extra polymeric substances induced the formation of aggregates (Figure 8). The settling velocities of the aggregates are expected to be higher than that of the individual particles.

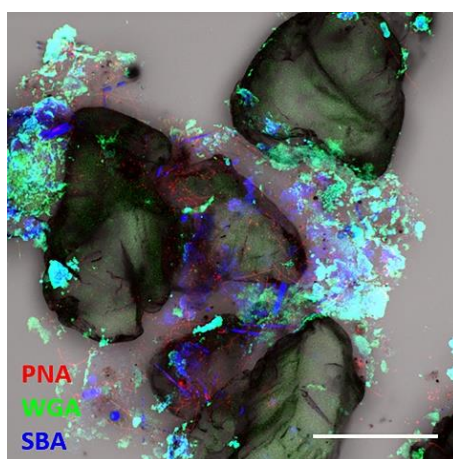


Figure 8: Confocal laser scanning microscope image of the aggregation of polystyrene particles after 10 weeks of incubation. Peanut agglutinin (PNA), wheat germ agglutinin (WGA), and soybean agglutinin (SBA) lectins visualize the EPS matrix in a red, green, and blue overlay. The length of the scale bar is 150 μm .

The residence times in the lake compartments during thermal stratification simulated with the 3-box model suggested that particle size has a significant effect on the residence time of the microplastic particles. For instance, the residence times of the 1 and 1000 μm particles in the

100 m lake water column were in order of 10^5 and 10^{-1} days respectively. The effect of lake hydrodynamics on the residence times of the microplastic was also noticeable. The residence time of the microplastic in the metalimnion is relatively short compared to the epilimnion and hypolimnion due to the lack of mixing processes as well as its limited thickness. The extremely long residence time for the small microplastic particles in the lake water column suggests that these particles should not be found in the sediment unless some other processes such as aggregation, packaging of microplastic into faecal pellets, or biofouling increase their settling velocity.

4.2 Systematic evaluation of physical parameters affecting the terminal settling velocity of microplastic particles in lakes using CFD (study 2).

<https://doi.org/10.3389/fenvs.2022.875220>

In this study, we systematically evaluated the effect of various factors, such as particle density, size, shape, and hydrophobicity, as well as water temperature on the terminal settling velocity. We conducted 683 individual CFD simulations of settling velocity. We then compared the simulation results to two semi-empirical equations as well as to the laboratory settling experiments in study 1. This aimed at understanding the behaviour of microplastic in lake systems and how this can control their exposure time to lake organisms.

The CFD results provided an improved evaluation of the relative effects of the different key factors controlling the residence time of microplastic in the lake water column. In accordance with study 1, the CFD model presented that particle size (volume) and particle density are the most important factors controlling the settling velocities of the particles under laminar conditions. Other factors such as particle shape and water temperature have less effect on the settling velocity of microplastics under laminar conditions than that of density and size. By doubling the density of a given particle size, the settling velocity was increased by ~ 380 and 480% for irregular and regular particles respectively. Increases up to ~ 95 and 225% could be obtained by doubling the volume of irregular and regular particles respectively. This could be attributed to the fact that increasing the density of a given particle increases the mass and thus the gravitational forces while it has no effect on the particle's volume and surface area, which would in turn change buoyancy and drag. The effects of temperature changes on the settling velocity of microplastic indicated that typical temperature differences between the compartments of a stratified lake in a temperate climate would lead to differences up to ~ 46% in the settling velocities. The changes in particle roundness only affected the settling velocity

of particles larger than 1 mm in diameter, while the smallest particles (0.5 mm diameter) were unaffected (Figure 9).

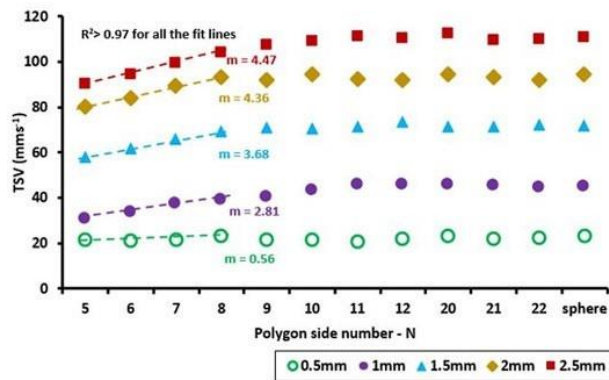


Figure 9: Effects of increasing roundness on TSV of MP particles for five different particle sizes.

Although the initial and boundary conditions of the CFD model were defined according to the real experimental setup, the CFD results still overestimated the settling velocities from the laboratory experiments. This was also the same case for the settling velocity results calculated using Dietrich (1982). This is probably due to the hydrophobic nature of microplastic that was not incorporated into both models (Figure 10).

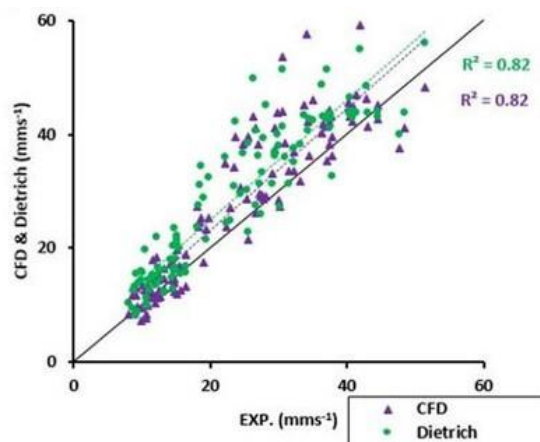


Figure 10: A comparison between CFD, laboratory results (EXP), and calculations using Dietrich (1982), where the red line represents the 1:1 line.

4.3 Quantifying microplastic residence times in lakes using mesocosm experiments and transport modelling (study 3)

In this work, we conducted a series of microplastic addition experiments to an in-lake mesocosm deployed at Großer Brombachsee using various microplastic sizes during lake stratification in summer and turnover in autumn and combined this with random walk modeling. This aimed at quantitatively analyzing the processes governing microplastic transport in the lake water column such as lake hydrodynamics as well as particle sizes. The experiments were

conducted over one year using three size ranges of fluorescent microspheres (1-5, 28-48, and 53-63 μm), capturing stratified and unstable conditions within the mesocosm.

The mesocosm experiments showed that changes in the lake hydrodynamics driven by seasonal temperature changes have a significant effect on the residence times of the microplastic particles in the lake water column. During thermal stratification in summer, the temperature gradient, and thus the strong density gradient during lake stratification, formed a very stable water column inside the mesocosm. In contrast, during lake turnover in autumn, the water column inside the mesocosm was unstable. This likely led to the onset of natural convective mixing in the lake water column, transporting the plastics to the bottom of the mesocosm much faster than that during summer. The convective mixing was supported by the high values of Rayleigh number ($>10^9$). Hence, the residence time of the smallest particles (1-5 μm) during lake turnover in autumn in the mesocosm was ~ 13 times shorter than during thermal stratification in summer. The mesocosm experiments also proved that particle size is an important factor controlling the residence time and thus the exposure time of microplastic in the lake water column. During summer, the residence time of the 28-48 μm particles was ~ 2.7 times longer than that for the 53-63 μm particles.

The simulated residence times during thermal stratification in summer using a random walk model were longer than the real residence times in the mesocosm, especially for the simulations using settling velocity results calculated using Stokes equation. For instance, the simulated residence times in the mesocosm using Stokes velocities for the 1-5 μm particles during summer were ~ 10 times longer than the actual residence times in the mesocosm. This could be attributed to the effect of microplastic-particle interaction (i.e. formation of aggregates) in the mesocosm caused by the large surface area and the surface charge of the 1-5 μm particles. Such aggregates are large and likely to have higher settling velocities compared to the individual pristine microplastic particles used in Stokes model. In contrast, the simulated residence times of the 1-5 μm particles using the effective settling velocity values during summer (32 days) were close to the actual residence times in the mesocosm during thermal stratification (24 days) (Figure 11). This is due to the fact that the effective settling velocity was derived directly from the mesocosm data. As such the effective settling velocity implicitly incorporates processes influencing settling velocities in the mesocosm such as particle-microplastic interactions and hydrodynamic conditions. The simulated residence times using PIV velocities for the large 28-48 and 53-63 μm particles were comparable to the actual residence times in the mesocosm during summer with a difference of ~ 1.4 and 1.9 times. This is likely to be attributed to the relatively lower surface area of the large particles which subsequently reduces the potential

particle-microplastic interactions and formation of aggregates. Finally, during lake turnover in autumn, the modelled residence times of the 1-5 μm particles were considerably longer than the actual residence times in the mesocosm. The simulation results using Stokes and effective settling velocities were ~ 113 and 8.5 times longer than the actual residence times respectively. This could be attributed to the complexity of the lake hydrodynamics during natural convection, which cannot be represented by the simplified lake physics present in the random walk model.

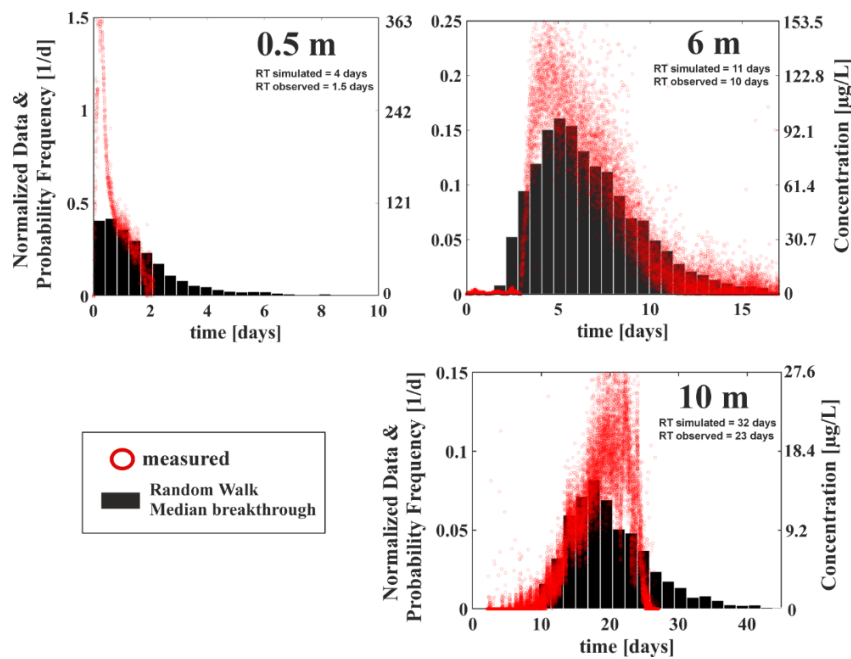


Figure 11: Simulated and measured particle breakthroughs at 0.5, 6 and 10m depth. Shown are the residence time distribution(RT) for the 1-5 μm particles in the summer experiment using the random walk model in combination with effective settling velocity.

The residence times calculated from the mesocosm experiments are considered more realistic than residence times calculated based on previous modeling and laboratory experiments existing in the literature. However, the conditions in the mesocosm are still likely to be quite different from real lakes. This could be due to various factors such as the boundary effect of the mesocosm walls, the limited area of the mesocosm ($\sim 7 \text{ m}^2$), and the isolation of the water inside the mesocosm from the rest of the lakes. This is expected to limit the size of turbulent eddies that can develop in the water column and the influence of other hydrodynamics.

4.4 Filter feeders are key to residence times of small microplastic particles in stratified lakes: a virtual experiment (study 4)

In this work, we used laboratory and virtual experiments to quantify the residence times of 0.5, 5, and 15 μm PS particles in a purely physical system controlled by sinking and mixing and compare this to a system where daphnia package microplastic into faecal pellets. The

simulations were parametrized using data from Lake Constance, Germany, and Esthwaite Water, UK as well as from existing literature and our own laboratory experiments.

The simulation results showed the importance of microplastic uptake for the residence time. Without the biological pathway, the residence times for both 0.5 and 5 μm microplastic particles in the water column of Lake Constance (>15 years) were significantly longer than the retention time of Lake Constance (4 years). This was similar for the Esthwaite Water as the residence times of the particles were ~ 60 (for the 0.5 μm) and 8 (for the 5 μm) times longer than the retention time of the lake (13 weeks). This suggests that these small pristine particles will transport through the lake water column and should not be found in lake sediment unless some other processes will happen such as aggregation, or biofouling. However, the residence times of the 15 μm particles were much shorter than the flushing time for Lake Constance and Esthwaite Water. This suggests that these 'large' particles could be found in the sediment layer of both lakes and especially in the shallow water column of Esthwaite Water.

After adding daphnia to the model, more than 90% of the particles reached the lake sediment in less than 1 year regardless of lake size and particle size. However, the significance of the biological pathway is controlled by the number of daphnia present in the epilimnion. For instance, during winter when daphnia numbers are insignificant, microplastic numbers increased to their maximum levels, while microplastic numbers were significantly reduced during the clear water phase as most of the water in the epilimnion passes through the model organisms. These results indicate the significance of microplastic packaging into the faecal pellets of lake organisms and how this will affect the residence time of small particles as the majority of small microplastic can cycle through organisms before reaching the sediment.

5. Conclusion and outlook

5.1 Conclusion

In order to comprehensively understand the transport and behavior of microplastic in lake systems, we investigated the key factors controlling the residence times of microplastic in the lake water column. This is essential as residence time is related to the exposure time of microplastic to lake organisms. By combining the results from the laboratory experiments and lake model (study 1) and CFD modeling (study 2) with the mesocosm experiments and random walk model (study 3) and virtual experiments (study 4) we can draw the following conclusions:

- The residence time of microplastic particles can vary over a very wide range of different time scales depending on key factors such as particle density and size, which can affect the residence time significantly. Other factors such as particle shape and roundness as well as water temperature had less effect on the settling velocity and the residence time than that of density and size.
- The hydrophobic nature of pristine microplastic can lead to rapid colonization of microplastic by biofilm. This means that pristine microplastics are unlikely to be found in natural aquatic environments as they are usually rapidly colonized by biofilms or adsorb natural material such as dissolved organic carbon or mineral precipitates. Also, the biofilm structure can be formed in dense patches rather than a uniform layer of biofilm. However, the formation of the EPS matrix can increase the tendency for microplastic aggregation as it likely works as an adhesive. Such aggregates are expected to sink faster than individual particles.
- Although the initial and boundary conditions of the CFD model were defined according to the real experimental setup, the CFD results still overestimated the settling velocities from the laboratory experiments. This was the same case for the settling velocity calculations using Dietrich (1982) and Waldschläger and Schüttrumpf (2019). These results show that the hydrophobic surface properties of the pristine microplastic should be considered in future modeling.
- Lake hydrodynamics play an important role in microplastic residence time in the lake water column. The turbulent mixing in the epilimnion during thermal stratification in summer likely causes resuspension of the settling particles and increases their residence

times compared to that in the laminar metalimnion. During lake turnover in autumn, the residence time of the settling particles can be significantly shorter than that during thermal stratification. This is attributed to instability in the lake water column which leads to the onset of natural convection resulting in a rapid sinking of microplastic particles.

- The modeled residence time of small pristine microplastic particles during thermal stratification can exceed the retention times of the lake. This suggests that these particles should not be found in the sediment layer unless some other processes increase their settling velocity. In the real lake water column, however, significant changes in particle properties caused by several factors such as biofouling, formation of aggregates, hydrophobic adhesion of microplastic with fine air bubbles, or interaction with lake organisms can occur during their residence time in the lake water column. This shows that microplastic behavior in lake systems is more complex than the simplified calculations of lake physics used in the models.
- The ingestion of microplastic by filter feeders and their egestion within the faecal pellets has shown to be significant when investigating microplastic behavior in lake systems. The residence times of the microplastic particles embedded in faecal pellets were orders of magnitude shorter than that of pristine particles. This causes a rapid removal of microplastic from the lake water column. This however is controlled by the number of organisms and the size of the particles.

5.2 Research outlook

Although we have presented in this dissertation a comprehensive investigation of microplastic behavior in lake systems through laboratory experiments, field experiments, lake models, and CFD modelling, there are remaining points that should be covered by future studies.

Firstly, in our laboratory experiments, we mainly used irregular particles with similar shapes. This resulted in a knowledge gap about the effect of particle roundness and shape on the settling velocities and how this controls the residence times of microplastic. Hence, future research should consider other geometries such as cylinders, cubes, and fibers and investigate how this affects the behavior of microplastic in the lake systems.

Secondly, the incubation periods of microplastic in the pond were relatively short. In nature, microplastic can be exposed for significant periods to the biofilm-building organisms during

their residence times in the lake water column which can change the properties of the particles, affecting their residence times in the lake water column. Also, the effect of season and incubation depth should be investigated to understand how these factors can affect the behavior of microplastic in lake system.

Thirdly, the lake models expected very significant residence times of the small particles compared to that measured in the mesocosm. These models, however, are highly simplified and theoretical representations of residence times. Real lake systems are considerably more complex than these simplified representations of lake physics. In future modelling, factors such as the potential aggregation of microplastic with existing lake particles should be considered. Also, the effect of the complex hydrodynamic conditions during lake turnover should be inspected.

Finally, the hydrodynamic conditions in the mesocosm are still likely to be quite different from a real lake. We suspect that the biological and chemical conditions inside the mesocosm were different from that in the surrounding lake. Also, there were some limitations caused by the field instruments. For instance, the microplastic concentrations and residence times were calculated depending on the signals detected by the fluorometers, with the best case being measurements at three depths. This resulted in a lack of knowledge about the behavior of the microplastic particles over the extent of the entire water column. In addition, we only used pristine spherical microplastic in the mesocosm experiment and did not use irregular shapes, fibers, or incubated particles. Therefore, future experiments investigating microplastic transporting lake systems should be conducted using a wide range of plastics and complex setups that are capable of representing microplastic transport in real lake systems.

6. References

- Ahmadi, P., Elagami, H., Dichgans, F., Schmidt, C., Gilfedder, B.S., Frei, S., Peiffer, S., Fleckenstein, J.H., 2022. Systematic Evaluation of Physical Parameters Affecting the Terminal Settling Velocity of Microplastic Particles in Lakes Using CFD. *Front. Environ. Sci.* 10.
- Aljaibachi, R., Callaghan, A., 2018. Impact of polystyrene microplastics on *Daphnia magna* mortality and reproduction in relation to food availability. *PeerJ* 6, e4601.
- Bagaev, A., Chubarenko, I., 2017. microplastics, numerical modelling, the Baltic Sea, anthropogenic pollution, in: Proceedings of International Conference "Managing risks to coastal regions and communities in a changing world" (EMEC'S'11 - SeaCoasts XXVI). Managing risks to coastal regions and communities in a changing world, Saint-Petersburg. Academus Publishing, p. 1.
- Bailly-Comte, V., Durepaire, X., Batiot-Guilhe, C., Schnegg, P.-A., 2018. In situ monitoring of tracer tests: how to distinguish tracer recovery from natural background. *Hydrogeol J* 26 (6), 2057–2069.
- Barnes, D.K.A., Galgani, F., Thompson, R.C., Barlaz, M., 2009. Accumulation and fragmentation of plastic debris in global environments. *Philosophical transactions of the Royal Society of London. Series B, Biological sciences* 364 (1526), 1985–1998.
- Bastviken, D.T.E., Caraco, N.F., Cole, J.J., 1998. Experimental measurements of zebra mussel (*Dreissena polymorpha*) impacts on phytoplankton community composition. *Freshwater Biology* 39 (2), 375–386.
- Bigalke, M., Fieber, M., Foetisch, A., Reynes, J., Tollan, P., 2022. Microplastics in agricultural drainage water: A link between terrestrial and aquatic microplastic pollution. *The Science of the total environment* 806 (Pt 4), 150709.
- Boos, J.-P., Gilfedder, B.S., Frei, S., 2021. Tracking Microplastics Across the Streambed Interface: Using Laser-Induced-Fluorescence to Quantitatively Analyze Microplastic Transport in an Experimental Flume. *Water Resources Research* 57 (12).
- Browne, M.A., Galloway, T., Thompson, R., 2007. Microplastic--an emerging contaminant of potential concern? *Integrated environmental assessment and management* 3 (4), 559–561.
- Cai, Y., Li, C., Zhao, Y., 2021. A Review of the Migration and Transformation of Microplastics in Inland Water Systems. *International journal of environmental research and public health* 19 (1).
- Canniff, P.M., Hoang, T.C., 2018. Microplastic ingestion by *Daphnia magna* and its enhancement on algal growth. *The Science of the total environment* 633, 500–507.

- Cannon, D.J., Troy, C., Bootsma, H., Liao, Q., MacLellan-Hurd, R.-A., 2021. Characterizing the Seasonal Variability of Hypolimnetic Mixing in a Large, Deep Lake. *JGR Oceans* 126 (11).
- Cole, M., Lindeque, P.K., Fileman, E., Clark, J., Lewis, C., Halsband, C., Galloway, T.S., 2016. Microplastics Alter the Properties and Sinking Rates of Zooplankton Faecal Pellets. *Environmental science & technology* 50 (6), 3239–3246.
- Cowan, E., Booth, A.M., Misund, A., Klun, K., Rotter, A., Tiller, R., 2021. Single-Use Plastic Bans: Exploring Stakeholder Perspectives on Best Practices for Reducing Plastic Pollution. *Environments* 8 (8), 81.
- D'Avignon, G., Gregory-Eaves, I., Ricciardi, A., 2022. Microplastics in lakes and rivers: an issue of emerging significance to limnology. *Environ. Rev.* 30 (2), 228–244.
- Dietrich, W.E., 1982. Settling velocity of natural particles. *Water Resources Research* 18 (6), 1615–1626.
- Effler, S.W., Spada, M.E., Gelda, R.K., Peng, F., Matthews, D.A., Kearns, C.M., Hairston, J.N.G., 2015. Daphnia grazing, the clear water phase, and implications of minerogenic particles in Onondaga Lake. *IW* 5 (4), 317–330.
- Elagami, H., Ahmadi, P., Fleckenstein, J.H., Frei, S., Obst, M., Agarwal, S., Gilfedder, B.S., 2022. Measurement of microplastic settling velocities and implications for residence times in thermally stratified lakes. *Limnology & Oceanography* 67 (4), 934–945.
- Farhat, N.M., Vrouwenvelder, J.S., van Loosdrecht, M.C.M., Bucs, S.S., Staal, M., 2016. Effect of water temperature on biofouling development in reverse osmosis membrane systems. *Water research* 103, 149–159.
- Geyer, R., Jambeck, J.R., Law, K.L., 2017. Production, use, and fate of all plastics ever made. *Science advances* 3 (7), e1700782.
- Ghawi, A.H., Kris, J., 2012a. A Computational Fluid Dynamics Model of Flow and Settling in Sedimentation Tanks, in: Woo Oh, H. (Ed.), *Applied Computational Fluid Dynamics*. IntechOpen, Erscheinungsort nicht ermittelbar.
- Ghawi, A.H., Kris, J., 2012b. A Computational Fluid Dynamics Model of Flow and Settling in Sedimentation Tanks, in: Oh, H.W. (Ed.), *Computational Fluid Dynamics (CFD) and Discrete Element Method (DEM) Applied to Centrifuges*. INTECH Open Access Publisher.
- Holtappels, M., Lorke, A., 2011. Estimating turbulent diffusion in a benthic boundary layer. *Limnol. Oceanogr. Methods* 9 (1), 29–41.

- Huret, M., Runge, J.A., Chen, C., Cowles, G., Xu, Q., Pringle, J.M., 2007. Dispersal modeling of fish early life stages: sensitivity with application to Atlantic cod in the western Gulf of Maine. *Mar. Ecol. Prog. Ser.* 347, 261–274.
- IEEE Computer Society, 2007. 31st Annual International Computer Software and Applications Conference, 2007: COMPSAC 2007 ; 24 - 27 July 2007, Beijing, China ; proceedings. IEEE Computer Society, Los Alamitos, Calif.
- Khatmullina, L., Isachenko, I., 2017. Settling velocity of microplastic particles of regular shapes. *Marine pollution bulletin* 114 (2), 871–880.
- Kirillin, G., Grossart, H.-P., Tang, K.W., 2012. Modeling sinking rate of zooplankton carcasses: Effects of stratification and mixing. *Limnology & Oceanography* 57 (3), 881–894.
- Kreft, A., Zuber, A., 1978. On the physical meaning of the dispersion equation and its solutions for different initial and boundary conditions. *Chemical Engineering Science* 33 (11), 1471–1480.
- Lacerda, A.L.D.F., Rodrigues, L.D.S., van Sebille, E., Rodrigues, F.L., Ribeiro, L., Secchi, E.R., Kessler, F., Proietti, M.C., 2019. Plastics in sea surface waters around the Antarctic Peninsula. *Scientific reports* 9 (1), 3977.
- Lavoie, J., Boulay, A.-M., Bulle, C., 2021. Aquatic micro- and nano-plastics in life cycle assessment: Development of an effect factor for the quantification of their physical impact on biota. *J of Industrial Ecology*.
- Lebreton, L., Andrady, A., 2019. Future scenarios of global plastic waste generation and disposal. *Palgrave Commun* 5 (1).
- Leiser, R., Wu, G.-M., Neu, T.R., Wendt-Potthoff, K., 2020. Biofouling, metal sorption and aggregation are related to sinking of microplastics in a stratified reservoir. *Water research* 176, 115748.
- Małozzewski, P., Zuber, A., 1982. Determining the turnover time of groundwater systems with the aid of environmental tracers. *Journal of Hydrology* 57 (3-4), 207–231.
- Meides, N., Menzel, T., Poetschner, B., Löder, M.G.J., Mansfeld, U., Strohriegel, P., Altstaedt, V., Senker, J., 2021. Reconstructing the Environmental Degradation of Polystyrene by Accelerated Weathering. *Environmental science & technology* 55 (12), 7930–7938.
- Michels, J., Stippkugel, A., Lenz, M., Wirtz, K., Engel, A., 2018. Rapid aggregation of biofilm-covered microplastics with marine biogenic particles. *Proceedings. Biological sciences* 285 (1885).
- Murawski, J., She, J., Frishfelds, V., 2022. Modeling drift and fate of microplastics in the Baltic Sea. *Front. Mar. Sci.* 9.

- Nelms, S.E., Galloway, T.S., Godley, B.J., Jarvis, D.S., Lindeque, P.K., 2018. Investigating microplastic trophic transfer in marine top predators. *Environmental pollution (Barking, Essex : 1987)* 238, 999–1007.
- Pérez-Guevara, F., Roy, P.D., Kuttralam-Muniasamy, G., Shruti, V.C., 2021. A central role for fecal matter in the transport of microplastics: An updated analysis of new findings and persisting questions. *Journal of Hazardous Materials Advances* 4, 100021.
- Reid, W.H., Harris, D.L., 1958. Some Further Results on the Bénard Problem. *Phys. Fluids* 1 (2), 102.
- Renner, G., Nellessen, A., Schwieters, A., Wenzel, M., Schmidt, T.C., Schram, J., 2020. Hydrophobicity-water/air-based enrichment cell for microplastics analysis within environmental samples: A proof of concept. *MethodsX* 7, 100732.
- Reynolds, C.S., Wiseman, S.W., 1982. Sinking losses of phytoplankton in closed limnetic systems. *J Plankton Res* 4 (3), 489–522.
- Ross, O.N., 2006. Particles in motion: How turbulence affects plankton sedimentation from an oceanic mixed layer. *Geophys. Res. Lett.* 33 (10), n/a-n/a.
- Rowe, M.D., Anderson, E.J., Wynne, T.T., Stumpf, R.P., Fanslow, D.L., Kijanka, K., Vanderploeg, H.A., Strickler, J.R., Davis, T.W., 2016. Vertical distribution of buoyant *Microcystis* blooms in a Lagrangian particle tracking model for short-term forecasts in Lake Erie. *JGR Oceans* 121 (7), 5296–5314.
- Rummel, C.D., Jahnke, A., Gorokhova, E., Kühnel, D., Schmitt-Jansen, M., 2017. Impacts of Biofilm Formation on the Fate and Potential Effects of Microplastic in the Aquatic Environment. *Environ. Sci. Technol. Lett.* 4 (7), 258–267.
- Sánchez, M.I., Paredes, I., Lebouvier, M., Green, A.J., 2016. Functional Role of Native and Invasive Filter-Feeders, and the Effect of Parasites: Learning from Hypersaline Ecosystems. *PloS one* 11 (8), e0161478.
- SAPEA, 2019. A scientific perspective on microplastics in nature and society. Evidence review report no. 4. SAPEA, Berlin.
- Scherer, C., Brennholt, N., Reifferscheid, G., Wagner, M., 2017. Feeding type and development drive the ingestion of microplastics by freshwater invertebrates. *Scientific reports* 7 (1), 17006.
- Singh, P., Bagrania, J., Haritash, A.K., 2019. Seasonal behaviour of thermal stratification and trophic status in a sub-tropical Palustrine water body. *Appl Water Sci* 9 (5).

- Stein, R.A., DeVries, D.R., Dettmers, J.M., 1995. Food-web regulation by a planktivore: exploring the generality of the trophic cascade hypothesis. *Can. J. Fish. Aquat. Sci.* 52 (11), 2518–2526.
- Sun, J., Dai, X., Wang, Q., van Loosdrecht, M.C.M., Ni, B.-J., 2019. Microplastics in wastewater treatment plants: Detection, occurrence and removal. *Water research* 152, 21–37.
- Visser, A.W., 1997. Using random walk models to simulate the vertical distribution of particles in a turbulent water column. *Mar. Ecol. Prog. Ser.* 158, 275–281.
- Waldschläger, K., Schüttrumpf, H., 2019. Effects of Particle Properties on the Settling and Rise Velocities of Microplastics in Freshwater under Laboratory Conditions. *Environmental science & technology* 53 (4), 1958–1966.
- Wang, C., O'Connor, D., Wang, L., Wu, W.-M., Luo, J., Hou, D., 2022. Microplastics in urban runoff: Global occurrence and fate. *Water research*, 119129.
- Weeraratne, D., Manga, M., 1998. Transitions in the style of mantle convection at high Rayleigh numbers. *Earth and Planetary Science Letters* 160 (3-4), 563–568.
- Weller, H.G., Tabor, G., Jasak, H., Fureby, C., 1998. A tensorial approach to computational continuum mechanics using object-oriented techniques. *Comput. Phys.* 12 (6), 620.
- Woods, J.S., Verones, F., Jolliet, O., Vázquez-Rowe, I., Boulay, A.-M., 2021. A framework for the assessment of marine litter impacts in life cycle impact assessment. *Ecological Indicators* 129, 107918.
- Worm, B., Lotze, H.K., Jubinville, I., Wilcox, C., Jambeck, J., 2017. Plastic as a Persistent Marine Pollutant. *Annu. Rev. Environ. Resour.* 42 (1), 1–26.
- Wüest, A., Lorke, A., 2003. SMALL-SCALE HYDRODYNAMICS IN LAKES. *Annu. Rev. Fluid Mech.* 35 (1), 373–412.
- Wüest, A., Lorke, A., 2009. Small-Scale Turbulence and Mixing: Energy Fluxes in Stratified Lakes, in: *Encyclopedia of Inland Waters*. Elsevier, pp. 628–635.
- Yan, M., Wang, L., Dai, Y., Sun, H., Liu, C., 2021. Behavior of Microplastics in Inland Waters: Aggregation, Settlement, and Transport. *Bulletin of environmental contamination and toxicology* 107 (4), 700–709.
- Zettler, E.R., Mincer, T.J., Amaral-Zettler, L.A., 2013. Life in the "plastisphere": microbial communities on plastic marine debris. *Environmental science & technology* 47 (13), 7137–7146.

7. Contribution statement

Study 1: Measurement of microplastic settling velocities and implications for residence time in thermally stratified lakes.

Authors: **Hassan Elagami**, Pouyan Ahmadi, Jan H. Fleckenstein, Sven Frei, Martin Obst, Seema Agarwal, Benjamin S. Gilfedder.

Status: Published in *Association for the Science of Limnology and Oceanography*, Volume 67, Issue 4 April 2022 Pages 934-945. <https://doi.org/10.1002/lno.12046>

Own contribution: concept and study design 70%, data acquisition 80%, data analyses and figures 80%, modelling 40%, discussion of results 70%, manuscript writing 80%

Author contribution: HE performed the laboratory experiments, whole lake modeling, data interpretation, and worked on the manuscript. PA and JHF assisted in data interpretation and writing the manuscript. SF developed the whole lake model, conducted the simulations, and contributed to writing the manuscript. MO performed the confocal laser scanning microscopy and assisted with analysis and interpretation of the biofilm data. SA provided the microplastics, and assisted in data interpretation from the settling column, especially relating to the surface chemistry of plastic polymers. BSG conceived the project, and assisted in data interpretation and writing and editing the manuscript.

Study 2: Systematic evaluation of physical parameters affecting the terminal settling velocity of microplastic particles in lakes using CFD

Authors: Pouyan Ahmadi, **Hassan Elagami**, Franz Dichgans, Christian Schmidt, Benjamin S. Gilfedder, Sven Frei, Stefan Peiffer, Jan H. Fleckenstein

Status: Published in *Frontiers in Environmental Science*, Volume 10, 2022. <https://doi.org/10.3389/fenvs.2022.87522>

Own contribution: concept and study design 50%, data acquisition 50%, data analyses and figures 30%, discussion of results 50%, manuscript writing 30%.

Author contribution: PA set up the CFD modeling framework, conducted the CFD simulations, designing the additional experiments, data interpretation and writing the manuscript. HE performed the laboratory experiments, assisted in data interpretation and writing the manuscript. FD contributed to the initial set-up of the CFD modeling framework, to data interpretation and writing of the manuscript. CS assisted in data interpretation and writing the manuscript. BSG assisted in data interpretation and writing the manuscript. SF assisted in data interpretation and writing the manuscript. SP assisted in data interpretation and writing the

manuscript. JHF conceived the project, assisted in data interpretation and contributed to writing and editing of the manuscript.

Study 3: Quantifying microplastic residence times in lakes using mesocosm experiments and transport modelling

Authors: **Hassan Elagami**, Sven Frei, Jan-Pascal Boos, Gabriele Trommer, Benjamin S. Gilfedder.

Status: Submitted to *Water Research* on 22nd Aug. 2022

Own contribution: concept and study design 80%, data acquisition 80%, data analyses and figures 80%, modeling 20%, discussion of results 80%, manuscript writing 80%

Author contribution: HE built the mesocosm setup, performed all experiments, worked on data analysis and interpretation, and wrote the manuscript. SF built the mesocosm, helped with conducting the experiments, assisted in data interpretation, built the random walk model, did all simulations, and worked on writing and editing the manuscript. JPB assisted in data interpretation and worked on writing and editing the manuscript. GT assisted with planning the experiments and provided lake monitoring data and logistics. BSG conceived the project, built the mesocosm, helped with conducting the experiments, assisted in data interpretation, and worked on writing and editing the manuscript.

Study 4: Filter feeders are key to residence times of small microplastic particles in stratified lakes: a virtual experiment

Authors: Benjamin-Silas Gilfedder, **Hassan Elagami**, Jan-Pascal Boos, Julian Brehm, Mathias Schott, Lorenz Witt, Christian Laforsch, Sven Frei

Status: Submitted to *Association for the Science of Limnology and Oceanography* on 12th Sep. 2022.

Own contribution: concept and study design 10%, data acquisition 5%, data analyses and figures 5%, modeling 5%, discussion of results 10%, manuscript writing 5%

Author contribution: BSG was responsible for the paper concept, writing the paper, and data analysis. HE was responsible for data assimilation from existing literature and paper revision and discussion of results. JPB conducted the PIV measurements to quantify the settling velocities of *Daphnia* faeces and editing of the paper. JB, MS, and LW designed, conducted and analysed the data from the *Daphnia* faeces settling experiments, while CL supervised these experiments and assisted with the data analysis. SF designed and conducted all of the modelling, helped with the interpretation of the data and assisted in writing the paper.

Chapter 2: Publications

Study 1: Measurement of microplastic settling velocities and implications for residence times in thermally stratified lakes

Hassan Elagami, Pouyan Ahmadi, Jan H. Fleckenstein, Sven Frei, Martin Obst, Seema Agarwal, Benjamin S. Gilfedder

Published in *Association for the Science of Limnology and Oceanography*, Volume 67, Issue 4 April 2022 Pages 934-945. <https://doi.org/10.1002/lno.12046>

Measurement of microplastic settling velocities and implications for residence times in thermally stratified lakes

Hassan Elagami^{1,2*}, Pouyan Ahmadi,³ Jan H. Fleckenstein,^{3,4} Sven Frei,² Martin Obst,⁵ Seema Agarwal,⁶ Benjamin S. Gilfedder^{1,2}

¹Limnological Research Station, Bayreuth Center of Ecology and Environmental Research, University of Bayreuth, Bayreuth, Germany

²Department of Hydrology, Bayreuth Center of Ecology and Environmental Research (BayCEER), University of Bayreuth, Bayreuth, Germany

³Department of Hydrogeology, Helmholtz Centre for Environmental Research – UFZ, Leipzig, Germany

⁴Hydrologic Modelling Unit, Bayreuth Center of Ecology and Environmental Research (BayCEER), University of Bayreuth, Bayreuth, Germany

⁵Experimental Biogeochemistry, BayCEER, University of Bayreuth, Bayreuth, Germany

⁶Macromolecular Chemistry II, University of Bayreuth, Bayreuth, Germany

Abstract

Microplastics residence times in lakes are currently poorly understood. In this work, settling experiments with pristine and biofilm-colonized microplastic particles were combined with model calculations to evaluate settling velocities, particle distributions, and residence times in the epilimnion, metalimnion, and hypolimnion of a hypothetical stratified lake broadly based on Upper Lake Constance. Settling velocities of various biodegradable and nonbiodegradable polymers of various shapes, sizes, and biofilm colonization were measured in a settling column. The settling velocities ranged between ~ 0.30 and $\sim 50 \text{ mm s}^{-1}$. Particle sizes and polymer densities were identified as primary controls on settling rates. Microplastic particles that had been exposed to a lake environment for up to 30 weeks were colonized by a range of biofilms and associated extracellular polymeric substances; surprisingly, however, the settling velocity did not vary significantly between pristine and colonized microplastic particles. Simulated microplastic residence times in the model lake varied over a wide range of time scales (10^{-1} to 10^5 d) and depended mainly on the size of the particles and depth of the lake layer. Long residence times on the order of 10^5 d (for $1\text{-}\mu\text{m}$ microplastic particles) imply that for small microplastic particles there is a high probability that they will be taken up at some stage by lake organisms. As the lake retention time (~ 4.5 years) is considerably shorter than the residence time of small microplastics, negligible quantities of these microplastic particles should be found in the lake sediment unless some other process increases their settling velocity.

*Correspondence: hassan.elagami@uni-bayreuth.de

This is an open access article under the terms of the Creative Commons Attribution License, which permits use, distribution and reproduction in any medium, provided the original work is properly cited.

Additional Supporting Information may be found in the online version of this article.

Author Contribution Statement: H.E. performed the laboratory experiments, whole lake modeling and worked on the manuscript. P.A. and J.H.F. assisted in data interpretation and writing the manuscript. S.F. developed the whole lake model, conducted the simulations, and contributed to writing the manuscript. M.O. performed the confocal laser scanning microscopy and assisted with analysis and interpretation of the biofilm data. S.A. provided the microplastics, and assisted in data interpretation from the settling column, especially relating to the surface chemistry of plastic polymers. B.S.G. conceived the project, and assisted in data interpretation and writing and editing the manuscript.

Over the past 70 years, plastic polymers have established themselves as cost-effective and durable materials that are used ubiquitously in industry, agriculture, and domestic applications. In 2015, global annual production of plastic polymers reached ~ 322 Mt (Worm et al. 2017). Roughly 50% of the plastic volume produced is made for single-use applications, and in particular for packaging purposes (Worm et al. 2017). By 2015, ~ 6300 Mt of plastic waste had been produced, of which approximately 9% was recycled, while 79% accumulated in landfills and the environment (Geyer et al. 2017). The majority of the plastic debris found in nature are high molar mass polymers such as polyethylene and polyethylene terephthalate (Agarwal 2020).

Rivers and streams are considered the dominant transport pathway moving plastic from terrestrial sources to the marine

sink (Fischer et al. 2016). In contrast to fluvial systems, lakes and reservoirs are mostly considered as permanent or temporary sinks for plastics due to their low-energy hydrodynamic regimes. Plastics in lakes and rivers originate predominantly from terrestrial sources such as effluents from waste-water treatment plants (Sun et al. 2019), agriculture, and improper dumping of plastic waste (Bellasi et al. 2020). During the transport of plastic in freshwater systems, it is exposed to various physical, chemical, and biological degradation processes (Browne et al. 2007; Meides et al. 2021). Fragmentation and degradation processes in natural environments transform plastic fragments larger than 5 mm into microplastics < 5 mm (Arthur et al. 2009) and nanoplastics (Toussaint et al. 2019).

As the density of pristine nonbuoyant plastic polymers lies close to that of water, microplastics are expected to remain in suspension for a substantial time before sedimentation to lake sediments. Long residence times in the water column increases the probability of uptake by organisms such as zooplankton (Nguyen et al. 2020) as such organisms cannot differentiate between microplastics and natural particulate matter used as food (Aljaibachi and Callaghan 2018).

Once microplastics have entered the food chain, organisms including zooplankton and fish uptake microplastics through ingestion via predation (Nelms et al. 2018). After microplastics have been ingested, they can also be egested within fecal pellets (Cole et al. 2016). As fecal pellets are a source of food for many aquatic organisms, the ingestion of these microplastic-containing pellets facilitates the transfer of microplastics to various trophic levels (Nelms et al. 2018). Fecal pellets may also form a pathway for microplastic sedimentation, removing them from the lake water column (Cole et al. 2016), although this remains poorly understood.

Existing studies have proposed that the physical properties of microplastics such as polymer density, shape, and size control the settling velocity of pristine microplastics (Khatmullina and Isachenko 2017; Waldschläger and Schüttrumpf 2019) and the residence time in the water column (Nguyen et al. 2020). Since most of microplastics in aquatic systems are irregularly shaped, they tend to have a larger surface area compared to spherical particles. The high surface area of the irregular particles leads to increased hydrodynamical friction and drag forces, resulting in lower settling velocities compared to ideal spheres (Dietrich 1982).

Pristine microplastics are also exposed to various types of biofilm-building microorganisms over time scales that are largely dependent on residence times of the particles in the water column and polymer properties (Zettler et al. 2013; Leiser et al. 2020; Ramsperger et al. 2020). Also, the hydrophobic nature of pristine microplastics favors biofilm formation (Zettler et al. 2013; Rummel et al. 2017; Lacerda et al. 2019). Accumulation of biofilms and attachment of microorganisms on the surfaces of pristine microplastics can potentially alter their density (Rummel et al. 2017; Michels et al. 2018) and thus their settling velocities (Kaiser et al. 2017). While some

studies have suggested that the development of biofilms on microplastic surfaces increases the settling velocity (Kaiser et al. 2017), other recent studies have found no substantial changes in the settling rates (Leiser et al. 2020). However, there is still very little known about how the physical, biological, and chemical conditions in lakes (which are very different from oceans) affect the formation of biofilm on microplastics and how this affects their settling behavior (Leiser et al. 2020). For example, biofilms may make the surface of colonized particles “stickier,” facilitating the formation of aggregates with other suspended materials such as mineral sediments or organic matter (Rummel et al. 2017).

The temperature gradient in the stratified lake water column is associated with changes in the density and the viscosity of water. As a consequence, drag forces exerted on particles increase from the relatively warm epilimnion (lower viscosity) to the cold hypolimnion (higher viscosity). Microplastic transport is also influenced by turbulence occurring in the epilimnion, which is mainly driven by wind (Singh et al. 2019), and in the hypolimnion caused by internal hydrodynamic forces such as seiches, currents, and bed roughness (Kirillin et al. 2012; Nishri et al. 2015). Compared to laminar conditions in the metalimnion, turbulent mixing in the epilimnion and hypolimnion likely causes resuspension of the settling particles and increases their residence time in these zones (Reynolds 2006, pp. 70–71). Due to the largely laminar conditions in the metalimnion, the residence time of microplastics only depends on the settling velocity of the particle and the thickness of the layer.

In this work, we combine systematic laboratory experiments, lake incubations, and model calculations to understand the effect of microplastic properties on sedimentation behavior. We then estimate the residence time, accumulation in, and transfer of microplastics between, lake compartments via virtual lake simulations. The residence time is presented as a critical parameter for determining accumulation of microplastics in the water column and potential uptake and transfer within the lake ecosystem. We anticipate that the residence times of pristine microplastics are controlled by the physical properties of the particles, as well as lake properties, such as turbulent mixing and depth.

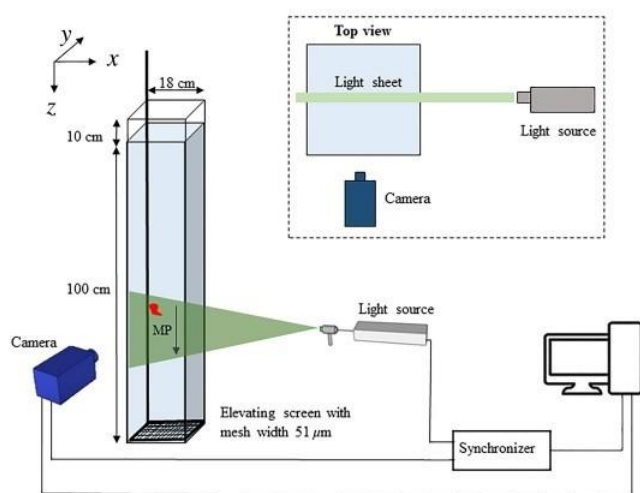
Methods

Characterization of microplastic particles

All biodegradable and nonbiodegradable fragments were provided by the Department of Macromolecular Chemistry at the University of Bayreuth, Germany. The selected polymers (Table 1) capture the dominant plastics produced by the plastic industry (Wright et al. 2013; Rocha-Santos and Duarte 2015). The size of the particles ranged between ~ 150 and ~ 2200 μm . The selection of various particles and polymer types aimed at assessing the effect of particle size, and polymer density on the settling velocity. The distinction between

Table 1. A list of all polymers used during settling velocity experiments and their measured densities.

Polymer	Abbreviation	Density (g cm^{-3})	Type
Polystyrene	PS	1.03	Nonbiodegradable
Polyamide 66	PA66	1.12	Nonbiodegradable
Polyvinylchloride	PVC	1.38	Nonbiodegradable
Polycaprolactone	PCL	1.14	Biodegradable
Poly lactide	PLLA	1.20	Biodegradable
Polybutylenadipate terephthalate	PBAT	1.22	Biodegradable

**Fig. 1.** The water column and the setup of the two-dimensional particle image velocimetry system.

biodegradable and nonbiodegradable polymers was aimed at assessing the potential effect of polymer surface chemistry and polymer type on the settling behavior of microplastic particles in lakes. Also, several recent studies, such as Bagaev et al. (2017) and Waldschläger and Schüttrumpf (2019), focus mainly on non-biodegradable polymers. Our work extends the types of polymers assessed in sinking experiments to a potentially important class of plastics that may become more prevalent in the future as society move toward biodegradable plastics.

Particle geometries were determined in the laboratory using a light microscope and a high definition digital single-lens reflex camera (Zeiss Axioplan microscope and Cannon EOS 5D respectively). The maximum particle length A [L] and the minimum particle length C [L] in the XY -plane of each irregularly shaped particle were measured based on these images using ImageJ software (Schindelin et al. 2012) (Supporting Information Fig. S1). The XZ -plane length B [L] was estimated as the average of A and C as a necessary approximation due to only being able to acquire two-dimensional images with the microscope available. As all particles used in the experiments were irregularly shaped (Supporting Information Fig. S1, S2), the equivalent diameter of each particle was calculated based on the best-fitting ellipsoid. The equivalent spherical diameter for

each particle D_{eq} [L] was then calculated according to Eq. 1 using the value from the ellipsoid. The Corey shape factor (CSF) was also calculated as in Eq. 2. The CSF is widely used to describe the overall shape of the particles and can be calculated as the thickness of the particle divided by the geometric average of the other two dimensions. It ranges from 0 to 1.0 and it is correlated with particle flatness.

$$D_{\text{eq}} = \sqrt[3]{ABC}, \quad (1)$$

$$\text{CSF} = \frac{C}{\sqrt{A.B}}. \quad (2)$$

The density of each nonbuoyant polymer was determined according to the procedure described in Waldschläger and Schüttrumpf (2019): Each particle was placed in a 50-mL glass beaker of distilled water. After the particle had sunk to the bottom, $1 \mu\text{L}$ of zinc chloride solution was added. This procedure was repeated until the particle was in a stable suspension. One milliliter of the solution was then weighed to determine the density of the particle. This process was repeated three times for each polymer using three different particles and the average polymer density was calculated. Some of the particles initially did not sink, despite their densities exceeding that of water. This is thought to be due to the hydrophobic surface chemistry of the pristine plastic. To avoid this, the particles were pretreated for 20 min in an ultrasonic bath. The hydrophobicity effect was particularly noticeable for polystyrene as its polymer density 1.03 g cm^{-3} is very close to that of water.

Settling velocity measurements

Settling velocities of the microplastic particles were measured in a water-filled glass column with a cross-section of $18 \text{ cm} \times 18 \text{ cm}$ and a height of 1.10 m (Fig. 1) based on the design of Khatmullina and Isachenko (2017). At the bottom of the column, a filter mesh (width $51 \mu\text{m}$) was used to collect and retrieve the individual particles after each settling experiment. The glass column was also equipped with two thermometers to measure the water temperature during each experiment. The laboratory was air-conditioned at $20 \pm 1^\circ\text{C}$. Settling velocities were measured using tap water (density = 0.998 g cm^{-3} , kinematic viscosity = $0.01 \text{ cm}^2 \text{ s}^{-1}$, and oxygen content = 9.45 mg L^{-1}).

The settling velocity for each microplastic particle was determined using a two-dimensional particle image velocimetry system iLa 5150. The system consists of a high-speed camera (80 frames per second), a light source (high-power light-emitting diodes) with a wavelength = 530 nm, and hardware for synchronization (Fig. 1). The software can determine the settling velocities in two dimensions using the recorded image stream by cross-correlation of sequential pairs of images. The image pairs were used to analyze the settling path of each particle and the time elapsed. The system was tested for accuracy and precision. A reference particle (polyamide 66) with an equivalent diameter of 1.75 mm was measured seven times under identical conditions. After each measurement, the particle was collected using the mesh. The mean and relative standard deviation (RSD%) was $32 \text{ mm s}^{-1} \pm 7\%$.

Each particle was lowered slowly into the settling column using tweezers and released a few centimeters below the water surface. The settling velocity of each particle was measured after the particle had reached its estimated (Stokes) terminal velocity and a stable orientation in the water column. The particle image velocimetry setup was placed at the lowest third of the settling column. In total, between 60 and 70 settling experiments were conducted for each polymer amounting to a total of about 400 settling experiments.

Lake incubations

To measure the effects of biofilm colonization on microplastic settling behavior, polyamide 66, polystyrene, polyvinylchloride, polycaprolactone, polylactide, and polybutylenadipate terephthalate particles with a size range from 300 to 2200 μm , used previously as part of the settling experiments, were incubated in a pond close to the University of Bayreuth. All incubations started in January and the incubation periods were 6, 8, 10, and 30 weeks. Each particle was incubated in a separate glass tube that was sealed at both ends using stainless steel screens with a mesh size of 51 μm (Supporting Information Fig. S3). This design allowed microorganisms to enter the tubes and to colonize microplastic particles but did not allow the particles to be lost from the tubes. Several polystyrene particles (300 to 350 μm) were incubated in the same tube for 10 weeks to investigate potential particle-particle interactions and how this may be influenced by biofilms. The changes in size, density, and shape of each incubated particle were characterized following the same procedures as described for the pristine particles.

Colonization of microplastic particle surface with biofilm-building microorganisms was characterized by confocal laser scanning microscopy. Colonized microplastic particles were incubated in 100 μL staining solution for 20 min. All dyes and lectin-dye conjugates were used in a concentration of 1 $\mu\text{g ml}^{-1}$. DNA/RNA was stained using Syto 40. The DNA/RNA signal was used to visualize microbial cells whereas lectin-fluorophore conjugates were used to visualize the

extracellular polymeric substances (wheat germ agglutinin—Alexa Fluor 555, soybean agglutinin—Alexa Fluor 488, and peanut agglutinin—Alexa Fluor 647). After incubating the particles in the dyes, the samples were rinsed three times with tap water. Aggregates were analyzed in a Petri dish in their original hydrated condition. The images were collected with $\times 10$ and $\times 20$ water immersion lenses with numerical apertures of 0.3 and 0.6, respectively.

Finally, after incubation, the changes in the settling velocity of each particle were evaluated by comparing the settling velocity between the pristine and incubated particles. The density of the incubated particle was determined after the settling velocity measurements to keep the biofilm in its original state as the zinc chloride solution is likely to destroy the biofilm structure. In addition, the settling column was filled with filtered lake water so that changes in osmotic pressure would not disturb the delicate biofilm structure. The density and the viscosity of the filtered lake water were determined in the laboratory. The physical properties of the filtered lake water were essentially the same as tap water.

Settling velocity model

As most of the particles were irregularly shaped and relatively large ($> 0.1 \text{ mm}$) (Supporting Information Figs. S1, S2), the hydrodynamic flow conditions around the particles were likely to be at Reynolds number > 1.0 . To account for the non-spherical geometry of the particles the semiempirical model of Dietrich (1982) was used to calculate the theoretical settling velocities. Rather than expressing the results in the terms of Reynolds number and drag coefficient, Dietrich (1982) uses the terms of dimensionless particle size and dimensionless settling velocity (Supporting Information Eq. S4a–f). For small particles, Dietrich (1982) converges on Stokes' law (at about a dimensionless particle size less than 2.0). For the "large" particles, the model accounts for the progressive growth in the flow field separation which increases the drag pressure more rapidly for a given increase in the settling velocity. However, Dietrich (1982) notes that the equation should not be used for dimensionless particle size greater than 5×10^9 as the boundary layer around the particles becomes fully turbulent, reducing the flow separation and thus pressure drag. The Reynolds number and dimensionless particle size were checked for each particle to investigate the flow regime around the particles. The settling velocity formulas are presented in the Supporting information (Eq. S4a–f).

Continuum model for microplastic particles in a stratified lake

The residence times and particle number within a hypothetical lake system and the flux between lake compartments (epilimnion, metalimnion, and hypolimnion) were modeled using a generic continuum model for vertical microplastic transport. The model represents a lumped parameter approach

consisting of three interacting model sub-systems representing the epilimnion, metalimnion, and hypolimnion. For the epilimnion and hypolimnion, the model assumes fully mixed (turbulent) conditions represented by exponential transfer functions (i.e., exponential residence time distributions) as first implemented by Reynolds and Wiseman (1982) and Reynolds (1984, pp. 46–50) and summarized by Reynolds (2006, pp. 70–71) and Lampert and Sommer (2010, pp. 48–49). In this approach, rather than representing the hydrodynamic conditions of the different lake compartments explicitly using, for example, an eddy diffusion coefficient and calculating fluxes in one dimension, the effect of turbulent mixing was simplified using the transfer functions so that each sub-system could be treated as zero-dimensional. In reality, this means that the eddy diffusion coefficient is large enough that the system can be treated as well mixed on time-scales relevant for microplastic transport. For the metalimnion, the model assumes laminar flow conditions and settling behavior, where particles have a single residence time. The combination of the three lake compartments gives a set of three differential equations that are solved simultaneously (Eq. 3a–c):

$$\frac{dN_{\text{epi}}}{dt} = N_{\text{in}} - k_{\text{epi}}N_{\text{epi}}(t), \quad (3a)$$

$$\frac{dN_{\text{meta}}}{dt} = k_{\text{epi}}N_{\text{epi}}(t) - k_{\text{epi}}N_{\text{epi}}(t - \tau_{\text{meta}}), \quad (3b)$$

$$\frac{dN_{\text{hypo}}}{dt} = k_{\text{epi}}N_{\text{epi}}(t - \tau_{\text{meta}}) - k_{\text{hypo}}N_{\text{hypo}}(t). \quad (3c)$$

Equation 3a describes the dynamic change of microplastics in the epilimnion, where N_{in} [particles T^{-1}] represents a defined input flux of particles into the lake (e.g., via an inflowing river), $-k_{\text{epi}}N_{\text{epi}}(t)$ [particles T^{-1}] is the loss of particles to the metalimnion, and k_{epi} [T^{-1}] is a first-order exchange coefficient. Equation 3b calculates the microplastic particles in the metalimnion where τ_{meta} [T] is the residence time of the particles. The particle flux from the metalimnion into the hypolimnion is $-k_{\text{epi}}N_{\text{epi}}(t - \tau_{\text{meta}})$ [particles T^{-1}] while Eq. 3c represents the dynamic change of particles in the hypolimnion. The loss of particles from the lake to the sediments is $k_{\text{hypo}}N_{\text{hypo}}(t)$ [particles T^{-1}] where k_{hypo} [T^{-1}] is a first-order exchange coefficient similar to that in the epilimnion. The first-order exchange coefficients k_{epi} and k_{hypo} [T^{-1}] were calculated by $k_{\text{epi,hypo}} = \frac{1}{\tau_{\text{epi,hypo}}}$ with τ [T] being the mean residence time in each respective layer.

In the well-mixed layers, the residence times τ_{epi} [T] and τ_{hypo} [T] were defined as the time required until the particle number was reduced to $1/e \approx 0.368$ (i.e., 36%) of the initial

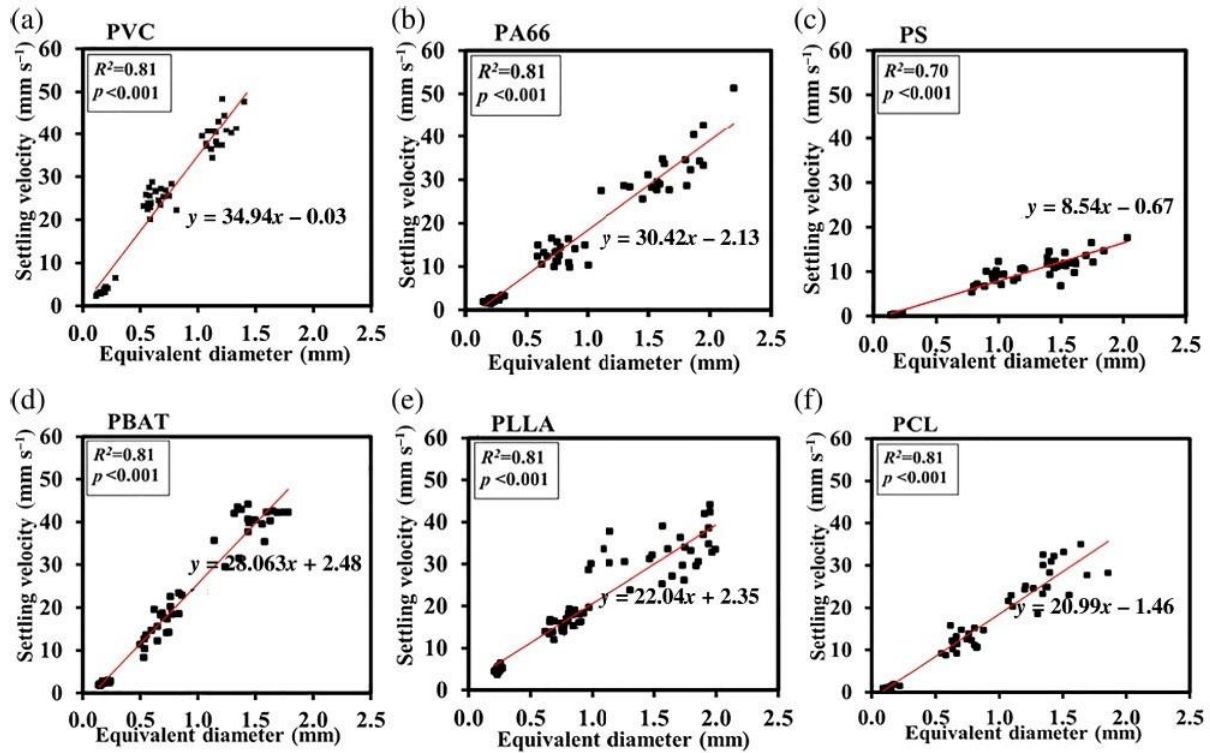


Fig. 2. Results of the experimentally measured settling velocities vs. equivalent diameter of the polyvinylchloride (PVC), polyamide 66 (PA66), polystyrene (PS), polybutylenadipate terephthalate (PBAT), polylactide (PLLA), and polycaprolactone (PCL) fragments, where p is the probability obtained from the t -test, R^2 (–) is the coefficient of determination, and the red line represents the regression line.

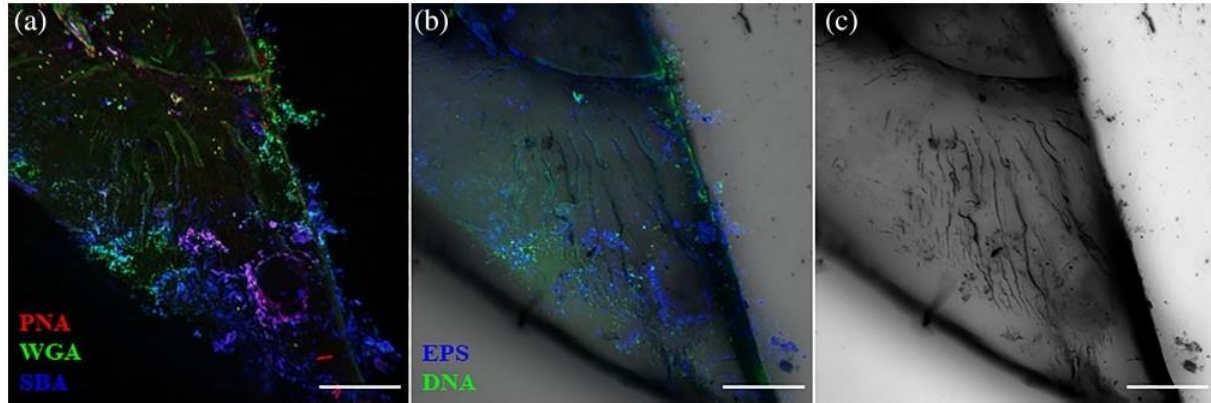


Fig. 3. Confocal laser scanning microscope images for the extracellular polymeric substances (EPS matrix) and microbial cells (DNA) colonizing the surfaces of a polyamide 66 particle after 10 weeks of incubation. **(a)** Peanut agglutinin (PNA), wheat germ agglutinin (WGA), and soybean agglutinin (SBA) lectins visualize the EPS matrix in a red, green, and blue overlay; **(b)** the EPS matrix and DNA are visible on the particle; and **(c)** the surface of the microplastic is shown in gray scale. The length of the scale bar is 150 μm .

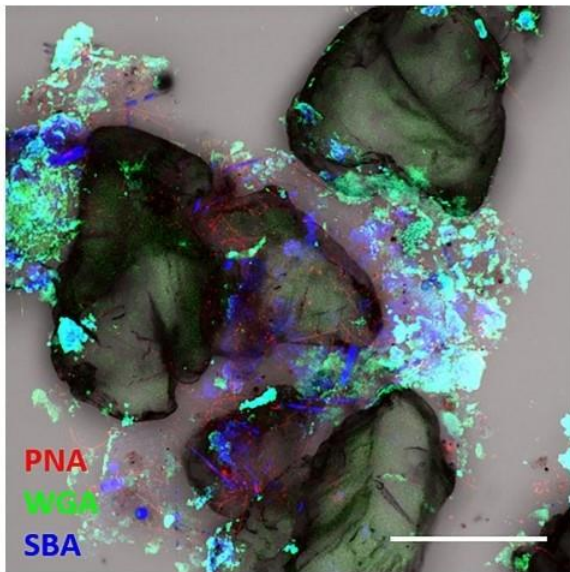


Fig. 4. A confocal laser scanning microscope image of the aggregation of polystyrene particles after 10 weeks of incubation. Peanut agglutinin (PNA), wheat germ agglutinin (WGA), and soybean agglutinin (SBA) lectins visualize the EPS matrix in a red, green, and blue overlay. The length of the scale bar is 150 μm .

particle concentrations (Reynolds 2006, pp. 70–71). The residence time in the metalimnion τ_{meta} [T] was calculated by dividing the thickness z_{meta} [L] of the layer by the laminar settling velocity of the particle. Values for the mean residence time were estimated according to Eq. 4, where v_s [LT^{-1}] represents the laminar settling velocities for microplastics in the relevant lake compartment and z [L] is the corresponding thickness of the epilimnion, metalimnion, or hypolimnion.

$$\tau_{\text{epi,meta,hypo}} = \frac{z_{\text{epi,meta,hypo}}}{v_{s,\text{epi,meta,hypo}}} \quad (4)$$

For simplicity, and to illustrate the effect of microplastic particle size on residence time, the model was run using settling velocity data from polystyrene spheres. The laminar settling velocities of the polystyrene spheres (1, 10, 500, and 1000 μm) were measured using the same procedures mentioned before. To account for the changes in the settling velocities of the microplastics due to the change of the water temperature in each lake compartment, the settling velocities were corrected as in Ghawi and Kris (2012) using their eq. S5. The dynamic model was constructed and solved using the Simulink toolbox included in MATLAB.

In addition to the dynamic model above, a simplified steady-state solution for Eqs. 3a–c assuming a constant particle influx $\dot{N}_{\text{in}} = \text{const}$, was derived for the particle number in each lake compartment:

$$N_{\text{epi}} = \frac{\dot{N}_{\text{in}}}{k_{\text{epi}}} = \dot{N}_{\text{in}} \tau_{\text{epi}}, \quad (5a)$$

$$N_{\text{meta}} = \frac{\dot{N}_{\text{in}}}{k_{\text{epi}}} \left[e^{(k_{\text{epi}} \tau_{\text{meta}})} - 1 \right], \quad (5b)$$

$$N_{\text{hypo}} = \frac{\dot{N}_{\text{in}}}{k_{\text{hypo}}} = \dot{N}_{\text{in}} \tau_{\text{hypo}}. \quad (5c)$$

This steady-state solution was used to quantify the relative distribution of microplastic particles in each lake compartment of thermally stratified lakes. In particular, the ratio between particles located in the epilimnion and hypolimnion ($N_{\text{epi}}/N_{\text{hypo}}$) was used as a characteristic parameter to compare lake systems. This ratio can be used to rapidly determine if most microplastic particles will be found in the epilimnion or the hypolimnion, which is important as the epilimnion is where microplastics are most likely to be taken up by organisms such as filter feeders. In this model, the ratio $N_{\text{epi}}/N_{\text{hypo}}$ only

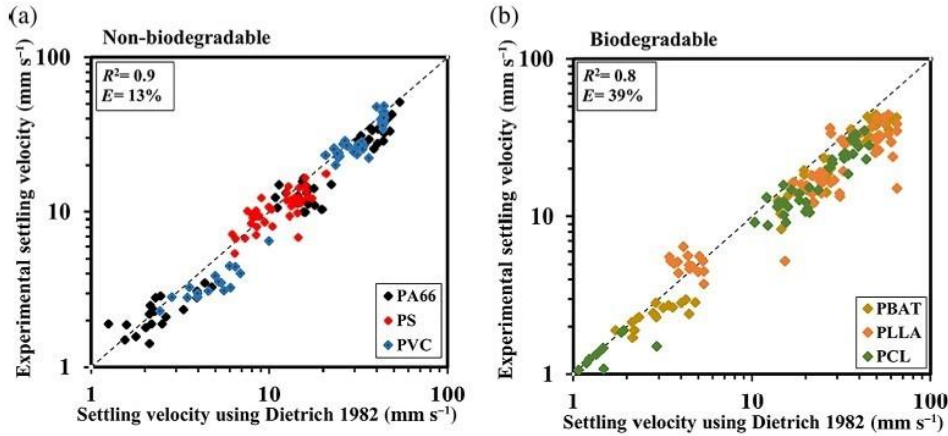


Fig. 5. A comparison between the experimental settling velocities and Dietrich model for the nonbiodegradable polyvinylchloride (PVC), polyamide 66 (PA66), polystyrene (PS), and biodegradable polybutylenadipate terephthalate (PBAT), polylactide (PLLA), and polycaprolactone (PCL) particles, where E is the relative error (%), and R^2 (–) is the coefficient of determination. The dashed line presents the 1 : 1 line.

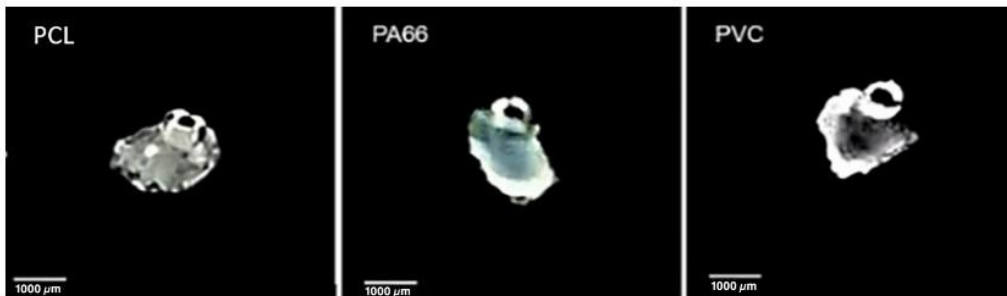


Fig. 6. Attachment of fine air bubbles on the surfaces of polycaprolactone (PCL), polyamide 66 (PA66), and polyvinylchloride (PVC) particles during the settling velocity experiments.

depends on $\tau_{\text{epi}}/\tau_{\text{hypo}}$, which can be expressed as $\frac{v_{s,\text{epi}}}{v_{s,\text{hypo}}} \cdot \frac{Z_{\text{epi}}}{Z_{\text{hypo}}}$. The relationship $N_{\text{epi}}/N_{\text{hypo}} = f(v_{s,\text{epi}}/v_{s,\text{hypo}}, Z_{\text{epi}}/Z_{\text{hypo}})$ is universally valid for all types of microplastics (independent of size, shape, and density) as long as the ratio $v_{s,\text{epi}}/v_{s,\text{hypo}}$ in a lake system is constant. This implies that $N_{\text{epi}}/N_{\text{hypo}}$ only depends on lake characteristics such as the temperature and thickness of each compartment.

Results

Settling velocities of pristine particles

The settling velocities for the six polymers ranged between ~ 0.30 and ~ 50 mm s⁻¹ (Fig. 2). Supporting Information Fig. S6 presents the distribution of the CSF of the microplastic particles. The results show a clear dependence of the settling velocities on particle size, with a coefficient of determination (R^2) between 0.70 and 0.81 and a high statistical significance ($p < 0.001$). In addition, the effect of polymer density on the settling velocity was clearly visible in the slope of the regression lines. Polymers with high density were consistently associated with a steeper slope, and thus a faster settling velocity. The calculated Reynolds number for the particles varied

between 0.05 and 130, thus being at the transition between laminar and the intermediate regimes.

Biofilm-coated particles

No significant changes were observed in the density, shape, or roundness of the incubated particles, even after 30 weeks of incubation (Supporting Information Fig. S7). However, the confocal laser scanning microscope images at 10 weeks incubation clearly showed a varying abundance of biofilms on the microplastic particle surface (Fig. 3). These were mainly composed of microbial cells and extra polymeric substances. The surfaces of the particles were only partially covered with biofilm, where it was concentrated in a few dense spots.

The potential formation of aggregates was investigated by incubating various polystyrene particles with an average equivalent diameter between 300 and 350 μm for 10 weeks in a single tube. The sample shown in Fig. 4 has a high abundance of extra polymeric substances despite the surface of the particles not being densely colonized by microbial cells. It also shows that individual polystyrene particles in combination

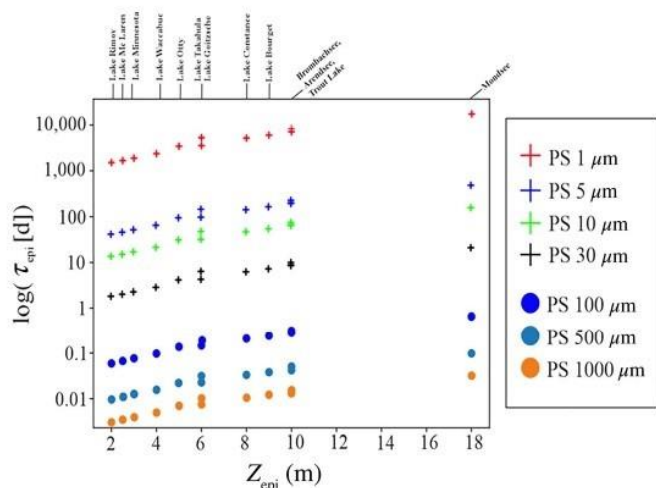


Fig. 7. Dependency of the mean residence time τ (d) on the particle size of the polystyrene (PS) particles, and depth of the epilimnion Z_{epi} (m). Note the logarithmic scale.

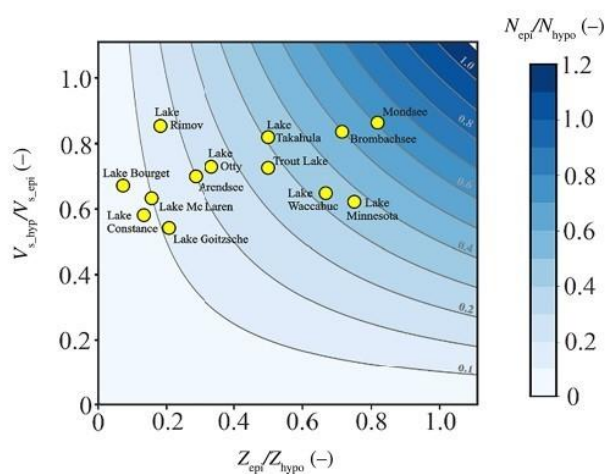


Fig. 8. Relative abundance for microplastics ($N_{\text{epi}}/N_{\text{hypo}}$) in the epilimnion and hypolimnion assuming steady-state conditions for different lake systems as a function of the settling velocity ($v_{s,\text{hypo}}/v_{s,\text{epi}}$) and depth ($Z_{\text{epi}}/Z_{\text{hypo}}$) ratios.

with the extra polymeric substances form a larger aggregate with the biofilm appearing to act as an “adhesive.”

After 6, 8, 10, and 30 weeks of incubation, no substantial differences in sedimentation rates between pristine and incubated microplastic particles were observed (Supporting Information Fig. S8). The maximum deviation in the mean settling velocities was $\pm 5\%$ which is within the measurement error of the particle image velocimetry system. An F -test and paired t -test confirmed that there was no significant difference ($p > 0.05$) before and after incubation in either means or variance. Both incubated and pristine particles followed much the

same settling trajectories after the incubation periods (Supporting Information Fig. S9).

Calculated settling velocity

Despite significant scatter in the data, the measured settling velocities were systematically lower than those calculated using Dietrich (1982) (Fig. 5). The nonbiodegradable particles had significantly less scatter around the 1 : 1 line than biodegradable polymers (Fig. 5). During the experiments, it was observed that fine air bubbles tend to attach to the surfaces of all polymer types and most obviously on the biodegradable microplastic particles (Fig. 6), despite all particles being pretreated in an ultrasonic bath prior to the experiments.

Residence times of microplastics in stratified lakes

The effect of particle size on the mean residence time in the epilimnion for 13 different lake systems is shown in Fig. 7. The mean depths of the epilimnion (Z_{epi}) during summer during stratified conditions ranged from 2 to 18 m. The modeled epilimnic mean residence times for the various lakes depended strongly on particle size and to a lesser extent on the polymer type. For the large microplastic particles (100–1000 μm), the modeled mean residence time was less than 1 d for all lakes. In contrast, the mean residence times for the smallest microplastic particles (1–30 μm) were orders of magnitudes higher, with residence times up to 10,000 d for 1- μm particles in the Mondsee.

Relative particle abundance ($N_{\text{epi}}/N_{\text{hypo}}$) for the selected lake systems during steady-state conditions is shown in Fig. 8. These lakes show a large variation in the $Z_{\text{epi}}/Z_{\text{hypo}}$ ratios, ranging between 0.1 and 0.8. As the lake data was measured entirely during stratification in the summer months, water temperatures for the hypolimnion were consistently lower than the epilimnion, leading to $v_{s,\text{hypo}}/v_{s,\text{epi}} < 1$ (higher viscosities in the cold hypolimnion). The $N_{\text{epi}}/N_{\text{hypo}}$ ranged between < 0.1 for the larger lakes such as Lake Constance in Germany and 0.6 for the Mondsee in Austria and shows that the proportion of microplastics found in either the epilimnion or hypolimnion scales with the $Z_{\text{epi}}/Z_{\text{hypo}}$. Interestingly, the Mondsee has the highest $N_{\text{epi}}/N_{\text{hypo}}$ ratio (> 0.6), meaning the majority of microplastics will be found in the epilimnion and the highest mean epilimnic residence time ($\sim 10,000$ d for 1- μm particles). This maximizes the probability of microplastic uptake by filter feeders and other organisms at the base of the food chain that are generally found in the epilimnion. In contrast, for Lake Constance, Lake Bourget, and Lake McLaren most of the microplastics should be found in the hypolimnion ($N_{\text{epi}}/N_{\text{hypo}} < 0.1$) despite often substantial residence time in the epilimnion (Fig. 8).

As an example to demonstrate how the redistribution of particles occurs between the different lake compartments, the dynamic model was used to calculate the flux of polystyrene spheres (Supporting Information Fig. S10) with a size range of 1, 10, 500, and 1000 μm to a virtual lake loosely based on Upper Lake Constance (Fig. 9). One hundred meters of the stratified lake water column were modeled using the data from

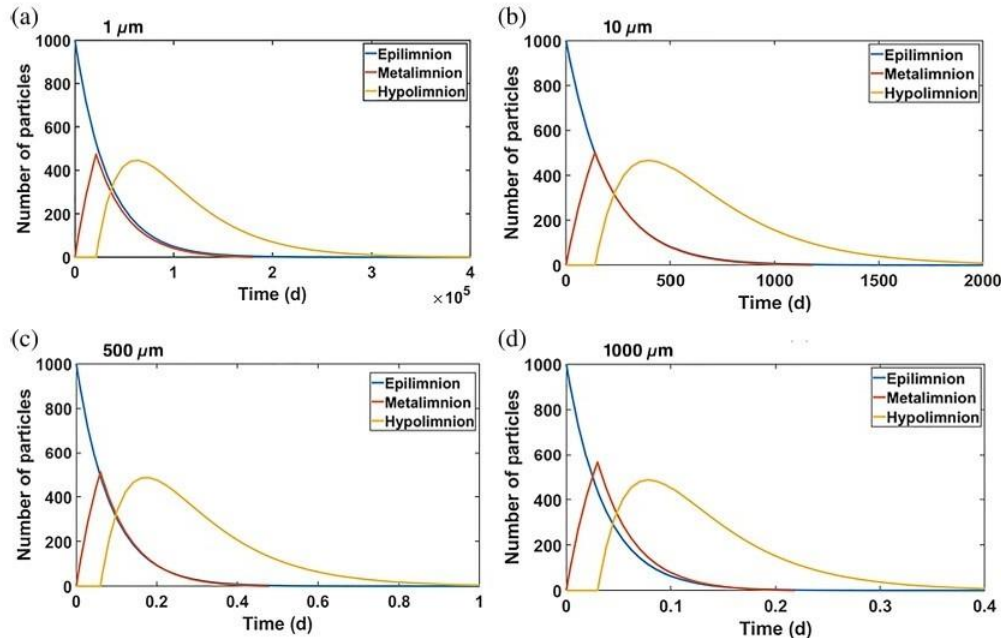


Fig. 9. Simulation results of 1-, 10-, 500-, and 1000- μm polystyrene spheres showing the modeled numbers of the accumulated microplastics in each lake compartment vs. elapsed time in Upper Lake Constance on Day 319 according to lake data from Appt et al. (2004). The simulations were initiated with a pulse of 1000 spherical polystyrene particles uniformly distributed in the well-mixed epilimnion.

Appt et al. (2004) (Supporting Information Table S11). The simulations were initiated with a pulse of 1000 spherical polystyrene particles that were uniformly distributed in the well-mixed epilimnion (Fig. 9). The microplastic numbers in the epilimnion decreased exponentially following the pulse. In contrast, in the metalimnion and the hypolimnion, the microplastic numbers initially increased as they received particles from the overlying lake layer. Microplastic numbers in the metalimnion and hypolimnion started to decrease after the loss rate to the underlying layer (or sediment in the case of the hypolimnion) exceeded the input rate from the overlying layer. The modeling results showed that the residence time τ (d) in each layer was very strongly dependent on particle size, similarly to the steady-state model.

Discussions

Various factors such as particle size, polymer density, hydrophobicity of the particle surface, biofouling, water temperature, and turbulent mixing control the residence times of microplastics in lakes. These factors, combined with high or constant input of microplastics will increase the probability that microplastics will be ingested by aquatic organisms and potentially be transferred within the lake food chain (Nelms et al. 2018).

The experimentally determined settling velocities showed that the density and size of the microplastics are the most critical parameters controlling the settling velocity. Since the

microplastic settling velocity during laminar conditions depends on their weight, drag forces, and buoyancy forces, all large and dense particles have significantly higher settling velocities than the smaller and lighter microplastics.

As the CSF describes the flatness of the particle and it depends only on the ratio between the three axes of the particles rather than its size, it was experimentally difficult to isolate the effect of particle shape on the settling velocity, separating it from that of density and size. This problem was exacerbated by the fact that all particles were similar in shape, despite being irregular (having similar CSF) (Supporting Information Fig. S1, S2) and no fibers or special geometric objects such as cubes, cylinders, or discs were used in the experiments.

We originally expected rapid and somewhat uniform colonization of the particles by biofilms (Zettler et al. 2013; Rummel et al. 2017). However, the confocal laser scanning microscope images showed that the biofilm rather forms dense patches with large parts of the particles left uncolonized. The formation of biofilm and in particular the presence of a thick extra polymeric substance increased the tendency for microplastic aggregation, which is consistent with findings from Rummel et al. (2017). Such aggregates are larger and likely to have different surface properties, densities, and shapes compared to the pristine particles, which should result in different physical behavior within the water column (Leiser et al. 2020).

The literature suggests that the colonization process alters the polarity of the plastic surface, changing it from hydrophobic to hydrophilic (Michels et al. 2018; Tu et al. 2020; van

Melkebeke et al. 2020), increases the density of the particle (Rummel et al. 2017; Michels et al. 2018), and reduces the attachment of air bubbles on the surface (Renner et al. 2020). Therefore, it was anticipated that the settling velocity would increase after incubation. However, no measurable changes in the physical properties or sedimentation behavior were observed. This may be due to the “short” incubation periods of 6, 8, 10, and 30 weeks. Also, the pond was frozen for the first 3 weeks of incubation during the winter season which may explain the small volumes of biofilm accumulated on the particle surface, assuming that the metabolism of the biofilm-building organisms was affected by the low temperatures (Farhat et al. 2016).

In accordance with Waldschläger and Schüttrumpf (2019); van Melkebeke et al. (2020), the settling velocities of the microplastics were not well described using the traditional sediment settling equation of Dietrich (1982). We believe this is due to the hydrophobicity of the microplastic surfaces, which is conducive to the formation of fine air bubbles, which then increased the buoyancy force exerted on the settling particle and reduced their settling velocity. Since Dietrich (1982) was originally developed for mineral particles, the hydrophobic adhesion between microplastics and air bubbles did not play a role in the settling behavior. Whether microplastic remains hydrophobic in the environment or not likely depends on microplastic surface properties, for example, after biofilm colonization. Pristine microplastics are unlikely to be found in natural aquatic environments as they are usually rapidly colonized by biofilms or adsorb natural material such as dissolved organic carbon or mineral precipitates (e.g., iron oxides) (Leiser et al. 2020). Also, measuring the size of particles from two-dimension images may not properly capture the third dimension of the particles. This is a potential source of error in the calculations of the theoretical settling velocities. These observations suggest, however, that the settling behavior of microplastic is more complex than in simplified theoretical models and more advanced methods such as computational fluid dynamics should be used to investigate this more exactly.

In the lake model, the epilimnion and the hypolimnion were presented as well-mixed systems to mimic turbulent processes within these layers during the thermal stratification. In contrast, the metalimnion was assumed to be laminar. The residence time of microplastics in the metalimnion is relatively short compared to the epilimnion and hypolimnion due to the lack of mixing processes as well as to a limited thickness. The extremely long residence time for small microplastic particles in the epilimnion in particular forms a high uptake probability for aquatic organisms such as filter feeders. This lake model has, however, a highly simplified and theoretical representation of residence times in the three lake compartments. Real lake systems are considerably more complex than these simplified representations of lake physics. In real lakes, the residence times of the settling microplastics are likely coupled with the changes in lakes' hydrodynamics such as temperature fluctuation, waves, transient turbulence, or

lake mixing in autumn and spring as stratification destabilizes. Also, lake retention time (flushing time), which is strongly dependent on the internal physical processes and water fluxes from the catchment (Ambrosetti et al. 2003), plays a decisive role in how long the microplastics will actually reside in a lake, and thus how long organisms have the opportunity to ingest them. Calculated residence times were on the order of 10^5 d for the smallest particles, meaning that the flushing time is significantly shorter than the residence time for most lakes, and thus is not really a meaningful number for a real lake system such as Lake Constance, which has a theoretical average flushing time of 4.5 years (Wessels 2015). It does suggest, however, that there should only be a negligible amount of microplastics of this size range found in the lake sediments unless some process increases their settling velocity, for example, aggregation with existing lake particles and detritus or uptake and death of organisms or egestion via fecal pellets. In addition, the biologically driven mixing of the water column due to the vertical migration of zooplankton increase turbulence in the water column (Dean et al. 2016) which may cause resuspension and redistribution of the microplastics, which may be particularly important in the hypolimnion.

Conclusion

This research aimed to identify the primary controls and time scales of microplastic residence times in stratified lake systems. By combining laboratory experiments and modeling, it was clear that microplastic residence times in the lake water column highly depend on the size and to a less extent the density of the particle, varying over many orders of magnitude. The comparison between laboratory-measured and calculated settling velocities using Dietrich (1982) showed that hydrophobic surface properties of the pristine microplastics are a key factor that needs to be considered when estimating settling velocities. It is expected that the hydrophobic adhesion between pristine microplastics and fine air bubbles can increase the buoyancy forces exerted on the particles and increase their residence time in the lake water column.

The microplastic polymers incubated in a small lake were effectively and rapidly colonized by biofilm and included bacteria cells and extra polymeric substances. However, the settling experiments did not show any substantial differences in the sedimentation trajectories and velocities between individual (i.e., not aggregates) pristine and incubated microplastics. The presence of biofilms on the surfaces of incubated microplastics did tend to favor the formation of aggregates. These aggregates are expected to sink faster and to have shorter residence time than individual pristine microplastics because of their increase in size and changes in surface properties.

Our lumped parameter modeling approach is a simple way to estimate residence times, fluxes, and numbers of microplastics in the epilimnion, metalimnion, and hypolimnion during both steady-state and dynamic conditions. The functional relationship

$N_{\text{epi}}/N_{\text{hypo}}$ allows a rapid assessment of where most microplastics will be found in different lakes and is independent of the input influx to the lake as long as the ratio $v_{s,\text{epi}}/v_{s,\text{hypo}}$ is constant. Also, the modeling approach was capable of showing the dynamic redistribution of microplastics in the stratified lake water column. The accumulated numbers and residence times of microplastics in the three lake compartments varied over several orders of magnitude and were strongly dependent on particle size as well as physical lake properties such as depth and temperature of the hypolimnion, metalimnion, and epilimnion. This is crucial for the uptake of microplastics by, for example, filter feeders, in lake systems. The simulated residence times suggest that significant numbers of microplastics should be found in lake sediment as long as their residence time is shorter than lake flushing time. In contrast, small microplastics with residence times significantly longer than lake flushing time are unlikely to be found in large numbers in lake sediment unless some biological or physical processes increase their settling velocity to deliver them to the lake bottom.

Data availability statement

Data are archived on CRC 1357 cloud storage and available on request.

References

- Agarwal, S. 2020. Biodegradable polymers: Present opportunities and challenges in providing a microplastic-free environment. *Macromol. Chem. Phys.* **221**: 2000017. doi:10.1002/macp.202000017
- Aljaibachi, R., and A. Callaghan. 2018. Impact of polystyrene microplastics on *Daphnia magna* mortality and reproduction in relation to food availability. *PeerJ* **6**: e4601. doi:10.7717/peerj.4601
- Ambrosetti, W., L. Barbanti, and N. Sala. 2003. Residence time and physical processes in lakes. *J. Limnol.* **62**: 1. doi:10.4081/jlimnol.2003.s1.1
- Appt, J., J. Imberger, and H. Kobus. 2004. Basin-scale motion in stratified Upper Lake Constance. *Limnol. Oceanogr.* **49**: 919–933. doi:10.4319/lo.2004.49.4.0919
- Arthur, C., J. Baker, and H. Bamford. 2009. Proceedings of the International Research Workshop on the Occurrence, Effects and Fate of Microplastic Marine Debris, 9–11 September 2008. NOAA Technical Memorandum NOS-OR&R-30.
- Bagaev, A., A. Mizyuk, L. Khatmullina, I. Isachenko, and I. Chubarenko. 2017. Anthropogenic fibres in the Baltic Sea water column: Field data, laboratory and numerical testing of their motion. *Sci. Total Environ.* **599–600**: 560–571. doi:10.1016/j.scitotenv.2017.04.185
- Bellasi, A., G. Binda, A. Pozzi, S. Galafassi, P. Volta, and R. Bettinetti. 2020. Microplastic contamination in freshwater environments: A review, focusing on interactions with sediments and benthic organisms. *Environments* **7**: 30. doi:10.3390/environments7040030
- Browne, M. A., T. Galloway, and R. Thompson. 2007. Microplastic—An emerging contaminant of potential concern? *Integr. Environ. Assess. Manag.* **3**: 559–561. doi:10.1002/ieam.5630030412
- Cole, M., P. K. Lindeque, E. Fileman, J. Clark, C. Lewis, C. Halsband, and T. S. Galloway. 2016. Microplastics alter the properties and sinking rates of zooplankton faecal pellets. *Environ. Sci. Technol.* **50**: 3239–3246. doi:10.1021/acs.est.5b05905
- Dean, C., A. Soloviev, A. Hirons, T. Frank, and J. Wood. 2016. Biomixing due to diel vertical migrations of zooplankton: Comparison of computational fluid dynamics model with observations. *Ocean Model.* **98**: 51–64. doi:10.1016/j.ocemod.2015.12.002
- Dietrich, W. E. 1982. Settling velocity of natural particles. *Water Resour. Res.* **18**: 1615–1626. doi:10.1029/WR018i006p01615
- Farhat, N. M., J. S. Vrouwenvelder, M. C. M. van Loosdrecht, S. S. Bucs, and M. Staal. 2016. Effect of water temperature on biofouling development in reverse osmosis membrane systems. *Water Res.* **103**: 149–159. doi:10.1016/j.watres.2016.07.015
- Fischer, E. K., L. Paglialonga, E. Czech, and M. Tamminga. 2016. Microplastic pollution in lakes and lake shoreline sediments—a case study on Lake Bolsena and Lake Chiusi (Central Italy). *Environ. Pollut.* **213**: 648–657. doi:10.1016/j.envpol.2016.03.012
- Geyer, R., J. R. Jambeck, and K. L. Law. 2017. Production, use, and fate of all plastics ever made. *Sci. Adv.* **3**: e1700782. doi:10.1126/sciadv.1700782
- Ghawi, A. H., and J. Kris. 2012. A computational fluid dynamics model of flow and settling in sedimentation tanks. *In* H. W. Oh [ed.], *Computational fluid dynamics (CFD) and discrete element method (DEM) applied to centrifuges*. INTECH Open Access Publisher.
- Kaiser, D., N. Kowalski, and J. J. Waniek. 2017. Effects of biofouling on the sinking behavior of microplastics. *Environ. Res. Lett.* **12**: 124003. doi:10.1088/1748-9326/aa8e8b
- Khatmullina, L., and I. Isachenko. 2017. Settling velocity of microplastic particles of regular shapes. *Mar. Pollut. Bull.* **114**: 871–880. doi:10.1016/j.marpolbul.2016.11.024
- Kirillin, G., H.-P. Grossart, and K. W. Tang. 2012. Modeling sinking rate of zooplankton carcasses: Effects of stratification and mixing. *Limnol. Oceanogr.* **57**: 881–894. doi:10.4319/lo.2012.57.3.0881
- Lacerda, A. L. D. F., and others. 2019. Plastics in sea surface waters around the Antarctic Peninsula. *Sci. Rep.* **9**: 3977. doi:10.1038/s41598-019-40311-4
- Lampert, W., and U. Sommer. 2010. *Limnology*. *In* *The ecology of lakes and streams*, 2nd ed. Univ. Press.
- Leiser, R., G.-M. Wu, T. R. Neu, and K. Wendt-Potthoff. 2020. Biofouling, metal sorption and aggregation are related to sinking of microplastics in a stratified reservoir. *Water Res.* **176**: 115748. doi:10.1016/j.watres.2020.115748

- Meides, N., and others. 2021. Reconstructing the environmental degradation of polystyrene by accelerated weathering. *Environ. Sci. Technol.* **55**: 7930–7938. doi:10.1021/acs.est.0c07718
- Michels, J., A. Stippkugel, M. Lenz, K. Wirtz, and A. Engel. 2018. Rapid aggregation of biofilm-covered microplastics with marine biogenic particles. *Proceedings. Biological sciences* **285**: 20181203. doi:10.1098/rspb.2018.1203
- Nelms, S. E., T. S. Galloway, B. J. Godley, D. S. Jarvis, and P. K. Lindeque. 2018. Investigating microplastic trophic transfer in marine top predators. *Environ. Pollut.* **238**: 999–1007. doi:10.1016/j.envpol.2018.02.016
- Nguyen, T. H., F. H. M. Tang, and F. Maggi. 2020. Sinking of microbial-associated microplastics in natural waters. *PLoS One* **15**: e0228209. doi:10.1371/journal.pone.0228209
- Nishri, A., A. Rimmer, and Y. Lechinsky. 2015. The mechanism of hypolimnion warming induced by internal waves. *Limnol. Oceanogr.* **60**: 1462–1476. doi:10.1002/lno.10109
- Ramsperger, A. F. R. M., and others. 2020. Structural diversity in early-stage biofilm formation on microplastics depends on environmental medium and polymer properties. *Water* **12**: 3216. doi:10.3390/w12113216
- Renner, G., A. Nellessen, A. Schwiers, M. Wenzel, T. C. Schmidt, and J. Schram. 2020. Hydrophobicity-water/air-based enrichment cell for microplastics analysis within environmental samples: A proof of concept. *MethodsX* **7**: 100732. doi:10.1016/j.mex.2019.11.006
- Reynolds, C. S. 1984. *The ecology of freshwater phytoplankton*. Cambridge Univ. Press.
- Reynolds, C. S. 2006. *The ecology of phytoplankton*. Cambridge Univ. Press.
- Reynolds, C. S., and S. W. Wiseman. 1982. Sinking losses of phytoplankton in closed limnetic systems. *J. Plankton Res.* **4**: 489–522. doi:10.1093/plankt/4.3.489
- Rocha-Santos, T., and A. C. Duarte. 2015. A critical overview of the analytical approaches to the occurrence, the fate and the behavior of microplastics in the environment. *TrAC Trends Anal. Chem.* **65**: 47–53. doi:10.1016/j.trac.2014.10.011
- Rummel, C. D., A. Jahnke, E. Gorokhova, D. Kühnel, and M. Schmitt-Jansen. 2017. Impacts of biofilm formation on the fate and potential effects of microplastic in the aquatic environment. *Environ. Sci. Technol. Lett.* **4**: 258–267. doi:10.1021/acs.estlett.7b00164
- Schindelin, J., and others. 2012. Fiji: An open-source platform for biological-image analysis. *Nat. Methods* **9**: 676–682. doi:10.1038/nmeth.2019
- Singh, P., J. Bagrania, and A. K. Haritash. 2019. Seasonal behaviour of thermal stratification and trophic status in a sub-tropical Palustrine water body. *Appl. Water Sci.* **9**: 139. doi:10.1007/s13201-019-1011-z
- Sun, J., X. Dai, Q. Wang, M. C. M. van Loosdrecht, and B.-J. Ni. 2019. Microplastics in wastewater treatment plants: Detection, occurrence and removal. *Water Res.* **152**: 21–37. doi:10.1016/j.watres.2018.12.050
- Toussaint, B., and others. 2019. Review of micro- and nanoplastic contamination in the food chain. *Food Addit. Contam. Part A Chem. Anal. Control Expo. Risk Assess.* **36**: 639–673. doi:10.1080/19440049.2019.1583381
- Tu, C., T. Chen, Q. Zhou, Y. Liu, J. Wei, J. J. Wanick, and Y. Luo. 2020. Biofilm formation and its influences on the properties of microplastics as affected by exposure time and depth in the seawater. *Sci. Total Environ.* **734**: 139237. doi:10.1016/j.scitotenv.2020.139237
- van Melkebeke, M., C. Janssen, and S. de Meester. 2020. Characteristics and sinking behavior of typical microplastics including the potential effect of biofouling: Implications for remediation. *Environ. Sci. Technol.* **54**: 8668–8680. doi:10.1021/acs.est.9b07378
- Waldschläger, K., and H. Schüttrumpf. 2019. Effects of particle properties on the settling and rise velocities of microplastics in freshwater under laboratory conditions. *Environ. Sci. Technol.* **53**: 1958–1966. doi:10.1021/acs.est.8b06794
- Wessels, M. 2015. Bathymetry of Lake Constance—A high-resolution survey in a large, deep Lake. *zfv – Zeitschrift für Geodäsie, Geoinformation und Landmanagement.* **140**: 203–210. doi:10.12902/zfv-0079-2015
- Worm, B., H. K. Lotze, I. Jubinville, C. Wilcox, and J. Jambeck. 2017. Plastic as a persistent marine pollutant. *Annu. Rev. Env. Resour.* **42**: 1–26. doi:10.1146/annurev-environ-102016-060700
- Wright, S. L., R. C. Thompson, and T. S. Galloway. 2013. The physical impacts of microplastics on marine organisms: A review. *Environ. Pollut.* **178**: 483–492. doi:10.1016/j.envpol.2013.02.031
- Zettler, E. R., T. J. Mincer, and L. A. Amaral-Zettler. 2013. Life in the “plastisphere”: Microbial communities on plastic marine debris. *Environ. Sci. Technol.* **47**: 7137–7146. doi:10.1021/es401288x

Acknowledgments

Funded by the Deutsche Forschungsgemeinschaft (DFG, German Research Foundation)—Project Number 391977956—SFB 1357. The authors would like to thank Peter Strohriegel for providing microplastic particles for the settling experiments, Antonia Freiberger for her support during confocal laser scanning microscope experiments, and Ulrich Mansfeld and Martina Heider for the scanning electron microscope images. Open Access funding enabled and organized by Projekt DEAL.

Conflict of interest

None declared.

Submitted 09 August 2021

Revised 16 November 2021

Accepted 06 February 2022

Associate editor: Yong Liu

Supplementary Information

Measuring of microplastics settling velocities and implications for residence times in thermally stratified lakes

Hassan Elagami^{1,3*}, Pouyan Ahmadi², Jan H. Fleckenstein^{2,6}, Sven Frei³, Martin Obst⁴, Seema Agarwal⁵, Benjamin S. Gilfedder^{1,3}

¹Limnological Research Station, Bayreuth Center of Ecology and Environmental Research
University of Bayreuth, Bayreuth, Germany

²Department of Hydrogeology, Helmholtz Centre for Environmental Research – UFZ, Leipzig,
Germany

³Department of Hydrology, Bayreuth Center of Ecology and Environmental Research (BayCEER),
University of Bayreuth, Bayreuth, Germany

⁴Experimental Biogeochemistry, BayCEER, Bayreuth, Germany

⁵Macromolecular Chemistry II, University of Bayreuth, Bayreuth, Germany

⁶Hydrologic Modelling Unit, Bayreuth Center of Ecology and Environmental Research (BayCEER),
University of Bayreuth, Bayreuth, Germany

Corresponding Author:

Hassan Elagami: Limnological Research Station, & Department of Hydrology, Bayreuth Center of Ecology and Environmental Research (BayCEER), University of Bayreuth, Bayreuth, Germany; orcid.org/0000-0002-2919-5230; Email: hassan.elagami@uni-bayreuth.de

S1) Characterization of microplastics from various polymer types

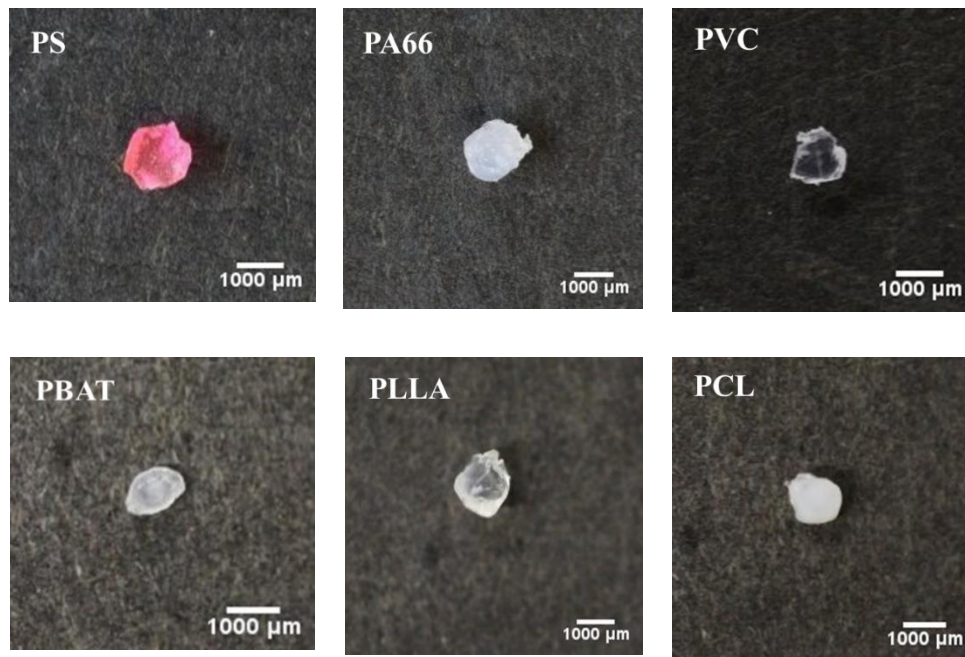


Figure S1: An example of polystyrene (PS), polyamide 66 (PA66), polyvinylchloride (PVC), polycaprolactone (PCL), polylactide (PLLA), and polybutylenadipate terephthalate (PBAT) particles investigated under the camera.

S2) Polystyrene fragments investigated under scanning electron microscope

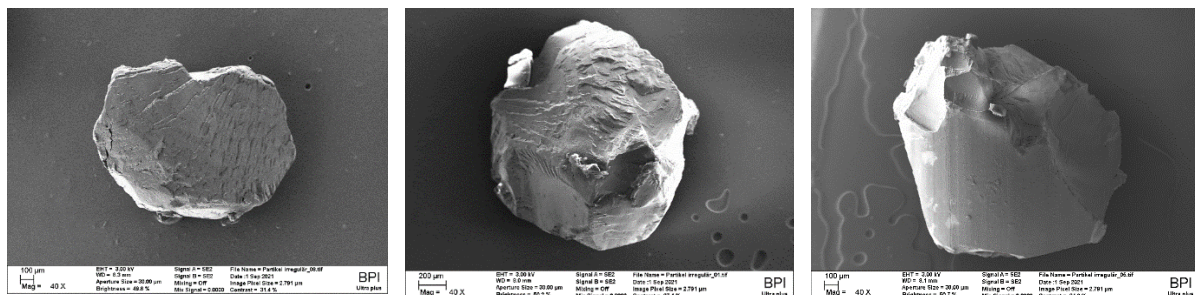


Figure S2: An example of the polystyrene fragments used in the settling velocity experiments under scanning electron microscope.

S3) The glass tubes used during the lake incubations



Figure S3: Example of the glass tubes used to incubate microplastic fragments in the lake.

S4) Dietrich (1928) settling velocity model

The theoretical settling velocity of each microplastic particle was calculated using the following equations:

$$W = \left(\frac{\rho_s - \rho}{\rho} g v W_* \right)^{1/3} \quad \text{a}$$

$$W_* = R^3 10^{R_1 + R_2} \quad \text{b}$$

$$R_1 = -3.76715 + 1.92944(\log D_*) - 0.09815(\log D_*)^{2.0} - 0.00575(\log D_*)^{3.0} + 0.00056(\log D_*)^{4.0} \quad \text{c}$$

$$R_2 = \left(\log \left(1 - \frac{1 - CSF}{0.85} \right) \right) - (1 - CSF)^{2.3} \tanh(\log D_* - 4.6) + 0.3(0.5 - CSF)(1 - CSF)^{2.0}(\log D_* - 4.6) \quad \text{d}$$

$$R_3 = \left(0.65 - \left(\frac{CSF}{2.83} \tanh(\log D_* - 4.6) \right) \right)^{\left(1 + \frac{(3.5 - P)}{2.5} \right)} \quad \text{e}$$

$$D_* = \frac{(\rho_p - \rho_w) g D_{eq}^3}{\rho_w \nu^2} \quad \text{f}$$

where W_* [-] is the dimensionless settling velocity, W [$L T^{-1}$] is the settling velocity of the particle, ρ_s [$M L^{-3}$] is the density of the particle, ρ [$M L^{-3}$] is the density of the fluid, ν [$L^2 T^{-1}$] is the kinematic viscosity of the fluid, R_1 [-] is a size factor, R_2 [-] is a shape factor, R_3 [-] is a

roundness factor, D^* [-] is the dimensionless diameter, CSF [-] is Corey shape factor, D_{eq} [L] is the equivalent particle diameter, and P [-] is Powers roundness.

S5) Correction of settling velocity according to water temperature in each layer

The experimental settling velocities were corrected according to (Ghawi and Kris, 2012b) using the following equation:

$$V_{ST_2} = V_{ST_1} \left(\frac{10^{\left[\frac{247.8}{T_1 + 133.15} \right]}}{10^{\left[\frac{247.8}{T_2 + 133.15} \right]}} \right)$$

where V_{ST_1} [LT^{-1}], V_{ST_2} [LT^{-1}], T_1 [$^{\circ}C$], and T_2 [$^{\circ}C$] are the settling velocity measured in the laboratory at $20^{\circ}C$, the corrected settling velocity in the lake compartments, water temperature in the laboratory, and the temperature of the lake compartment respectively.

S6) Spread of the Corey shape factor of the particles used in the settling velocity experiments

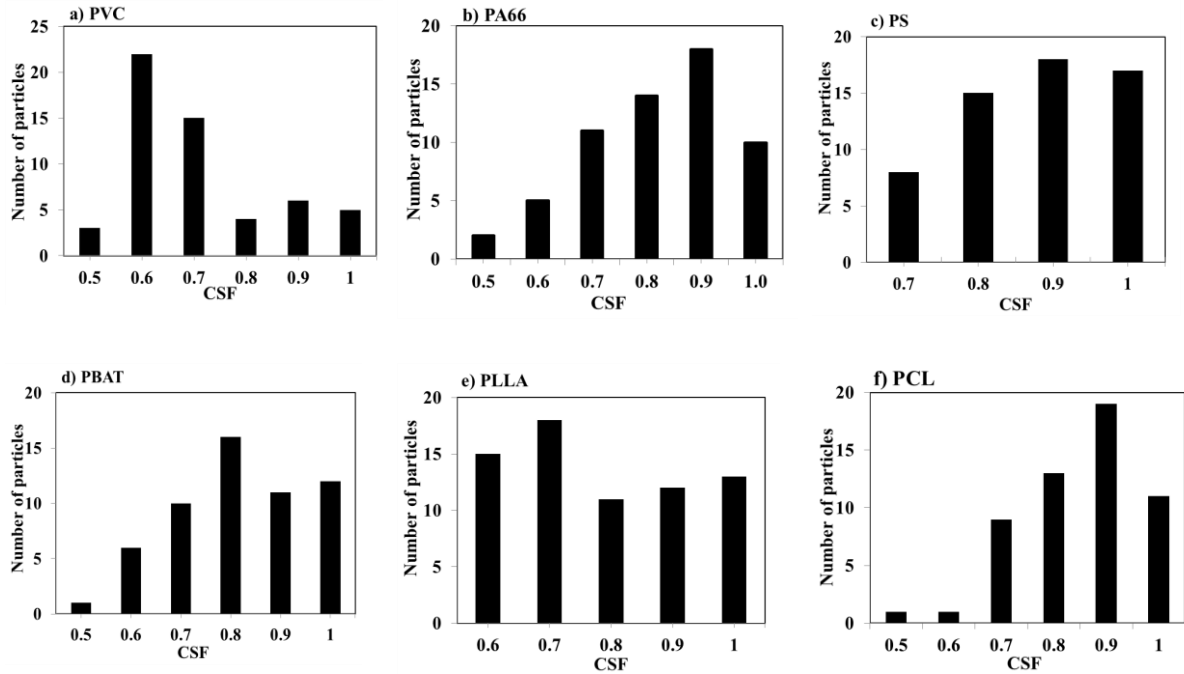


Figure S6: Distribution of Corey shape factor (CSF) of the polystyrene (PS), polyamide 66 (PA66), polyvinylchloride (PVC), polycaprolactone (PCL), polylactide (PLLA), and polybutylenadipate terephthalate (PBAT) particles across the experimental samples.

S7) Accumulation of biofilm on the surfaces of the incubated microplastics

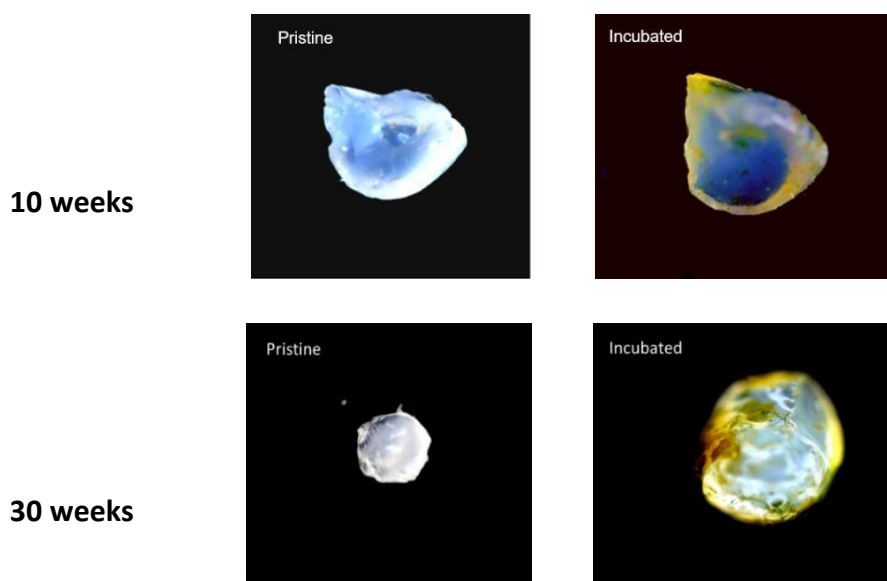


Figure S7: Comparison between pristine and biofilm-coated polyamide 66 particles after 10 and 30 weeks of incubation.

S8) Settling velocities of pristine and incubated microplastics

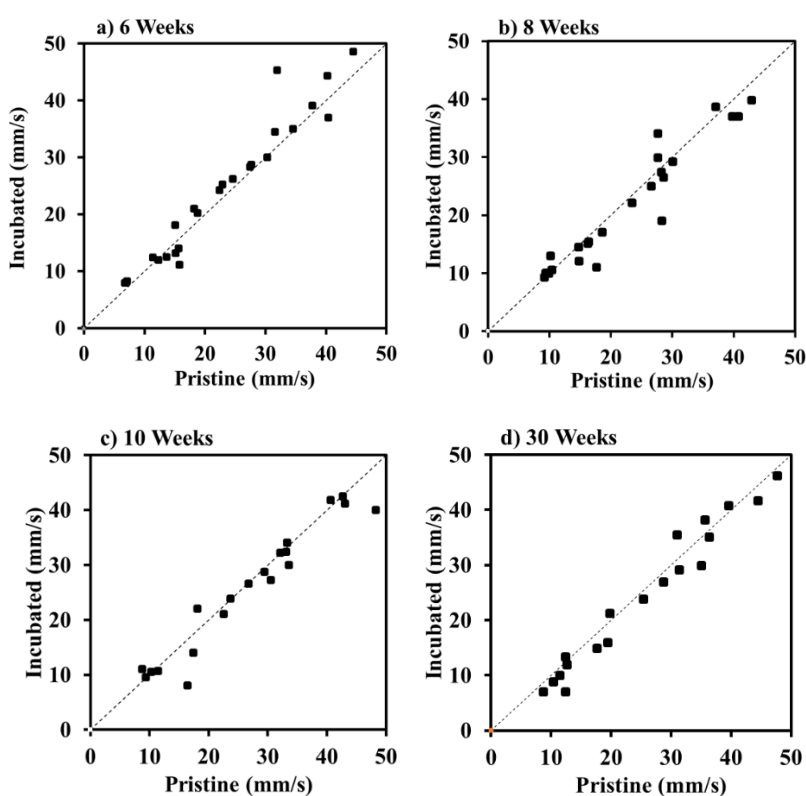


Figure S8: Comparison between experimentally determined the settling velocity of the pristine and incubated microplastics after different lake incubations. The dashed line presents the 1:1 line.

S9) Tracking the settling paths before and after incubation

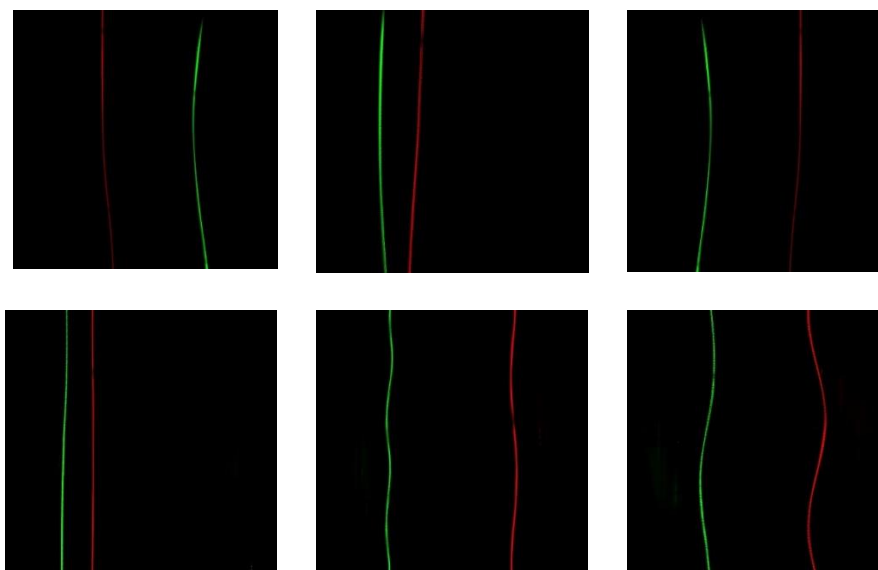


Figure S9: The sinking trajectories of 6 different particles after 30 weeks of incubation. The red trajectories and the green trajectories represent pristine and colonized microplastics respectively. The size of the frame is 30cm X 30cm.

S10) An example of the polystyrene spheres used in the lake model

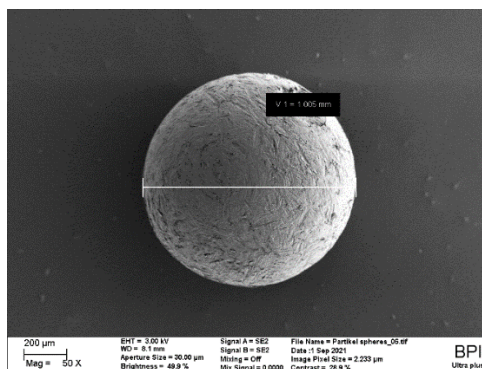


Figure S10: A scanning electron microscope image of a 1000 µm polystyrene sphere used in the lake model.

S11) Residence time the polystyrene spheres in each lake compartment

Table S11: Layer depth (m), water temperatures T ($^{\circ}C$), and the residence time τ (d) of the microplastics in the epilimnion, metalimnion, and hypolimnion of Upper lake Constance on day 319 according to Appt et al. (2004).

The residence times τ (d) of the microplastics in each individual compartment were calculated according to equation 4.

Layer	Depth (m)	T ($^{\circ}C$)	$\tau_{1\mu m}$ (d)	$\tau_{10\mu m}$ (d)	$\tau_{500\mu m}$ (d)	$\tau_{1000\mu m}$ (d)
Epilimnion	30	9.0	30750	200	0.08	0.04
Metalimnion	20	7.5	21400	140	0.06	0.03
Hypolimnion	50	5.5	56695	370	0.16	0.07

Study 2: Systematic evaluation of physical parameters affecting the terminal settling velocity of microplastic particles in lakes using CFD

Pouyan Ahmadi, **Hassan Elagami**, Franz Dichgans, Christian Schmidt, Benjamin S. Gilfedder, Sven Frei, Stefan Peiffer, Jan H. Fleckenstein

Published in *Frontiers in Environmental Science*, Volume 10, 2022.

<https://doi.org/10.3389/fenvs.2022.87522>



Systematic Evaluation of Physical Parameters Affecting the Terminal Settling Velocity of Microplastic Particles in Lakes Using CFD

Pouyan Ahmadi^{1*}, Hassan Elagami^{2,3}, Franz Dichgans¹, Christian Schmidt^{1,4}, Benjamin S. Gilfedder^{2,3}, Sven Frei³, Stefan Peiffer³ and Jan H. Fleckenstein^{1,5*}

¹Department of Hydrogeology, Helmholtz-Centre for Environmental Research, UFZ, Leipzig, Germany, ²Limnological Research Station, Bayreuth Center of Ecology and Environmental Research, University of Bayreuth, Bayreuth, Germany, ³Department of Hydrology, Bayreuth Center of Ecology and Environmental Research (BayCEER), University of Bayreuth, Bayreuth, Germany, ⁴Department of Aquatic Systems Analysis and Management, Helmholtz-Centre for Environmental Research, UFZ, Leipzig, Germany, ⁵Hydrologic Modelling Unit, Bayreuth Center of Ecology and Environmental Research (BayCEER), University of Bayreuth, Bayreuth, Germany

OPEN ACCESS

Edited by:

Ping Wang,
Beijing Forestry University, China

Reviewed by:

Veerasingam S.,
Qatar University, Qatar
Qiqing Chen,
East China Normal University, China

*Correspondence:

Pouyan Ahmadi
pouyan.ahmadi@ufz.de
Jan H. Fleckenstein
jan.fleckenstein@ufz.de

Specialty section:

This article was submitted to
Freshwater Science,
a section of the journal
Frontiers in Environmental Science

Received: 13 February 2022

Accepted: 24 March 2022

Published: 13 April 2022

Citation:

Ahmadi P, Elagami H, Dichgans F,
Schmidt C, Gilfedder BS, Frei S,
Peiffer S and Fleckenstein JH (2022)
Systematic Evaluation of Physical
Parameters Affecting the Terminal
Settling Velocity of Microplastic
Particles in Lakes Using CFD.
Front. Environ. Sci. 10:875220.
doi: 10.3389/fenvs.2022.875220

Microplastic (MP) particles are commonly found in freshwater environments such as rivers and lakes, negatively affecting aquatic organisms and potentially causing water quality issues. Understanding the transport and fate of MP particles in these environments is a key prerequisite to mitigate the problem. For standing water bodies (lakes, ponds) the terminal settling velocity (TSV) is a key parameter, which determines particle residence times and exposure times of organisms to MP in lakes. Here we systematically investigate the effects of the physical parameters density, volume, shape and roundness, surface roughness and hydrophobicity and lake water temperature on the TSV of a large number of particles with regular and irregular shapes (equivalent diameters: 0.5–2.5 mm) and different polymer densities using computational fluid dynamics (CFD) simulations. Simulation results are compared to laboratory settling experiments and used to evaluate existing, semi-empirical relationships to estimate TSV. The semi-empirical relationships were generally found to be in reasonable agreement with the CFD simulations ($R^2 > 0.92$). Deviations were attributed to simplifications in their descriptions of particle shapes. Overall the CFD simulations also matched the TSVs from the experiments quite well, ($R^2 > 0.82$), but experimental TSVs were generally slower than model TSVs with the largest differences for the irregular particles made from biodegradable polymers. The deviations of up to 58% were found to be related to the attachment of air bubbles on irregularities in the particle surfaces caused by the hydrophobicity of the MP particles. Overall, density was the most decisive parameter for TSV with increases in TSV of up to 400% followed by volume (200%), water temperature (47%) and particle roundness (45%). Our simulation results provide a frame of reference for an improved evaluation of the relative effects of different particle characteristics on their TSV in lakes. This will in turn allow a more robust estimation of particle residence times and potential exposure times of organism to MP in the different compartments of a lake.

Keywords: CFD, Navier-Stokes equations, OpenFOAM, microplastic particles, terminal settling velocity

1 INTRODUCTION

Plastic products have a broad range of applications in all fields of daily life due to their useful properties such as durability and ductility (Derraik, 2002; North and Halden, 2013). Their widespread use, in turn, has led to large amounts of plastic waste, which, if mismanaged, may pose a threat to the environment (Derraik, 2002; Barnes et al., 2009; Claessens et al., 2011). Plastic debris, in a wide variety of sizes, can be found in the oceans, as well as in terrestrial freshwater systems and the atmosphere (Barnes et al., 2009; de Souza Machado et al., 2018; Rochman, 2018; Frias and Nash, 2019; Liao and Chen, 2021). A significant share of the plastic found in the terrestrial and marine environments belongs to the microplastic (MP) fraction (<5 mm (Barnes et al., 2009)). These MP particles may enter the environment as primary MP via the release from cosmetic products and cleaners, via losses from production plants and during transport (Gregory, 1983; Gregory, 1996; Fendall and Sewell, 2009; Doyle et al., 2011) or as secondary MP resulting from the break-down and erosion of larger plastic debris in the environment (Williams and Simmons, 1996; Browne et al., 2011; Wright et al., 2020). Although different size ranges have been used to define MP (Claessens et al., 2011; Van Cauwenberghe et al., 2013), an upper size limit of 5,000 μm has been introduced as the definition of MP by the National Oceanic and Atmospheric Administration (Lambert and Wagner, 2018; Sighicelli et al., 2018) and is commonly accepted as the upper size limit in the literature. The lower size limit is not as clearly defined and may vary between different studies depending on their scope and questions (Khatmullina and Isachenko, 2017; Kaiser et al., 2019; Waldschlager and Schuttrumpf, 2019).

Freshwater lakes are amongst the main receptors of MP in the terrestrial environment (Zbyszewski et al., 2014; Ballent et al., 2016; Fischer et al., 2016; Anderson et al., 2017; Vaughan et al., 2017; Hendrickson et al., 2018; Sighicelli et al., 2018). MP particles can be taken up by organisms in different compartments of a lake with detrimental effects on the organisms as well as other organisms at higher trophic levels (Cole et al., 2013; Wright et al., 2013; Cole et al., 2016; Coppock et al., 2019). Transport vectors of MP particles determine their horizontal and vertical distribution patterns in a lake (Khatmullina and Isachenko, 2017; Kaiser et al., 2019; Waldschlager and Schuttrumpf, 2019; Isachenko, 2020) and in turn control residence times in the lake compartments as well as exposure of organisms to MP particles. It is therefore of particular importance to understand the physical controls of particle settling in lakes (Elagami et al., 2022). Vertical transport vectors are strongly controlled by physical parameters that define the force balance between downward gravitational forces, drag forces and upward buoyant forces acting on the body of an individual MP particle. A terminal settling velocity (TSV) is reached at the point where the summation of drag and buoyant forces is approximately equal to the weight force (Chubarenko et al., 2016; Khatmullina and Isachenko, 2017; Zhang, 2017).

Several experimental studies have investigated the TSV of MP particles primarily in marine systems (Arora et al., 2010; Wright

et al., 2013; Chubarenko et al., 2016; Kooi et al., 2016; Kowalski et al., 2016; Khatmullina and Isachenko, 2017; Zhang, 2017; Chubarenko et al., 2018; Akdogan and Guven, 2019; Kaiser et al., 2019), with studies explicitly addressing freshwater systems being rare (Khatmullina and Isachenko, 2017; Kaiser et al., 2019; Waldschlager and Schuttrumpf, 2019; Elagami et al., 2022). In some of these studies specific semi-empirical relationships have been developed to predict the TSV of MP particles in water considering particle size, density, and roundness as well as water density and kinematic viscosity (Dietrich, 1982; Khatmullina and Isachenko, 2017; Kaiser et al., 2019; Waldschlager and Schuttrumpf, 2019; Elagami et al., 2022). Comparisons with earlier, well established relationships developed for mineral particles (Dietrich, 1982) suggest that for certain MP characteristics adjustments to the known relationships are needed (Khatmullina and Isachenko, 2017; Waldschlager and Schuttrumpf, 2019). However, adjustments or new formulations on the basis of experiments only reflect the specific shapes of MP particles being used in the experiment and a more general, systematic assessment of the relative importance of different particle characteristics for TSV estimates would be useful. We take a first step in this direction.

Models are a useful tool for a systematic evaluation of particle transport in aquatic environments. Different types of models have been used to simulate the settling and transport of plastic debris, MP particles and individual MP particle in water bodies over a wide range of spatial scales. At global and regional scales studies have focused on MP transport in oceans using Eulerian circulation models for flow in combination with Lagrangian (Berlemont et al., 1990; Maximenko et al., 2012; Jalon-Rojas et al., 2019; Nooteboom et al., 2020; Guerrini et al., 2021) or Eulerian (advective dispersive) (Mountford and Morales Maqueda, 2019) transport formulations. These types of models rely on an adequate description of particle settling, which is typically obtained from semi-empirical relationships derived from experiments. At the smaller, process scale the direct forces acting on particles or sets of particles have been simulated using computational fluid dynamics (CFD) (Zhang, 2017; Jeremy et al., 2020) or Lattice Boltzmann methods (Trunk et al., 2021). While those approaches are computationally expensive they can account for arbitrary particle shapes and properties and provide valuable mechanistic insights into the dominant factors controlling particle settling. In turn they can also be used to validate and refine semi-empirical relationships from experiments. Following this argument, the main objective of this study is to systematically evaluate different factors, such as particle density, size (or volume) and shape, water temperature, and initial orientation of the particle, which control the settling behavior and in turn the TSV of MP particles. We further hypothesize that the hydrophobicity of the surfaces of pristine MP particles will significantly affect their settling behavior and TSV. Along those lines we quantify TSV of MP particle using CFD simulations of a large set of individual particles representing the following seven different polymers: Polystyrene (PS), Polyamide 66 (PA66), Polycaprolacton (PCL), Polylactic acid (PLA), Poly (L-lactic) acid (PLLA), Polybutylenadipate terephthalate (PBAT), Polyvinyl chloride (PVC), which are commonly found in the lake environment

(Webb et al., 2013; Wright et al., 2013; Rocha-Santos and Duarte, 2015) over a range of shapes, densities and sizes. First we verify our simulation approach against a set of laboratory experiments using physical conditions and particle parameters in our simulations, which are identical to those from the laboratory experiments of (Elagami et al., 2022). We then compare our simulation results to existing semi-empirical relationships developed for estimating the TSV of mineral (Dietrich, 1982) and MP particles (Waldschläger and Schüttrumpf, 2019) before conducting a systematic, model-based evaluation of the key parameters controlling TSV and their relative importance.

2 METHODS

Three methods were used to investigate the TSV of MP particles i) numerical simulations, ii) laboratory settling experiments, iii) semi-empirical settling relationships. For our analyses we used two general classes of particles in terms of their shapes: a) regular spherical particles and b) irregular particles with arbitrary shapes. Additionally we generated a set of virtual, axis-symmetrical (regular) particles derived from revolved polygons (see **Section 2.4.1**) for a systematic evaluation of the effects of particle roundness, which were only evaluated with the CFD model. The irregular MP particles were selected from larger sets of particles made from seven abundant polymers (PS, PA66, PCL, PLLA, PLA, PBAT, and PVC). These MP particles can be categorized into biodegradable (PCL, PLA and PLLA) versus non-biodegradable (PS, PA66, PBAT, PVC) polymers. Their size and density ranged from 500 to 2,200 μm and 1.03 to 1.38 kgm^{-3} , respectively (cf. **Supplementary Material S1, Supplementary Table S1**). All biodegradable and non-biodegradable particles were provided by the Department of Macromolecular Chemistry at the University of Bayreuth, Germany. MP particles with sizes smaller than 500 μm were intentionally not considered as the simulation of their settling would require very fine numerical meshes in the simulations and excessive numerical costs, in particular if many particles are to be simulated. Furthermore the settling of very small particles will increasingly be affected by their electro-chemical surface properties and less by their physical shapes and properties (Zhang et al., 2017), so that other tools and methods would be required for an assessment of their settling. The same holds true for very specific shapes like fibers (Wei et al., 2021). Our study specifically focuses on particle settling in standing freshwater (e.g., freshwater lakes), which is in line with the experimental data available for verification. However, it is generally possible to also apply our methodology to other environments such as saltwater lakes, simply by changing the properties of the water in the model. Numerical simulations form the core of this work, while the experiments and semi-empirical relationships are used to provide a reference for the simulations. In the following the three different methods are described in more detail.

2.1 Model Setup and Boundary Conditions

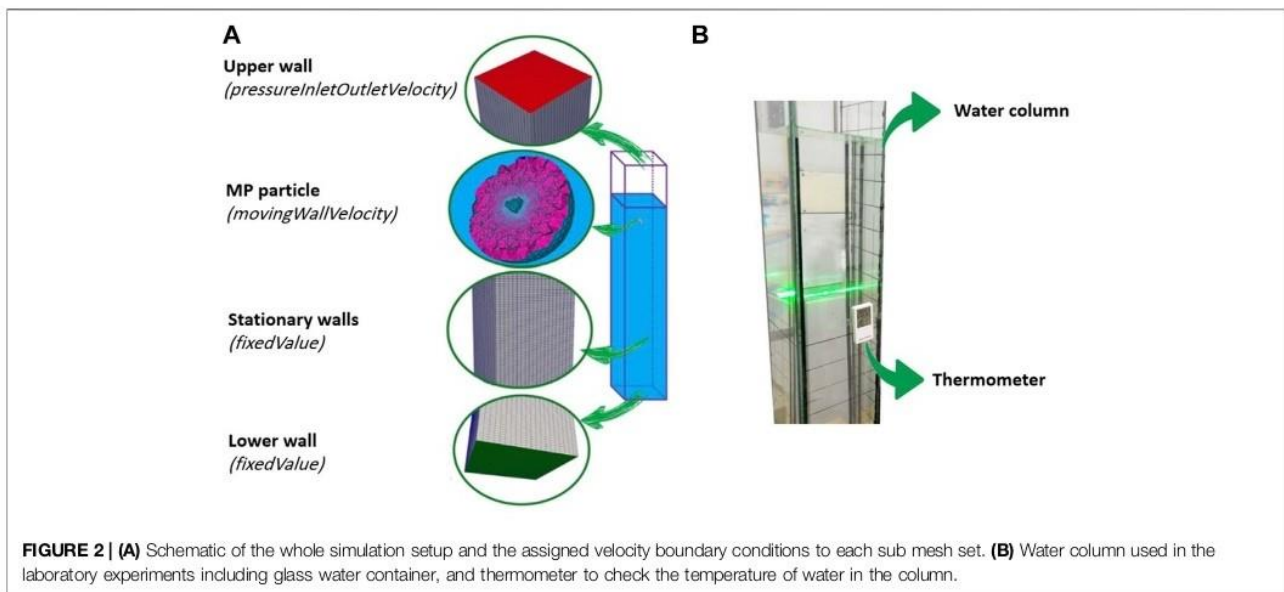
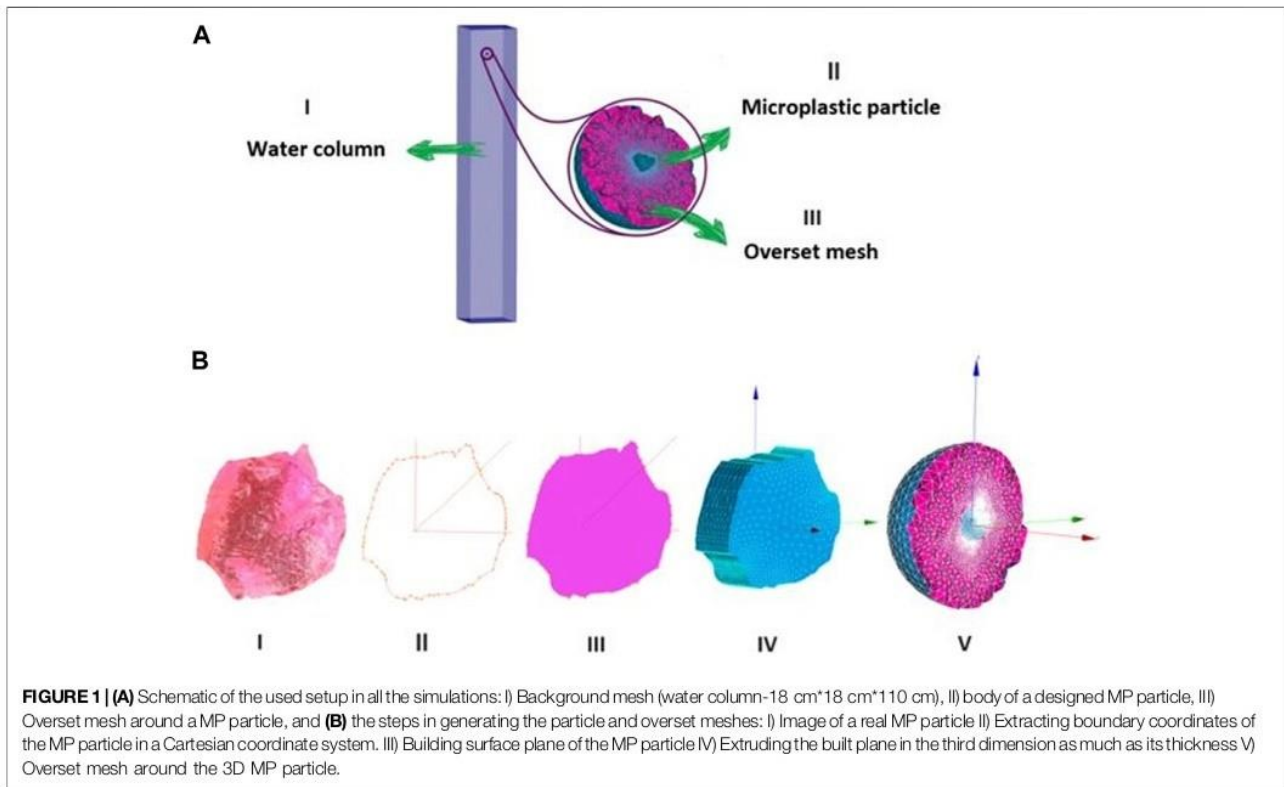
To simulate the TSV of MP particles, we use the solver `overInterDyMFoam` out of the open source C++ toolbox

`OpenFOAM v1812` (Weller et al., 1998). The used solver is for two incompressible, immiscible fluids (water and air in this application), which employs the volume-of-fluid method to capture the water-air interface. It solves the Navier-Stokes equations and supports moving meshes using the overset method. In the present study, we employed the overset method (also known as Chimera framework (Houzeaux et al., 2014)), as it allows to simulate MP settling in a deep-water column without the need for any mesh deformation.

The general simulation setup consists of two mesh domains for i) the water column (background mesh) and ii) the particle and its close surroundings (overset mesh) as shown in **Figure 1A**. As the two mesh sets are disconnected, the approach allows for a large freedom in movement (6 DOF) of the simulated object, especially compared to traditional approaches which employ mesh morphing/deformation. While the background mesh remains stationary, the overset mesh can move according to the calculated forces on the enclosed object. During each time step, the cells covered by the overset mesh are removed from the background mesh (cell type “hole”). The results are exchanged/interpolated at the boundary between the background and overset mesh using specific patch types. As the overset mesh is moving, the holes and interfacial patch cells are re-defined for each time step based on the current position of the overset mesh.

Figure 1B illustrates the design steps taken to mesh the arbitrarily shaped MP particle based on images taken from the particles in the laboratory experiments and how the overset mesh encloses the particle's body. The SALOME 9.4 (Ribes and Caremoli, 2007) software was used to generate the numerical meshes for all simulation setups. The software ParaView (Ahrens et al., 2005) was used for visualization of the conducted simulations.

Figure 2A illustrates the general setup of the simulations representing the water column dimensions and the boundary conditions in the experiments (see **Section 2.2** for more details). To implement the same condition as in the experiments, in all of the performed simulations $1 \text{ mm}^2\text{s}^{-1}$ and 0.9982 gcm^{-3} were considered as water kinematic viscosity and density at 20°C respectively. Moreover, the velocity boundary condition of “`pressureInletOutletVelocity`” was set to keep the upper side of the column open and in contact with air. In turn an air/water interfacial tension of “`sigma: 0.007 kgs-2`” was set for all simulations. The outer surface of the MP particle which is settling in the water (a viscous fluid), is surrounded by stationary walls of the column. Hence, to represent the velocity boundary conditions accordingly, the boundary types “`movingWallVelocity`” and “`fixedValue`” in OpenFOAM were used for the walls of the MP particle and water column, respectively. More details concerning the applied initial and boundary conditions for pressure, phase saturation and velocity have been provided in **Supplementary Table S2**. Quantities such as particle volume, mass, center of mass (COM), location, and moment of inertia (MOI) (cf. **Supplementary Material S3**), are important input parameters for the OpenFOAM solver and had to be accurately calculated beforehand.



2.2 Experiment Setup and Data

We used TSVs measured in the laboratory for a set of spherical and irregularly shaped MP particles (Elagami et al., 2022) for comparison with the CFD results. Besides that, we carried out an additional set of experiments to test our hypothesis, that the

hydrophobicity of MP particles will affect their TSV. Settling experiments were first run for pristine, untreated PLA and PS particles in the size range from 1 to 2 mm and then repeated after the particles had been treated by immersion in a surfactant (Tween-20) for 2 hours. All the experiments were conducted

using the same experimental setup as in (Elagami et al., 2022) consisting of a water column with the dimensions of 18 cm*18 cm*110 cm and a Particle Image Velocimetry (PIV) system to measure the settling velocity (**Figure 2B**). The 2D-PIV system (iLA 5,150) consists of a LED light sheet with 530 nm wave length as light source, a 40 fps high speed camera to track MP velocities during settlement, and also the hardware to synchronize the image acquisition frequency with the light source. The air conditioned laboratory and the water temperature were kept constant at 20°C and two thermometers were used to record the temperature of water during the experiments.

2.3 Comparison of Simulations to Semi-Empirical Relationships and Experimental Data

Comparison of the model with results from experiments and semi-empirical relationships was carried out in two steps: First, simulations of 120 irregular MP particles made of the polymers PS, PA66, PCL, PLLA, PLA, and PBAT from the experiments in (Elagami et al., 2022) were conducted to quantify their TSV and the findings were compared to the TSVs measured in the laboratory experiments. Images of some of these MP particles and the associated “model designed” particles for the numerical mesh in the simulations are illustrated in **Supplementary Table S3** (cf. **Supplementary Material S4**) as an example. In the second step, simulated TSVs were compared to TSVs estimated based on two existing semi-empirical relationships between TSV and particle characteristics, namely i) the relationship originally proposed by Dietrich (1982), Dietrich, (1982) for mineral particles, which has been shown to return acceptable TSVs for regular MP particles (Khatmullina and Isachenko, 2017; Kaiser et al., 2019), and ii) the relationship formulated by Waldschläger et al. (2019) (Waldschläger and Schüttrumpf, 2019) for a broad size and shape range of MP particles. TSV of spherical particles with ten different sizes (0.5, 0.6, 0.75, 1, 1.25, 1.5, 1.75, 2, 2.25, and 2.5 mm) were simulated for each polymer with densities of 1.03 (PS), 1.12 (PA66), 1.14 (PCL), 1.20 (PLLA), and 1.38 gcm⁻³ (PVC), and then the simulation results were compared to the TSV results of the same particles returned by the two semi-empirical relationships.

2.4 Evaluating the Influence of Physical Parameters on TSV of MP Particles

After confirming adequate performance of the model in the previous stage, the impact of particle roundness, size and density as well as water temperature on TSV were systematically evaluated to assess the sensitivity of the TSV of MP particles to the variation of each of the these physical parameters.

2.4.1 Effects of Shape Characteristics

To systematically investigate the effect of different levels of roundness on TSV we used regular polygons (**Figure 3B**). Increasing the number N of sides of a regular polygon, yields

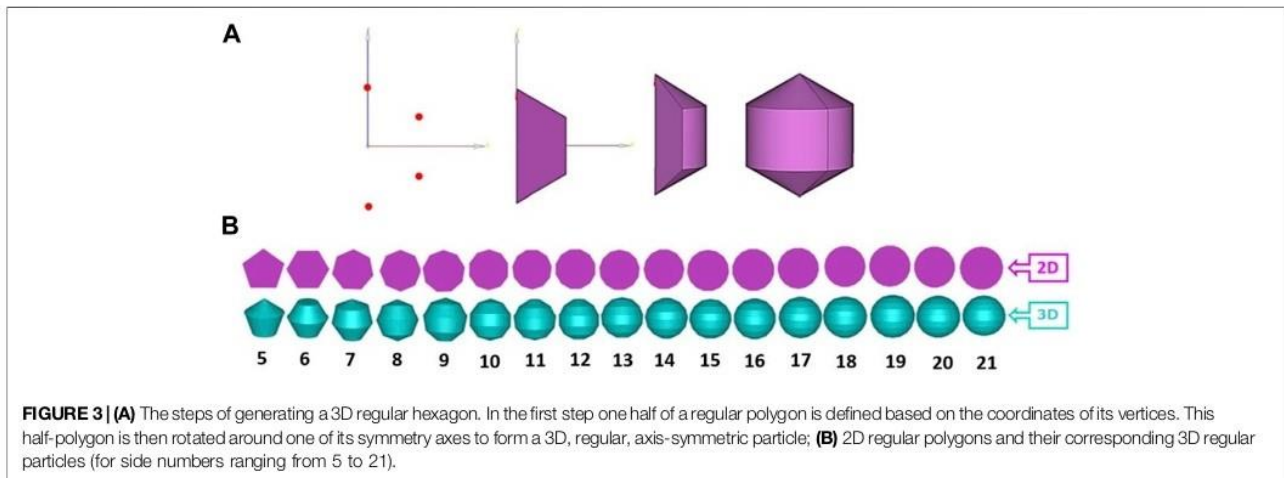
polygons with a growing number of sides of shorter length and more internal angles, which evolve towards a perfect circle when N approaches infinity. Revolving such regular polygons with identical areas around one of their symmetry axes, produces 3D shapes with equal volumes (**Figure 3A**). This procedure was followed to produce five series of regular polygons with the same areas of their 2D projections as circles with diameters of 0.5, 1, 1.5, 2, and 2.5 mm (cf. **Supplementary Material S5**, **Supplementary Figure S2**) to generate a set of “virtual particles” with increasing levels of roundness but the same volumes for a model-based assessment of the effects of roundness on TSV. To reduce the computational costs, simulations were only carried out for virtual particles with a density of 1.38 gcm⁻³ (PVC), to show the general trend of the impact of roundness on the TSV of MP particles.

The level of roundness of the irregular MP particles used in our study was classified based on the Powers scale of roundness and the Corey Shape Factor (CSF), both of which are metrics having commonly been used in other studies (Dietrich, 1982; Khatmullina and Isachenko, 2017; Kaiser et al., 2019; Waldschläger and Schüttrumpf, 2019). The Powers scale of roundness is a measure, which defines particle roundness on a scale from 1 (very angular) to 6 (well rounded) based on the average of two assessments by independent observers using a graphical chart for comparison (Powers, 1953). The CSF is a measure of the flatness of a particle and is determined based on the lengths of its shortest, intermediate and longest perpendicular axes (Corey, 1949).

The surface area to volume ratio (SA:V) is also an important physical characteristic of MP particles, derived from their shape. It determines how drag forces are exerted on a MP particle and how these forces are distributed across its surface. The larger the SA:V, the more friction forces relative to gravitational forces will be exerted on the particle and consequently the less TSV the particle will have and vice versa. The SA:V was determined based on calculations of the particle surface area and volume from the numerical mesh for all regular and irregular MP particles.

2.4.2 Impact of Particle Density and Volume

First we selected a distinct set of polygon-shaped particles from the analysis of roundness and systematically increased their densities and sizes. These peculiar shapes of the particles were intentionally chosen to be able to simultaneously evaluate the relative influence of evolving particle roundness versus the effects of increasing particles size and density. To this end, the polygons with areas identical to a sphere with 1 mm diameter and the density of $\rho_{PVC} = 1.1 \text{ gcm}^{-3}$ were selected for the analysis. By choosing this initial size, the new set of virtual particles with increased sizes approximately stays within the size range of the MP definition. To examine the size effects, generated particles corresponding to the polygons with 5, 6, 7, 8, and 12 sides as well as a sphere were chosen and their volume enlarged by 10, 20, 50, and 100%. Similarly, the same percentages were used to increase the density of the original particles, which means that the initial density of $\rho_{PVC} = 1.1 \text{ gcm}^{-3}$ was increased by 10, 20, 50, and 100% to yield particle densities of 1.21, 1.32, 1.65, and 2.2 gcm⁻³ respectively. The highest density obtained using this procedure

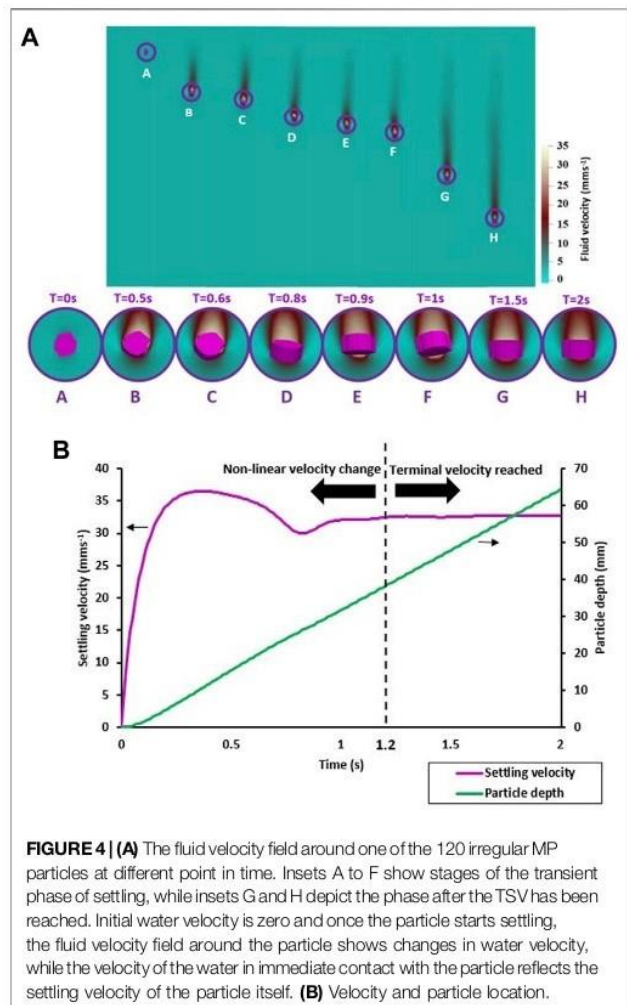


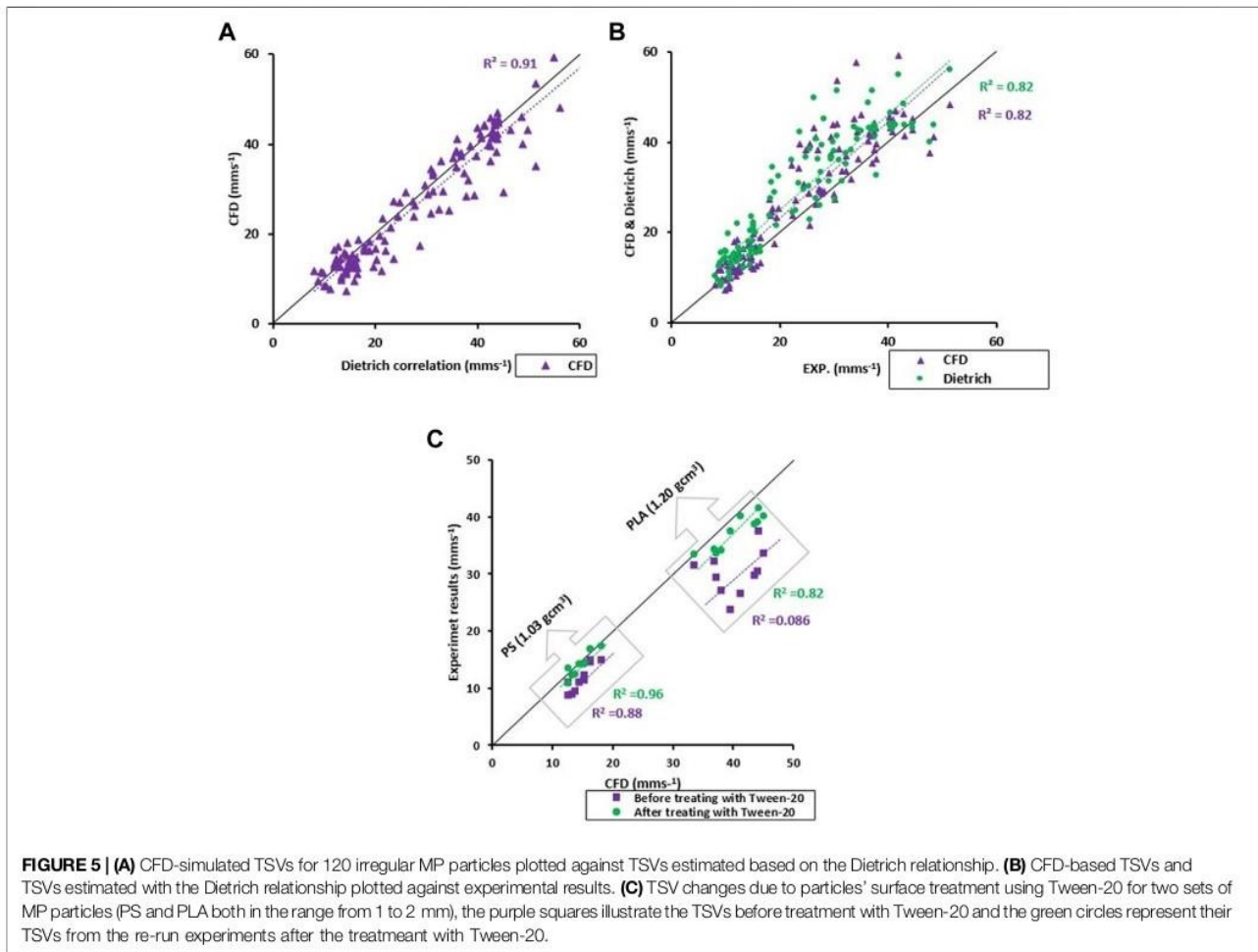
is only found in very heavy polymers (e.g., polytetrafluoroethylene ($2.1\text{--}2.3\text{ gcm}^{-3}$) (Chubarenko et al., 2016)), which may be found less frequently in the environment. However, for the purpose of a systematic evaluation of density effects this was assumed to be acceptable.

In addition 10 irregular MP particles (from the particles used in Section 2.2) with an equivalent diameter range from 1 to 2 mm, a Powers scale of roundness (Powers, 1953) of 4 and a Corey Shape Factor (CSF), (Corey, 1949), ranging from 0.7 to 0.85, were selected as model particles to investigate the impact of an increase in size and density on TSVs. The initial density of the particles was assumed to be 1.1 gcm^{-3} , and similar scenarios with respect to increasing volume and density as performed for regular particles were repeated for the irregular ones as well.

2.4.3 Temperature

Vertical temperature gradients and the associated changes in water density result in a thermal stratification of lakes during summer with the formation of an epilimnion, metalimnion, and hypolimnion (Herschy, 2012; Singh et al., 2019). The vertical temperature variations lead to changes in the kinematic viscosity of the water and the resulting TSV of the particles as the move from the relatively warm epilimnion, via the metalimnion to the colder hypolimnion (Gorham and Boyce, 1989; Singh et al., 2019). These changes in TSV will affect the residence times of MP particles in the different compartments of a stratified lake system. To quantify the effects of temperature changes on TSV in the different compartments, TSVs were simulated for the different temperature regimes. In temperate climates water temperatures in the three main compartments typically range from 18 to 24°C, 18–7.5°C, and 7.5–4°C in the epilimnion, metalimnion, and hypolimnion, respectively (Boehrer and Schultze, 2008). TSVs for 30 randomly selected irregular PVC particles (from the set of particles used in Section 2.3) were simulated for temperatures of 20, 10 and 4°C as characteristic temperatures for the epilimnion, metalimnion and hypolimnion respectively. The densities and kinematic viscosities of water at 10 and 4°C are 0.9997 gcm^{-3} , $1.3063\text{ mm}^2\text{s}^{-1}$ and 1 gcm^{-3} , $1.5674\text{ mm}^2\text{s}^{-1}$, respectively (Wagner and Kretzschmar, 2008).





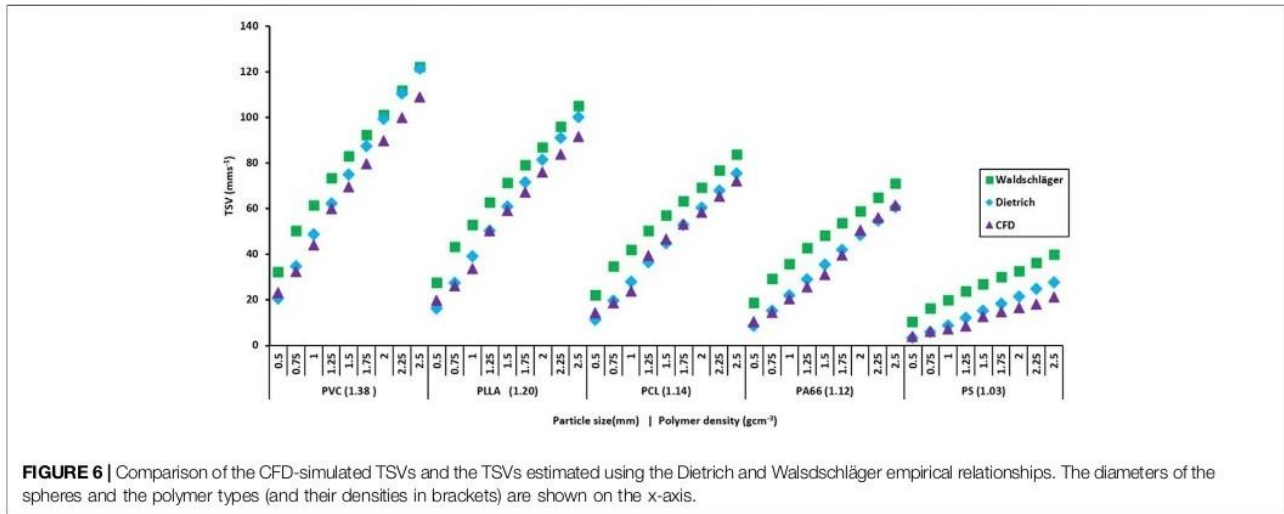
3 RESULTS

3.1 CFD Results for Irregular MP Particles Compared to Experimental Results and the Dietrich Relationship

The settling process for one of the 120 simulated irregular MP particles is illustrated in **Figure 4A**. In the initial phase of the settling the particle velocity dynamically changes as the particle shows secondary movements such as rotations and tumbling (**Figure 4B** at $t = 1.2$ s and **Figure 4A**, in-set A-F) before the particle reaches a stable orientation in the fluid with a constant settling velocity at $t = 1.2$ s. This initial, dynamic phase lasted around one second for all simulated particles. The second phase was characterized by a stable particle orientation (**Figure 4A**, G and H) and constant settling velocities for most particles. Some particles, however, showed small harmonic oscillations in their continuing downward movement, but with a constant average TSV.

Simulated TSVs of 120 individual MP particles are plotted against the TSVs estimated by the Dietrich relationship in

Figure 5A. CFD results are scattered along the 1:1 line with a slope of 0.95 and a coefficient of determination (R^2) of 0.91. In **Figure 5B** TSVs simulated with CFD as well as TSVs from the Dietrich semi-empirical relationship are plotted against TSVs from the settling experiments. TSVs from CFD simulations as well as estimates based on the Dietrich relationship overestimate TSVs compared to the settling experiments. The coefficients of determination still showed relatively high values at 0.82 for both correlations and both trend lines have roughly the same slope of about 1.059. The strongest deviations were found for the biodegradable polymers (i.e., PCL, PLA and PLLA). However, a deviation was observed for PS, as a non-biodegradable polymer, as well. For PLA and PS particles an additional set of settling experiments were performed, initially with pristine untreated particles and subsequently with particles being treated with a surfactant to assess the effects of hydrophobicity on the TSV. Results of these additional experiments are plotted in **Figure 5C**. While the untreated particles show significantly slower experimental TSVs compared to the TSVs obtained from the CFD model, this deviation between simulated and experimental TSVs is practically removed for the treated particles. The R^2 improved from $R^2 = 0.88$ to $R^2 = 0.96$ and from $R^2 = 0.086$ to $R^2 =$



0.82 between the untreated and treated particles for the PS- and PLA-particles respectively (Figure 5C).

3.2 Evaluation of CFD Results for Spherical MP Particles Against the Semi-Empirical Relationships

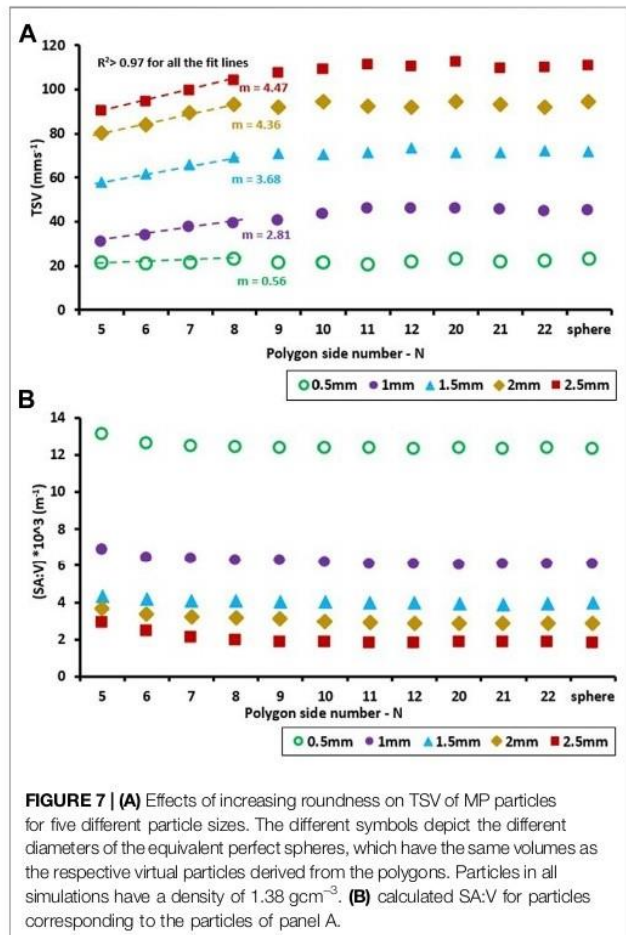
In Figure 6 the CFD-simulated TSVs are plotted against particle size and density for a set of spherical particles. For comparison the TSVs estimated based on the (Waldschläger and Schüttrumpf, 2019) and (Dietrich, 1982) relationships are plotted for the same particles. For all polymers TSVs increased quasi-linearly with particle diameter. However, the slope of the quasi-linear relationship decreased with declining polymer density (density declines from left to right in Figure 6).

Overall the TSVs simulated with CFD are quite well matched by the values estimated from the Dietrich equation ($R^2 > 0.98$). This is especially the case for the smallest diameters (0.5 and 0.75 mm), for which the simulated and estimated TSVs match very closely for all polymer types and densities. For larger diameters the match slightly deteriorates. In contrast, the TSVs predicted by the Waldschläger relationship are systematically biased towards higher TSV values for all particle sizes and diameters. This bias gets slightly smaller with increasing particle size and density.

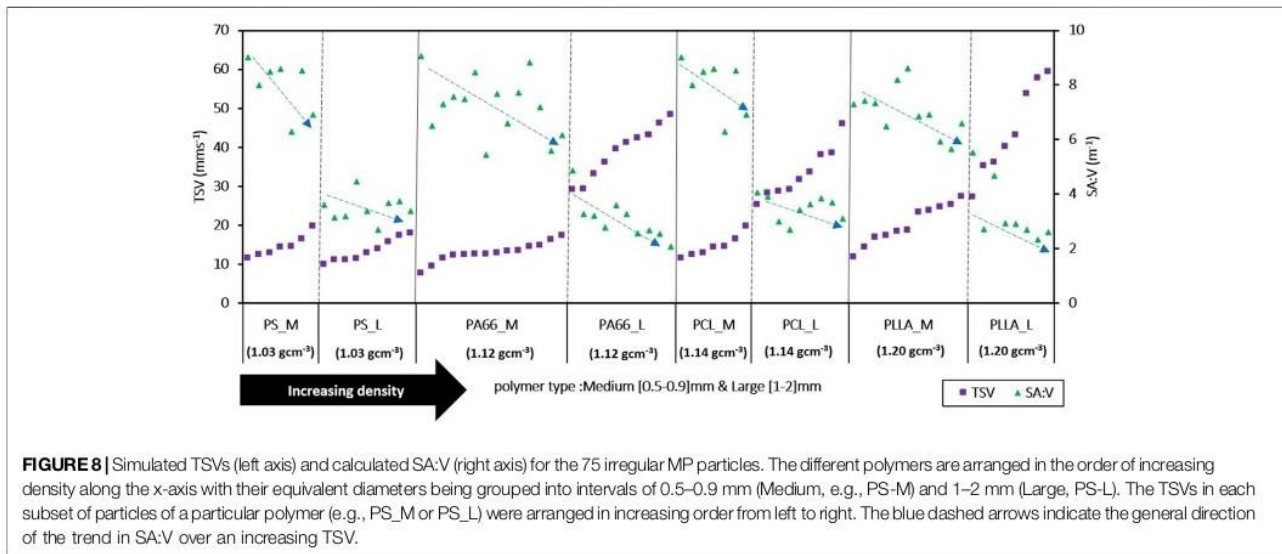
3.3 Systematic Investigation of the Relative Importance of Different Parameters on TSV

3.3.1 Roundness

Increasing the degree of roundness of the virtual particles from $N = 5$ to 9 causes a linear increase in TSVs for all the examined particle sizes (Figure 7A). Linear regressions between the degree of roundness (N) and the TSV yield coefficients of determination (R^2) larger than 0.97 for all particles. The slope of the linear regressions steadily grows from the smallest (0.5 mm) to the largest (2.5 mm) particle diameter.



Comparing the changes in SA:V for increasing side numbers (Figure 7B) with the corresponding changes in TSVs (Figure 7A), shows that for a given particle diameter a



decreasing SA:V is associated with an increase in TSV. However, for all the investigated particle diameters a threshold in N emerges at the value of 8, beyond which a further increase in N does not yield further increases in TSV. Beyond this threshold changes in SA:V with increasing N become minimal and in turn show little to no effect on the simulated TSVs. In this range TSV stays quasi-constant only showing minimal, non-systematic variations (Figure 7A, $N > 8$). Since the magnitudes of TSV and SA:V for $N > 8$ were very similar, we removed the data for $13 \leq N \leq 19$ to improve the readability of the figure.

3.3.2 Surface Area to Volume Ratio—Particles With Irregular Shapes

The general relationship between SA:V and TSV, was also evaluated for all the 75 irregular MP particles used in the simulations in Section 3.1 (Figure 8). Sorting the TSVs in ascending order for each type of polymer depicted descending trends for SA:V ratios (dashed blue arrows in Figure 8). This inverse relationship indicates that lower SA:V generally facilitate faster TSVs. However, this trend shows significant scatter, in particular for the lighter polymers such as PS. Spearman rank correlations between the SA:V and TSV for each of the polymer classes yielded values ranging from 0.31 to 0.9, indicating only mild correlations between the two variables. In contrast spearman rank correlations between the particle volumes and TSV showed generally higher values ranging from 0.58 to 0.99, indicating that variability in TSV for the irregular particles investigated here is predominantly driven by variability in particle volume (i.e., weight), while the effect of variability in the SA:V is secondary.

3.3.3 Effects of Increasing Particle Size and Density on TSV

3.3.3.1 MP Particles With Regular Shapes

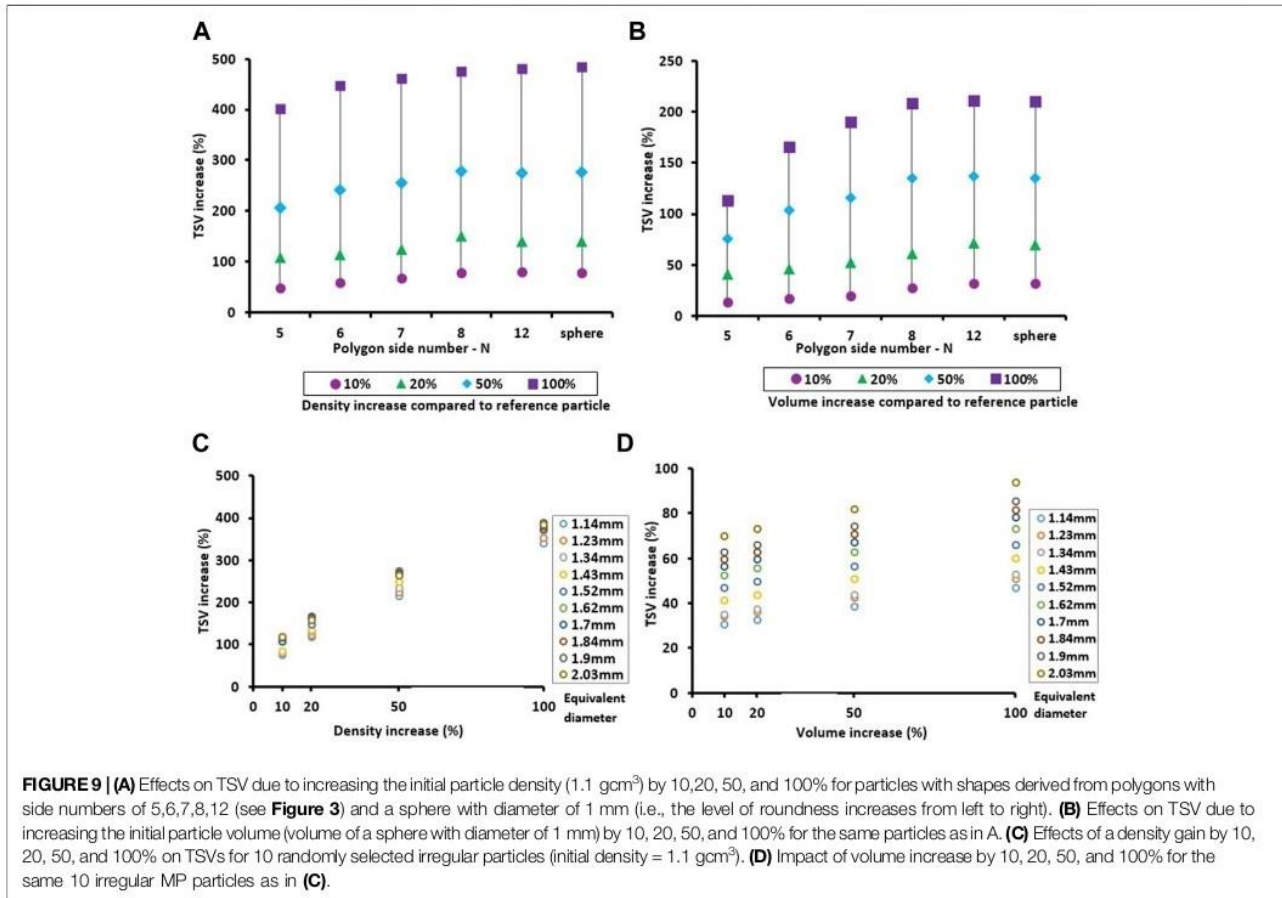
Effects of density and size (volume) on the TSV of the MP particles are depicted in Figure 9. For a 10% increase in density

the TSV increases from 48% for the least rounded particle ($N = 5$) to 78% for a perfect sphere with a gradual increase with the degree of roundness. For density increases of 20, 50 and 100% the associated increases in TSV range between 107 and 139%, 206 and 275% and 401 and 483% respectively. The largest effects on TSV by increasing density can generally be seen for a perfect sphere, which has the smallest SA:V. Doubling the density of a sphere increases the associated TSV by approximately 50% compared to a respective particle derived from a polygon with five sides.

Plotting the increases in TSV for the same particles used in Figure 9A over the same percent increases in volume (Figure 9B) reveals similar patterns as for the increases in density, but at significantly lower magnitude. Increases in TSV for the least rounded particles ($N = 5$) ranged from 13 to 112% when and from 32 to 223% for a perfect sphere ($N = \infty$). Similar to the effects of increasing density the largest effect on TSV can be seen for particles approaching the shape of a sphere ($N > 8$).

3.3.3.2 MP Particles With Irregular Shapes

The effect of increasing the density of the irregular MP particles on their TSVs was generally quite similar to that observed for the regular particles (Figure 9C). For example, doubling the density of these particles led to an increase in TSV of up to five times, only slightly less than the maximum increase for the regular particles. However, the effect of increasing volume on TSV for the irregular MP particles deviated in magnitude from that of particles with regular shapes. While doubling the volume of the regular particles with a high level of roundness (e.g. $N > 8$) led to TSV increases of 200% (Figure 9B), the irregular particles only reached maximum TSV increases around 90% (Figure 9C). However, the regular particles with the least degree of roundness ($N = 5$) generally showed significantly smaller TSV increases (<120%), which are more in the range observed for the irregular particles. Interestingly, the clear sorting of the volume related TSV-increases for the irregular particles by their equivalent

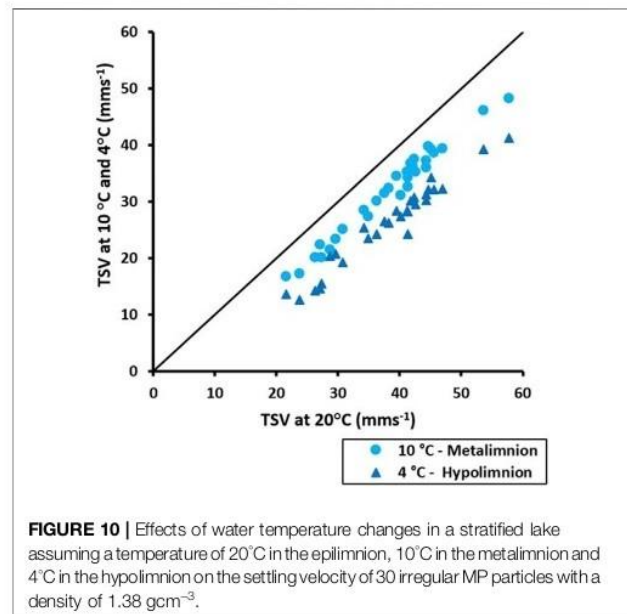


diameter (**Figure 9D**) was not seen for the effects of density-increases (**Figure 9C**). This indicates that changes in surface drag due to the increase in surface area resulting from the volume-increase is directly related to the particle's equivalent diameter, while the equivalent diameter does not directly affect TSV changes due to an increase in density.

Calculating the coefficients of determination for the correlation between simulated TSVs, and the corresponding particles volumes and densities yielded values of $R^2 > 0.90$, and $R^2 > 0.94$, respectively. This implies that variations in particle TSV can be largely explained by variations in particle density and volume and that shape characteristics of the investigated particles play less of a role in determining the settling velocity.

3.3.4 Effects of Water Temperature on TSV

The TSVs in the epilimnion with an assumed reference temperature of 20°C are plotted against the TSVs in the metalimnion, with an assumed temperature of 10°C (light blue circles), and the hypolimnion with an assumed temperature of 4°C (dark blue triangles) for 30 MP particles (**Figure 10**). The average decrease in TSVs resulting from the temperature drop between the epilimnion and the hypolimnion is 32%. The largest temperature effects on TSVs can be seen for the smallest particles



[equivalent diameter (cf. **Supplementary Material S4**, Eq. 5) from 0.57 to ~1 mm], with a drop in TSVs from 32 to 46% compared to the reference temperature of 20°C.

4 DISCUSSION

4.1 CFD-Based Assessment of the Initial Settling Process

Although the main purpose of our simulations was to quantify the TSVs of MP particles, which defines their overall settling times in lentic water bodies such as lakes (Lambert and Wagner, 2018), the transient CFD simulations also allow to evaluate the dynamic initial behavior during settling. The settling of all particles, with regular or irregular shape, showed two distinct phases during the initial settling period. The first phase represents the time period before the particle reaches the TSV. In this phase the irregular particles often show dynamic movements including rotations and tumbling with dynamical changes in settling velocities before they finally reach a stable settling position at the TSV. This marks the beginning of the second phase, in which the particles settle with a quasi-steady TSV. However, even after a steady TSV is reached, gentle secondary particle movements are possible depending on the particle's shape. The specific time to reach the TSV needs to be considered in experimental setups (Khatmullina and Isachenko, 2017; Waldschläger and Schüttrumpf, 2019) to ensure that velocity measurements are done at a point where the forces exerted on the particle are balanced and the TSV has truly been reached. In our simulations, the initial phase of settling with transient velocities only lasted for a fraction of a second (usually $t < 0.5$ s) for symmetric particles such as spheres. In contrast for asymmetric particles with different roundness levels and stronger secondary movements, this phase could last up to one second (more details on the behavior of MP particles before reaching TSV, cf. **Supplementary Material S6**). The beginning of phase two is marked by the point when the particles reach their stable settling position at a steady TSV. However, some particles showed small oscillating secondary movements with very small harmonic velocity fluctuations around a steady average TSV during this phase. These oscillating, rotating, and tumbling secondary movements have also been reported from experimental work in the laboratory (Khatmullina and Isachenko, 2017; Waldschläger and Schüttrumpf, 2019). Given that the TSVs of the particles are reached very fast, the initial phase with transient velocities is negligible in terms of an assessment of the settling of particles in larger stagnant water bodies such as lakes.

4.2 Comparison of TSVs From CFD-Simulations, Semi-Empirical Relationships and Settling Experiments

The CFD model accounts for the exact particle shape and density and all the hydrodynamic forces that are exerted on the particle body. Therefore CFD simulations can be considered to reflect the true movement of a particle in water. As such CFD results can be used on the one hand to evaluate the accuracy of commonly used

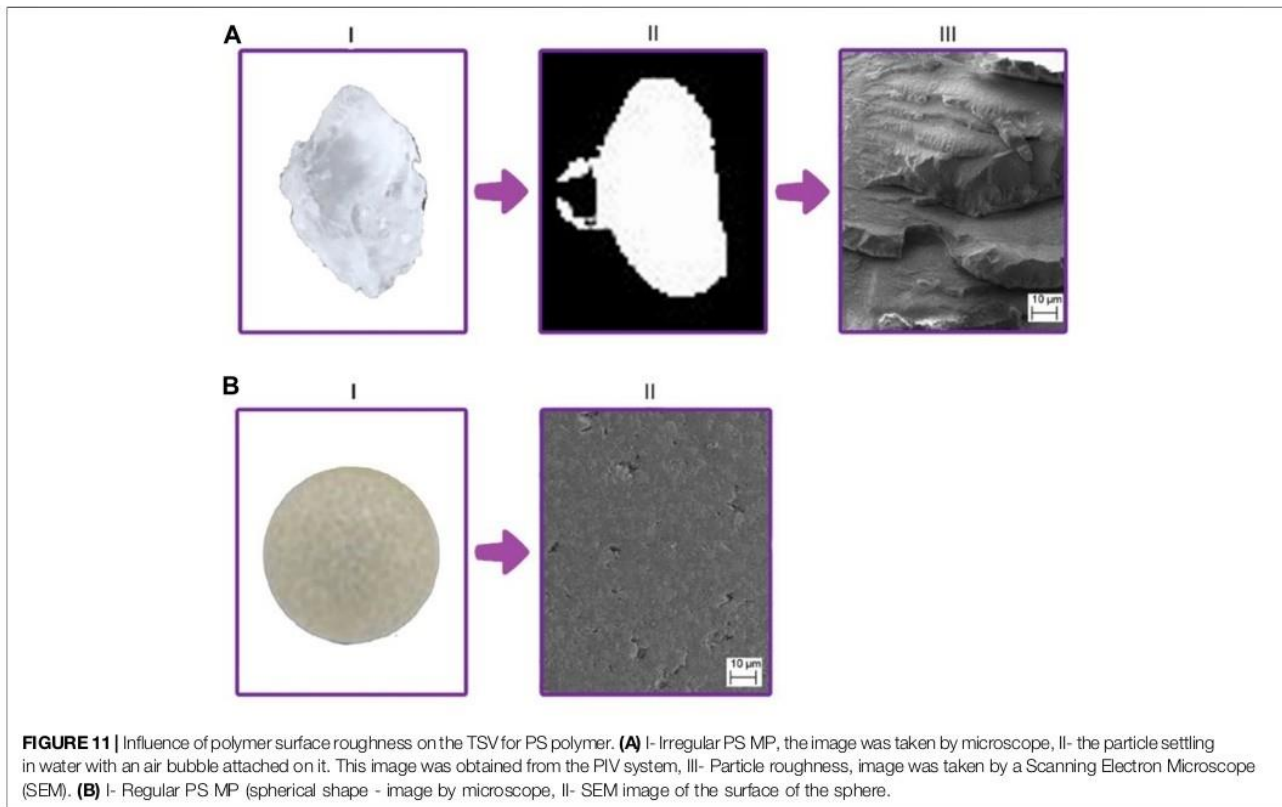
semi-empirical relationships, which make simplifications in the description of particles shapes, and on the other hand reveal additional non-hydrodynamic effects on particle TSVs by comparison with the results from settling experiments with the real MP particles of the same shapes and densities. In the following we will first briefly discuss the results from the spherical particles (**Section 3.2**) and then move to a more detailed discussion of the results from the irregular particles (**Section 3.1**).

4.2.1 Regular, Spherical Particles

For the spherical particles the CFD-simulated TSVs were generally better matched by estimates from the Dietrich relationship than by estimates obtained from the Waldschläger relationship (Waldschläger and Schüttrumpf, 2019) (**Figure 6**). The Dietrich relationship (Dietrich, 1982) had originally been developed for mineral particles of significantly higher densities ($>2.2 \text{ gcm}^{-3}$) than the polymers investigated in this study ($<1.4 \text{ gcm}^{-3}$). Surprisingly, however, it also yielded very reasonable TSV estimates for the much lower-density MP particles. This good agreement is likely due to the strong shape similarities between the mineral particles used to develop the Dietrich relationship (including smooth spheres, prolate ellipsoids, natural and crushed sediments (Dietrich, 1982)) and the MP particles we used in this study. In contrast the study by Waldschläger et al. (2019) (Waldschläger and Schüttrumpf, 2019) also included particles with significantly different shapes and also with lower densities and is in turn adapted to accommodate a broader range of particle characteristics. While we used very detailed descriptions of 3D particles shapes in our simulations, Waldschläger et al. (2019) only used the relatively coarse measures of the Powers scale of roundness and the CSF to describe particle shapes in their empirical relationships. These measures may not fully define all shape characteristics that affect the hydrodynamic forces acting on the particles during settling. This presumably explains the larger offset between the CFD-simulated TSVs and the TSV estimates based on the Waldschläger relationship.

4.2.2 Irregular Particles

Comparing the CFD-based TSVs with the TSVs obtained from the Dietrich semi-empirical relationship for the corresponding irregular MP particles yielded a strong correlation with an R^2 of 0.91 and a deviation of the slope of the regression line to the 1:1 line of only 5% (**Figure 5A**). This indicates that the Dietrich relationship generally provides a good estimate of the TSVs of the particles with their respective shapes and densities. The scatter of the data points along the 1:1 line we attribute to the fact that the Dietrich relationship uses only three principal dimensions of a particle (i.e., longest, intermediate, shortest perpendicular axes) to calculate the particle equivalent diameter and its relative flatness (CSF) (Dietrich, 1982), which does not allow to account for individual details in differences in particle shapes. Furthermore, the Powers scale of roundness, a measure used in the Dietrich relationship to define the roundness of a particle is an observational measure, which for well-rounded elliptical and



spherical particles with only small differences in their shapes will yield the same values.

Although the comparison between the CFD-simulated TSVs and the TSV estimates from the Dietrich semi-empirical relationship with the TSVs from the settling experiments overall showed a good agreement ($R^2 = 0.82$), simulated (CFD) and estimated (Dietrich relationship) TSVs were generally biased towards faster TSVs compared to the experimentally determined values (**Figure 5B**). The strongest deviations we observed for the biodegradable polymers (PLLA, PCL, PLA), however, also MP particles of PS, a non-biodegradable light polymer, showed a noticeable deviation. We suspect that the hydrophobicity of the particle surfaces may have been the reason for this deviation between simulated and observed TSVs (**Figure 5C**). Hydrophobicity is a common characteristic of the surfaces of most polymers typically found in waste (Al Harraq and Bharti, 2021) and can enhance the sorption of hydrophobic contaminants to MP particles (Kwon et al., 2017) leading to bioaccumulation of these contaminants (Ziccardi et al., 2016). It can also potentially lead to the adhesive attachment of air (Al Harraq and Bharti, 2021). The latter process will change the net density of the particles by adding an additional upward force, which will affect their movement in water. This phenomenon is in fact a commonly used method to separate MP particles from water filled sediments (Renner et al., 2020).

The fact that the treatment with the surfactant Tween-20 shifted the experimental TSVs of PLA and PS particles to the CFDs-simulated TSV values (**Figure 5C**), strongly suggests that the observed TSVs deviations are related to effects of surface hydrophobicity. This general interpretation is further corroborated by the observation of discrete, large air bubbles at surface irregularities on some of the particles during settling in PIV images (**Figure 11A-II**). We attribute the generally stronger deviation of the experimentally determined TSVs from the respective CFD-simulated TSVs for the biodegradable polymers to the fact that the surfaces of biodegradable polymers tend to have higher surface roughness to facilitate better degradation (Szewczyk et al., 2019; Moghadam and Tafreshi, 2020). Very small surface heterogeneities associated with those rougher surfaces (Al Harraq and Bharti, 2021) probably facilitate enhanced adhesive attachment of air at surface irregularities. Air-attachment, with potential effects on TSV, will also occur on the rough surface of non-biodegradable particles, but presumably to a lesser degree (**Figure 11A-III**). This could explain why we also observed a noticeable deviation of the experimental TSV from the respective CFD-estimate for the irregular particles made of PS (**Figure 5C**), a non-biodegradable polymer with a density (1.03 g cm^{-3}) very close to that of water. The low density of the PS particles makes them more susceptible to changes in TSV due to attached air than the non-biodegradable particles made of denser polymers, for which

no significant deviations between experiment and CFD had been observed.

The images of particles (taken by a light microscope, Zeiss Axioplan) and a high definition digital single lens reflex (DSLR) camera Cannon EOS 5D)) and their surfaces in **Figure 11** generally illustrate the differences in the surface roughness of an irregular, non-biodegradable particle (**Figure 11A-I**) and a spherical non-biodegradable particle (**Figure 11B-I**) made from the same type of polymer (PS). The surface of the irregular particle shows larger irregularities and a generally rougher surface structure (**Figure 11A-III**) compared to the spherical particle with a relatively smooth surface (**Figure 5B-II**). The surface irregularities and the rougher surface of an irregular PS particle will better facilitate the attachment of larger air bubbles than the smoother surface of a respective spherical PS particle. This interpretation is further supported by earlier settling experiments using spherical particles with and without treatment with Tween-20, which had been conducted at the Limnological Research Station at Bayreuth University (personal communication, Hassan Elagami), which had practically shown no difference in the TSVs before and after treatment with Tween-20.

4.3 Roundness and SA:V Relationship and its Influence on TSVs of MP Particles

In previous studies the degree of roundness of a particle has commonly been considered as an important parameter for estimating the TSV of particles and it has usually been described by using the CSF and the Powers scale of roundness (Dietrich, 1982; Khatmullina and Isachenko, 2017; Waldschläger and Schüttrumpf, 2019). We examined the effect of roundness more systematically using exact 3D particle shapes obtained from revolving polygons with an increasing number of sides (see **Section 2.4.1** for more details). Increasing the level of roundness leads to a decrease in SA:V (**Figure 7B**) and thus less drag forces being exerted on the particles body resulting in a faster TSV. This general inverse relationship between SA:V and TSV can be observed for the regular, spherical particles (**Figure 7A**) as well as the irregular particles (**Figure 8**). However, it is more evident for the virtual, regular particles investigated here as they all have the same volumes and densities, isolating roundness and the associated SA:V as the only variable parameters (**Figure 7**). However, even for the irregular MP particles shown in **Figure 8**, which have variable volumes, the general descending trend in SA:V for increasing TSVs is clearly discernable.

The gradual increase of the slopes of the regression lines for increasing particle diameters (**Figure 7A**) suggests that the magnitude of the effect of increasing roundness on a particle's TSV increases with particle diameter. While the larger particles show significant increases in TSV over the initial increases in roundness, the smallest particles with a diameter of 0.5 mm practically do not show any significant change in TSV over the same increase in roundness. We attribute this to the drastic increase in SA:V when moving from particles with 1 mm diameter to the smallest particles with a diameter of

0.5 mm (**Figure 7B**). For these very small particles the SA:V is very high and in turn their TSV is driven more by the drag forces resulting from their large surface area relative to their volume than by additional hydrodynamic forces resulting from changes in their roundness.

4.4 Particle Density and Volume Effects on TSV

A comparison of the magnitudes of TSV increases associated with a density increase versus a volume increase for regular and irregular particles, respectively, showed a clear dominance of density over volume effects on TSV for the same percent increases in either parameter (**Figure 9**). By increasing the density of a MP particle, the only force that is amplified is weight, which will accelerate the downward movement of the particle. For the same percentage increase in volume in turn, the respective increase in weight and downward gravitational force is counteracted by additional upward forces resulting from an increase in drag due to the enlarged surface area and in the buoyancy of the particle, both attenuating the increase in TSV.

The relative increases in TSV in percent for the same percentage increases in density were very similar between the regular (**Figure 9A**) and irregular particles (**Figure 9C**) with values exceeding 400% for a doubling of the density. This was not the case for the same percentage increases in volume. While we observed TSV increases of up to 200% for the regular particles (**Figure 9B**) the irregular particles only showed TSV increases of less than 100% (**Figure 9D**). This illustrates the crucial role of shape irregularities in affecting the hydrodynamic forces (e.g., drag) acting on the irregular particles during settling and the resulting slow-down of their TSVs. Volume increases seem to amplify the effect of such irregularities causing a non-linear increase of the drag forces on the particles for increasing volumes. Interestingly for the irregular particles the ranking of their TSV increases relative to their equivalent particle diameter changed over the different increments in density gain (**Figure 9C**), while it stayed the same for volume increases. Likely the simultaneous increase in weight, drag and buoyancy associated with a volume increase maintains a certain balance in downward and upward forces acting on a particle of a specific shape. In contrast the more dramatic gains in weight due to the density increases seem to result in significant differences in the hydrodynamics forces (drag) that act on particles of different shapes and in turn counteract the gain in gravitational force.

4.5 Impact of Water Temperature on TSV

Our simulations on the effects of temperature on the TSV of MP particles (**Figure 10**) indicate that typical temperature differences between the compartments of a stratified lake in a temperate climate, will lead to significant differences in TSV (up to 46%). Differences in temperature and in turn density and kinematic viscosity of water in the different lake compartments have an influence on the drag forces exerted on the particles altering their TSVs. This temperature dependency of TSV can significantly affect the residence times of particles in the different lake compartments (Cole et al., 2016) and with that the exposure

time of organisms to the MP particles (Elagami et al., 2022). This implies that the seasonal temperature evolution in the different lake compartments needs to be considered when evaluating exposure. In addition to the temperature effect, however, other parameters such as water oxygen content, salinity, water pH and changes in food quality and availability have to be taken into account to assess the complex patterns of interactions between organisms and MP particles in the different lake compartments (Migwi et al., 2020; Hiltunen et al., 2021; Höffschroerer et al., 2021).

4.6 The Relative Importance of the Different Parameters Affecting Particle TSV

As highlighted by our analyses the TSV of MP particles in lakes and stagnant water bodies is affected by a range of different physical parameters such as density, volume, shape, surface roughness and hydrophobicity of the particles as well as the temperature and in turn density and viscosity of water. Evaluating the relative impact of these parameters on the TSV of MP particles quantitatively is challenging, as some of the parameters are coupled and their effects on TSV will overlap (Al Harraq and Bharti, 2021). Furthermore the settling of particles in the investigated size range (0.5–2.2 mm) is largely outside the true Stokes range of a laminar regime and hydrodynamic forces induced by turbulence will affect particle settling specifically for the larger particles. However, our rigorous, model-based evaluation of the hydrodynamic effects of the parameters listed above on particle TSVs, combined with respective laboratory settling experiments, including modifications to the particles' hydrophobicity, allowed a more systematic, qualitative assessment of the relative importance of the different parameters. In the following we will compare the relative change of TSV in percent over the parameter ranges evaluated in our analyses, which reflect the ranges typically observed for MP particles found in the environment.

Our analyses demonstrate the importance of particle density for controlling TSV. While an increase in particle density directly affects the gravitational force driving settling, it has no impact on the particle's volume and surface area, which would in turn change buoyancy and drag. A doubling of particle density led to TSV increases of up to 483 and 388% for regular and irregular particles respectively. In contrast, TSV increases of only 224% for the regular and 93% for the irregular particles could be realized for a doubling of particle volume. We attribute the significantly smaller TSV increase for the irregular particles to effects of the enlarged surface irregularities on drag and turbulence at the particle-water interface slowing down the settling velocity. The attachment of air on the surfaces of some of the biodegradable MP particles led to a reduction of the TSV by up to 58%, followed by relatively similar maximum changes in TSV of 47 and 45% due changes in water temperature and particle roundness respectively. Changes in particle roundness only significantly affected the TSVs of particles larger than 1 mm in diameter, while the smallest particles (0.5 mm diameter) were unaffected and their TSVs seemed to be controlled by their large SA:V. While

the effects of water temperature and particle roundness similarly affected particles of all shapes and polymer types, effects of air attachment were most pronounced for particles with significant shape irregularities and rough surfaces (mainly the biodegradable particles in our study), but also evident for irregular particles made of the lightest polymer PS with a density close to that of water ($= 1.03 \text{ gcm}^{-3}$). In contrast, regular, spherical particles with smooth surfaces did not show any significant effects of air attachment on TSV in our experiments.

5 SUMMARY AND CONCLUSION

In this study we systematically investigated the effects of different physical parameters on the TSV of MP particles in stagnant water bodies such as lakes. Parameters, which were varied over ranges typical for MP particles found in the environment, included particle density, volume, shape and roundness, surface hydrophobicity and water temperature. In total we conducted 683 individual CFD simulations of the settling behavior of MP particles of regular and irregular shapes and compared the simulation results to two semi-empirical equations to estimate particle TSVs as well as to laboratory settling experiments with the respective particles.

Our CFD simulations illustrated the peculiar, shape-dependent movement of irregular particles in the initial, transient phase of settling before reaching a quasi-steady TSV. This transient phase was found to be short, usually not exceeding one second, and is therefore negligible for estimating the time-scales of particle settling in larger stagnant water bodies such as lakes. The CFD-based calculations of TSV for MP particles of regular and irregular shapes were found to be in good agreement ($R^2 = 0.91$) with TSV estimates obtained from the semi-empirical Dietrich equation (Dietrich, 1982), which is based on simple shape metrics and was originally developed for mineral (sediment) particles. Deviations from the CFD results can be attributed to the simplicity of the shape metrics used, which presumably play out more significantly for the lighter MP particles than for the heavier mineral particles, for which the relationship was originally developed. Surprisingly the comparison of our CFD-based TSVs with values obtained from another semi-empirical relationship, which was specifically developed for MP fragments, pellets and spheres (Waldschläger and Schüttrumpf, 2019) yielded a poorer agreement. We suspect that this deviation is related to differences between the shapes of the particles used to derive this relationship and the particle shapes in our study.

A comparison between the CFD-based TSV values and the experimentally determined values for the irregular particles also showed a good general agreement ($R^2 = 0.82$), but with some more significant deviations for the particles made of biodegradable polymers and the very light non-biodegradable polymer PS ($=1.03 \text{ gcm}^{-3}$). Separating the data from the biodegradable particles from the other data revealed a significantly weaker correlation ($R^2 = 0.09$), which we hypothesized to be related to the attachment of air on the

particle surface due to its hydrophobicity. Our hypothesis was corroborated by the results of additional settling experiments, in which the MP particles were treated with a surfactant to reduce their surface hydrophobicity, which brought the experimental results into good agreement with the CFD results ($R^2 = 0.82$). Maximum changes in TSV related to effects of hydrophobicity were on the order of 58%. Our results further indicated that the magnitude of air attachment on the hydrophobic particle surfaces seems to be related to the presence of larger surface irregularities as well as to the generally rougher surfaces of the bio-degradable polymers. The effects observed for the irregular, non-biodegradable PS particles are presumably related to their low density, which makes them more susceptible to TSV changes even at smaller magnitudes of air attachment. Regular, spherical particles with relatively smooth surfaces in contrast, did not show any measurable effects of air attachment on their TSVs.

For an evaluation of the relative importance of the different physical parameters investigated we conclude that density is the most decisive parameter for the TSV as it predominantly affects particle weight and in turn the gravitational force controlling TSV. Increases in TSV in excess of 400% could result from a doubling of density. In contrast, gains in weight due to a doubling of particle volume are counteracted by increases in buoyancy of the larger particle and drag on the enlarged particle surface leading to comparably smaller TSV increases on the order of 100–200%. Effects of air attachment follow with TSV changes of up to 58%, but they are restricted to particles with specific shape and surface characteristics. Effects of water temperature and particle roundness were responsible for maximum TSV changes of 47 and 45% respectively. Our systematic evaluation of the effects of key physical parameters on TSV provides a framework to evaluate their relative importance in future studies on the behavior of MP particles in lakes and can help to design future experiments on MP particle settling. It is clear, however, that the settling of MP particles in real lakes will also be affected by processes such as the formation of biofilms and/or mineral crusts on particle surfaces (Kaiser et al., 2017; Chen et al., 2019; Leiser et al., 2020; Elagami et al., 2022), the sorption of metals on particle surfaces (Leiser et al., 2021), particle interactions and aggregation (Leiser et al., 2021; Elagami et al., 2022; Wu et al., 2022), particle aging (Brandon et al., 2016) or the uptake and excretion by organisms (Koelmans et al., 2022), and turbulent flows (Kumar et al., 2021). How these processes interact with the basic physical processes investigated in this study and how that

may change the settling behavior of MP particles remains to be investigated in future work.

DATA AVAILABILITY STATEMENT

The original contributions presented in the study are included in the article/**Supplementary Material**, further inquiries can be directed to the corresponding authors.

AUTHOR CONTRIBUTIONS

PA: Set up the CFD modeling framework, conducted the CFD simulations, designing the additional experiments, data interpretation and writing the manuscript. HE: Performed the laboratory experiments, assisted in data interpretation and writing the manuscript. FD: Contributed to the initial set-up of the CFD modeling framework, to data interpretation and writing of the manuscript. CS: Assisted in data interpretation and writing the manuscript. BG: Assisted in data interpretation and writing the manuscript. SF: Assisted in data interpretation and writing the manuscript. SP: Assisted in data interpretation and writing the manuscript. JF: Conceived the project, assisted in data interpretation and contributed to writing and editing of the manuscript.

FUNDING

Funded by the Deutsche Forschungsgemeinschaft (DFG, German Research Foundation)–Project Number 391977956–SFB 1357.

ACKNOWLEDGMENTS

We would like to thank Ulrich Mansfeld and Martina Heider for taking the SEM images.

SUPPLEMENTARY MATERIAL

The Supplementary Material for this article can be found online at: <https://www.frontiersin.org/articles/10.3389/fenvs.2022.875220/full#supplementary-material>

REFERENCES

- Ahrens, J., Geveci, B., and Law, C. (2005). Paraview: An End-User Tool for Large Data Visualization. *The visualization handbook*, 717–731(8). doi:10.1016/b978-012387582-2/50038-1
- Akdogan, Z., and Guven, B. (2019). Microplastics in the Environment: A Critical Review of Current Understanding and Identification of Future Research Needs. *Environ. Pollut.* 254, 113011. doi:10.1016/j.envpol.2019.113011
- Al Harraq, A., and Bharti, B. (2021). Microplastics through the Lens of Colloid Science. *ACS Environ. Au* 2 (1), 3–10. doi:10.1021/acsenvironau.1c00016
- Anderson, P. J., Warrack, S., Langen, V., Challis, J. K., Hanson, M. L., and Rennie, M. D. (2017). Microplastic Contamination in lake Winnipeg, Canada. *Environ. Pollut.* 225, 223–231. doi:10.1016/j.envpol.2017.02.072
- Arora, C., Kumar, B. P., and Narayana, A. C. (2010). Influence of Particle Shape on Drag Coefficient for Commonly Occurring sandy Particles in Coastal Areas. *Int. J. Ocean Clim. Syst.* 1 (2), 99–112. doi:10.1260/1759-3131.1.2.99
- Ballent, A., Corcoran, P. L., Madden, O., Helm, P. A., and Longstaffe, F. J. (2016). Sources and Sinks of Microplastics in Canadian Lake Ontario Nearshore, Tributary and beach Sediments. *Mar. Pollut. Bull.* 110 (1), 383–395. doi:10.1016/j.marpolbul.2016.06.037
- Barnes, D. K. A., Galgani, F., Thompson, R. C., and Barlaz, M. (2009). Accumulation and Fragmentation of Plastic Debris in Global

- Environments. *Phil. Trans. R. Soc. B* 364 (1526), 1985–1998. doi:10.1098/rstb.2008.0205
- Berlemont, A., Desjonqueres, P., and Gouesbet, G. (1990). Particle Lagrangian Simulation in Turbulent Flows. *Int. J. Multiphase Flow* 16 (1), 19–34. doi:10.1016/0301-9322(90)90034-g
- Boehrer, B., and Schultze, M. (2008). Stratification of Lakes. *Rev. Geophys.* 46 (2), RG2005. doi:10.1029/2006rg000210
- Brandon, J., Goldstein, M., and Ohman, M. D. (2016). Long-term Aging and Degradation of Microplastic Particles: Comparing *In Situ* Oceanic and Experimental Weathering Patterns. *Mar. Pollut. Bull.* 110 (1), 299–308. doi:10.1016/j.marpolbul.2016.06.048
- Browne, M. A., Crump, P., Niven, S. J., Teuten, E., Tonkin, A., Galloway, T., et al. (2011). Accumulation of Microplastic on Shorelines Worldwide: Sources and Sinks. *Environ. Sci. Technol.* 45 (21), 9175–9179. doi:10.1021/es201811s
- Chen, X., Xiong, X., Jiang, X., Shi, H., and Wu, C. (2019). Sinking of Floating Plastic Debris Caused by Biofilm Development in a Freshwater lake. *Chemosphere*. 222, 856–864. doi:10.1016/j.chemosphere.2019.02.015
- Chubarenko, I., Bagaev, A., Zobkov, M., and Esiukova, E. (2016). On Some Physical and Dynamical Properties of Microplastic Particles in marine Environment. *Mar. Pollut. Bull.* 108 (1–2), 105–112. doi:10.1016/j.marpolbul.2016.04.048
- Chubarenko, I., Esiukova, E., Bagaev, A., Isachenko, I., Demchenko, N., Zobkov, M., et al. (2018). “Behavior of Microplastics in Coastal Zones,” in *Microplastic Contamination in Aquatic Environments*. Editors E. Y. Zeng (Elsevier), 175–223. doi:10.1016/b978-0-12-813747-5.00006-0
- Claessens, M., De Meester, S., Van Landuyt, L., De Clerck, K., and Janssen, C. R. (2011). Occurrence and Distribution of Microplastics in marine Sediments along the Belgian Coast. *Mar. Pollut. Bull.* 62 (10), 2199–2204. doi:10.1016/j.marpolbul.2011.06.030
- Cole, M., Lindeque, P., Fileman, E., Halsband, C., Goodhead, R., Moger, J., et al. (2013). Microplastic Ingestion by Zooplankton. *Environ. Sci. Technol.* 47 (12), 6646–6655. doi:10.1021/es400663f
- Cole, M., Lindeque, P. K., Fileman, E., Clark, J., Lewis, C., Halsband, C., et al. (2016). Microplastics Alter the Properties and Sinking Rates of Zooplankton Faecal Pellets. *Environ. Sci. Technol.* 50 (6), 3239–3246. doi:10.1021/acs.est.5b05905
- Coppock, R. L., Galloway, T. S., Cole, M., Fileman, E. S., Queirós, A. M., and Lindeque, P. K. (2019). Microplastics Alter Feeding Selectivity and Faecal Density in the Copepod, *Calanus helgolandicus*. *Sci. total Environ.* 687, 780–789. doi:10.1016/j.scitotenv.2019.06.009
- Corey, A. T. (1949). *Influence of Shape on the Fall Velocity of Sand Grains*. Fort Collins, CO: Colorado A & M College.
- Derraik, J. G. B. (2002). The Pollution of the marine Environment by Plastic Debris: a Review. *Mar. Pollut. Bull.* 44 (9), 842–852. doi:10.1016/s0025-326x(02)00220-5
- de Souza Machado, A. A., Kloas, W., Zarfl, C., Hempel, S., and Rillig, M. C. (2018). Microplastics as an Emerging Threat to Terrestrial Ecosystems. *Glob. Change Biol.* 24 (4), 1405–1416. doi:10.1111/gcb.14020
- Dietrich, W. E. (1982). Settling Velocity of Natural Particles. *Water Resour. Res.* 18 (6), 1615–1626. doi:10.1029/wr018i006p01615
- Doyle, M. J., Watson, W., Bowlin, N. M., and Sheavly, S. B. (2011). Plastic Particles in Coastal Pelagic Ecosystems of the Northeast Pacific Ocean. *Mar. Environ. Res.* 71 (1), 41–52. doi:10.1016/j.marenvres.2010.10.001
- Elagami, H., Ahmadi, P., Fleckenstein, J. H., Frei, S., Obst, M., Agarwal, S., et al. (2022). Measurement of Microplastic Settling Velocities and Implications for Residence Times in Thermally Stratified Lakes. *Limnology & Oceanography* Ino.12046, 1–12. doi:10.1002/Ino.12046
- Fendall, L. S., and Sewell, M. A. (2009). Contributing to marine Pollution by Washing Your Face: Microplastics in Facial Cleansers. *Mar. Pollut. Bull.* 58 (8), 1225–1228. doi:10.1016/j.marpolbul.2009.04.025
- Fischer, E. K., Paglialonga, L., Czech, E., and Tamminga, M. (2016). Microplastic Pollution in Lakes and lake Shoreline Sediments - A Case Study on Lake Bolsena and Lake Chiusi (central Italy). *Environ. Pollut.* 213, 648–657. doi:10.1016/j.envpol.2016.03.012
- Frias, J. P. G. L., and Nash, R. (2019). Microplastics: Finding a Consensus on the Definition. *Mar. Pollut. Bull.* 138, 145–147. doi:10.1016/j.marpolbul.2018.11.022
- Gorham, E., and Boyce, F. M. (1989). Influence of lake Surface Area and Depth upon thermal Stratification and the Depth of the Summer Thermocline. *J. Great Lakes Res.* 15 (2), 233–245. doi:10.1016/s0380-1330(89)71479-9
- Gregory, M. R. (1983). Virgin Plastic Granules on Some Beaches of Eastern Canada and Bermuda. *Mar. Environ. Res.* 10 (2), 73–92. doi:10.1016/0141-1136(83)90011-9
- Gregory, M. R. (1996). Plastic ‘scrubbers’ in Hand Cleansers: a Further (And Minor) Source for marine Pollution Identified. *Mar. Pollut. Bull.* 32 (12), 867–871. doi:10.1016/s0025-326x(96)00047-1
- Guerrini, F., Mari, L., and Casagrandi, R. (2021). The Dynamics of Microplastics and Associated Contaminants: Data-Driven Lagrangian and Eulerian Modelling Approaches in the Mediterranean Sea. *Sci. Total Environ.* 777, 145944. doi:10.1016/j.scitotenv.2021.145944
- Hendrickson, E., Minor, E. C., and Schreiner, K. (2018). Microplastic Abundance and Composition in Western Lake Superior as Determined via Microscopy, Pyr-GC/MS, and FTIR. *Environ. Sci. Technol.* 52 (4), 1787–1796. doi:10.1021/acs.est.7b05829
- Hersch, R. W., Herschy, R. W., Wolanski, E., Andutta, F., Delhez, E., Fairbridge, R. W., et al. (2012). Ecological Threat to Lakes and Reservoirs. *Encyclopedia of Lakes and Reservoirs*, 233–234. doi:10.1007/978-1-4020-4410-6_74
- Hiltunen, M., Vehniäinen, E.-R., and Kukkonen, J. V. K. (2021). Interacting Effects of Simulated Eutrophication, Temperature Increase, and Microplastic Exposure on *Daphnia*. *Environ. Res.* 192, 110304. doi:10.1016/j.envres.2020.110304
- Hoffschröder, N., Grassl, N., Steinmetz, A., Sziegoleit, L., Koch, M., and Zeis, B. (2021). Microplastic burden in *Daphnia* Is Aggravated by Elevated Temperatures. *Zoology (Jena)*. 144, 125881. doi:10.1016/j.zool.2020.125881
- Houzeaux, G., Eguzkitza, B., Aubry, R., Owen, H., and Vázquez, M. (2014). A Chimera Method for the Incompressible Navier-Stokes Equations. *Int. J. Numer. Meth. Fluids*. 75 (3), 155–183. doi:10.1002/fld.3886
- Isachenko, I. (2020). Catching the Variety: Obtaining the Distribution of Terminal Velocities of Microplastics Particles in a Stagnant Fluid by a Stochastic Simulation. *Mar. Pollut. Bull.* 159, 111464. doi:10.1016/j.marpolbul.2020.111464
- Jalón-Rojas, I., Wang, X. H., and Fredj, E. (2019). A 3D Numerical Model to Track marine Plastic Debris (TrackMPD): Sensitivity of Microplastic Trajectories and Fates to Particle Dynamical Properties and Physical Processes. *Mar. Pollut. Bull.* 141, 256–272. doi:10.1016/j.marpolbul.2019.02.052
- Jérémy, R., Gaston, L. P., and Valyrakis, M. (2020). Coupled CFD-DEM Modelling to Assess Settlement Velocity and Drag Coefficient of Microplastics. *EGU General Assembly 2020*. doi:10.5194/egusphere-egu2020-10049
- Kaiser, D., Estelmann, A., Kowalski, N., Glockzin, M., and Waniek, J. J. (2019). Sinking Velocity of Sub-millimeter Microplastic. *Mar. Pollut. Bull.* 139, 214–220. doi:10.1016/j.marpolbul.2018.12.035
- Kaiser, D., Kowalski, N., and Waniek, J. J. (2017). Effects of Biofouling on the Sinking Behavior of Microplastics. *Environ. Res. Lett.* 12 (12), 124003. doi:10.1088/1748-9326/aa8e8b
- Khatmullina, L., and Isachenko, I. (2017). Settling Velocity of Microplastic Particles of Regular Shapes. *Mar. Pollut. Bull.* 114 (2), 871–880. doi:10.1016/j.marpolbul.2016.11.024
- Koelmans, A. A., Redondo-Hasselerharm, P. E., Nor, N. H. M., de Ruijter, V. N., Mintenig, S. M., and Kooi, M. (2022). Risk Assessment of Microplastic Particles. *Nat. Rev. Mater.*, 1–15. doi:10.1038/s41578-021-00411-y
- Kooi, M., Reisser, J., Slat, B., Ferrari, F. F., Schmid, M. S., Cunsolo, S., et al. (2016). The Effect of Particle Properties on the Depth Profile of Buoyant Plastics in the Ocean. *Sci. Rep.* 6 (1), 33882–33910. doi:10.1038/srep33882
- Kowalski, N., Reichardt, A. M., and Waniek, J. J. (2016). Sinking Rates of Microplastics and Potential Implications of Their Alteration by Physical, Biological, and Chemical Factors. *Mar. Pollut. Bull.* 109 (1), 310–319. doi:10.1016/j.marpolbul.2016.05.064
- Kumar, R., Sharma, P., Verma, A., Jha, P. K., Singh, P., Gupta, P. K., et al. (2021). Effect of Physical Characteristics and Hydrodynamic Conditions on Transport and Deposition of Microplastics in Riverine Ecosystem. *Water* 13 (19), 2710. doi:10.3390/w13192710
- Kwon, J.-H., Chang, S., Hong, S. H., and Shim, W. J. (2017). Microplastics as a Vector of Hydrophobic Contaminants: Importance of Hydrophobic Additives. *Integr. Environ. Assess. Manag.* 13 (3), 494–499. doi:10.1002/ieam.1906

- Lambert, S., and Wagner, M. (2018). Microplastics Are Contaminants of Emerging Concern in Freshwater Environments: An Overview. *Freshw. microplastics*, 1–23. doi:10.1007/978-3-319-61615-5_1
- Leiser, R., Jongsma, R., Bakenhus, I., Möckel, R., Philipp, B., Neu, T. R., et al. (2021). Interaction of Cyanobacteria with Calcium Facilitates the Sedimentation of Microplastics in a Eutrophic Reservoir. *Water Res.* 189, 116582. doi:10.1016/j.watres.2020.116582
- Leiser, R., Wu, G.-M., Neu, T. R., and Wendt-Potthoff, K. (2020). Biofouling, Metal Sorption and Aggregation Are Related to Sinking of Microplastics in a Stratified Reservoir. *Water Res.* 176, 115748. doi:10.1016/j.watres.2020.115748
- Liao, J., and Chen, Q. (2021). Biodegradable Plastics in the Air and Soil Environment: Low Degradation Rate and High Microplastics Formation. *J. Hazard. Mater.* 418, 126329. doi:10.1016/j.jhazmat.2021.126329
- Maximenko, N., Hafner, J., and Niiler, P. (2012). Pathways of marine Debris Derived from Trajectories of Lagrangian Drifters. *Mar. Pollut. Bull.* 65 (1-3), 51–62. doi:10.1016/j.marpolbul.2011.04.016
- Migwi, F. K., Ogunah, J. A., and Kiratu, J. M. (2020). Occurrence and Spatial Distribution of Microplastics in the Surface Waters of Lake Naivasha, Kenya. *Environ. Toxicol. Chem.* 39 (4), 765–774. doi:10.1002/etc.4677
- Moghadam, A., and Vahedi Tafreshi, H. (2020). On Liquid Bridge Adhesion to Fibrous Surfaces under normal and Shear Forces. *Colloids Surf. A: Physicochemical Eng. Aspects.* 589, 124473. doi:10.1016/j.colsurfa.2020.124473
- Mountford, A. S., and Morales Maqueda, M. A. (2019). Eulerian Modeling of the Three-Dimensional Distribution of Seven Popular Microplastic Types in the Global Ocean. *J. Geophys. Res. Oceans.* 124 (12), 8558–8573. doi:10.1029/2019jc015050
- Nooteboom, P. D., Delandmeter, P., van Sebille, E., Bijl, P. K., Dijkstra, H. A., and von der Heydt, A. S. (2020). Resolution Dependency of Sinking Lagrangian Particles in Ocean General Circulation Models. *PLoS one.* 15 (9), e0238650. doi:10.1371/journal.pone.0238650
- North, E. J., and Halden, R. U. (2013). Plastics and Environmental Health: The Road Ahead. *Rev. Environ. Health.* 28 (1), 1–8. doi:10.1515/reveh-2012-0030
- Powers, M. C. (1953). A New Roundness Scale for Sedimentary Particles. *J. Sediment. Res.* 23 (2), 117–119. doi:10.1306/d4269567-2b26-11d7-8648000102c1865d
- Renner, G., Nellessen, A., Schwiens, A., Wenzel, M., Schmidt, T. C., and Schram, J. (2020). Hydrophobicity-water/air-based Enrichment Cell for Microplastics Analysis within Environmental Samples: A Proof of Concept. *MethodsX.* 7, 100732. doi:10.1016/j.mex.2019.11.006
- Ribes, A., and Caremoli, C. (2007). “Salome Platform Component Model for Numerical Simulation,” in 31st annual international computer software and applications conference (COMPSAC 2007): IEEE, 553–564.
- Rocha-Santos, T., and Duarte, A. C. (2015). A Critical Overview of the Analytical Approaches to the Occurrence, the Fate and the Behavior of Microplastics in the Environment. *Trac Trends Analytical Chemistry.* 65, 47–53. doi:10.1016/j.trac.2014.10.011
- Rochman, C. M. (2018). Microplastics Research-From Sink to Source. *Science.* 360 (6384), 28–29. doi:10.1126/science.aar7734
- Sighicelli, M., Pietrelli, L., Lecce, F., Iannilli, V., Falconieri, M., Coscia, L., et al. (2018). Microplastic Pollution in the Surface Waters of Italian Subalpine Lakes. *Environ. Pollut.* 236, 645–651. doi:10.1016/j.envpol.2018.02.008
- Singh, P., Bagrania, J., and Haritash, A. (2019). Seasonal Behaviour of thermal Stratification and Trophic Status in a Sub-tropical Palustrine Water Body. *Appl. Water Sci.* 9 (5), 1–6. doi:10.1007/s13201-019-1011-z
- Szewczyk, P. K., Ura, D. P., Metwally, S., Knapczyk-Korczak, J., Gajek, M., Marzec, M. M., et al. (2019). Roughness and Fiber Fraction Dominated Wetting of Electrospun Fiber-Based Porous Meshes. *Polymers (Basel).* 11 (1), 34. doi:10.3390/polym11010034
- Trunk, R., Bretl, C., Thäter, G., Nirschl, H., Dorn, M., and Krause, M. J. (2021). A Study on Shape-dependent Settling of Single Particles with Equal Volume Using Surface Resolved Simulations. *Computation.* 9 (4), 40. doi:10.3390/computation9040040
- Van Cauwenberghe, L., Claessens, M., Vandegehuchte, M. B., Mees, J., and Janssen, C. R. (2013). Assessment of marine Debris on the Belgian Continental Shelf. *Mar. Pollut. Bull.* 73 (1), 161–169. doi:10.1016/j.marpolbul.2013.05.026
- Vaughan, R., Turner, S. D., and Rose, N. L. (2017). Microplastics in the Sediments of a UK Urban lake. *Environ. Pollut.* 229, 10–18. doi:10.1016/j.envpol.2017.05.057
- Wagner, W., and Kretschmar, H.-J. (2008). “IAPWS Industrial Formulation 1997 for the Thermodynamic Properties of Water and Steam,” in International steam tables: properties of water and steam based on the industrial formulation IAPWS-IF97, 7–150.
- Waldschläger, K., and Schüttrumpf, H. (2019). Effects of Particle Properties on the Settling and Rise Velocities of Microplastics in Freshwater under Laboratory Conditions. *Environ. Sci. Technol.* 53, 1958–1966. doi:10.1021/acs.est.8b06794
- Webb, H., Arnott, J., Crawford, R., and Ivanova, E. (2013). Plastic Degradation and its Environmental Implications with Special Reference to Poly (Ethylene Terephthalate). *Polymers* 5, 1–18. doi:10.3390/polym5010001
- Wei, X.-F., Bohlén, M., Lindblad, C., Hedenqvist, M., and Hakonen, A. (2021). Microplastics Generated from a Biodegradable Plastic in Freshwater and Seawater. *Water Res.* 198, 117123. doi:10.1016/j.watres.2021.117123
- Weller, H. G., Tabor, G., Jasak, H., and Fureby, C. (1998). A Tensorial Approach to Computational Continuum Mechanics Using Object-Oriented Techniques. *Comput. Phys.* 12 (6), 620–631. doi:10.1063/1.168744
- Williams, A. T., and Simmons, S. L. (1996). The Degradation of Plastic Litter in Rivers: Implications for Beaches. *J. Coast Conserv.* 2 (1), 63–72. doi:10.1007/bf02743038
- Wright, S. L., Thompson, R. C., and Galloway, T. S. (2013). The Physical Impacts of Microplastics on marine Organisms: a Review. *Environ. Pollut.* 178, 483–492. doi:10.1016/j.envpol.2013.02.031
- Wright, S. L., Ulke, J., Font, A., Chan, K. L. A., and Kelly, F. J. (2020). Atmospheric Microplastic Deposition in an Urban Environment and an Evaluation of Transport. *Environ. Int.* 136, 105411. doi:10.1016/j.envint.2019.105411
- Wu, J., Ye, Q., Wu, P., Xu, S., Liu, Y., Ahmed, Z., et al. (2022). Heteroaggregation of Nanoplastics with Oppositely Charged Minerals in Aquatic Environment: Experimental and Theoretical Calculation Study. *Chem. Eng. J.* 428, 131191. doi:10.1016/j.cej.2021.131191
- Zbyszewski, M., Corcoran, P. L., and Hockin, A. (2014). Comparison of the Distribution and Degradation of Plastic Debris along Shorelines of the Great Lakes, North America. *J. Great Lakes Res.* 40 (2), 288–299. doi:10.1016/j.jglr.2014.02.012
- Zhang, H. (2017). Transport of Microplastics in Coastal Seas. *Estuarine, Coastal Shelf Sci.* 199, 74–86. doi:10.1016/j.ecss.2017.09.032
- Zhang, Y., Xie, M., Adamaki, V., Khanbareh, H., and Bowen, C. R. (2017). Control of Electro-Chemical Processes Using Energy Harvesting Materials and Devices. *Chem. Soc. Rev.* 46 (24), 7757–7786. doi:10.1039/c7cs00387k
- Ziccardi, L. M., Edgington, A., Hentz, K., Kulacki, K. J., and Kane Driscoll, S. (2016). Microplastics as Vectors for Bioaccumulation of Hydrophobic Organic Chemicals in the marine Environment: A State-Of-The-Science Review. *Environ. Toxicol. Chem.* 35 (7), 1667–1676. doi:10.1002/etc.3461

Conflict of Interest: The authors declare that the research was conducted in the absence of any commercial or financial relationships that could be construed as a potential conflict of interest.

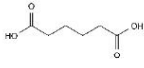
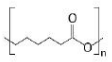
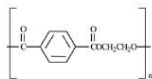
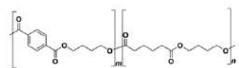
Publisher's Note: All claims expressed in this article are solely those of the authors and do not necessarily represent those of their affiliated organizations, or those of the publisher, the editors and the reviewers. Any product that may be evaluated in this article, or claim that may be made by its manufacturer, is not guaranteed or endorsed by the publisher.

Copyright © 2022 Ahmadi, Elagami, Dichgans, Schmidt, Gilfedder, Frei, Peiffer and Fleckenstein. This is an open-access article distributed under the terms of the Creative Commons Attribution License (CC BY). The use, distribution or reproduction in other forums is permitted, provided the original author(s) and the copyright owner(s) are credited and that the original publication in this journal is cited, in accordance with accepted academic practice. No use, distribution or reproduction is permitted which does not comply with these terms.

Supplementary Material

S1: Details on the used polymers in the carried out experiments and simulations

Table S1. Properties of the seven abundant polymers used in this study.

Polymer name	Abbreviation	Structure	Density (gcm ⁻³)	Type
Polystyrene	PS		1.030	Non-biodegradable
Polyamide 66	PA66		1.12	Non-biodegradable
Polycaprolacton	PCL		1.14	Biodegradable
Poly(lactic acid)	PLA		1.20	Biodegradable
Poly(L-lactic acid)	PLLA		1.20	Biodegradable
Polybutylenadipate terephthalate	PBAT		1.22	Non-biodegradable
Polyvinyl chloride	PVC		1.38	Non-biodegradable

S2: Adjusted initial and boundary conditions in all the conducted simulations**Table S2.** The used initial and boundary conditions in the simulations conducted by OpenFOAM.

		Velocity	Pressure	Phase Saturation
Upper wall	type	inletOutlet;	fixedValue;	fixedValue;
	value	internalField	internalField	uniform 0;
MP particle	type	movingWallVelocity	fixedFluxPressure;	zeroGradient;
	value	internalField	-	-
Side walls	type	fixedValue	fixedFluxPressure;	zeroGradient;
	value	internalField	-	-
Lower wall	type	fixedValue	fixedFluxPressure;	zeroGradient;
	value	internalField	-	-

S3: Calculation of MOI for an arbitrary particle

The following equations are used to calculate mass (m) and mass moment of inertia (I_o) of particle with arbitrary shape (Ehrlich and Weinberg, 1970; Peraire and Widnall, 2008; Tang and Shangguan, 2011) (Figure S1) in which r_i is a vector that points out to the position of the i^{th} cell in the mesh of a designed particle within a Cartesian coordinate system and $\rho(r_i)$ is the particle density in the i^{th} cell:

$$m = \int_{v(r)} \rho(r_i) dV(\vec{r}) \quad (1)$$

$$I_o = \int_{v(r)} \rho(r_i) r_i^2 dV(\vec{r}) = \int \begin{bmatrix} x_i^2 + y_i^2 & -x_i y_i & -x_i z_i \\ -x_i y_i & x_i^2 + y_i^2 & -y_i z_i \\ -x_i z_i & -y_i z_i & x_i^2 + y_i^2 \end{bmatrix} \rho(r_i) dV(\vec{r}) \quad (2)$$

Origin is the rotational axis of the particle's moment of inertia which is calculated by equation 2. Having the coordinate of the particle's center of mass (\vec{c}) (equation 3) and using the parallel axes theorem, MOI of the particles around their center of gravity can be calculated using equation 4.

$$\vec{c} = \frac{1}{m} \int_{v(r)} \vec{r}_i \rho(r_i) dV(\vec{r}) \quad (3)$$

$$I_o = \int \begin{bmatrix} x_i^2 + y_i^2 & -x_i y_i & -x_i z_i \\ -x_i y_i & x_i^2 + y_i^2 & -y_i z_i \\ -x_i z_i & -y_i z_i & x_i^2 + y_i^2 \end{bmatrix} \rho(r_i) dV(\vec{r}) - \int_{v(r)} \rho(r_i) dV(\vec{r}) \begin{bmatrix} C_y^2 + C_z^2 & -C_x C_y & -C_x C_z \\ -C_x C_y & C_x^2 + C_z^2 & -C_y C_z \\ -C_x C_z & -C_y C_z & C_x^2 + C_y^2 \end{bmatrix} \quad (4)$$

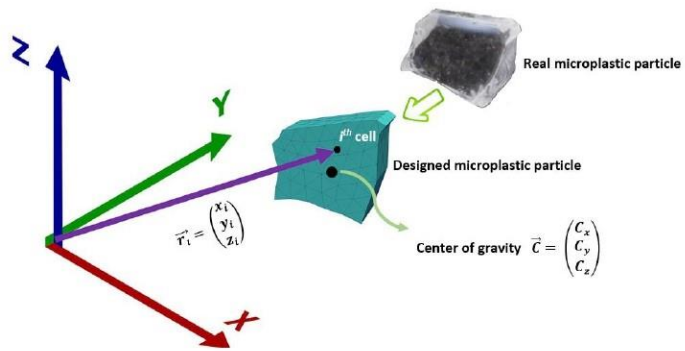
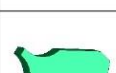
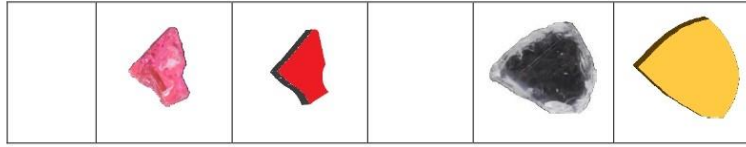


Figure S1. Position vector and center of mass location of an irregularly shaped MP particle.

S4: A number of the designed irregularly shaped MP particles and their real images

Table S3. Some of the designed particles based on the shape of real irregularly shaped MP particles.

Polymer type	Real MP particle	Simulated MP particle	Polymer type	Real MP particle	Simulated MP particle
PLLA			PA66		
					
					
PCL			PBAT		
					
					
PS			PVC		
					



In the table a selection of the real MP particles used in the experiments and their designed shapes using the meshing software SALOME 9.4 software (Ribes and Caremoli, 2007) are depicted. The simulation results for three random particles software are visualized using ParaView software (Ahrens et al., 2005) (see supplementary animation (Video 1)). In order to compare their sizes in the interpretations, equation 5 was used to calculate the diameter of spheres with volumes identical to the volumes of the MP particles.

$$D_{eq} = \sqrt[3]{ABC} \quad (5)$$

A and C are the longest and shortest lengths of each particle and B is the arithmetic average of A and C (Kooi et al., 2016; Waldschläger and Schüttrumpf, 2019).

S5: Calculating side length of the polygons with identical areas to generate particles of the same volumes

A regular polygon with N sides is a cyclic polygon which is described using two circles, an inscribed circle that forms the tangent to the middle points of all sides of a regular polygon, and a circumscribed circle which passes through all its vertices. As the number of sides of a polygon increase towards infinity, the lengths of its sides converge to zero, so that the inscribed and circumscribed circles eventually overlap. Knowing the side length and the number of sides, equation 6 returns the area of a regular polygon. Figure S2 has been drawn based on equation 6 so that considering areas equal to circles with diameters of 0.5 mm, 1mm, 1.5mm, 2mm, and 2.5mm, the side length (a) of the polygons with areas equal to their corresponding circles were calculated.

$$A = \frac{1}{4} na^2 \cot \frac{\pi}{n} \quad (6)$$

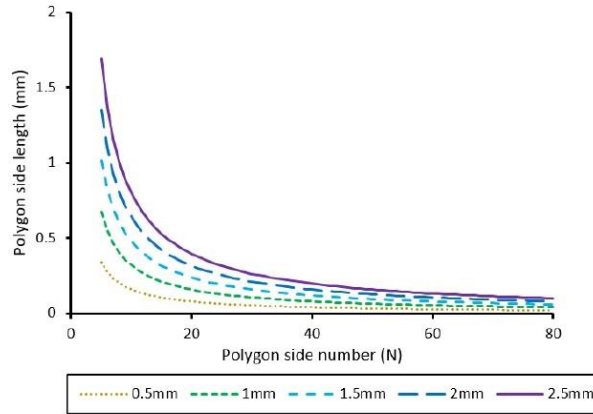


Figure S2. The side lengths of regular 2D polygons with areas identical to a circle derived from a polygon with an infinite number of sides (legend shows the diameters of the circles).

S6. Behavior of a particle before and after reaching its terminal settling velocity (TSV)

Figure S3-A illustrates the evolution of the settling velocity in the initial transient phase of settling for four particles with different shapes, which show different, shape-dependent behavior. Figure S3-B shows the velocity evolution for 5 triangular particles entering the water column with different orientations at angles of 45°, 90°, 135°, and 180°. The velocity evolution in the transient phase of settling before reaching a constant terminal settling velocity (TSV) clearly depends on the orientation of the particle when entering the water column (Figure S3-B). In this transient phase the settling velocity can fluctuate around the TSV as a result of secondary oscillating, rotating and tumbling movements of the MP particles. Those types of secondary movements were also observed in the settling experiments in the present as well as other studies (Khatmullina and Isachenko, 2017).

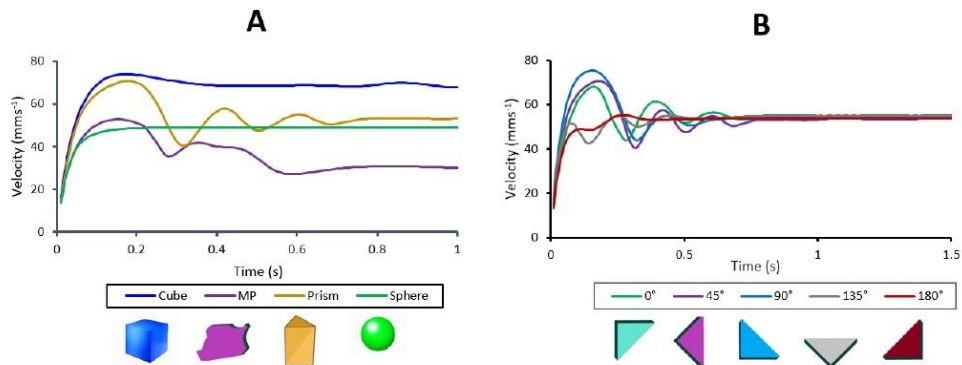


Figure S3. Velocity profile before and after reaching TSV for (A) three different regular particles (cube, prism, and sphere) and an irregular MP particle, (B) Evolution of the settling velocity of a triangular particle entering the water column with orientations at different angles (0°, 45°, 90°, 135°, 180°).

References

- Ahrens, J., Geveci, B., and Law, C. (2005). Paraview: An end-user tool for large data visualization. *The visualization handbook* 717(8).
- Ehrlich, R., and Weinberg, B. (1970). An exact method for characterization of grain shape. *Journal of sedimentary research* 40(1), 205-212.
- Khatmullina, L., and Isachenko, I. (2017). Settling velocity of microplastic particles of regular shapes. *Marine pollution bulletin* 114(2), 871-880.
- Kooi, M., Reisser, J., Slat, B., Ferrari, F.F., Schmid, M.S., Cunsolo, S., et al. (2016). The effect of particle properties on the depth profile of buoyant plastics in the ocean. *Scientific reports* 6(1), 1-10.
- Peraire, J., and Widnall, S. (2008). Lecture L26-3D Rigid Body Dynamics: The Inertia Tensor. *Dynamics*.
- Ribes, A., and Caremoli, C. (Year). "Salome platform component model for numerical simulation", in: *31st annual international computer software and applications conference (COMPSAC 2007)*: IEEE), 553-564.
- Tang, L., and Shangguan, W.-B. (2011). An improved pendulum method for the determination of the center of gravity and inertia tensor for irregular-shaped bodies. *Measurement* 44(10), 1849-1859.
- Waldschläger, K., and Schüttrumpf, H. (2019). Effects of particle properties on the settling and rise velocities of microplastics in freshwater under laboratory conditions. *Environmental science & technology* 53(4), 1958-1966.

Study 3: Quantifying microplastic residence times in lakes using mesocosm experiments and transport modelling

Hassan Elagami, Sven Frei, Jan-Pascal Boos, Gabriele Trommer, Benjamin S. Gilfedder.

Submitted to *Water Research* on 22nd Aug. 2022

Abstract

Microplastic residence time in lakes is a key factor controlling uptake by lake organisms. In this work, we have used a series of in-lake mesocosm experiments combined with random walk modeling to quantify microplastic residence times in the lake water column. Three size ranges of fluorescent microplastic (1-5, 28-48, and 53-63 μm) were added to a 12m deep mesocosm and detected using high resolution in-situ fluorescence detectors. Experiments were conducted over one year capturing stratified and unstable conditions within the water column. The measured residence times in summer ranged between ~ 1 and 24 days, and depended largely on particle size. The modeled residence time for the smallest particles using Stokes velocity ($>200\text{d}$) was considerably longer than the measured residence times in the mesocosm ($\sim 24\text{d}$). We believe that the discrepancy during the summer is due to interactions between the small microplastic particles and existing particles in the lake. In contrast, large Rayleigh numbers during autumn suggest that instabilities in the water column likely led to turbulent convective mixing and rapid microplastic transport within the mesocosm. This work shows that microplastic transport within lakes is complex, especially for the smallest plastic sizes, and involves interactions between physical, physicochemical and biological processes.

1. Introduction

Plastic production has increased rapidly since the middle of the 20th century, with an estimated total global production of 8300 million Mt in 2015 (Worm et al., 2017). This will likely increase owing to innovations in the plastic industry which lead to novel and low-cost synthetic polymers combined with an increase in consumer demand (Lebreton and Andrady, 2019). The majority of the global plastic volume produced is typically made for single-use, particularly as packaging (D'Avignon et al., 2022). Ideally, after use, the polymer is recycled and reenters the production stream. However, evidence from life cycle studies (Lavoie et al., 2021; Woods et al., 2021) show that improper disposal of plastic is significant, leading to its migration and accumulation in the environment (e.g., in inland waters) before it reaches the ocean (Cai et al., 2021). For

example, it is estimated that roughly 5% of the plastic produced in 2015 was recycled, while 91% was either incinerated or accumulated in landfills and the environment (Worm et al., 2017).

Plastic transport through inland waters is an important pathway between environmental compartments and ultimately is responsible for delivering plastic debris to the ocean (Yan et al., 2021). Plastic debris is classified according to size into macro plastics (>5 mm), microplastics (1 μm to 5 mm), and nano plastics (<1 μm) (SAPEA, 2019). As macro plastic is exposed to a wide range of physical and biological degradation processes during its transport through catchments, it tends to lose its structure and physical integrity over time and degrade also into micro-and nano plastic (D'Avignon et al., 2022).

Since non-buoyant pristine microplastic particles are small in size and have polymer densities close to that of water, they are expected to have significant residence times in lake systems (Elagami et al., 2022). During their residence in the lake water column, they are exposed to a wide range of lake organisms (e.g., zooplankton, fish). This results in a high likelihood of uptake by lake organisms before the plastic reaches the lake sediment, or before they are flushed from the lake via outlets (Canniff and Hoang, 2018; D'Avignon et al., 2022). Recent studies have shown that lake organisms such as zooplankton have a limited ability to distinguish between their food, which is usually composed of natural particulate organic carbon either from the lake or its catchment, and microplastic particles (Aljaibachi and Callaghan, 2018). Once microplastic particles have entered the food web, they can migrate to higher trophic levels through direct ingestion or indirect ingestion of microplastic containing organisms by predators (D'Avignon et al., 2022; Nelms et al., 2018).

The settling velocity of microplastic is controlled by key physical particle properties such as density and size (Ahmadi et al., 2022; Elagami et al., 2022; Khatmullina and Isachenko, 2017; Waldschlager and Schuttrumpf, 2019). Physical-chemical factors such as hydrophobic adhesion

between pristine particles and fine air bubbles, formation of aggregates with existing lake particles, as well as biofouling can affect the buoyancy of the microplastic, modify its settling velocity and thus also influence its residence time in lakes (Elagami et al., 2022; Leiser et al., 2020; Renner et al., 2020).

Lake hydrodynamics can also influence the residence times of microplastic within the water column. For instance, turbulent mixing in the epilimnion during summer is expected to cause a significant increase in the residence times of sinking particles compared to particles in the 'laminar' metalimnion (Elagami et al., 2022; Kirillin et al., 2012; Reynolds and Wiseman, 1982). However, the behavior of microplastic during lake turnover is expected to be very different from that during the stratification period. This is due to the instability of the lake column which leads to the onset of natural (turbulent) convective mixing (Cannon et al., 2021). The role that such complex hydrodynamic processes play in determining residence time is currently poorly understood.

Despite the growing number of studies focusing on understanding microplastic behavior in lake systems, the majority of existing research is mainly based on laboratory experiments and modeling (Ahmadi et al., 2022; Elagami et al., 2022; Khatmullina and Isachenko, 2017; Waldschläger and Schüttrumpf, 2019). Unlike laboratory experiments which are conducted in artificial settings, field experiments are conducted in conditions similar to reality and encompass the many of the complexities of real lake settings.

In this work, we have performed microplastic addition experiments in a 3 x 12 m mesocosm located in lake Großer Brombachsee, Germany. Experiments were conducted for one year encompassing various lake conditions and microplastic sizes to understand microplastic transport processes in lakes. The results from the mesocosm experiments were compared with results from a random walk model to quantitatively analyze the underlying processes affecting microplastic transport in lakes and determine how well physical transport processes can explain

observations from the complex experimental mesocosm system. The primary aim was to develop a quantitative understanding of the primary processes influencing microplastic transport in the lake water column, and how this may influence the exposure of organisms to this emerging pollutant.

2. Methodology

2.1. Study region

All field experiments were conducted at lake Großer Brombachsee in the German federal state of Bavaria. The Großer Brombachsee is a 5.1 km long, 2.0 km wide water reservoir with a maximum depth of 32.5 m covering an area of $\sim 8.50 \text{ km}^2$. The thermal stratification period extends from May until the end of October. Lake turnover typically begins in November. The lake has an intermediate level of productivity and is classified as mesotrophic. According to long term monitoring data of the Water Management Authority Office, the average annual total nitrogen and phosphorus concentrations over lake depth are ~ 0.95 and 0.025 mg l^{-1} respectively. The experimental site was situated at the border of a nature reserve, located on the southwestern side of the lake (Figure 1). The water depth at the mesocosm site varied between 10 and 12 m depending on the season extraction for water supply.

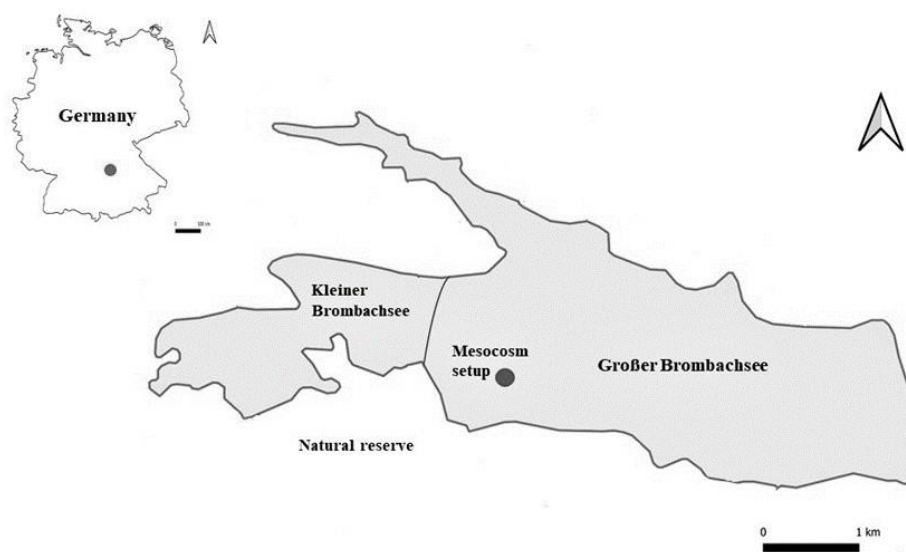


Figure 1: A map showing the location of the experimental setup at Großer Brombachsee in Bavaria, Germany

2.2. Mesocosm setup

The mesocosm setup (Aquatic Research Instruments (USA)) consists of a 12 m long and 3 m diameter impermeable polyethylene plastic enclosure with 80% light transmittance, reinforced with nylon fibers (Figure 2 and Figure S1). The enclosure was also fitted with side loops at 3m intervals to stabilize the mesocosm. The upper end of the mesocosm was fitted with a 3m diameter ring buoy constructed from a foam-filled corrugated drain pipe. The bottom of the enclosure was fixed to the sediment layer using 5x20 kg concrete ballasts. The enclosure was freely open from the top, but partially sealed from the bottom with a mesh. The mesocosm was lowered slowly into the lake before the mesh was installed shortly after the mesocosm. No filling (pumping) was required. A U-shaped pontoon was fixed around the mesocosm and adopted as a platform for fixing the instruments. The whole setup was anchored to the lake bed with 4 anchors and the ropes were tensioned to prevent the setup from drifting and rotating. The mesocosm was deployed in May 2021 and left for two months to allow the water column to equilibrate with the surrounding lake water before conducting the first experiment.

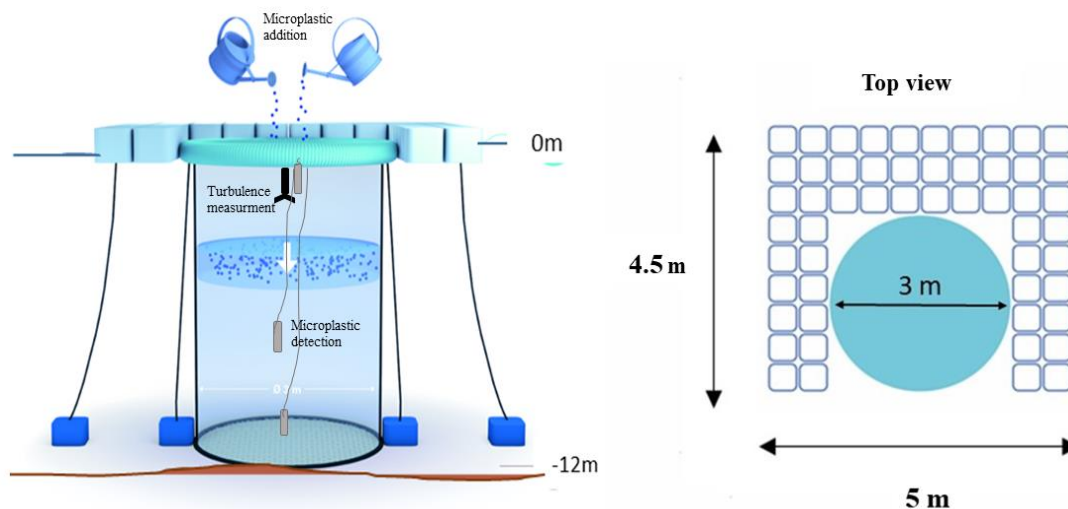


Figure 2: A sketch of the mesocosm setup at Großer Brombachsee

2.3. Microplastic particles

All microspheres were supplied by Cospheric LLC in green fluorescent dry powder. The fluorescent dye had maximum excitation and emission wave lengths of 414 and 514 nm

respectively. Microspheres were used exclusively during the experiments due to the limited availability of fluorescent microplastic. Table 1 shows the polymers, their densities, particle sizes and the amounts of the microplastic used in each experiment. The 1-5 μm particles were composed of a propriety polymer of unknown chemical structure, whereas the larger particles were polyethylene. Aqueous microplastic solutions with concentrations of 1.0 g l^{-1} were prepared in the laboratory prior to each experiment. Due to the hydrophobic nature of Cospheric particles, the stock solutions were prepared using distilled water and mixed with 0.1 g of surfactant (Tween 20) per 100 ml of water. This also prevented the microplastic from agglomerating or floating on the surface of the water while preparing the solution. The solutions were then preserved in clean sealed buckets in a cool room before transportation to the lake.

Table 1: A list of polymer names, particle sizes, densities, and amount of the microplastic microspheres used in the experiments.

Polymer	Density (g cm^{-3})	Amount (g)	Diameter (μm)	Time of experiment
Polyethylene	1.10	20	53-63	Summer 2021
Polyethylene	1.10	20	28-48	Summer 2021
Unknown (Proprietary Polymer)	1.30	5	1-5	Summer 2022
Unknown (Proprietary Polymer)	1.30	5	1-5	Autumn 2021

2.4. Microplastic addition to the mesocosm

Prior to each experiment, the surface of the water inside the mesocosm was cleaned using fine nets. The stock solutions were stirred until all settled particles were resuspended and uniformly distributed in the solution. The particles were then added as a pulse from the top of the mesocosm simultaneously by two persons using two metal watering cans fitted with wide

sprinklers to ensure a uniform distribution of the microplastic in the mesocosm (Figure S2). The particle additions are estimated to have lasted a maximum of five minutes.

2.5. Field measurements

Water temperatures were measured in the center of the mesocosm at the start and during each experiment using Hobo TidbiT temperature loggers at 1 m intervals and with a sampling resolution of 30 minutes. Temperature profiles were also taken outside the mesocosm before the start of each experiment. The temperature data were used to infer the stability and stratification of the water column.

A 3D acoustic doppler velocimeter (ADV, Nortek vector 300) was used to measure 3D water velocities inside the mesocosm, and infer the turbulent kinetic energy and turbulent diffusion. The ADV was fixed in the center of the mesocosm at 1m below the water surface. The instrument was set to sample at burst intervals of 600 Sec with 100 samples per burst at 8 Hz. The ADV was set to detect flow velocities in the East-North-Up (ENU) directions in a sampling volume of $\sim 1.5 \text{ cm}^3$. The instrument is equipped with a magnetometer and tilt sensors to correct measured velocities for movement of the instrument in the water column.

The fluorescent microplastic was measured in the center of the mesocosm using submersible field fluorometers from Albillia GGUN-FL24 (Bailly-Comte et al., 2018). The fluorometers used an excitation wavelength of 470 nm to excite the green microplastic particles and the fluorescent intensity was measured in the ‘uranine’ channel. The fluorometers were calibrated in the laboratory following the same procedures as presented in Boos et al. (2021). At least 8 calibration points were used. The only difference to Boos et al. (2021) is that calibration solutions were prepared using filtered lake water rather than distilled water. The calibrations are presented in Figure S3. The minimum detection limits of the 1-5, 28-48, and 53-63 μm particles were approximately 2, 100, and 200 $\mu\text{g l}^{-1}$ respectively. The fluorometers were less sensitive to the 28-48 and 53-63 μm microspheres due to the lower particle abundance and

higher scattering in the measuring cell (Figure S3). The measurement frequency of the fluorometers in the mesocosm was selected according to the expected residence times of the particles based on their laminar settling velocities. Thus, the sampling interval was fixed at 2 and 120 seconds for the large (fast) and the small (slow) particles, respectively. During lake stratification, the fluorometers were positioned at 0.5 m below the water surface, the epilimnion-metalimnion interface, and 1m from the bottom of the mesocosm. During lake turnover in autumn, the fluorometers were only positioned at 0.5 m below the water surface and 1 m over lake sediment.

2.6. Microplastic settling velocity

In this work we have used three characteristic settling velocities for the microplastic particles. Firstly, Stokes equation was used to calculate the settling velocities of the small 1-5 μm particles (v_{s_Stokes}) [LT^{-1}]. Secondly, the settling velocities of particles outside Stokes range (28-48 and 53-63 μm) were measured experimentally under laminar conditions using particle image velocimetry system (PIV). The measured velocities were then corrected to the water temperature of each lake compartment in the mesocosm. The corrected settling velocities were denoted as v_{s_PIV} [LT^{-1}]. Finally, effective settling velocities for all microplastic particles were calculated using the experimental data from the mesocosm (v_{s_eff}) [LT^{-1}].

Stokes settling velocities were calculated according to:

$$v_{s_Stokes} = \frac{2(\rho_p - \rho_w)}{9\mu} gR^2 \quad 1$$

Where ρ_p [M L^{-3}] is the density of the particle, ρ_w [M L^{-3}] is the density of the lake water, R [L] is the radius of the particle, g [LT^{-2}] is the acceleration due to gravity, and μ [$\text{M L}^{-1} \text{T}^{-1}$] is the dynamic viscosity of the water.

The laminar settling velocities of the large 28-48 and 53-63 μm microspheres were measured in the laboratory using the same two-dimensional iLa 5051 PIV system used by Elagami et al. (2022). The system consists of a high-speed camera (40 frames per second) and a light source

(high-power light-emitting diodes) with a wavelength of 530 nm. The settling velocities were measured in a 10 cm x 10 cm x 40 cm glass column filled with filtered lake water based on the design of Khatmullina and Isachenko (2017). The room temperature was kept constant at 20°C. Approximately 1 ml of the stock microplastic solution was added carefully at the top of the column as a pulse (cloud) in the water column. The average settling velocity of each particle cloud was calculated based on the PIV images. The laboratory-measured settling velocities were corrected as in Ghawi and Kris (2012a) using the water temperature of each lake compartment using equation S4.

The effective settling velocities from the mesocosm experiments were calculated for all microplastic sizes by dividing the depth of each compartment (i.e. epilimnion or metalimnion) by the time required until 50% of the particles were lost from the compartment:

$$v_{s_effect} = \frac{z}{\tau_{50\%}} \quad 2$$

Where z [L] is the depth of the compartment, and $\tau_{50\%}$ [T] is the time elapsed until 50% of particles was lost from that compartment.

2.7. Hydrodynamic calculations

The temperature data inside the mesocosm was used to calculate the Rayleigh number to elucidate if natural convection was occurring in the water column during the autumn experiment. The Rayleigh number was calculated according to equation 3 (Weeraratne and Manga, 1998):

$$Ra = \frac{\alpha g \Delta T z^3}{\nu \beta} \quad 3$$

where α is the thermal expansion coefficient of water ($210 \times 10^{-6} \text{ C}^{-1}$), g is the acceleration due to gravity, ΔT [°C] is the temperature difference between the bottom and top boundaries, z is the thickness of the compartment, ν [$\text{L}^2 \text{ T}^{-1}$] is the kinematic viscosity of water, and β [$\text{L}^2 \text{ T}^{-1}$] is thermal diffusivity of water.

The 3D water velocity data were used to calculate the turbulence kinetic energy (TKE) [$L^2 T^{-2}$] in the mesocosm. The time series for TKE of each burst was calculated using equation 4 as in Wüest and Lorke (2003):

$$TKE = \frac{1}{2} (\sigma_{East}^2 + \sigma_{North}^2 + \sigma_{Up}^2) \quad 4$$

Where, σ_{East} , σ_{North} , and σ_{up} [$L T^{-1}$], are the standard deviations of the fluctuations in velocity components during each burst.

The vertical component of the velocity data was also used to calculate the vertical eddy diffusivity (D) [$L^2 T^{-1}$] for each burst. Since velocities were measured in the Eulerian frame of reference, where the flow moves past the velocity sensor fixed at 1m below the water surface, D can be estimated from Taylor's approach using (Holtappels and Lorke, 2011)

$$D = w' \cdot L_E \quad 5$$

$$L_E = \int_0^{\infty} E_r \cdot dr \quad 6$$

Where, w' is the standard deviation of the vertical velocities [$L T^{-1}$], L_E [L] is the Eulerian integral length scale, E_r [-] is the spatial correlation coefficient, and r [L] is the spatial distance. For simplification, L_E [L] was assumed to be equal to the Lagrangian length scale (L_L) [L] as also done by Holtappels and Lorke (2011). Hence, D [$L^2 T^{-1}$] was calculated as follows:

$$D = w' \cdot L_L \quad 7$$

$$L_L = w' \cdot T_L \quad 8$$

$$T_L = \int_0^{\infty} R_L \cdot d\tau \quad 9$$

Where T_L [T] is the Lagrangian time scale, R_L [-] is the Lagrangian velocity autocorrelation, and τ [T] is the time interval between two velocity measurements (0.125 s).

2.8. Calculation of residence times in the mesocosm

The residence time of the microplastic in each compartment was calculated as the delay between the time required for 95% of the microplastics to be lost from the compartment and the time of microplastic input to that compartment. For instance, the residence time in the epilimnion (τ_{epi}) [T] was calculated as the difference between the time required until 95% of the particles were lost from the epilimnion and the time when the microplastic was added to the mesocosm. The residence time in the metalimnion (τ_{meta}) [T] was calculated as the delay between the time where 95% of the particles was lost from the metalimnion and the start of the pulse detected by the fluorometer positioned at the epilimnion-metalimnion interface. During lake turnover in the autumn, the mesocosm was treated as one mixed compartment and thus the residence time was calculated for the whole mesocosm (τ_{tot}) [T]. The total residence times in the mesocosm during autumn (τ_{tot}) and summer experiments were calculated as the difference between the time required until 95% of the particles passed the deepest fluorescence detector and the time of adding the microplastic to the mesocosm.

2.9. Modelling of microplastic sinking trajectories and residence times

Particle sinking trajectories and residence times in the mesocosm were modeled using a Lagrangian particle tracking technique based on the Huret et al. (2007); Visser (1997) scheme which was later modified and applied by Rowe et al. (2016) and Ross (2006) to simulate the vertical distribution of bacteria and plankton under turbulent conditions in lakes. The effect of turbulent motion on particle trajectories and residence times in the water column is represented by a 1D random walk assuming a vertically heterogeneous turbulence field:

$$z(t + \Delta t) = z(t) + v_s \Delta t + D'(z(t)) \Delta t + R \sqrt{\frac{2D(\tilde{z}) \Delta t}{r}} \quad 10$$

where the vertical particle trajectory $z(t+\Delta t)$ [L] for a time increment Δt [T] can be estimated based on the current particle location $z(t)$ [L], the depth specific particle settling velocity v_s [LT^{-1}]

¹], the depth gradient of the turbulent diffusivity $D' = \frac{dD}{dz}$ [LT^{-1}], a normally distributed random number R [-] in the range of $R \in [-1, 1]$ with zero mean and a variance of $r = 1/3$ and the turbulent diffusivity $D(\tilde{z})$ [$\text{L}^2 \text{T}^{-1}$] at an intermediate location $\tilde{z} = z(t) + 0.5 \frac{dD(z(t))}{dz} \Delta t$.

For representation of the vertical turbulent diffusivity, a power a law model similar to Kirillin et al. (2012) was used:

$$K(z) = \begin{cases} D_S^{(1-z/H_E)} D_M^{z/H_E} & \text{at } z \leq H_E \\ D_M & \text{at } H_E < z < H_M \\ D_M^{(H-z/H_H)} D_H^{z-(H_M+H_E)/H_H} & H_M < z < H_H \end{cases} \quad 11$$

Where D_S , D_M and D_H [$\text{L}^2 \text{T}^{-1}$] are the turbulent diffusivities at the lake surface, the interface to the metalimnion and the lake bottom respectively. H_E , H_M and H_H [L] denote the thickness of the epilimnion, the metalimnion and the total depth of the lake respectively. Turbulent diffusivity at the lake surface D_S was estimated using the Taylor's approach based on the ADV data. Diffusivities at the interface to the metalimnion and the lake bottom were estimated by fitting the measured particle curves at each depth to an Advection-Dispersion-Model (A-D). The A-D model represents an analytical solution to the one-dimensional advection dispersion equation for a semi-infinite system with an instantaneous injection of a tracer (in our case microplastic particles) in the fluid flux (Kreft and Zuber, 1978; Małoszewski and Zuber, 1982). From the A-D fitting, the depth specific Peclet number $Pe = v_s z / D$ [-] can be derived, relating the effect of gravitational settling and turbulent diffusion for a specific depths z where microplastic concentrations were measured (Ross 2006). D values can then be derived from the Pe -number using the settling velocity (i.e. v_{s_Stokes} , v_{s_PIV} , v_{s_eff}). A detailed description of the A-D fitting procedure is provided as part of the supplementary information. Each breakthrough experiment was represented using 2500 particles in the random walk simulations. All parameters used to run the random walk model are provided in the supplementary information (S5 and S9).

3. Results

3.1. Mesocosm temperature profiles

The measurements at the start of the experiments showed that the water column inside and outside the mesocosm were near to identical and during summer was thermally stratified and divided into an epilimnion and metalimnion (Figure S6). The thickness of the epilimnion inside the mesocosm over the extent of the experiments were ~8, 9, and 6m for the first, second and third summer experiment, respectively (Figure 3). The thickness of the metalimnion during the three summer experiments were ~ 3, 2, and 4m. The water temperatures varied between 18 and 25°C for the epilimnion and 12 to 14°C for the metalimnion.

Prior to and during the autumn experiment, the temperature tended to be warmer at depth than at the surface. The differences between the lower (the warmer) and the upper (the cooler) layer inside and outside the mesocosm at the start of the experiment were ~ 0.80 and 0.85°C respectively (Figure S6). Also, the average temperature difference between the lower and the upper layer inside the mesocosm during the whole autumn experiment was ~ 0.8°C (over an extent of 11m). The Rayleigh number (equation 3) was calculated using investigate the propensity for natural convection in the mesocosm. The time series for the Rayleigh numbers is presented in Figure S7. The minimum Rayleigh number was ~ 4×10^{12} , considerably exceeding the critical value of ~1700 (Reid and Harris, 1958). The Rayleigh number also indicated that the convection was turbulent ($Ra > 10^9$).

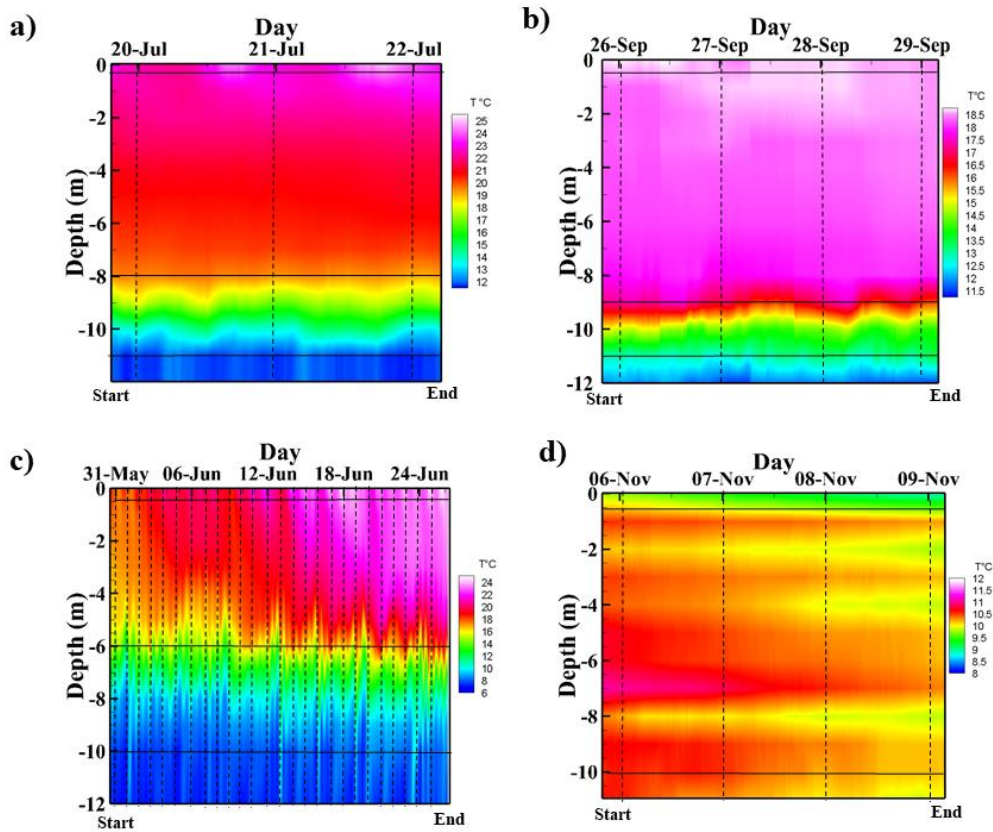


Figure 3: Temperature profiles inside the mesocosm for all experiments. Figures a), b), and c) show the temperature profiles during summer while figure d) shows the temperature profile during autumn. The horizontal lines show the location of the fluorometers which also define the lake epilimnion and hypolimnion. The vertical dashed lines represent midnight.

3.2. Turbulence kinetic energy

There were substantial fluctuations in the TKE in the epilimnion during summer experiments, especially for the experiment with the 1-5 μm particles (Figure 4). The maximum values for TKE during the summer experiments were $\sim 2.7 \times 10^{-3}$, 5×10^{-3} , and $6.6 \times 10^{-3} \text{ m}^2 \text{ s}^{-2}$ for the first, second, and third experiments respectively. The average TKE values were 3.5×10^{-4} , 5×10^{-4} , and $1 \times 10^{-4} \text{ m}^2 \text{ s}^{-2}$. During autumn, however, the fluctuations in the TKE values were much lower, showing much flatter TKE time series than that during summer experiments. The maximum and the average TKE values during autumn were 1.8×10^{-4} and $2 \times 10^{-5} \text{ m}^2 \text{ s}^{-2}$ respectively.

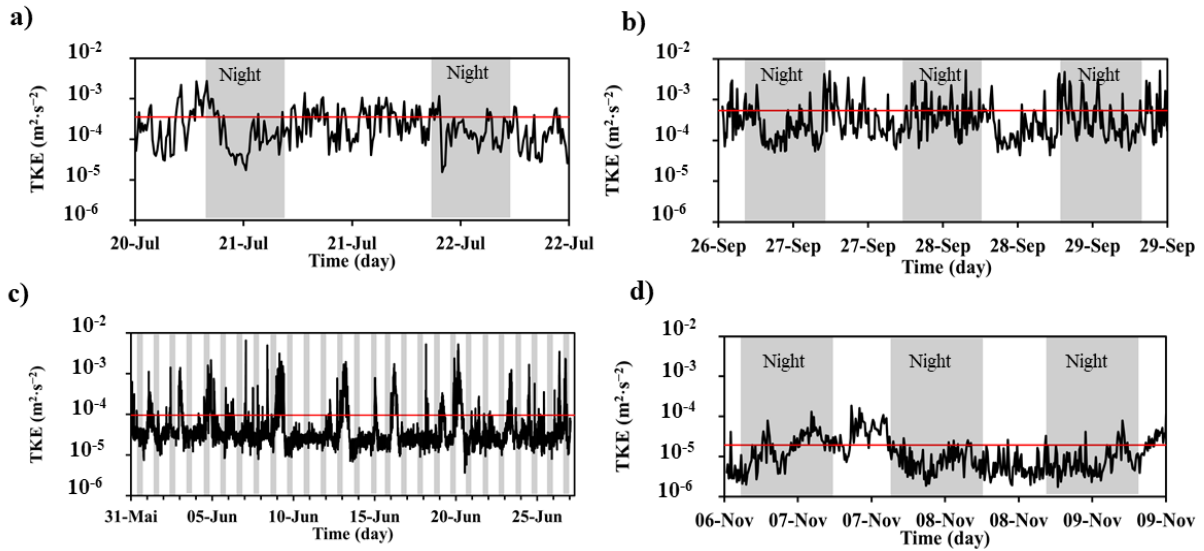


Figure 4: Time series of TKE for all experiments. Figures a), b), and c) present TKE during summer for the 53-63, 28-48, and 1-5 μm particles respectively. Figure d) shows TKE during autumn for the 1-5 μm microspheres. The gray intervals represent the night times. The red lines show the average TKE values. Note the logarithmic scale.

3.3. Microplastic concentrations in the mesocosm

Figures 5a, b, and c show the abundance and distribution of the microplastic in the mesocosm during the summer experiments. The maximum microplastic concentrations measured at 0.5m were approximately 15,000, 11,000, and 400 $\mu\text{g l}^{-1}$ during the first (53-60 μm), second (28-48 μm), and third (1-5 μm) experiments, respectively. The maximum concentrations at the epilimnion-metalimnion interface were approximately 10,000, 5000, and 200 $\mu\text{g l}^{-1}$ during the first, second, and third experiments respectively. At the bottom of the metalimnion, the maximum microplastic concentrations were approximately 2,500, 7,000, and 50 $\mu\text{g l}^{-1}$ for the first, second, and third experiments. The time required until 95% of the particles was lost from the epilimnion (τ_{epi}) was 0.8, 1.9, and 19.5 days for the first, second, and third summer experiments (Figures 5). For the metalimnion, τ_{meta} was 0.6, 1.4, and 22 days for the first, second, and third experiments (Figure 5). The total residence times in the mesocosm were 1, 2.5, and 24.7 days.

The measured particle concentrations during autumn are presented in Figure 5d. Surprisingly, the upper and the lower pulses showed an overlap of ~ 1 day. The maximum microplastic concentration detected by the upper fluorometer was $\sim 80 \mu\text{g l}^{-1}$. The lower pulse was divided into large initial and small subsequent pulses with maximum concentrations of ~ 55 and $25 \mu\text{g l}^{-1}$ respectively. The time until 95% of the particles had passed the lowest detector 1m over lake sediment (τ_{tot}) 1.9 days.

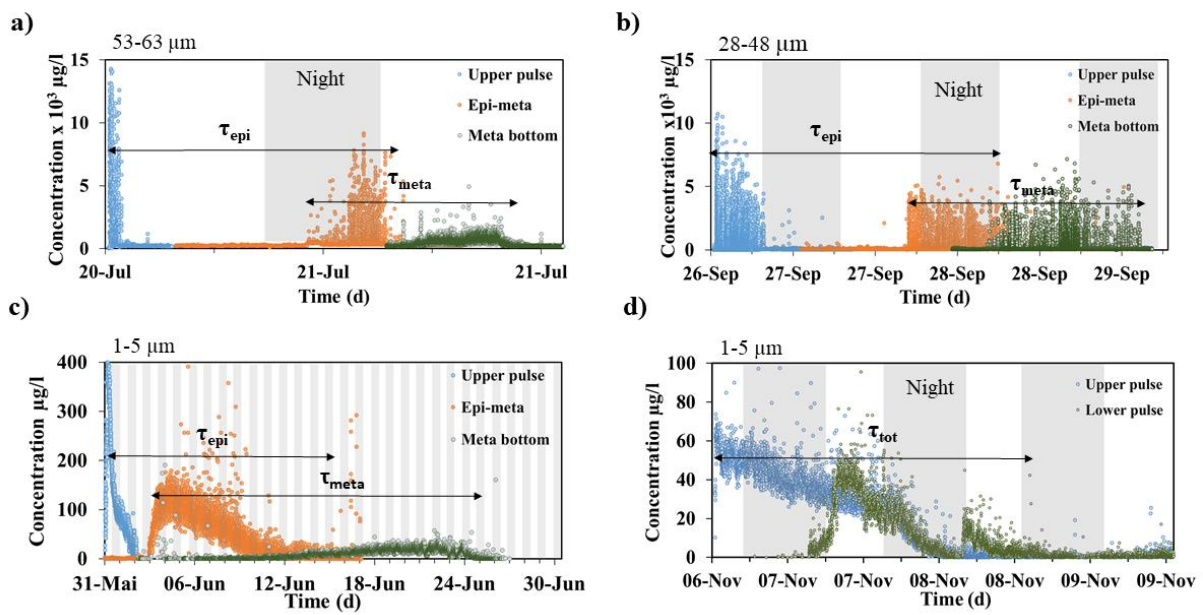


Figure 5: The measured concentrations of microplastic in the mesocosm. Figures a), b), and c) show particle concentrations during summer experiments. Figure d) shows particle concentrations during autumn. The gray intervals represent the night times. The blue, orange and green pulses represent the microplastic concentrations at 0.5 m below the water surface, epilimnion-metalimnion interface (in summer), and deepest fluorometer (bottom of the metalimnion in summer) respectively.

3.4. Settling velocity

Table S8 shows the values of the characteristic settling velocities (v_{s_Stokes} , v_{s_PIV} , and v_{s_eff}) used in the random walk model. For the 1-5 μm particles, the lowest velocities were estimated using Stokes Law (0.079 m d^{-1}) while the highest settling velocities were the v_{s_eff} (1.09 m d^{-1}). Also, for the 53-63 μm particles, v_{s_eff} was the highest (50 m d^{-1}), while v_{s_PIV} was the lowest

(17 m d⁻¹). In contrast, for the 28-48µm particles v_{s_PIV} was the highest (8.7 m d⁻¹) while v_{s_eff} was the lowest (0.16 m d⁻¹).

3.5 Eddy diffusivity

The A-D fitting routine provided estimates for the turbulent diffusivities that were comparable to those derived using Taylor's approach and the ADV data for the summer experiments using the 1-5 µm particles (Figure S9). The turbulent diffusivities ranged between $D_H = 1.12 \times 10^{-6}$ and $D_s = 6.7 \times 10^{-6} \text{ m}^2 \text{ s}^{-1}$ (Table S10). For the summer experiments using 28-48 and 53-63 µm the A-D fitting was less successful so that the random walk modelling relied primarily on D values derived from Taylor's approach. This ranged from 3×10^{-6} to $1 \times 10^{-5} \text{ m}^2 \text{ s}^{-1}$ depending on experiment and depth (Table S10). During autumn, our modeling depended exclusively on the D values calculated from Taylor's approach.

3.6. Random walk model

The random walk model was run using the three different settling velocities v_{s_Stokes} , v_{s_PIV} and v_{s_eff} depending on the experiment being simulated. The distribution in residence times of the individual simulated particles (i.e. microplastic residence time distribution) were then used to calculate the time until 95 % of particles had passed a specified depth in the water column. This is defined as the virtual microplastic residence time. The simulations using v_{s_Stokes} (summer experiment 1-5 µm) are shown in Figure 6, and have a rapid rise as the particle pulse reaches the measurement depth, and then a long tail as particles are transported by a combination of settling and turbulence from the water column. The simulated residence times were considerably longer than the measured values, with ~ 135 days for the first 0.5 m, 225 days for the epilimnion (6 m) and 239 days for the whole mesocosm water column (10 m).

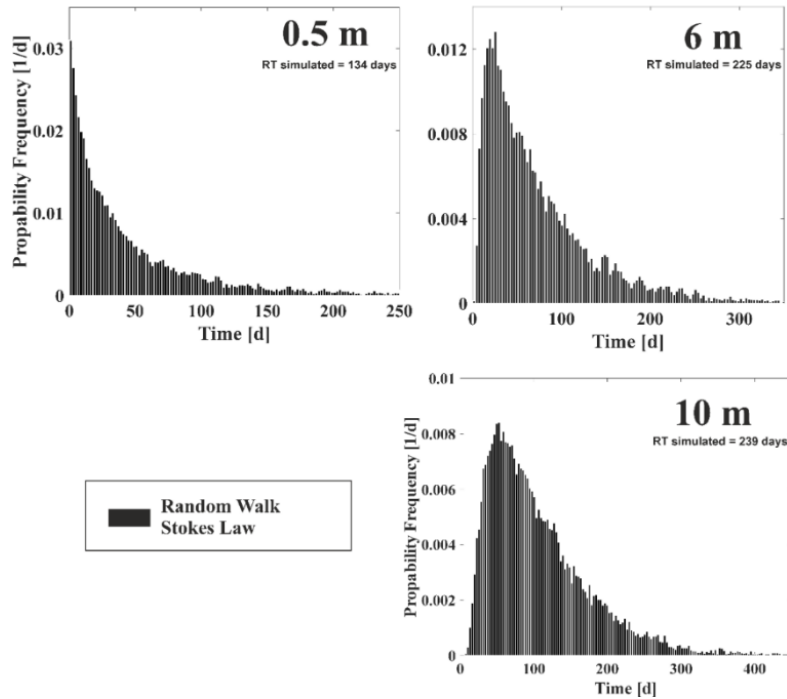


Figure 6: Simulated residence time distribution (RT) at 0.5, 6 and 10 m depth for the 1-5 μm particles of the summer experiment using v_{s_Stokes} .

When using v_{s_eff} for the same model run, the simulated microplastic residence times of the 1-5 μm particles in summer were similar to that inferred from microplastic concentrations in the mesocosm (Figure 7). All distributions showed the characteristic shape of the A-D model with a fast increase, a local maxima and a slowly decaying tail (Figure S9). The only parts that could not accurately be represented by the random walk model were the initial peak in particle concentrations at 0.5 m and the rapidly decaying tails at 0.5 and 10m depth (Figure 7). Using v_{s_eff} , the residence times were 4 days for 0.5 m, 11 days for the epilimnion (6 m) and 32 days for the whole 10 m water column.

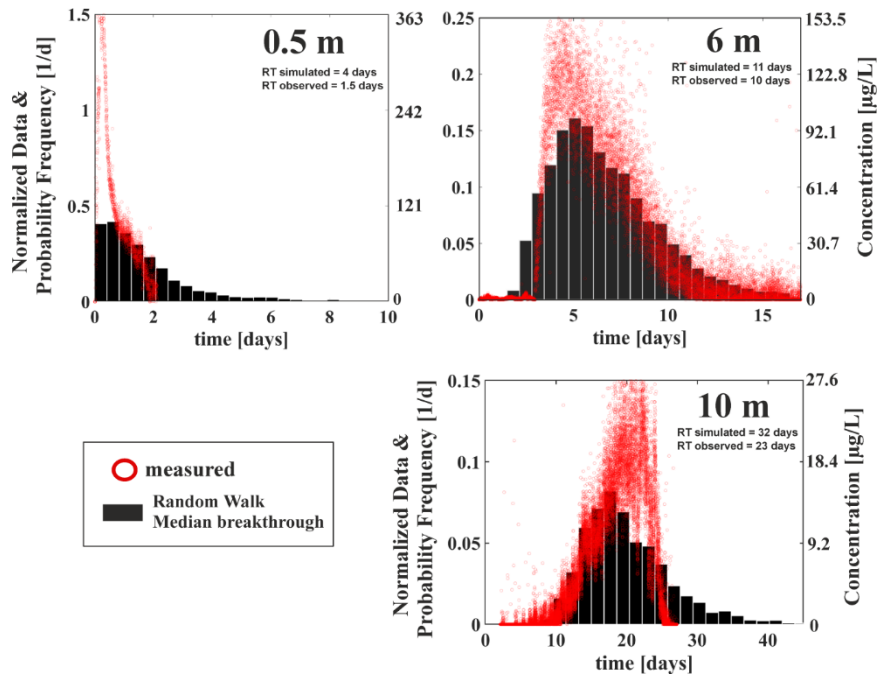


Figure 7: Simulated and measured particle breakthroughs at 0.5, 6 and 10m depth. Shown are the residence time distribution (RT) for the 1-5 μm particles in the summer experiment using the random walk model in combination with v_{s_eff} . The measured particle concentrations are presented as a concentration (secondary Y-axis) and as normalized data (primary Y-axis). Data normalization (described in detail as part of the supplement) was necessary to compare the output of the random walk model to the measured particle breakthrough curves.

Results from simulations for the 28-48 and 53-63 μm particles in summer and the 1-5 μm particles in autumn experiment are summarized in Table 2. As the v_{s_eff} method did not work well for the larger particle sizes (28-48 μm) due to a noisy signal from the detectors, the random walk simulations for this size class were parameterize using v_{s_PIV} only. The results show that while the random walk model can reproduce the measured residence times for the larger particles relatively well (e.g. 0.8 vs. 0.62 days for the 53-63 μm particles), it significantly over estimated the residence times for the small particles in the autumn experiments independent of the settling velocity used (2 vs. 17-225 days).

Table 2: A comparison between actual residence times in the mesocosm and simulated residence times using

v_{s_Stokes} , v_{s_PIV} v_{s_eff} .

Experiment	Depth (m)	Residence time in days calculated from			
		Mesocosm (actual)	v_{s_Stokes}	v_{s_PIV}	v_{s_eff}
Summer 53-63 μm	11	0.9	-	0.62	-
Summer 28-48 μm	11	2.5	-	1.39	-
Summer 1-5 μm	10	24	239	-	32
Autumn 1-5 μm	10	2	225	-	17

4. Discussions

Microplastic abundance in lake systems is associated with negative impacts on lake organisms and ecosystem functioning (Aljaibachi and Callaghan, 2018; D'Avignon et al., 2022). Uptake from the water column by lake organisms such as filter feeders is highly dependent on the residence time in the water column, and particularly in the epilimnion where most organisms reside. Several factors such as particle size, polymer density, water temperature, and lake hydrodynamics affect the residence times of microplastic (Waldschläger and Schüttrumpf 2019; Elagami et al. 2022; Ahmadi et al. 2022). These factors coupled with the abundance of microplastic in lakes control the uptake probability of microplastic by lake organisms and their potential transfer through the food web (D'Avignon et al., 2022; Nelms et al., 2018).

The temperature gradient, and thus the strong density gradient during lake stratification, formed a very stable water column inside the mesocosm. The water column was divided into a turbulent epilimnion and a more-or-less laminar metalimnion. This shows maximum TKE values at the 1 m below the water surface (top of the epilimnion) of $\sim 2.7 \times 10^{-3}$, 5×10^{-3} , and $6.6 \times 10^{-3} \text{ m}^2 \text{ s}^{-2}$ for the first, second and third experiments respectively. The major source of the high TKE in

the surface layer during turbulent mixing is the wind (Cannon et al., 2021; Singh et al., 2019). The waves in the lake impacting directly on the mesocosm walls and the platform could also have contributed to the relatively high TKE in the surface layer. The D values calculated from the A-D fitting for the 1-5 μm particles during summer experiments were similar to those calculated from ADV data and Taylor's approach ($\sim 10^{-6} \text{ m}^2 \text{ s}^{-1}$). The calculated D_S , D_M , and D_H values were in a similar range, but at the lower end of typical D values in stratified lakes (10^{-7} to $10^{-2} \text{ m}^2 \text{ s}^{-2}$) (Wüest and Lorke, 2009)

In contrast to the summer experiments, the average temperature difference between the bottom part of the mesocosm and the water surface was $\sim 0.8^\circ\text{C}$. This temperature difference and subsequently the density difference, combined with the 11m depth of the water column and the temperature fluctuations in the water column resulted in a highly unstable water column. This instability resulted in Rayleigh numbers ($>10^{12}$) which were significantly higher than the critical values, suggesting that the water column was mixed by turbulent convection. The maximum TKE values at 1m below the water surface during this period was one order of magnitude lower than that during summer ($\sim 1.8 \times 10^{-4} \text{ m}^2 \text{ s}^{-2}$). The major source of TKE is convection during autumn which results in the sinking of the upper (cool) water parcels. Finally, the calculated D values in autumn (in the range of $10^{-7} \text{ m}^2 \text{ s}^{-1}$) were considerably lower than during the summer and at the lower end of the compilation of D values in Wüest and Lorke (2009).

Microplastic concentrations were affected by the hydrodynamic conditions in the mesocosm. For instance, the maximum microplastic concentrations during summer were ~ 5 times higher than that in autumn for the same 1-5 μm particles (Figure 5c and d). The distribution of microplastic inside the mesocosm was also affected by season. Unlike the summer experiment, the upper pulse at 0.5 m below water surface and the lower pulse at 1m over sediment during autumn experiment had an overlap of ~ 1 day (Figure 5c and d). Furthermore, the fluorometer at 1m over the lake sediment detected two subsequent microplastic pulses during autumn

experiment. The maximum concentration of the two pulses at 1m over sediment were 55 and 25 $\mu\text{g l}^{-1}$. Surprisingly however, the measurements suggest that turbulent convection seemed to be not strong enough to start resuspension of settled microplastic, as neither fluorometer detected any microplastic after the end of the pulse. These differences between microplastic behaviors during summer and autumn experiments are to be attributed to the instability in the water column that likely led to turbulent convective mixing and rapid microplastic transport within the mesocosm.

As also found in modelling studies by Elagami et al. (2022), the microplastic residence times were significantly affected by the size of the particles in the stratified water column. When increasing the particle size from 1-5 to 53-63, the residence time in the whole column decreased by ~25 times. By comparing the residence times in the mesocosm for the particle group 1-5 μm during summer (thermal stratification) with that during autumn (lake convection), the total residence time in summer was ~ 13 times longer than that during autumn. This shows that in addition to size, hydrodynamics can play a critical role in microplastic transport, especially for the smallest particle sizes.

The simulated residence times using the random walk model differed from the actual residence times in the mesocosm, especially for the simulations using v_{s_Stokes} for the smallest particle sizes (Table 2). The simulated residence time of the 1-5 μm particles in summer using v_{s_Stokes} was ~ 10 times higher than that actual residence time in the mesocosm (Table2). This could be due to the effect of microplastic-particle interaction (i.e. formation of aggregates) in the mesocosm caused by the large surface area and the surface charge of the small microplastic particles. Such aggregates are large and likely to have higher settling velocities compared to the individual pristine microplastic particles used in Stokes calculations.

The simulated residence times of the 1-5 μm particles using v_{s_eff} values were very close to the actual residence times in the mesocosm. This is due to v_{s_eff} and D being derived directly from

the mesocosm data. As such v_{s_eff} implicitly incorporates processes influencing settling velocities in the mesocosm such as particle-microplastic interactions and hydrodynamic conditions. Such processes are not included in the laminar settling velocities in v_{s_Stokes} or v_{s_PIV} . The only part of the measured data that could not be represented by the random walk model for the 1-5 μm particles during summer using v_{s_eff} were the peak height and the rapidly decaying tail of the pulse at 0.5m below the water surface as well as the width of the pulse at the bottom of the metalimnion (Figure 7). This is likely due to the simplified way the random walk represents the complexities of real-world microplastic transport particularly that the model assumes one dimensional transport and uses predefined and stationary D values. In reality the TKE time series shows that the turbulent strength is transient and likely depends many interrelated factors such as winds, currents and waves that impact on the mesocosm.

For the summer experiments using the large 28-48 and 53-63 μm particles, the simulated residence times using v_{s_PIV} values were comparable to the actual residence times in the mesocosm with a difference of ~ 1.4 and 1.9 times. This is likely to be attributed to the relatively lower surface area of the large particles which subsequently reduces the potential particle-microplastic interactions and aggregation formation with organic matter (e.g. live and dead phytoplankton) inside the mesocosm.

During autumn, the modeled residence times of the 1-5 μm particles were considerably longer than those derived from the mesocosm. The simulation results using v_{s_Stokes} and v_{s_eff} were ~ 113 and 8.8 times higher than the actual residence time, respectively. These significant differences are likely due to the complex hydrodynamic conditions caused by the high instability in the lake water column, and particularly the initiation of natural convection which cannot be represented by the simplified lake physics used in the random walk model. Also during lake turnover, organic materials, cyanobacteria, and iron particles could resuspend and attach to the microplastic particles either increasing their density or building aggregates, both

of which would increase their settling velocity and reduce residence time in the mesocosm (D'Avignon et al., 2022). It is clear from the autumn experiment that the processes controlling microplastic settling velocities and residence times in lake systems during highly unstable hydrodynamic conditions need to be more deeply studied in future research.

The residence times calculated from the mesocosm experiments are considered more realistic than residence times calculated based on previous modelling or laboratory experiments, as mesocosm experiments more closely represent the complexities existing in lake systems. However, the conditions in the mesocosm are still likely to be quite different from a real lake. This could be due to several factors such as the boundary effect of the mesocosm walls, the small surface area of the mesocosm ($\sim 7 \text{ m}^2$), and the isolation of the water inside the mesocosm from the rest of the lakes. This will limit the size of turbulent eddies that can develop in the water column and the influence of other hydrodynamic processes such as seiches and currents that only develop in lake basins. We also noticed that the productivity in the mesocosm was higher than in the surrounding lake, making the likelihood and effect of interactions with plankton larger than in the real lake system. Also, there were some limitations caused by the field instruments. For example, microplastic concentrations and residence times were calculated depending solely on the signals detected in the measuring cells of the fluorometers, with the best case being measurements at three depths. This resulted in a lack of knowledge about the behavior of the microplastic particles over the extent of the entire water column. Finally, our understanding of the hydrodynamics inside the water column depended largely on the velocity measurements by the ADV at a single point fixed at 1m below the water surface. This also limits our understanding of the hydrodynamics conditions over the entire extent of the water column.

5. Conclusion

In this work we have, for the first time, conducted microplastic residence time experiments in a mesocosm deployed in a real lake system. The mesocosm setup and the detection and tracking methods have proven to be useful in quantifying the residence times of microplastic in lake systems under hydrodynamic conditions close to real conditions in lakes. The limitation of the model has also highlighted where real lake microplastic transport processes are more complex than pure physical transport based on sinking and turbulent diffusion.

Our field experiments have confirmed that particle size has a significant impact on the residence time during stratified summer conditions. The small microplastic particles had considerably longer mesocosm residence times than large particles. However, the residence times of these small particles were still 1 to 2 orders of magnitude shorter than predicted using a random walk model parameterized using the Stokes sinking velocities and turbulent dispersivities from the mesocosm. This was thought to be due to processes such as aggregation of the microplastic with existing lake particulate matter, and potentially the interactions with biota.

Lake hydrodynamics driven by seasonal temperature changes affected the residence time and distribution of microplastic in the mesocosm in autumn. The microplastic residence times were significantly shorter than during the summer experiment and the random walk simulations. It is thought that this was induced by the initiation of turbulent convection in the water column. This shows that the behavior of microplastic in real lake systems and the uptake probability by lake biota such as zooplankton is still poorly understood. Future work needs to incorporate processes such as heteroaggregation, biofouling, and uptake by lake organisms as well as lake hydrodynamics to quantitatively understand microplastic residence times and associated ecological effects of microplastic in these sensitive environments.

Acknowledgment

Funded by the Deutsche Forschungsgemeinschaft (DFG, German Research Foundation)—Project Number 391977956—SFB 1357. The authors would like to thank the technicians of Wasserwirtschaftsamt in Ansbach for their help and support during the deployment of the mesocosm. We would also like to thank Karel As, Peter Onyisi Uhuegbue, Marie Erler, Anna-Maria Seiverth, Isabel Piccon, and Bianca Burgesmeir for their help during the experiments.

Author Contribution Statement

HE built the mesocosm setup, performed all experiments, worked on data analysis and interpretation, and wrote the manuscript. SF built the mesocosm, helped with conducting the experiments, assisted in data interpretation, built the random walk model, did all simulations, and worked on writing and editing the manuscript. JPB assisted in data interpretation and worked on writing and editing the manuscript. GT assisted with planning the experiments and provided lake monitoring data and logistics. BSG conceived the project, built the mesocosm, helped with conducting the experiments, assisted in data interpretation, and worked on writing and editing the manuscript.

References

- Ahmadi, P., Elagami, H., Dichgans, F., Schmidt, C., Gilfedder, B.S., Frei, S., Peiffer, S., Fleckenstein, J.H., 2022. Systematic Evaluation of Physical Parameters Affecting the Terminal Settling Velocity of Microplastic Particles in Lakes Using CFD. *Front. Environ. Sci.* 10.
- Aljaibachi, R., Callaghan, A., 2018. Impact of polystyrene microplastics on *Daphnia magna* mortality and reproduction in relation to food availability. *PeerJ* 6, e4601.
- Bailly-Comte, V., Durepaire, X., Batiot-Guilhe, C., Schnegg, P.-A., 2018. In situ monitoring of tracer tests: how to distinguish tracer recovery from natural background. *Hydrogeol J* 26 (6), 2057–2069.
- Boos, J.-P., Gilfedder, B.S., Frei, S., 2021. Tracking Microplastics Across the Streambed Interface: Using Laser-Induced-Fluorescence to Quantitatively Analyze Microplastic Transport in an Experimental Flume. *Water Resources Research* 57 (12).

- Cai, Y., Li, C., Zhao, Y., 2021. A Review of the Migration and Transformation of Microplastics in Inland Water Systems. *International journal of environmental research and public health* 19 (1).
- Canniff, P.M., Hoang, T.C., 2018. Microplastic ingestion by *Daphnia magna* and its enhancement on algal growth. *The Science of the total environment* 633, 500–507.
- Cannon, D.J., Troy, C., Bootsma, H., Liao, Q., MacLellan-Hurd, R.-A., 2021. Characterizing the Seasonal Variability of Hypolimnetic Mixing in a Large, Deep Lake. *JGR Oceans* 126 (11).
- D'Avignon, G., Gregory-Eaves, I., Ricciardi, A., 2022. Microplastics in lakes and rivers: an issue of emerging significance to limnology. *Environ. Rev.* 30 (2), 228–244.
- Elagami, H., Ahmadi, P., Fleckenstein, J.H., Frei, S., Obst, M., Agarwal, S., Gilfedder, B.S., 2022. Measurement of microplastic settling velocities and implications for residence times in thermally stratified lakes. *Limnology & Oceanography* 67 (4), 934–945.
- Ghawi, A.H., Kris, J., 2012. A Computational Fluid Dynamics Model of Flow and Settling in Sedimentation Tanks, in: Woo Oh, H. (Ed.), *Applied Computational Fluid Dynamics*. IntechOpen, Erscheinungsort nicht ermittelbar.
- Holtappels, M., Lorke, A., 2011. Estimating turbulent diffusion in a benthic boundary layer. *Limnol. Oceanogr. Methods* 9 (1), 29–41.
- Huret, M., Runge, J.A., Chen, C., Cowles, G., Xu, Q., Pringle, J.M., 2007. Dispersal modeling of fish early life stages: sensitivity with application to Atlantic cod in the western Gulf of Maine. *Mar. Ecol. Prog. Ser.* 347, 261–274.
- Khatmullina, L., Isachenko, I., 2017. Settling velocity of microplastic particles of regular shapes. *Marine pollution bulletin* 114 (2), 871–880.
- Kirillin, G., Grossart, H.-P., Tang, K.W., 2012. Modeling sinking rate of zooplankton carcasses: Effects of stratification and mixing. *Limnology & Oceanography* 57 (3), 881–894.
- Kreft, A., Zuber, A., 1978. On the physical meaning of the dispersion equation and its solutions for different initial and boundary conditions. *Chemical Engineering Science* 33 (11), 1471–1480.

- Lavoie, J., Boulay, A.-M., Bulle, C., 2021. Aquatic micro- and nano-plastics in life cycle assessment: Development of an effect factor for the quantification of their physical impact on biota. *J of Industrial Ecology*.
- Lebreton, L., Andrady, A., 2019. Future scenarios of global plastic waste generation and disposal. *Palgrave Commun* 5 (1).
- Leiser, R., Wu, G.-M., Neu, T.R., Wendt-Potthoff, K., 2020. Biofouling, metal sorption and aggregation are related to sinking of microplastics in a stratified reservoir. *Water research* 176, 115748.
- Małozzewski, P., Zuber, A., 1982. Determining the turnover time of groundwater systems with the aid of environmental tracers. *Journal of Hydrology* 57 (3-4), 207–231.
- Nelms, S.E., Galloway, T.S., Godley, B.J., Jarvis, D.S., Lindeque, P.K., 2018. Investigating microplastic trophic transfer in marine top predators. *Environmental pollution (Barking, Essex : 1987)* 238, 999–1007.
- Reid, W.H., Harris, D.L., 1958. Some Further Results on the Bénard Problem. *Phys. Fluids* 1 (2), 102.
- Renner, G., Nellessen, A., Schwiers, A., Wenzel, M., Schmidt, T.C., Schram, J., 2020. Hydrophobicity-water/air-based enrichment cell for microplastics analysis within environmental samples: A proof of concept. *MethodsX* 7, 100732.
- Reynolds, C.S., Wiseman, S.W., 1982. Sinking losses of phytoplankton in closed limnetic systems. *J Plankton Res* 4 (3), 489–522.
- Ross, O.N., 2006. Particles in motion: How turbulence affects plankton sedimentation from an oceanic mixed layer. *Geophys. Res. Lett.* 33 (10), n/a-n/a.
- Rowe, M.D., Anderson, E.J., Wynne, T.T., Stumpf, R.P., Fanslow, D.L., Kijanka, K., Vanderploeg, H.A., Strickler, J.R., Davis, T.W., 2016. Vertical distribution of buoyant *Microcystis* blooms in a Lagrangian particle tracking model for short-term forecasts in Lake Erie. *JGR Oceans* 121 (7), 5296–5314.
- SAPEA, 2019. A scientific perspective on microplastics in nature and society. Evidence review report no. 4. SAPEA, Berlin.

- Singh, P., Bagrania, J., Haritash, A.K., 2019. Seasonal behaviour of thermal stratification and trophic status in a sub-tropical Palustrine water body. *Appl Water Sci* 9 (5).
- Visser, A.W., 1997. Using random walk models to simulate the vertical distribution of particles in a turbulent water column. *Mar. Ecol. Prog. Ser.* 158, 275–281.
- Waldschläger, K., Schüttrumpf, H., 2019. Effects of Particle Properties on the Settling and Rise Velocities of Microplastics in Freshwater under Laboratory Conditions. *Environmental science & technology* 53 (4), 1958–1966.
- Weeraratne, D., Manga, M., 1998. Transitions in the style of mantle convection at high Rayleigh numbers. *Earth and Planetary Science Letters* 160 (3-4), 563–568.
- Woods, J.S., Verones, F., Jolliet, O., Vázquez-Rowe, I., Boulay, A.-M., 2021. A framework for the assessment of marine litter impacts in life cycle impact assessment. *Ecological Indicators* 129, 107918.
- Worm, B., Lotze, H.K., Jubinville, I., Wilcox, C., Jambeck, J., 2017. Plastic as a Persistent Marine Pollutant. *Annu. Rev. Environ. Resour.* 42 (1), 1–26.
- Wüest, A., Lorke, A., 2003. SMALL-SCALE HYDRODYNAMICS IN LAKES. *Annu. Rev. Fluid Mech.* 35 (1), 373–412.
- Wüest, A., Lorke, A., 2009. Small-Scale Turbulence and Mixing: Energy Fluxes in Stratified Lakes, in: , *Encyclopedia of Inland Waters*. Elsevier, pp. 628–635.
- Yan, M., Wang, L., Dai, Y., Sun, H., Liu, C., 2021. Behavior of Microplastics in Inland Waters: Aggregation, Settlement, and Transport. *Bulletin of environmental contamination and toxicology* 107 (4), 700–709.

Supplementary information

S1) Mesocosm enclosure and mesocosm setup



Figure S1: The mesocosm enclosure and the mesocosm setup used for all experiments.

S2) Adding microplastics to the lake



Figure S2: Adding microplastics to the mesocosm using watering cans.

S3) Calibration lines

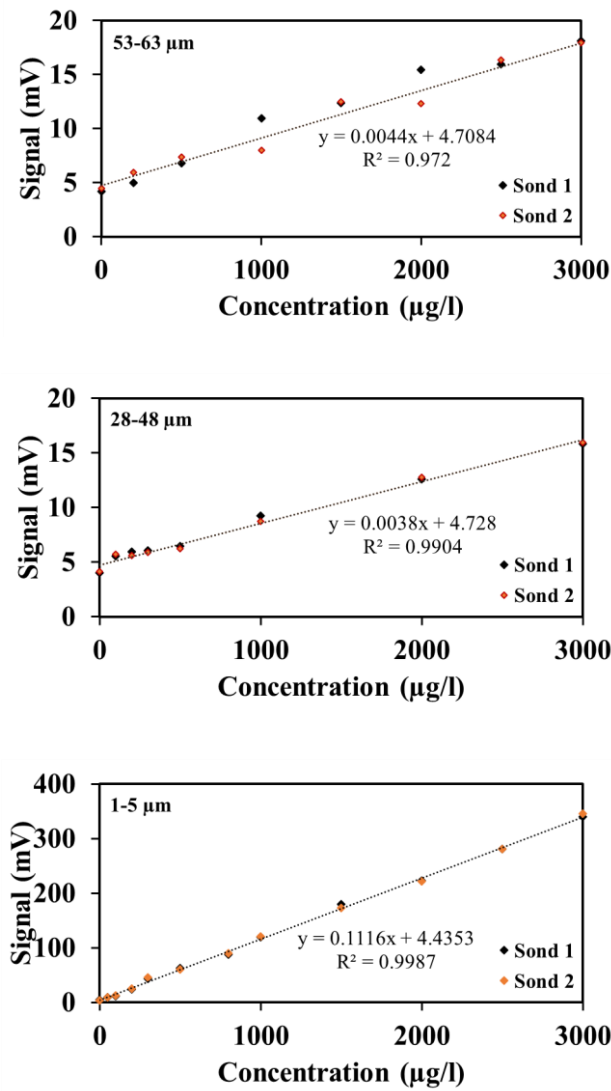


Figure S3: Calibration lines of the fluricence detectors.

S4) Corrected settling velocities

$$V_{S_PIV} = V_{ST_1} \left(\frac{10^{\left[\frac{247.8}{T_1 + 133.15} \right]}}{10^{\left[\frac{247.8}{T_2 + 133.15} \right]}} \right)$$

where V_{ST_1} [LT^{-1}], V_{S_PIV} [LT^{-1}], T_1 [$^{\circ}C$], and T_2 [$^{\circ}C$] are the settling velocity measured in the laboratory at $20^{\circ}C$, the corrected settling velocity for the lake compartments, water temperature in the laboratory, and the temperature of the lake compartment respectively.

S5) Advection-Dispersion-Model

$$pdf_{AD}(t-a) = \frac{1}{\tau_s \sqrt{4\pi Pe^{-\frac{t-a}{\tau_s}}}} e^{-\frac{\left(1-\frac{t-a}{\tau_s}\right)^2}{4Pe^{-\frac{t-a}{\tau_s}}}}$$

where $pdf_{AD}(t-a)$ [T⁻¹] is the A-D probability density function, a [T] is a time delay parameter, τ_s [T] is the mean residence time of microplastic and $Pe = v_s z / D$ [-] the Peclet-Number, relating vertical settling of particles v_s [LT⁻¹] for a given length scale z [L] (in our case the observation depths in the mesocosm) to the turbulent diffusivity D . Assuming that the vertical particle settling velocities v_s are known, Pe from a fitted A-D Model can be used to estimate the corresponding turbulent diffusivity D . For fitting the observed particle concentrations $c(t)$ [ML⁻³] to the A-D Model, the concentrations first have to be transformed into a corresponding probability frequency $f(t)$ [T⁻¹]:

$$f(t) = \frac{c(t)}{\sum c(t)\Delta t}$$

Where $\sum c(t)$ [ML⁻³] is the sum of all measured concentrations belonging to a breakthrough experiment and Δt [T] is the corresponding measurement resolution.

S6) Temperature profiles inside and outside the mesocosm

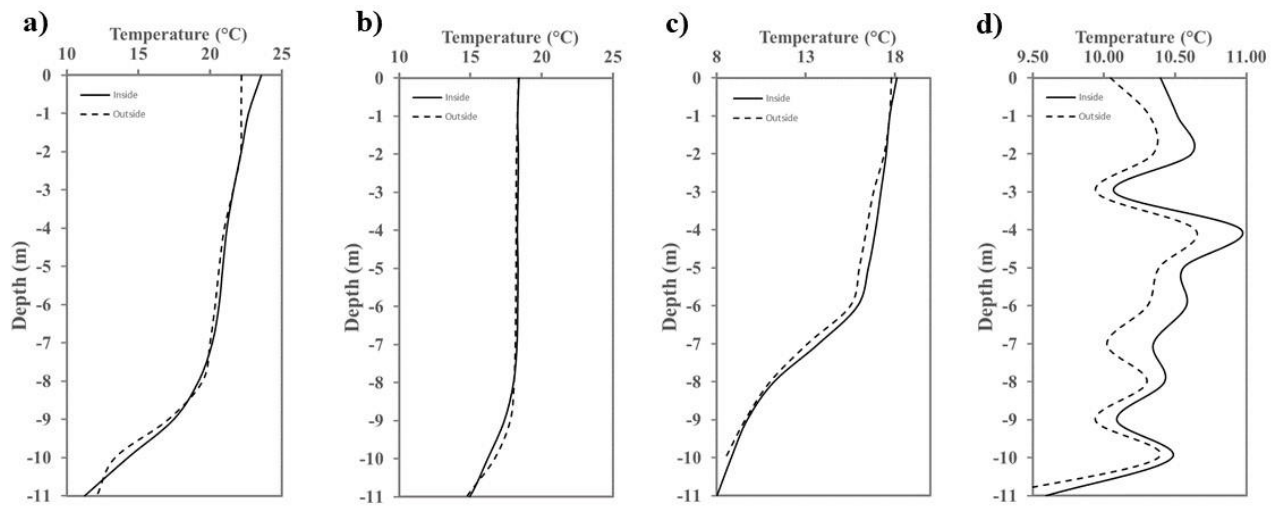


Figure S6: temperature profiles inside and outside the mesocosm before the start of each experiment. figures 5a, b, and c represent the temperature profiles during summer, while figure d represents the temperature profile during autumn.

S7) Calculated reyliegh numbers during autumn experiemnt

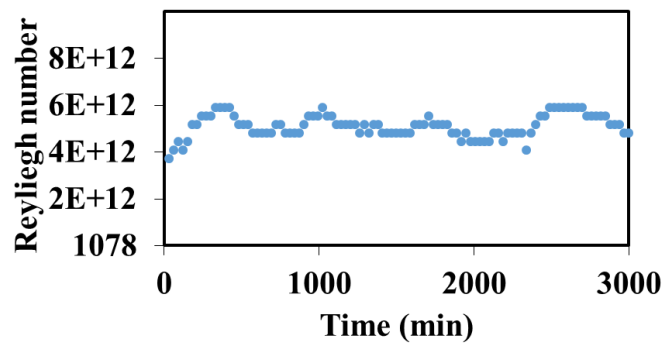


Figure S7: Calculated reyliegh numbers during autumn experiemnt at 30 minutes resolution.

S8) Characteristic settling velocities

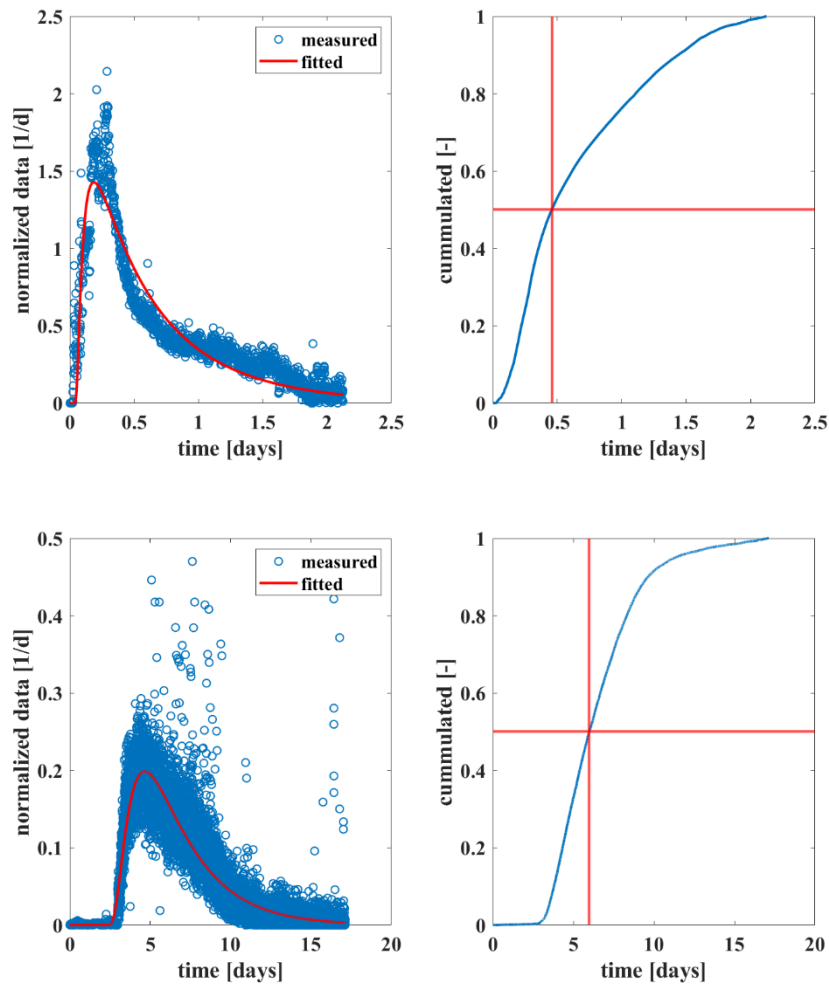
Experiment	Settling velocity	Settling velocity	Settling velocity
	Epi.	Metal.	Hypo.
	[m/d]	[m/d]	[m/d]
1-5 μm Summer	0.098 ¹	0.086 ¹	0.079 ¹
	1.09 ²	0.5 ²	0.5 ²
1-5 μm Autumn	0.077 ¹	0.077 ¹	0.077 ¹
	0.78 ²	0.78 ²	0.78 ²
28-48 μm Summer	0.16 ²	4.11 ²	5.15 ²
	8.7 ³	8.0 ³	8.0 ³
53-63 μm Summer	50.0 ²	50.0 ²	50.0 ²
	19.0 ³	17.0 ³	17.0 ³

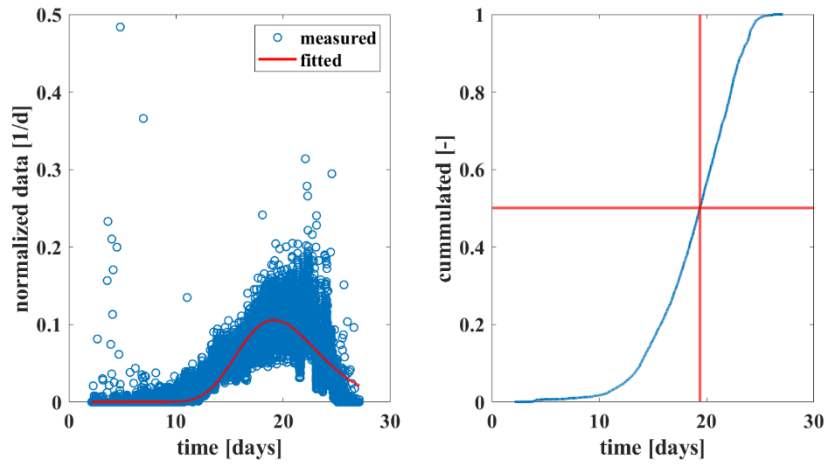
¹ V_{s_Stokes} ² V_{s_eff} ³ V_{s_PIV}

S9) A detailed description of the A-D fitting procedure

a) Summer 1-5 μm

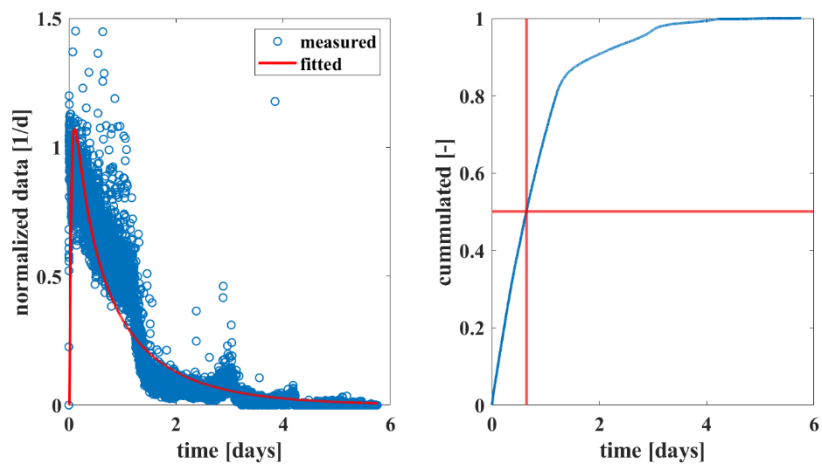
depth	Pe^{-1}	a	τ_s
[m]	[-]	[days]	[days]
0.5	0.63	0.028	0.29
6	0.22	2.10	3.19
10	0.019	0	19.37

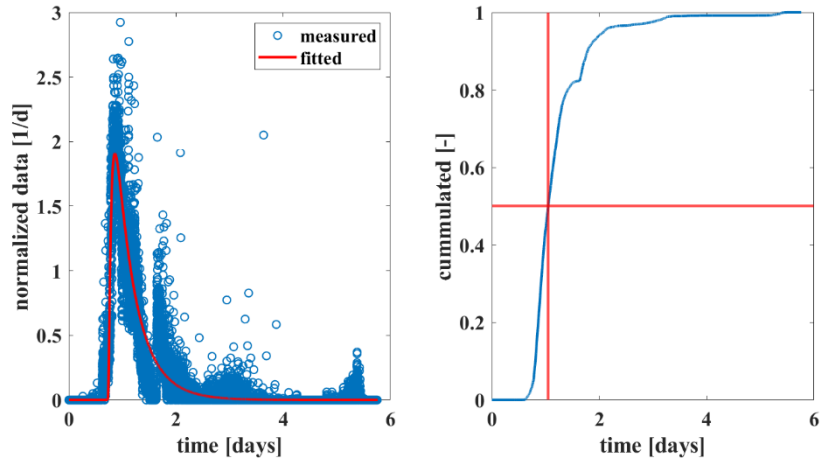




b) Autumn 1- 5 μ m

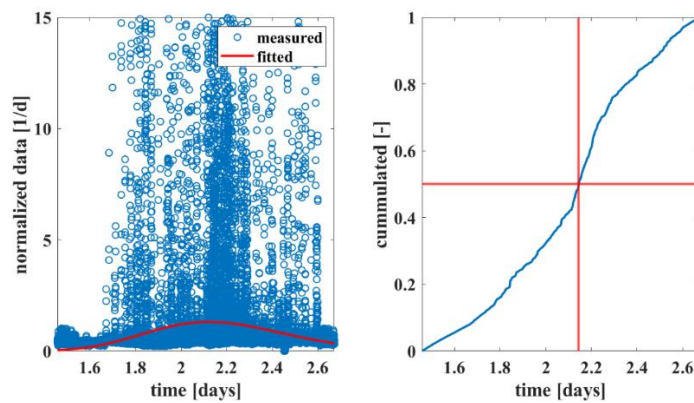
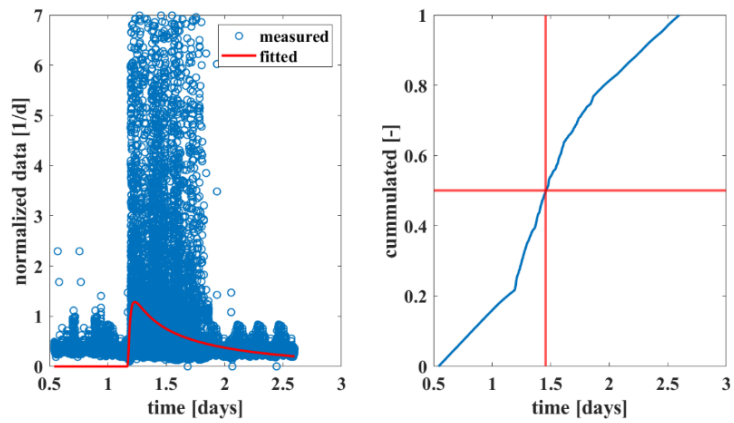
depth	Pe ⁻¹	a	τ_s
[m]	[-]	[days]	[days]
0.5	1.27	0	0.31
6	0.5	0.72	0.24
10	-	-	-





c) *Summer 28-48 μ m*

depth	Pe^{-1}	a	τ_s
[m]	[-]	[days]	[days]
0.5	5.762	0.34	0.37
6	1.68	1.16	0.24
11	0.0102	0	2.14



d) Summer 53-63 μ m

depth	Pe⁻¹	a	τ_s
[m]	[-]	[days]	[days]
0.5	1.41	0.0021	0.0048
6			
11			

S10) Random Walk Model Parametrization

Experiment	H _E	H _M	H _H	D _s	D _M	D _H
	[m]	[m]	[m]	[m ² /s]	[m ² /s]	[m ² /s]
1-5 μm Summer	8	2	11	6.7x10 ⁻⁶ ¹	6.7x10 ⁻⁶ ¹	1.12x10 ⁻⁶ ²
1-5 μm Autumn	9	1	11	9.2x10 ⁻⁷ ¹	9.2x10 ⁻⁷ ¹	9.2x10 ⁻⁷ ¹
28-48 μm Summer	8	3	11	1.07x10 ⁻⁵ ¹	3x10 ⁻⁶ ²	3x10 ⁻⁶ ²
53-63 μm Summer	8	3	11	4.6x10 ⁻⁶ ¹	4.6x10 ⁻⁶ ¹	4.6x10 ⁻⁶ ¹

Taylor's approach¹, AD fitting²

Study 4: Filter feeders are key to small microplastic cycling in stratified lakes: a virtual experiment

B.S Gilfedder, **H. Elagami**, J.P. Boos, J. Brehm, M. Schott, L.Witt, C. Laforsch, S. Frei

Submitted to *Association for the Science of Limnology and Oceanography* on 12th Sep. 2022

Abstract

Microplastic (MP) poses an uncertain risk to lake ecosystems. Its uptake is largely controlled by its residence time. Here we use laboratory and virtual experiments to quantify small MP (<15 μm) residence times in a large (Lake Constance) and small (Esthwaite Water) lake. The aims were to quantify MP residence times in a purely physical system controlled by sinking and mixing and compare this to a system where *Daphnia* additionally package MP into faecal pellets. The laboratory experiments showed that settling velocities increased from $\sim 5 \times 10^{-6}$ - 10^{-3} mm/s for pristine MP to ~ 1 mm/s for the faeces. Modeled 0.5 and 5 μm particles had very long lake residence times (>15 years) in the abiotic simulations but were reduced to ~ 1 year in the biotic model. The 15 μm particles had a residence time of 1-2.5 years in the abiotic system and <1.6 years once *Daphnia* were included. The ratio of the MP uptake velocity to the sinking velocity ($v_{\text{up}}/v_{\text{s_epi}}$) was used to compare the biological and physical systems. For the 0.5 and 5 μm particles $v_{\text{up}}/v_{\text{s_epi}}$ was $\gg 1$ in all cases for both lakes, while for the 15 μm MP there was a transition between biological and physical processes dominating depending on *Daphnia* numbers. These virtual experiments show that the packaging of small MP in faecal pellets by zooplankton will control its residence time in lakes. Moreover, the majority of small MP will cycle through organisms before reaching the sediment, increasing the likelihood of negative ecological effects and transfer in the food web.

Introduction

Microplastic (MP) is of growing concern for lake ecosystems as organisms can consume and transfer MP particles at all ecological levels with only poorly understood effects that potentially range from the individual to whole populations (Elizalde-Velázquez et al. 2020; Schwarzer et al. 2022; Trotter et al. 2021). Uptake by lake organisms and transfer within the food web is closely coupled with the MP cycle in lakes, which involves a number of complex interrelated processes such as transport within the water column, sedimentation to the lake sediments, uptake by biota, transfer within the food chain, and potentially degradation and colonisation of MP by biofilms (D'avignon et al. 2022). There is a growing body of literature that has documented the quantity and characteristics of MP polymers found in lake water (Tamminga and Fischer 2020), lake sediments (Su et al. 2016) as well as within lake organisms (Michler-Kozma et al. 2022; Yıldız et al. 2022). Although it is difficult to generalise MP numbers in lakes due to the large diversity of lake types and geographical settings as well as differing sampling and quantification techniques (e.g., lower MP size cut-off often differs between studies, (Stock et al. 2019)), recent reviews have estimated that MP numbers in the water column typically vary between 0.1 and 10 MP particles m^{-3} (D'avignon et al. 2022; Tanentzap

et al. 2021). While the highest MP numbers are usually found in highly populated industrialised areas (e.g. 15,000 MP particles m^{-3} in the water column of Lake Tai Hu, China (Su et al. 2016)), MP can also be found in regional (Tamminga and Fischer 2020) and remote areas in remarkably high numbers (e.g. Negrete Velasco et al. (2020) identified ~ 2600 MP particles m^{-3} in the water column and outlet of a frozen Swiss mountain lake), demonstrating the importance of long-range transport and local sources far from industrialised areas (Dong et al. 2021).

Lakes are often considered as MP sinks as MP numbers in their sediment are typically significantly higher than the water column (see data compilation in D'avignon et al. 2022). The lake serves as a permanent sink when MP is buried in lake sediments, or as a transitory storage when resuspension from the sediment releases MP back into the lake water column, or when there is a long residence time (RT) within the water column. The current understanding is that particle properties, lake properties and lake hydrodynamics largely determine whether a MP particle will be transported conservatively through a lake or be lost to the sediments (Elagami et al. 2022). Large dense particles (>10 's of μm) tend to sink rapidly, and thus are expected to have short RTs within the water column and accumulate in the lake sediments (Ahmadi et al. 2022; Khatmullina and Isachenko 2017; Waldschläger and Schüttrumpf 2019). In contrast small, low density particles ($<$ few μm) have slower settling velocities, longer RTs, and are more likely to be flushed through the lake before they can enter long-term storage in the sediments (Elagami et al. 2022). Due to limitations in sampling and analysis, the smallest MP particles are still able to be measured in lake water or sediments, although this is starting to change with the availability of ultra-high resolution FT-IR and Raman spectroscopy (Vinay Kumar et al. 2021).

The microplastic RT in the water column, and especially in the epilimnion, is an important parameter for evaluating the probability of ingestion by lake organisms. Lakes host a range of organisms from various trophic levels, with the potential for uptake either directly via filter-feeding (Scherer et al. 2017) or ingestion of MP-containing prey (Chae et al. 2018) with subsequent transfer within the aquatic food web (Yıldız et al. 2022). Long RTs in the epilimnion, where the majority of lake organisms reside, leads to a higher likelihood of uptake, especially by planktonic filter feeders such as *Daphnia*. In contrast, short RTs will give organisms a limited time to ingest MP particles. Uptake will also be influenced by MP size, as larger particles cannot pass the feeding apparatus (Ebert 2005). Filter feeders are central for MP entering into the food web, as they feed by consuming particulate organic carbon (POC) from the water column as their primary food source. This POC is typically phytoplankton, live or dead, and bacteria but also includes other POC sources such as detritus from the catchment

(Bell and Ward 1970; McMahon and Rigler 1965). At the population maximum zooplankton can remove most of the POC from the epilimnion in the ‘clear water phase’, where most, if not all water in the epilimnion passes through these organisms (Effler et al. 2015). This is followed by a rapid population decline due to the depleted food source and an increase in predation pressure. There is still very little known about how MP uptake affects freshwater aquatic organisms at concentrations relevant for real lake systems (O’connor et al. 2020). However, there are numerous studies that have shown detrimental effects of MP on lake biota at elevated MP concentrations and transfer within the lake food web (O’connor et al. 2020). However, there is little known about what uptake and release of MP imbedded in faeces means for MP transport within the water column. It seems reasonable to assume that once imbedded in zooplankton faeces the hydrodynamic properties of the MP should be controlled largely by the faeces properties rather than by those of the individual plastic particles, as has been observed in the ocean (Cole et al. 2016; Pérez-Guevara et al. 2021). Thus, the role of filter feeders in the lake MP cycle may be critical, particularly in determining microplastic RTs within the lake water column and the availability of MP for uptake by lake organisms.

In this work we use a series of generic virtual lake experiments to quantitatively study the role of *Daphnia*, a key lake zooplankton species, on microplastic cycling in lakes. The simulations are parametrised using data from a large (Lake Constance, Germany) and a small lake (Esthwaite Water, UK) as well as from existing literature and our own laboratory experiments. The aim is to elucidate how lake size and *Daphnia* population dynamics effect MP RTs in the lake water column. We focus on how ingestion of MP by *Daphnia* and egestion as part of their faeces influences the settling velocities and residence times in the water column of these two lakes. Essentially, we quantify (i) how long organisms will likely be exposed to MP in the lake water column, (ii) if lakes act as long-term sinks for MP particles or if they are only a transient storage before being transported out of the lake, and (iii) the role of filter feeding organisms such as *Daphnia* play in these processes.

Materials and Methods

Model Lake System

The transport and accumulation of MP particles with and without *Daphnia* was studied using an array of generic virtual experiments, using Lake Constance, Germany, to represent large lakes and Esthwaite Water, UK, to represent small lakes. The full mathematical description of the model can be found in the supplement. In the following we give a description of the most pertinent aspects of the model. Each model represents a stratified lake with a well-mixed (fully

turbulent) epilimnion and hypolimnion and a laminar Metalimnion similar to that described in Elagami et al. (2022) (Figure 1). Model parameters such as lake area, water residence time, mean depth and temperature for each lake layer are based on literature data (Achterberg et al. 1997; Isf 2016) (Table 1).

Table 1: Lake parameters used in the virtual experiments.

	Lake Constance	Esthwaite Water
Lake Area [km²]	472	1.0
Water Residence Time	4 years	13 weeks
Depth [m]		
<i>Epilimnion</i>	15	6
<i>Metalimnion</i>	10	2
<i>Hypolimnion</i>	65	4
Mean Temperature [°C]		
<i>Epilimnion</i>	15	15
<i>Metalimnion</i>	10	11
<i>Hypolimnion</i>	4.5	8

The abiotic model system includes an exponential RT distribution in the epilimnion and hypolimnion and one unique RT in the metalimnion based on its depth and the MP sinking velocity v_s (i.e. $t = \text{depth}/v_s$). The influence of *Daphnia* on MPs residence times was analysed for the epilimnion, metalimnion and hypolimnion simultaneously. The primary parameters were the *Daphnia* MP ingestion rate in the epilimnion, the MP RT in the *Daphnia* intestinal tract, the egestion rate of MP in *Daphnia* faeces, the settling velocity of these faeces and the *Daphnia* population numbers in the lake during the year. While we do not explicitly model ecosystem processes such as grazing or predator-prey relationships, these processes are implicitly included due to the use of measured population data from the two lakes.

Due to the lack of literature data for individual *Daphnia* species, we were required to pool data from various species for each model parameter. For example, only the total numbers of Cladocera were available from monthly monitoring at Lake Constance (Isf 2016) and Esthwaite Water (Talling 2003), while the *Daphnia* MP ingestion rates were specifically for *Daphnia magna* (Scherer et al. 2017). This mix of parameters introduces an inherent uncertainty in the model results as each species is likely to have a characteristic set of representative parameters.

This was addressed using an uncertainty analysis described in section 2.6. Each model lake system was run in two ways: 1) by exclusively simulating physical MP transport within the water column (abiotic system, Figure 1B), and 2) by accounting for physical MP transport and ingestion and egestion by *Daphnia* (biotic system, Figure 1A). Uptake of MP by *Daphnia* was assumed to occur only during night in the epilimnion as part of the diel vertical migration, with the model using a 12h day-night cycle. This is another simplification of reality, as real lakes are populated an array of *Daphnia* species with individual migration patterns that are often responding to predator (fish) behaviour and day length (Ringelberg 1999). However, this seems to be the most realistic way of simply representing the most important aspects of *Daphnia* feeding habits into the model. MP particles are released as part of *Daphnia* faeces into the epilimnion which then sink with a characteristic sinking velocity. Once the MP particles reach the lake sediments they were assumed to be permanently immobilized. For both model systems we further assume 1) both lakes are perpetually stratified and 2) once particles enter the lake they are uniformly distributed in the epilimnion. These are necessary simplifications as simulating the full hydrodynamics of the two lakes is not possible with our simplistic representation of the lake system as a series of transfer functions.

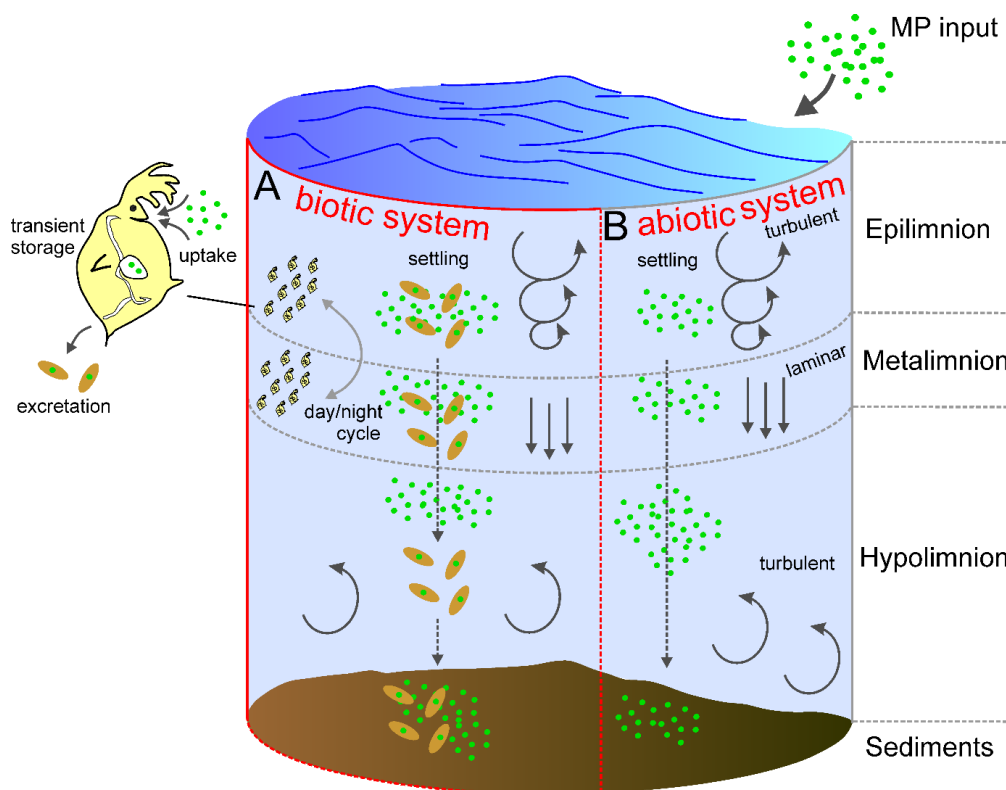


Figure 1: Conceptual model of the primary processes effecting MP transport and residence times in a stratified lake as implemented in the model. A) the model containing biological uptake and excretion by *Daphnia* plus physical transport, B) purely physical transport in the water column.

2.3 Settling Velocities for MP particles

Microplastic settling velocities for the different lake compartments were estimated using Stokes law for polystyrene ($\rho=1.050 \text{ kg m}^{-3}$) with particle diameters of 0.5 μm , 5 μm and 15 μm . Settling velocities of the particles were corrected for water temperature based on mean annual temperatures in each of the lake compartments by applying an empirical relationship that is dependent water density and dynamic viscosity (Elagami et al. 2022).

2.4 Uptake and Egestion of MP by *Daphnia*

Ingestion of particles into the digestive tract of *Daphnia* was represented by assuming proportionality between the particle uptake rate and MP numbers in the epilimnion (Eq. S1). $k_2(t)$ represents the time dependent MP uptake parameter for the entire population of *Daphnia* and essentially represents the proportion of the epilimnic water that passes through the *Daphnia* population per day. It requires 1) a representative filtration rate for a single daphnid individual m , 2) the total volume of the epilimnion V_{epi} , 3) the *Daphnia* population per lake area P as a function of time and 4) the corresponding lake area A . Data used to derive the filtration rate (Supplementary Figure S1A) were taken from MP feeding experiments presented in Scherer et al. (2017) while the population densities of Cladocera for Lake Constance and Esthwaite Water are based on Isf (2016) and Talling (2003) respectively (Supplementary Figure S1B).

$$k_2(t) = \frac{m}{V_{epi}} A P(t) \quad (3)$$

The faeces excretion rate (supplementary Eq S1) controlling the release of MP from the *Daphnia* into the epilimnion, was estimated from *D. magna* feeding experiments presented in Rosenkranz et al. (2009). An exponential model was used to represent the experimental data shown in Supplementary Figure 1C. The exponential model showed a very good fit ($r^2=0.99$), providing an estimate for the excretion rate of 14.5 d^{-1} which translates to a RT in the *Daphnia* of about 5 h for 95% of particles to leave the organism.

2.5 Faeces sinking velocities

There is currently no data available on the sinking velocities of *Daphnia* faeces containing MP from fresh water lakes. To quantify the sinking velocities of these MP imbedded faeces, experiments were conducted in the laboratory of Animal Ecology, University of Bayreuth, using the *D. magna* clone BL2.2 that originated from a small pond in Leuven (Belgium) (Imhof et al. 2017). Prior to the experiment, female *Daphnia* were cultured in 1.5 L jars containing 1 L artificial M4 medium at $20 \pm 0.5 \text{ }^\circ\text{C}$ and a 16 h:8 h light:dark regime with half an hour dusk and dawn respectively (Elendt and Bias 1990). *Daphnia* were fed ad libitum with the unicellular

green algae *Acutodesmus obliquus* three times a week. To avoid crowding effects, neonates of the first and second broods were removed within 24 h after release.

Microplastic used in the feeding experiments were wet ground PS fragments (diameter ~ 17.7 μm , PS158N/L; INEOS Styrolution Group GmbH, Germany) and red PS spheres (diameter ~ 3 μm ; Polybead®, Polysciences, Inc.; USA). Additionally, spray dried fluorescent labelled (rhodamine B) PS (\varnothing 10.4 μm ; Europäisches Zentrum für Dispersionstechnologien, Germany) was used to analyze the degree of MP incorporation into the faeces. Stock suspensions of PS particles were prepared following the protocol of Schür et al. (2020) ensuring that particles were well dispersed. Approximately 50 mg of the respective particles were suspended in 50 ml autoclaved M4 medium and shaken for 48 h at 100 rpm. Stock suspensions were then stored at 4 °C and continuously stirred before dilution. Finally, the particle concentration of stock suspensions was evaluated using a hemocytometer (Brand GmbH) prior to the experiments.

Third brood age synchronized primiparous *D. magna* were separated in 150 ml beakers containing 50 ml of the M4 medium, 2 mg C l⁻¹ of *A. obliquus* and 5000 particles ml⁻¹ of the respective MP particles. After 24h of exposure to the particles, *Daphnia* faeces were collected from the bottom of the beakers and gently transferred with 5 ml plastic pipettes to a plexiglass chamber (3 x 3 x 12 cm) filled with M4 medium for settling velocity measurements. Faeces settling velocities were measured using particle image velocimetry (PIV) (Elagami et al. 2022). Velocities were subsequently determined using the TrackMate plugin (Ershov et al. 2021) in ImageJ (Schindelin et al. 2012).

To determine if the MP were incorporated into the *Daphnia* faeces, the animals were exposed to the rhodamine B labelled PS as described above. After 24h, faecal pellets were collected, gently washed three times in ultrapure water, transferred to microscope slides, dried in a desiccator and imaged using a Leica M205 FCA fluorescence stereo microscope (excitation: 553 nm; emission: 627 nm; Leica Microsystems; Germany).

2.6 Physical sinking vs biological uptake

To determine if MP transport in the lake epilimnion is dominated by abiotic or biotic transport processes we calculate the ratio between the mean MP residence time in the epilimnion τ_{epi} , and a characteristic *Daphnia* ingestion time τ_{up} (Eq. 4). τ_{up} is the inverse of $k_2(t)$. v_{up} is $m P(t)$ and by using the definition of the mean residence time in the epilimnion (Supplementary equation 2a), the ratio in equation 4 can also be expressed in terms of the particle settling velocities and uptake velocities. When v_{up}/v_{s_epi} ratio is ~ 1 both uptake/excretion by *Daphnia* and physical sinking are equally important for MP residence times within the epilimnion, while at

$v_{up}/v_{s_epi} \gg 1$ biological uptake dominate, while $v_{up}/v_{s_epi} \ll 1$ indicate that physical transport dominate.

$$\frac{\tau_{epi}}{\tau_{up}} = \frac{m P(t)}{v_{s_epi}} = \frac{v_{up}}{v_{s_epi}} \quad (4)$$

2.6 Parameter Uncertainty

Data on MP uptake and excretion rates of MP by filter feeding organisms such as *Daphnia* are sparse, especially at the species level. We have been restricted to data from a limited number of sources and usually to one single *Daphnia* species, which also varies from parameter to parameter. To account for the uncertainty introduced into the simulation we performed an uncertainty analysis using a bootstrapping method. Egestion, filtration rates and *Daphnia* population dynamics were randomly selected as model input from a range of $\pm 50\%$ of the original values, assuming the original values represent the mean of a normal distribution. This changes the absolute numbers of each parameter, but not the temporal development of the population. In total 200 unique parameter sets for each lake system were generated and run through the model. All simulations were evaluated for the time it takes for 95% of the MP particles to reach the lake sediments, referred to as the lake residence time.

Results

The settling velocities of the MP-containing *Daphnia* faeces had a mean and standard error of 1.04 ± 0.07 (n=14) and 0.93 ± 0.13 mm s⁻¹ (n=13) for the 17.4 μ m and 3 μ m MP particles, respectively (Figure 2). In comparison, the Stokes sinking rates of pristine plastic of the same size was 7.5×10^{-3} and 2.2×10^{-4} mm s⁻¹. This shows that the sinking velocity of *Daphnia* faeces controlled the MP sinking rate, while the effect of MP size was only of minor importance in the faeces. The MP particles were clearly imbedded in the *Daphnia* faeces pellets (Figure 2). A sinking velocity of 1 mm s⁻¹ was used for all subsequent modelling of faeces sinking velocities, except for the sensitivity analysis where it was varied by $\pm 50\%$, as described above.

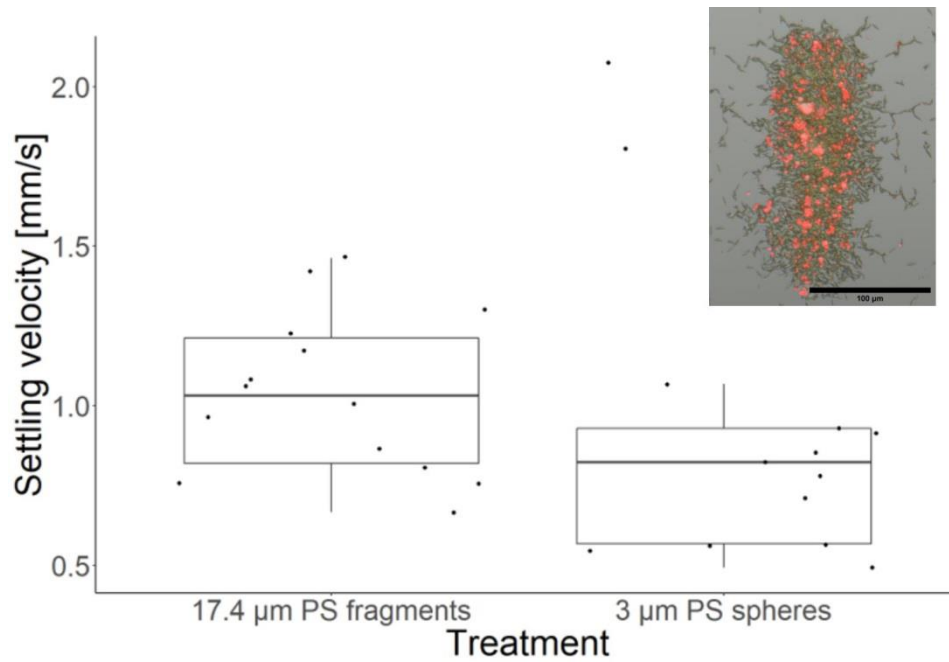


Figure 2: Settling velocities of *Daphnia magna* faeces containing PS MP (fragments $n = 14$; spheres $n = 13$). Mean settling velocities (\pm SE): fragments 1.04 ± 0.07 mm/s; spheres: 0.93 ± 0.13 mm/s. Inset is an image of *D. magna* faeces containing MP. Scale bar of inset faeces is $100 \mu\text{m}$.

Initially the model particle flux to both lakes was kept constant for one full year at 10^7 particles per day, which amounted to a total MP input to both lakes of 3.65×10^9 particles (Figures 3&4). Thereafter MP particle numbers in the epi-, meta-, and hypolimnion were solely controlled by in-lake processes. During the first year MP numbers increased rapidly in the epilimnion of both lakes. In the Lake Constance abiotic model MP numbers in the water column reached $\sim 3.6 \times 10^9$ particles for the $0.5 \mu\text{m}$ MP, 2.1×10^9 particles for the $5 \mu\text{m}$ MP, and 0.3×10^9 particles for the $15 \mu\text{m}$ MP (Figure 3). In the biotic system containing *Daphnia* the number of particles in the epilimnion were only 5-10 % of the abiotic system, with a maximum of 0.4×10^9 particles for both the 0.5 and $5 \mu\text{m}$ MP and $\sim 0.2 \times 10^9$ particles for the $15 \mu\text{m}$ MP. The maximum in MP numbers were not found at the end of the first year as in the abiotic system, but shortly before the maximum in the *Daphnia* populations. In the abiotic simulations for the smaller lake Esthwaite Water MP numbers in the epilimnion were similar to Lake Constance for the $0.5 \mu\text{m}$ particles, but were considerably lower for the $5 \mu\text{m}$ ($\sim 1.1 \times 10^9$) and especially the $15 \mu\text{m}$ ($\sim 0.1 \times 10^9$) particles (Figure 4). In the Esthwaite Water biotic model the highest MP numbers in the epilimnion were not found at the end of the first year, as also seen in Lake Constance, but slightly before the maximum in the *Daphnia* population, with $\sim 0.5 \times 10^9$ particles for the $0.5 \mu\text{m}$, 0.4×10^9 for the $5 \mu\text{m}$ particles, and 0.1×10^9 for the $15 \mu\text{m}$ particles. This is 14 %, 45% and

~100 % of the maximum particle numbers found in the abiotic system for the three particle sizes, respectively.

Lake Constance: abiotic system

Lake Constance: biotic system

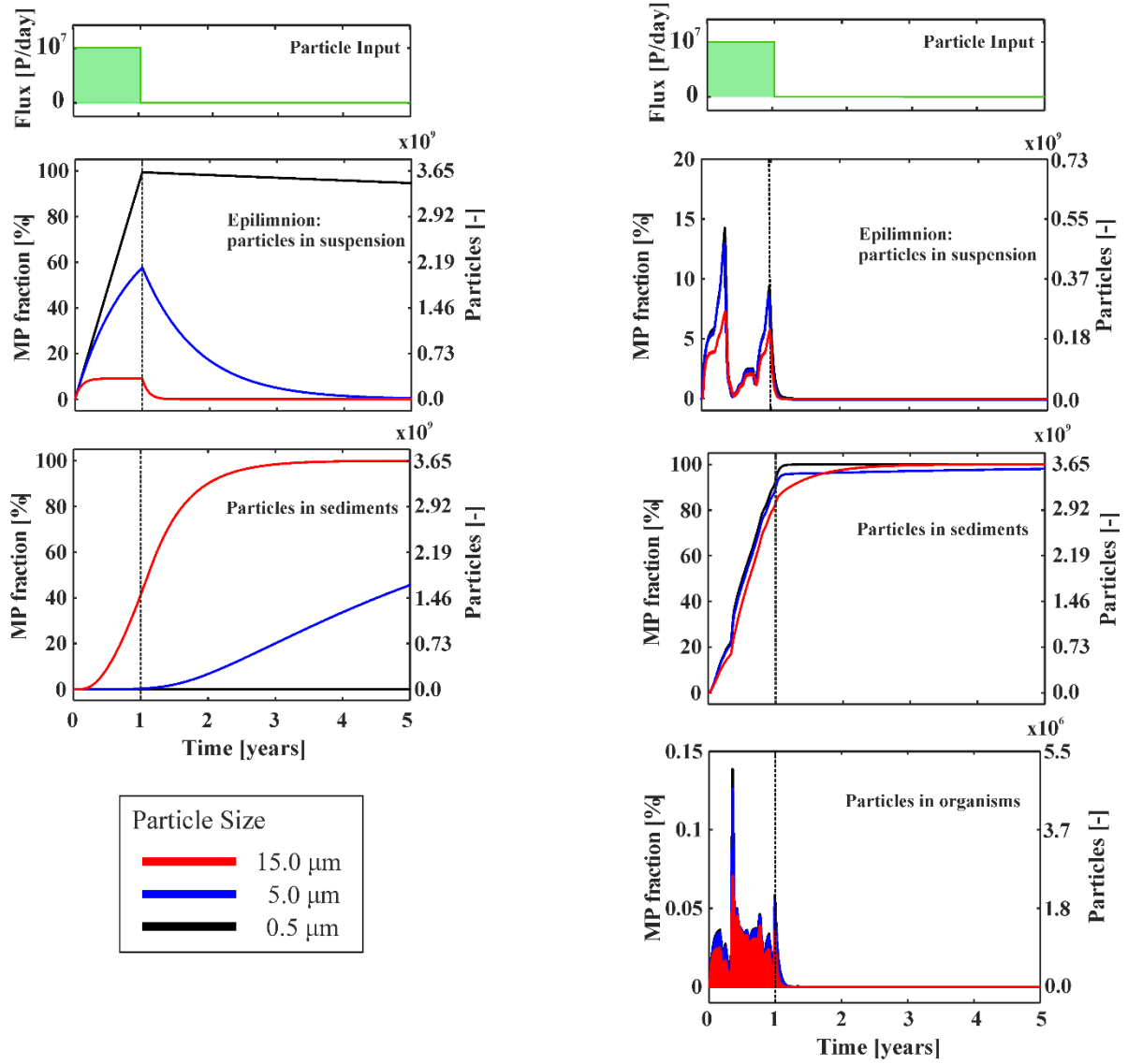


Figure 3: Comparison between simulated abiotic and biotic MP numbers and percent of total input in Lake Constance epilimnion, entering the sediments and in the *Daphnia* biomass.

Esthwaite Water: abiotic system

Esthwaite Water: biotic system

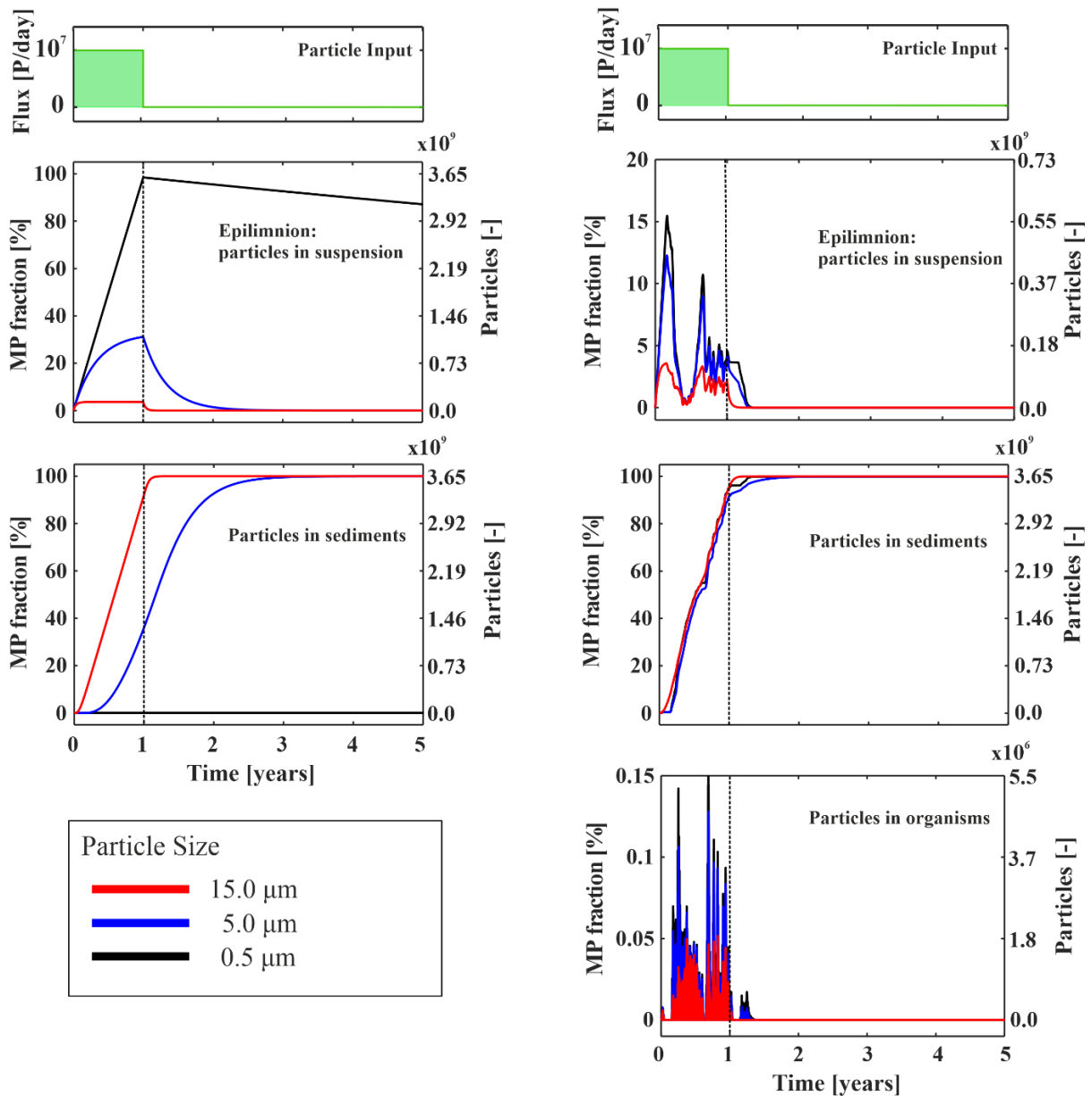


Figure 4: Comparison between simulated abiotic and biotic MP numbers and percent of total input in the Esthwaite Water epilimnion, entering the sediments and in the *Daphnia* biomass. In the abiotic simulations, once the MP flux ceased the numbers of 0.5 μm particles decreased very slowly in the epilimnion of both lakes; $\sim 95\%$ of the particles remained in the Lake Constance and $\sim 87\%$ in the Esthwaite Water epilimnion after 5 years simulation time (Figures 3&4). The 5 μm and especially the 15 μm particles exited the epilimnion considerably faster than the 0.5 μm particles in both lakes, with 95% of these larger particles lost $<1-3.5$ years. In contrast to the epilimnion, the time required for 95% of the particles to exit the entire lake water column and reach the sediments (MP lake residence time, τ) for the abiotic systems was in excess of 15 years for the 0.5 μm and 5 μm particles and ~ 2.4 years for the 15 μm particles

in Lake Constance (Table 2). In contrast the residence times for 5 μm and 15 μm particles in Esthwaite Water were only ~2.15 and 1.03 years due to the shallower lake depth. The 0.5 μm particles were calculated to have a residence time of >15 years, with no noticeable flux to the sediments over the entire 15 year simulated period. Only a very small proportion of MP was found in the *Daphnia* biomass at any one time, with a maximum of 0.15 % of the total MP added to the lake, and usually around 0.05 % (Figures 3&4). There were a larger number of the 0.5 μm and 5 μm particles stored in biomass than 15 μm particles.

Table 2: Microplastic residence time and uncertainties (from the sensitivity analysis) in the two lakes, defined as the time for 95 % of the particles to leave the lake and enter the sediments.

	Lake Constance residence time [years] (confidence interval)	Esthwaite Water residence time [years] (confidence interval)
0.5 μm		
bitotic system	1.02 (0.99-1.15)	1.19 (0.98-1.26)
abiotic system	>15	>15
5.0 μm		
bitotic system	1.1 (1.01-4.04)	1.2 (1.02-1.37)
abiotic system	>15	2.15
15.0 μm		
bitotic system	1.58 (1.33-1.9)	1 (0.98-1.01)

Apart from the 15 μm particles for Esthwaite Water, the MP residence times for both lake systems were significantly shorter in the biotic than in the abiotic simulations (Table 2). The largest difference in residence times were observed for the 0.5 μm particles, where 95% of the MP particles reached the sediments after ~1 year for both lakes in the biotic model while in the abiotic model it was >15 years. The reduction in residence time caused by introducing *Daphnia* into the model decreased with particle size, and lake depth, to the point where there was little (a few %) difference between abiotic and biotic residence times for the 15 μm particles in the

shallow Esthwaite Water. The temporal dynamics in particle numbers in both lakes was largely controlled by the *Daphnia* population dynamics, with the minimum MP numbers in the water column during the clear water phase when the *Daphnia* population was at its maximum. The highest numbers were in the winter months when there was nearly no *Daphnia* in both lakes. There was little noticeable effect of the diel feeding cycle on MP numbers.

The parameter uncertainty analysis for the biotic Lake Constance model indicated that the residence times of 0.5 μm , 5 μm and 15 μm particles were only minimally affected by parameters associated with ingestion and egestion of MP and *Daphnia* population dynamics (Table 2 & supplementary Figure 3). The estimated 95 % confidence intervals for residence times ranged between 0.99-1.15 years for 0.5 μm , 1.01-4.04 years for 5 μm and 1.33-1.9 years for 15 μm particles (Table 2). In the Esthwaite Water model parameter uncertainty only had a significant effect for the 0.5 μm and 5 μm particles. The 95 % confidence intervals ranged between 0.98-1.26 (0.5 μm), 1.02-1.37 (5 μm) and 0.98-1.01 years (15 μm). As would be expected, the combined effect of the filtering rate and the total numbers of *Daphnia* in the lake had the largest effect on MP residence times in the simulations. The combination of these two parameters quantifies the total amount of water, and thus also number of particles, that passes through the *Daphnia* population. The egestion rate has less of an effect on the residence times but controls the amount of MP stored in the organisms. The parameters associated with particle settling were not subject to the bootstrapping analysis, as the model uncertainty is assumed to be predominantly associated with the poorly constrained and often lumped biological parameters taken from the literature.

The ratio between the MP uptake rate by *Daphnia* and the sinking velocity of pristine MP in epilimnion (v_{up}/v_{s_epi}) was calculated as a dimensionless number to characterize the importance of the biotic versus abiotic pathways for MP residence times in the lake water column. A v_{up}/v_{s_epi} ratio of 1 indicates that sinking and uptake are of equal importance, $\gg 1$ indicates the biological pathway dominates while a value $\ll 1$ indicates that the abiotic sinking dominates. We define the transition zone to be from 0.1 to 10. This analysis showed that v_{up}/v_{s_epi} scales with the *Daphnia* population and particle size; and that the smaller the MP particle the more dominant is the biological pathway (Figure 5). For the 0.5 μm particles the biological pathway is always the dominant way for MP to leave the lake water column and enter long term storage in the sediments (as faeces), while for the 5 μm and 15 μm particles the biological pathway becomes dominant (>10) at *Daphnia* populations of 10,000 and 100,000 individuals per m^2 respectively. The 5 μm particles remain >1 for *Daphnia* numbers >1000 individuals per m^2 and v_{up}/v_{s_epi} is never below 0.1 for the populations recorded in both lakes. Only the 15 μm particles

produced a v_{up}/v_{s_epi} value smaller than 1 for the *Daphnia* populations measured in the lakes while the abiotic pathway becomes dominant (<0.1) at populations below 1000 individuals per m^2 .

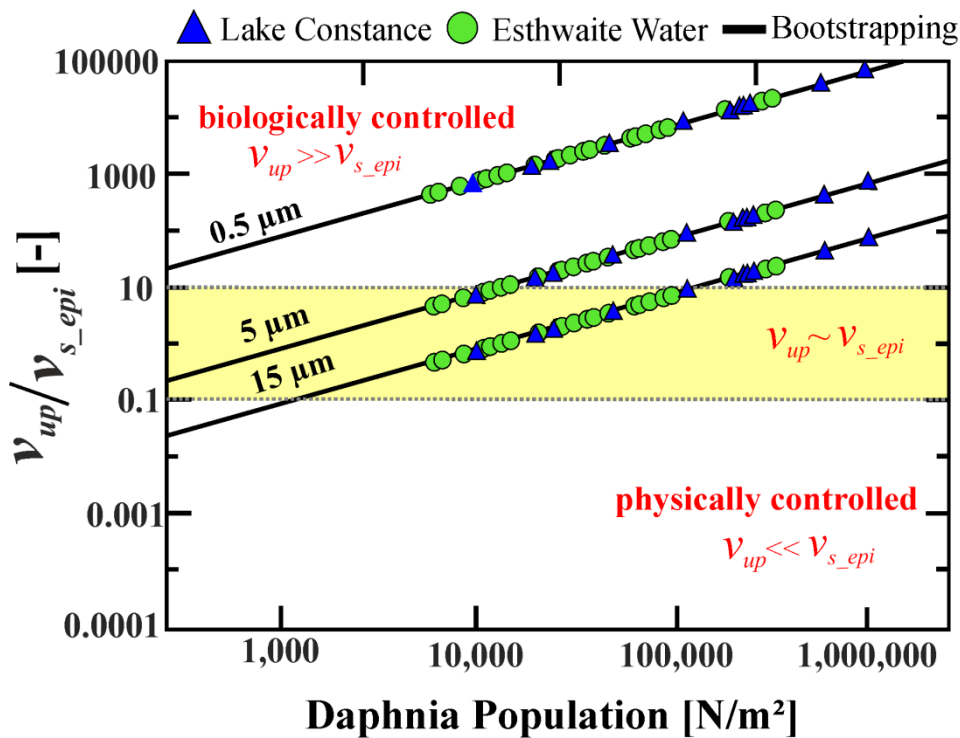


Figure 5: Ratio of *Daphnia* uptake vs. physical sediment as a function of the *Daphnia* population as an indicator of physically vs. biologically controlled MP removal from lake systems.

Discussion

Despite decades of plastic pollution research in the world's oceans, it is still in its infancy in limnic environments. Microplastic is of growing concern in these systems due to its ubiquitous presence, transfer within the food web and potentially adverse effects range from individual organisms to whole ecosystem scales (D'avignon et al. 2022; O'connor et al. 2020). The amount of plastic, and MP in particular, entering the terrestrial environment is expected to increase in the future (Lebreton and Andrady 2019), making it imperative to more deeply understand its transport through and between terrestrial compartments including aquatic environments.

Microplastic transport processes in the lentic water column control MP residence times, but these processes are poorly understood because of the complexity of various interacting factors. Residence time is important to quantify, however, as it controls the probability of uptake by filter feeding aquatic organisms such as *Daphnia*. The longer such organisms are exposed to MP, the higher the chance that it will be ingested and enter the lentic food web, and possibly be transferred between trophic levels (Yıldız et al. 2022). Previous research has focused

predominately on physical transport processes such as sinking velocities (Kaiser et al. 2019; Waldschläger and Schüttrumpf 2019) and mixing (Elagami et al. 2022) and how this is influenced by particle properties such as plastic polymer type, size and shape. There is currently little, if anything, known about the role of lake organisms for MP residence times in lakes. Evidence from the marine environment suggests that faeces can have a significant effect on settling velocities, but even these experiments assume laminar conditions which is a large simplification of reality (Pérez-Guevara et al. 2021).

The simulations performed here show that when neglecting the biological pathway residence times for small (0.5 and 5 μm) MP particles in Lake Constance are very long for both the epilimnion and the entire lake water column (both >15 years). The residence time for these particles was considerably longer than the lake flushing time (~ 4 years, defined as river discharge leaving lake divided by the lake volume), suggesting that MP will be transported conservatively through the lake rather than deposited in the sediments. This is similar for the Esthwaite Water, with the MP residence time ranging between >60 (0.5 μm) and ~ 8 (5 μm) times the flushing time (13 weeks) despite shorter MP residence times in this small lake. These results suggest that lakes will not act as a sink for small MP particles unless additional processes, such as uptake by filter feeders or possibly aggregation of MP with existing lake particles (Long et al. 2015; Schmidtman et al. 2022), significantly increases their settling velocities. The 15 μm particles are expected to reach the sediments as their residence times are only a fraction of the lake flushing time for both lakes, with this being more evident in Esthwaite Water due to its shallow depth.

When MP ingestion and egestion by *Daphnia* was introduced into the model structure the residence times for the small particles were drastically reduced for both the epilimnion and the entire lake water column. More than 90 % of MP, regardless of particle size and lake size, reached the sediments in less than a year. The importance of the biological pathway is also highlighted by particle numbers in the epilimnion being purely controlled by the number of *Daphnia* present. During winter when *Daphnia* numbers are low MP numbers increased to their highest levels, while they sank to near-zero in the clear water phase when *Daphnia* filter a significant portion of the POC, including MP, out of the lake epilimnion. The proportion of epilimnic water that passes through the *Daphnia* (k_2 in Eq. 3) each day controls MP uptake. At the height of the clear water phase in Lake Constance ($\sim 10^6$ *Daphnia* individuals m^{-2}), the whole of the epilimnic water volume passes through the organisms 2.5 times per day. This is a very high filtering capacity. To evaluate if this is plausible, we have conducted a simple calculation based on measured *Daphnia* filter rates from the literature (0.1-5 ml h^{-1} individual

¹, depending largely on *Daphnia* size (Burns 1969)), the *Daphnia* numbers in Supplementary Figure 1 (max. 10^6 individuals m^{-2}) and lake area and epilimnion depth given in Table 1. This calculation suggests that between 0.2 and 8 times the volume of the epilimnion can pass through the *Daphnia* population per day. While this calculation has several assumptions, such as uniform *Daphnia* numbers across the lake, our value for k_2 is in reasonable agreement with literature values. The sensitivity analysis supports this conclusion as it showed that the residence times are only minimally influenced by the selection of the biological parameters used, and the same interpretation would be made by varying the biological uptake rate, population density and excretion rate from 50-150 % of the original value.

The dominance of the biological pathway for the 0.5 μm and 5 μm MP particles is also clearly shown by the value of v_{up}/v_{s_epi} . In all cases the biological pathway dominates (>10) for the 0.5 μm MP, while it is dominant for the 5 μm particles for all but the winter *Daphnia* populations ($<10,000$ individuals m^{-2}). For the largest particles, the value of v_{up}/v_{s_epi} is consistently in the transition zone (ratio 0.1-10) where both biologically mediated transport and physical transport are important for MP residence times in the epilimnion.

Model Uncertainties

The model presented here is a highly simplified representation of reality, both in terms of the data used and the model physics. Parameter uncertainty is addressed to some extent by the sensitivity analysis, so that the largest uncertainties probably stem from the simplified way the model represents lake physics. For example, the model assumes that the virtual lakes are permanently stratified rather than mixing one or more times per year as is typical for mid latitude lakes such as Lake Constance and Esthwaite Water. These simplifications were necessary to avoid a full simulation of lake hydrodynamics, and then coupling the hydrodynamic model to a biological module and a particle transport module, all of which is not trivial. Lake turnover would have distributed the MP throughout the lake water column, rather than it being confined to the individual compartments where the residence time is controlled by the sinking velocity. It is difficult to predict what this mixing would imply for MP residence times, as MP from the epilimnion would be mixed into the hypolimnion, which may reduce the total residence time. Concurrently, MP from the hypolimnion would also be mixed back into the epilimnion, increasing the residence time, and leading to an enhanced exposure to organisms such as *Daphnia* with the potential for ingestion and egestion imbedded in faeces at the start of spring. In general, more MP is found in the hypolimnion at steady state in abiotic models (Elagami et al. 2022), suggesting that the mean RT may be increased by lake turnover.

We also assumed that the sediments act as a permanent sink. Given the low density of many plastic polymers and shear forces acting on the lake bed, especially in large lakes (Lorrai et al. 2011), it is possible that MP will be re-suspended back into the lake. This is expected to be enhanced during turnover due to the highly turbulent conditions induced by mixing events, even in the hypolimnion (Cannon et al. 2021). This would render these re-suspended particles available for uptake, effectively increasing their RT in the lake.

A potentially important biological assumption not directly related to transport is that the faecal pellets are assumed to undergo no changes while sinking to the sediments. It is known that *Daphnia* faecal pellets are fragile and are colonized by bacteria that can decompose the pellets in the water column (He and Wang 2006; Pérez-Guevara et al. 2021). This would reduce the sinking velocity of the pellets as mass is lost and they become smaller both of which would extend residence times. Pellets can also form a food source for higher organisms such as fish, in which case the MP would likely end up in large faecal material and sink more rapidly than in the *Daphnia* pellets (Pérez-Guevara et al. 2021). Finally, we have only used *Daphnia* as our ‘model’ filter feeding organism. Lakes host an array of filter feeding zooplankton, such as Copepods and rotifers, meaning that there is a large potential for more MP to enter the food web than predicted by the model. This MP would also be packed in faecal pellets and sink to the sediments. Despite uptake likely being somewhat species specific (e.g. general vs. selective feeders) we believe that our uptake rates are at the lower end of the expected range in nature as we have concentrated exclusively on *Daphnia* as a representative filter feeding organism. Despite these model uncertainties, we believe that our simplified model captures the most salient transport and uptake processes controlling the residence times of MP in lakes.

Conclusions

These virtual experiments highlight the importance of including lake ecology into calculations when estimating MP transport processes in physical models and in particular when assessing residence times. The model predicts that the residence time of small MP imbedded in faecal pellets will be orders of magnitude shorter than pristine plastic and is likely to play a critical part in determining MP residence times and uptake by zooplankton in lakes and ponds. It also shows that the vast majority of small MP will cycle through lake organisms rather than sinking to the sediments via physical transport processes, with potential negative effects to these organisms and ecosystems. It will be vital in the future to test these first model predictions with experimental data, and we hope these virtual experiments will stimulate both discussions and experiments to this effect.

Acknowledgments

Funded by the Deutsche Forschungsgemeinschaft (DFG, German Research Foundation)—
Project Number 391977956—SFB 1357.

References

- Achterberg, E. P., C. M. G. Van Den Berg, M. Boussemart, and W. Davison. 1997. Speciation and cycling of trace metals in Esthwaite Water: A productive English lake with seasonal deep-water anoxia. *Geochimica et Cosmochimica Acta* **61**: 5233-5253.
- Ahmadi, P. and others 2022. Systematic Evaluation of Physical Parameters Affecting the Terminal Settling Velocity of Microplastic Particles in Lakes Using CFD. *Frontiers in Environmental Science* **10**.
- Bell, R. K., and F. J. Ward. 1970. Incorporation of organic carbon by *Daphnia pulex*. *Limnology and Oceanography* **15**: 713-726.
- Burns, C. W. 1969. Relation between filtering rate, temperature, and body size in four species of *Daphnia*. *Limnology and Oceanography* **14**: 693-700.
- Cannon, D. J., C. Troy, H. Bootsma, Q. Liao, and R.-A. Maclellan-Hurd. 2021. Characterizing the Seasonal Variability of Hypolimnetic Mixing in a Large, Deep Lake. *Journal of Geophysical Research: Oceans* **126**: e2021JC017533.
- Chae, Y., D. Kim, S. W. Kim, and Y.-J. An. 2018. Trophic transfer and individual impact of nano-sized polystyrene in a four-species freshwater food chain. *Scientific Reports* **8**: 284.
- Cole, M. and others 2016. Microplastics Alter the Properties and Sinking Rates of Zooplankton Faecal Pellets. *Environmental Science & Technology* **50**: 3239-3246.
- D'avignon, G., I. Gregory-Eaves, and A. Ricciardi. 2022. Microplastics in lakes and rivers: an issue of emerging significance to limnology. *Environmental Reviews* **30**: 228-244.
- Dong, H. and others 2021. Microplastics in a Remote Lake Basin of the Tibetan Plateau: Impacts of Atmospheric Transport and Glacial Melting. *Environmental Science & Technology* **55**: 12951-12960.
- Ebert, D. 2005. *Ecology, Epidemiology, and Evolution of Parasitism in Daphnia*. National Library of Medicine.
- Effler, S. W. and others 2015. *Daphnia* grazing, the clear water phase, and implications of minerogenic particles in Onondaga Lake. *Inland Waters* **5**: 317-330.

- Elagami, H. and others 2022. Measurement of microplastic settling velocities and implications for residence times in thermally stratified lakes. *Limnology and Oceanography* **67**: 934-945.
- Elendt, B. P., and W. R. Bias. 1990. Trace nutrient deficiency in *Daphnia magna* cultured in standard medium for toxicity testing. Effects of the optimization of culture conditions on life history parameters of *D. magna*. *Water Research* **24**: 1157-1167.
- Elizalde-Velázquez, A., A. M. Carcano, J. Crago, M. J. Green, S. A. Shah, and J. E. Cañas-Carrell. 2020. Translocation, trophic transfer, accumulation and depuration of polystyrene microplastics in *Daphnia magna* and *Pimephales promelas*. *Environmental Pollution* **259**: 113937.
- Ershov, D. and others 2021. Bringing TrackMate in the era of machine-learning and deep-learning. *bioRxiv*: 2021.2009.2003.458852.
- He, X., and W.-X. Wang. 2006. Relative importance of inefficient feeding and consumer excretion to organic carbon flux from *Daphnia*. *Freshwater Biology* **51**: 1911-1923.
- Imhof, H. K., J. Rusek, M. Thiel, J. Wolinska, and C. Laforsch. 2017. Do microplastic particles affect *Daphnia magna* at the morphological, life history and molecular level? *PLOS ONE* **12**: e0187590.
- Isf, L. F. U. B.-W. 2016. Institut für Seenforschung, Arbeitsbericht 2016, p. <https://pudi.lubw.de/detailseite/-/publication/87532>.
- Kaiser, D., A. Estelmann, N. Kowalski, M. Glockzin, and J. J. Waniek. 2019. Sinking velocity of sub-millimeter microplastic. *Marine Pollution Bulletin* **139**: 214-220.
- Khatmullina, L., and I. Isachenko. 2017. Settling velocity of microplastic particles of regular shapes. *Marine Pollution Bulletin* **114**: 871-880; <https://doi.org/810.1016/j.marpolbul.2016.1011.1024>.
- Lebreton, L., and A. Andrady. 2019. Future scenarios of global plastic waste generation and disposal. *Palgrave Communications* **5**: 6.
- Long, M. and others 2015. Interactions between microplastics and phytoplankton aggregates: Impact on their respective fates. *Marine Chemistry* **175**: 39-46.
- Lorrai, C., L. Umlauf, J. K. Becherer, A. Lorke, and A. Wüest. 2011. Boundary mixing in lakes: 2. Combined effects of shear- and convectively induced turbulence on basin-scale mixing. *Journal of Geophysical Research: Oceans* **116**.

- Mcmahon, J. W., and F. H. Rigler. 1965. Feeding rate of daphnia magna straus in different foods labeled with radioactive phosphorus *Limnology and Oceanography* **10**: 105-113.
- Michler-Kozma, D. N., L. Kruckenfellner, A. Heitkamp, K. P. Ebke, and F. Gabel. 2022. Uptake and Transfer of Polyamide Microplastics in a Freshwater Mesocosm Study. *Water* **14**: 887.
- Negrete Velasco, A. D. J. and others 2020. Microplastic and Fibre Contamination in a Remote Mountain Lake in Switzerland. *Water* **12**: 2410.
- O'connor, J. D. and others 2020. Microplastics in Freshwater Biota: A Critical Review of Isolation, Characterization, and Assessment Methods. *Global Challenges* **4**: 1800118.
- Pérez-Guevara, F., P. D. Roy, G. Kutralam-Muniasamy, and V. C. Shruti. 2021. A central role for fecal matter in the transport of microplastics: An updated analysis of new findings and persisting questions. *Journal of Hazardous Materials Advances* **4**: 100021.
- Ringelberg, J. 1999. The photobehaviour of *Daphnia* spp. as a model to explain diel vertical migration in zooplankton. *Biological Reviews* **74**: 397-423.
- Rosenkranz, P., Q. Chaudhry, V. Stone, and T. F. Fernandes. 2009. A comparison of nanoparticle and fine particle uptake by *Daphnia magna*. *Environmental Toxicology and Chemistry* **28**: 2142-2149.
- Scherer, C., N. Brennholt, G. Reifferscheid, and M. Wagner. 2017. Feeding type and development drive the ingestion of microplastics by freshwater invertebrates. *Scientific Reports* **7**: 17006.
- Schindelin, J. and others 2012. Fiji: an open-source platform for biological-image analysis. *Nature Methods* **9**: 676-682.
- Schmidtman, J. and others 2022. Heteroaggregation of PS microplastic with ferrihydrite leads to rapid removal of microplastic particles from the water column. *Environmental Science: Processes & Impacts*.
- Schür, C., S. Zipp, T. Thalau, and M. Wagner. 2020. Microplastics but not natural particles induce multigenerational effects in *Daphnia magna*. *Environmental Pollution* **260**: 113904.
- Schwarzer, M. and others 2022. Shape, size, and polymer dependent effects of microplastics on *Daphnia magna*. *Journal of Hazardous Materials* **426**: 128136.

- Stock, F., C. Kochleus, B. Bänsch-Baltruschat, N. Brennholt, and G. Reifferscheid. 2019. Sampling techniques and preparation methods for microplastic analyses in the aquatic environment – A review. *TrAC Trends in Analytical Chemistry* **113**: 84-92.
- Su, L. and others 2016. Microplastics in Taihu Lake, China. *Environmental Pollution* **2016**: 711-719; [org/710.1016/j.envpol.2016.1006.1036](https://doi.org/10.1016/j.envpol.2016.1006.1036).
- Talling, J. F. 2003. Phytoplankton–zooplankton seasonal timing and the ‘clear-water phase’ in some English lakes. *Freshwater Biology* **48**: 39-52.
- Tammenga, M., and E. K. Fischer. 2020. Microplastics in a deep, dimictic lake of the North German Plain with special regard to vertical distribution patterns. *Environmental Pollution* **267**: 115507.
- Tanentzap, A. J. and others 2021. Microplastics and anthropogenic fibre concentrations in lakes reflect surrounding land use. *PLOS Biology* **19**: e3001389.
- Trotter, B. and others 2021. Long-term exposure of *Daphnia magna* to polystyrene microplastic (PS-MP) leads to alterations of the proteome, morphology and life-history. *Science of The Total Environment* **795**: 148822.
- Vinay Kumar, B. N., L. A. Löschel, H. K. Imhof, M. G. J. Löder, and C. Laforsch. 2021. Analysis of microplastics of a broad size range in commercially important mussels by combining FTIR and Raman spectroscopy approaches. *Environmental Pollution* **269**: 116147.
- Waldschläger, K., and H. Schüttrumpf. 2019. Effects of Particle Properties on the Settling and Rise Velocities of Microplastics in Freshwater under Laboratory Conditions. *Environmental Science & Technology* **53**: 1958-1966.
- Yıldız, D. and others 2022. Effects of a microplastic mixture differ across trophic levels and taxa in a freshwater food web: In situ mesocosm experiment. *Science of The Total Environment* **836**: 155407.

Supplementary Information

Mathematical Transport Model

A dynamic lake model was developed to represent the transport behaviour of MP for the biotic and abiotic systems. Similarly to Elagami et al. (2022) the model represents a lumped parameter approach that uses transfer functions to represent the behaviour of MP-particles in each lake compartment. The transfer functions represent transport, mixing and uptake processes occurring in the two lake water columns (Figure 1B). Particle numbers N_i in free suspension ($N_1 = \text{epi-}$, $N_2 = \text{meta-}$, $N_3 = \text{hypolimnion}$) in lake sediment (N_4) and within zooplankton faeces ($N_5 = \text{epi-}$, $N_6 = \text{meta-}$, $N_7 = \text{hypolimnion}$ and $N_8 = \text{lake sediments}$) were simulated for each of the lake compartments as well as within the digestive tract of the zooplankton (N_9) in the epilimnion. For the epi- and hypolimnion, the model assumes fully mixed (turbulent) conditions that are represented by exponential transfer functions (i.e., exponential residence time distributions). For the metalimnion, the model assumes laminar conditions, where particles have a single residence time, mathematically represented by a Delta-Dirac transfer function that is similar to a 'piston flow' type model. For all compartments the governing equations can be combined into a set of nine coupled ordinary differential equations:

$$\frac{d}{dt} \vec{N} = M \cdot \vec{N} + \vec{L} \quad (\text{S1})$$

In Equation S1 $\frac{d}{dt} \vec{N}$ [particles T^{-1}] represents the change of MP numbers in time for each model compartment $\vec{N} = (N_1 \dots N_9)$, M [T^{-1}] represents a matrix containing first order transfer coefficients k_1-k_6 [T^{-1}] defining the exponential transfer functions used to represent the effect of turbulent mixing for the epi- and hypolimnion as well as the uptake and excretion by *Daphnia* (Equation S2).

M (S2)

$$= \begin{bmatrix} -k_1 - k_2(t) & 0 & 0 & 0 & 0 & 0 & 0 & 0 & 0 \\ k_1 & 0 & 0 & 0 & 0 & 0 & 0 & 0 & 0 \\ 0 & 0 & -k_3 & 0 & 0 & 0 & 0 & 0 & 0 \\ 0 & 0 & k_3 & 0 & 0 & 0 & 0 & 0 & 0 \\ 0 & 0 & 0 & 0 & -k_5 & 0 & 0 & 0 & k_4 \\ 0 & 0 & 0 & 0 & k_5 & 0 & 0 & 0 & 0 \\ 0 & 0 & 0 & 0 & 0 & 0 & -k_6 & 0 & 0 \\ 0 & 0 & 0 & 0 & 0 & 0 & k_6 & 0 & 0 \\ k_2(t) & 0 & 0 & 0 & 0 & 0 & 0 & 0 & -k_4 \end{bmatrix}$$

\vec{L} [particles T⁻¹] is a vector containing information about the input of MP into the epilimnion $I(t)$ [particles T⁻¹] and fluxes associated with the laminar settling of MP and MP containing faeces in the metalimnion (Equation S3).

$$\vec{L} = \begin{bmatrix} I(t) \\ -k_1 N_1(t - \tau_1) \\ k_1 N_1(t - \tau_1) \\ 0 \\ 0 \\ -k_5 N_5(t - \tau_2) \\ k_5 N_5(t - \tau_2) \\ 0 \\ 0 \end{bmatrix} \quad (S3)$$

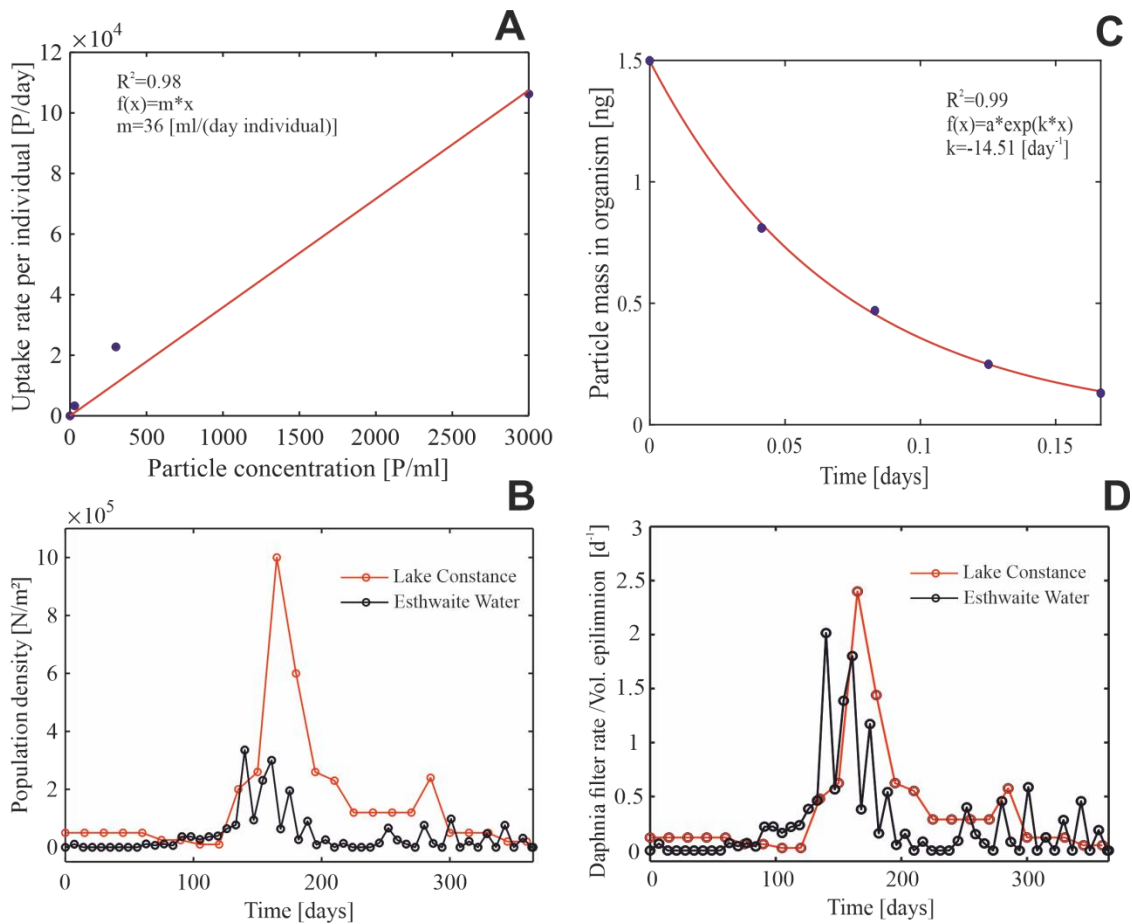
The first order exchange coefficients for the epi- and hypolimnion were estimated according to the definition of the mean lifetime of an exponential function $k = \frac{1}{\tau_{epi,hypo}}$ where $\tau_{epi,hypo}$ [T] are mean residence times of MP and MP containing faeces in the turbulent epi- and hypolimnion. Values for the mean residence times τ_{epi} , τ_{meta} and τ_{hypo} were calculated using equation S4a-c, where v_s [LT⁻¹] represents the laminar settling velocities for MP in each lake compartment and z [L] is the corresponding thickness of the epi- meta- and hypolimnion. The final set of coupled differential equations (shown in Figure S2) was solved

simultaneously for every timestep by using the SIMULINK toolbox in MATLAB. For both lake systems the model was run for a period of $t_{end} = 15$ years with variable time stepping.

$$\tau_{epi} = \frac{Z_{epi}}{v_{s_epi}} \quad (S4a)$$

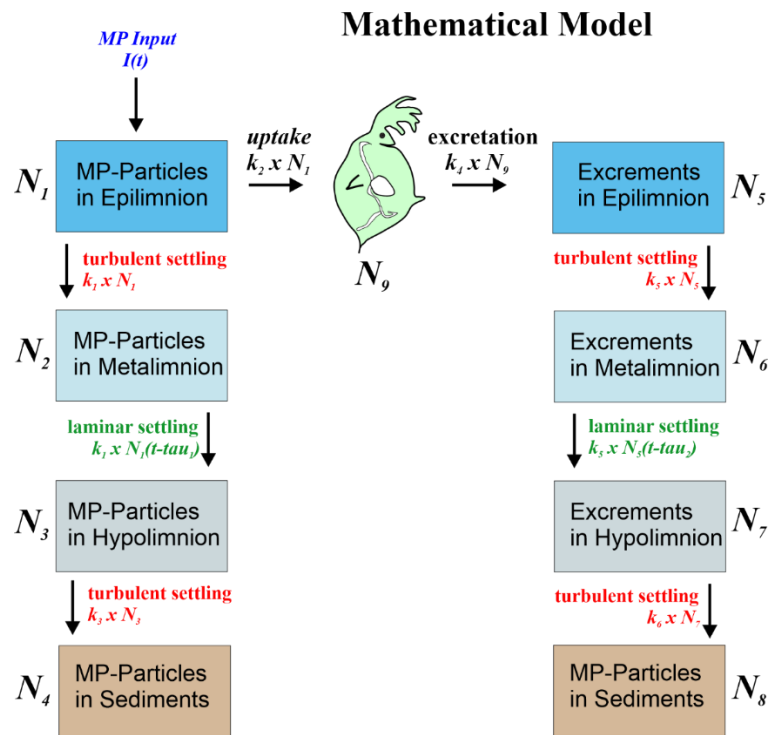
$$\tau_{meta} = \frac{Z_{meta}}{v_{s_meta}} \quad (S4b)$$

$$\tau_{hypo} = \frac{Z_{hypo}}{v_{s_hypo}} \quad (S4c)$$

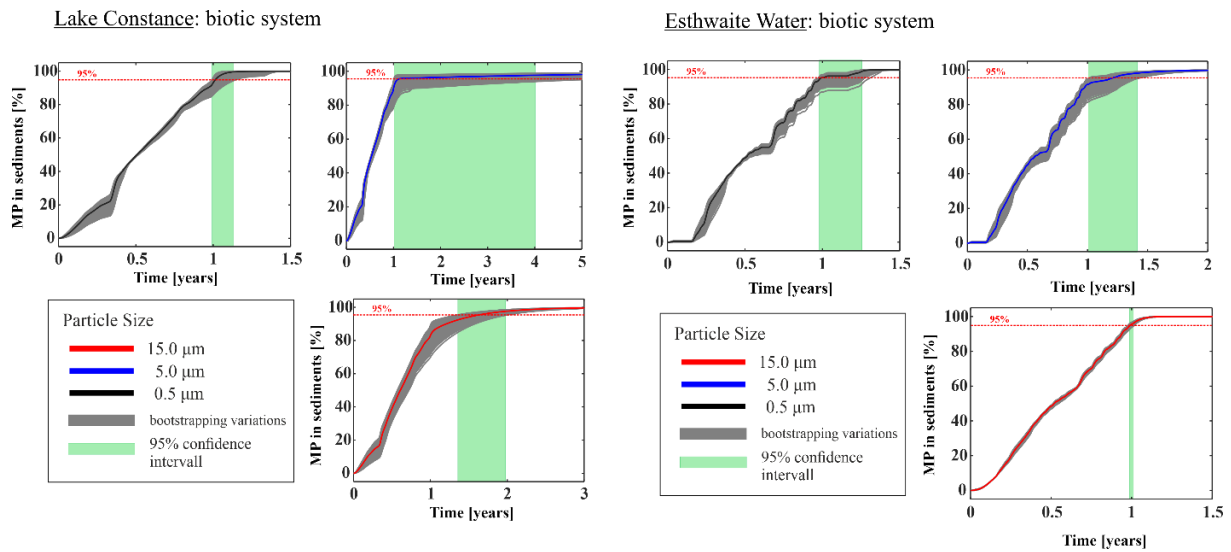


Supplementary S1: A) relationship between particle concentrations and uptake rate of MP for *Daphnia Magna* from Scherer et al. (2017). B) *Daphnia* population dynamics in Lake Constance and Esthwaite Water are from ISF (2016) and Achterberg et al. (1997), C) Data

used to calculate MP excretion rates of *Daphnia* faeces, and D) *Daphnia* filtration rate as a proportion of the epilimnion water volume.



Supplementary Figure S2: Graphical representation of the mathematic lake model including the most important parameters used in the calculations.



Supplementary Figure S3: Sensitivity analysis of the fraction of MP particles entering the sediments (residence times) in Lake Constance and Estwaite Water. Sedimentation rate, population density, egestion and filtration rates was varied from 50-150 % of their average values to quantify the effects of parameter selection on residence time estimates.

Achterberg, E.P., van den Berg, C.M.G., Boussemart, M., Davison, W., 1997. Speciation and cycling of trace metals in Estwaite Water: A productive English lake with seasonal deep-water anoxia. *Geochimica et Cosmochimica Acta*, 61(24): 5233-5253.

Elagami, H. et al., 2022. Measurement of microplastic settling velocities and implications for residence times in thermally stratified lakes. *Limnology and Oceanography*, 67(4): 934-945.

ISF, L.f.U.B.-W., 2016. Institut für Seenforschung, Arbeitsbericht 2016, Karlsruhe / Langenargen.

Scherer, C., Brennholt, N., Reifferscheid, G., Wagner, M., 2017. Feeding type and development drive the ingestion of microplastics by freshwater invertebrates. *Scientific Reports*, 7(1): 17006.

(Eidesstattliche) Versicherungen und Erklärungen

(§ 9 Satz 2 Nr. 3 PromO BayNAT)

Hiermit versichere ich eidesstattlich, dass ich die Arbeit selbstständig verfasst und keine anderen als die von mir angegebenen Quellen und Hilfsmittel benutzt habe (vgl. Art. 64 Abs. 1 Satz 6 BayHSchG).

(§ 9 Satz 2 Nr. 3 PromO BayNAT)

Hiermit erkläre ich, dass ich die Dissertation nicht bereits zur Erlangung eines akademischen Grades eingereicht habe und dass ich nicht bereits diese oder eine gleichartige Doktorprüfung endgültig nicht bestanden habe.

(§ 9 Satz 2 Nr. 4 PromO BayNAT)

Hiermit erkläre ich, dass ich Hilfe von gewerblichen Promotionsberatern bzw. -vermittlern oder ähnlichen Dienstleistern weder bisher in Anspruch genommen habe noch künftig in Anspruch nehmen werde.

(§ 9 Satz 2 Nr. 7 PromO BayNAT)

Hiermit erkläre ich mein Einverständnis, dass die elektronische Fassung meiner Dissertation unter Wahrung meiner Urheberrechte und des Datenschutzes einer gesonderten Überprüfung unterzogen werden kann.

(§ 9 Satz 2 Nr. 8 PromO BayNAT)

Hiermit erkläre ich mein Einverständnis, dass bei Verdacht wissenschaftlichen Fehlverhaltens Ermittlungen durch universitätsinterne Organe der wissenschaftlichen Selbstkontrolle stattfinden können.

.....
Ort, Datum, Unterschrift